**Electronic Supplementary Information** for "Stapling of two PEGylated side chains increases the conformational stability of the WW domain via an entropic effect"

Qiang Xiao, Natalie A. Bécar, Nathaniel P. Brown, Mason S. Smith, Kimberlee L. Stern, Steven R. E. Draper, Katherine P. Thompson, Joshua L. Price

Department of Chemistry and Biochemistry, Brigham Young University, Provo, Utah 84602, United States



## 1. Structure of WW variants

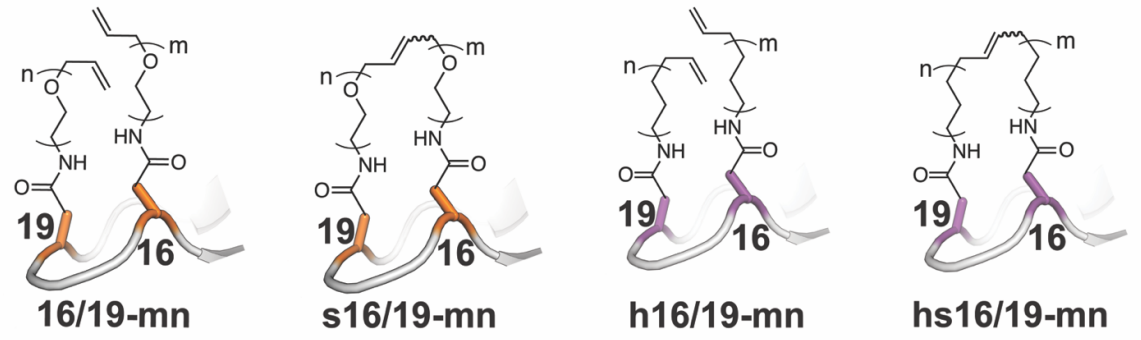


| Name | m | n |
|---|---|---|
| 16/19-11 | 1 | 1 |
| s16/19-11 | 1 | 1 |
| 16/19-12 | 1 | 2 |
| s16/19-12 | 1 | 2 |
| 16/19-22 | 2 | 2 |
| s16/19-22 | 2 | 2 |
| 16/19-23 | 2 | 3 |
| s16/19-23 | 2 | 3 |
| 16/19-33 | 3 | 3 |
| s16/19-33 | 3 | 3 |
| 16/19-34 | 3 | 4 |
| s16/19-34 | 3 | 4 |
| 16/19-44 | 4 | 4 |
| s16/19-44 | 4 | 4 |
| h16/19-22 | 2 | 2 |
| sh16/19-22 | 2 | 2 |
| h16/19-23 | 2 | 3 |
| sh16/19-23 | 2 | 3 |

**Figure S1**. Sequence and structures of WW variants

## 2. Synthesis of WW variants

**Peptide Synthesis:** All WW variants were synthesized as C-terminal acids on Fmoc-Gly-Wang LL resin (EMD Biosciences) by microwave-assisted solid phase peptide synthesis using a standard Fmoc Nα protection strategy. as described previously[1]. All Fmoc-protected amino acids were purchased from Advanced Chem Tech, except for the modified non-natural asparagine derivatives with PEG or hydrocarbon chain on the residue, which were synthesized as described in section **8** below. Unstapled WW variants were cleaved from resin and purified by preparative reverse-phase high-performance liquid chromatography (HPLC) on a C18 column using a linear gradient of water in acetonitrile with 0.1% v/v trifluoroacetic acid. Peptide identity was confirmed by electrospray ionization time-of-flight mass spectrometry.

We used an analogous approach to prepare the stapled WW variants, except we reduced the resin loading (i.e. the number of Fmoc-protected amino groups on resin) of the initial 40 μmol of resin by approximately 50% using a 1:1 mixture of Fmoc- and Boc-protected amino acids during the first coupling reaction. Attempts to perform the ring-closing metathesis reaction at higher resin loading were unsuccessful, presumably because of on-resin peptide aggregation. We performed all subsequent coupling and deprotection reactions with the resulting 20 μmol resin; after the final coupling and deprotection cycle, the resin was allowed to swell in dichloromethane for 10 minutes, and then rinsed three times with dichloroethane. A freshly made 0.5 M solution of the first-generation Grubbs ruthenium complex (purchased from Combi-Blocks) in dichloroethane (1.6 mL, 800 μmol; 40 eq. relative to resin) was then added to the resin and stirred for 2 h with bubbling $N_2$ (to facilitate removal of ethylene as the reaction progressed). Stapling of the Asn-linked olefin-terminated hydrocarbons in WW variants **h16/19-mn** was sufficiently complete at this point, and we proceeded with cleavage, purification, and characterization as described above.

For the less reactive O-allyl terminated Asn-linked PEGs in WW variants **16/19-mn** and **16/32-44**, additional steps were necessary. The catalyst solution was drained from the resin, which was rinsed three times with dichloroethane. A second aliquot of a freshly made solution of first-generation Grubbs ruthenium complex (1.6 mL, 800 μmol; 40 eq. relative to resin) was then added to the resin and stirred for 2 h at room temperature with bubbling $N_2$. Complete stapling of WW variant **16/32-44** required heating of the two metathesis reaction mixture to 60 °C, presumably because of the increased distance in primary sequence between the O-allyl Asn-linked PEGs in **16/32-44** (16 residues apart) relative to **16/19-44** (3 residues apart).

We note that using super-stoichiometric amounts of the first-generation Grubbs ruthenium complex was absolutely essential to generating enough of each stapled WW variant for subsequent purification, characterization, and thermodynamic experiments. Attempts to use catalytic (i.e., sub-stoichiometric) amounts did not result in enough of the desired stapled product, suggesting that the heterogeneous on-resin ring-closing metathesis reaction is much less efficient than the corresponding homogeneous solution-phase reaction.

### 3. Global Fitting of Variable Temperature CD Data

Following purification and characterization (as described above), the conformational stability of stapled and unstapled WW variants was assessed by variable-temperature circular dichroism spectropolarimetry. Data from three replicate variable temperature CD experiments on WW variants **16/19-00, 16/19-11, s16/19-11, 16/19-12, s16/19-12, 16/19-22, s16/19-22, 16/19-23, s16/19-23, 16/19-33, s16/19-33, 16/19-34, s16/19-34, 16/19-44, s16/19-44, h16/19-22, hs16/19-22, h16/19-23, hs16/19-23, 16/32-00, 16/32-44,** and **s16/32-44** were each fit globally to a model for a two-state thermally induced unfolding transition, as shown in equation S1:

$$[\theta] = [(c_n + d_n \bullet T) + K_f(a_n + b_n \bullet T)]/(1+K_f), \quad \text{(S1)}$$

where T is temperature in Kelvin, $c_n$ is the *y*-intercept and $d_n$ is the slope of the post-transition baseline for replicate *n* ($c_1$ and $d_1$ for replicate 1; $c_2$ and $d_2$ for replicate 2; $c_3$ and $d_3$ for replicate 3); $a_n$ is the *y*-intercept and $b_n$ is the slope of the pre-transition baseline for melt *n* ($a_1$ and $b_1$ for replicate 1; $a_2$ and $b_2$ for replicate 2; $a_3$ and $b_3$ for replicate 3); and $K_f$ is the temperature-dependent folding equilibrium constant. $K_f$ is related to the temperature-dependent free energy of folding $\Delta G_f$ according to the following equation:

$$K_f = \exp[-\Delta G_f / RT], \quad \text{(S2)}$$

where R is the universal gas constant (0.0019872 kcal/mol/K). $\Delta G_f$ is a function of temperature, as shown in the following equation:

$$\Delta G_f = \Delta H_0 \bullet (T_m - T)/T_m + \Delta C_p \bullet [T - T_m - T \bullet \ln(T/T_m)], \quad \text{(S3)}$$

where $T_m$ is the midpoint of the unfolding transition and the temperature at which $\Delta G_f = 0$; $\Delta H_0$ is the change in enthalpy upon folding at $T = T_m$; and $\Delta C_p$ is the change in heat capacity upon folding. The parameters for equations S1–S3 were used to calculate the values of $\Delta G_f$ for each WW variant in the main text and in the tables below. CD spectra and variable temperature CD data for each WW variant are shown in Figures S2–S23, along with the fit parameters (± standard error). Standard parameter errors were used to estimate the uncertainty in the thermodynamic values given in the main text by propagation of error.

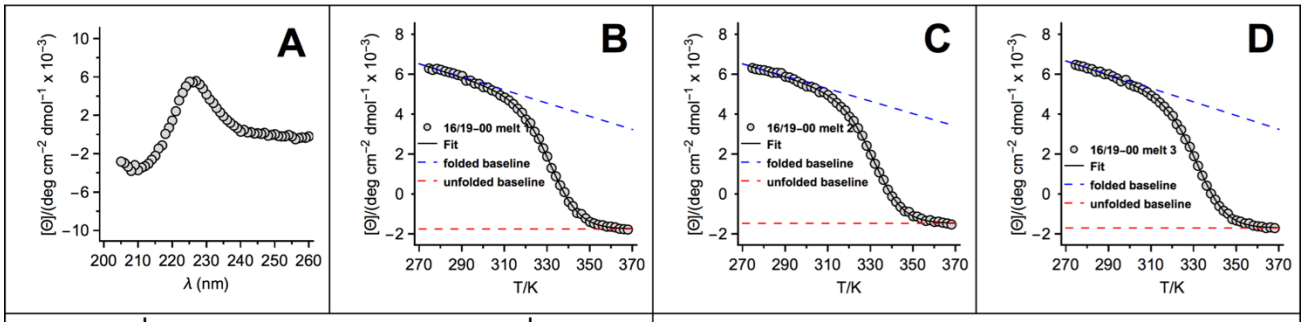


| Parameters | Values | Units | P–Values |
|---|---|---|---|
| $\Delta H_0$ | −31.0 ± 0.4 | kcal/mol | <0.001 |
| $T_m$ | 58.9 ± 0.2 | °C | <0.001 |
| $\Delta C_p$ | −0.34 ± 0.08 | kcal/mol/K | <0.001 |
| a1 | 15.4 ± 0.4 | deg cm$^2$ dmol$^{-1}$ x 10$^{-3}$ | <0.001 |
| b1 | −0.0329 ± 0.0015 | deg cm$^2$ dmol$^{-1}$ K$^{-1}$ x 10$^{-3}$ | <0.001 |
| c1 | −1.75 ± 0.02 | deg cm$^2$ dmol$^{-1}$ x 10$^{-3}$ | <0.001 |
| d1 | --- | --- | --- |
| a2 | 15.0 ± 0.4 | deg cm$^{-2}$ dmol$^{-1}$ x 10$^{-3}$ | <0.001 |
| b2 | −0.0313 ± 0.0015 | deg cm$^{-2}$ dmol$^{-1}$ K$^{-1}$ x 10$^{-3}$ | <0.001 |
| c2 | −1.47 ± 0.02 | deg cm$^{-2}$ dmol$^{-1}$ x 10$^{-3}$ | <0.001 |
| d2 | --- | --- | --- |
| a3 | 15.9 ± 0.4 | deg cm$^2$ dmol$^{-1}$ x 10$^{-3}$ | <0.001 |
| b3 | −0.0343 ± 0.0015 | deg cm$^2$ dmol$^{-1}$ K$^{-1}$ x 10$^{-3}$ | <0.001 |
| c3 | −1.70 ± 0.02 | deg cm$^{-2}$ dmol$^{-1}$ x 10$^{-3}$ | <0.001 |
| d3 | --- | --- | --- |

$R^2 = 0.9999$
sum residuals$^2$ = 0.2635

For **16/19–00**, when T = 332.02 K,
$\Delta G_f$ = 0.00 ± 0.02 kcal/mol
$\Delta H_f$ = −31.0 ± 0.4 kcal/mol
$-T\Delta S_f$ = 31.0 ± 0.4 kcal/mol

**Figure S2**. (A) CD spectra and (B–D) variable temperature CD data (triplicate) for 50 μM solutions of WW variant **16/19-00** in 20 mM sodium phosphate, pH 7. Fit parameters from equations S1–S3 appear in the table, as do calculated values for $\Delta G_f$, $\Delta H_f$, and $-T\Delta S_f$ at 332 K (the melting temperature of **16/19-00**), with the indicated standard errors.

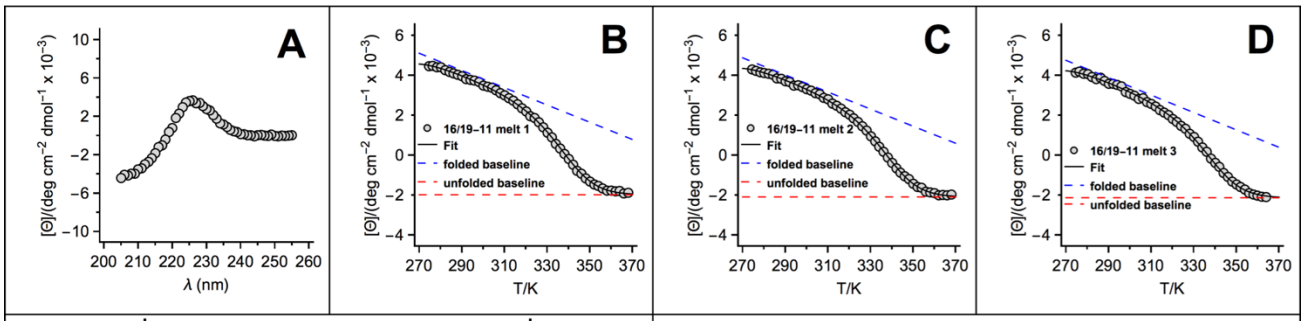


| Parameters | Values | Units | P–Values |
|---|---|---|---|
| $\Delta H_0$ | −25.6 ± 0.7 | kcal/mol | <0.001 |
| $T_m$ | 64.9 ± 0.3 | °C | <0.001 |
| $\Delta C_p$ | −0.52 ± 0.03 | kcal/mol/K | <0.001 |
| a1 | 16.8 ± 0.5 | deg cm$^2$ dmol$^{-1}$ x 10$^{-3}$ | <0.001 |
| b1 | −0.0432 ± 0.0018 | deg cm$^2$ dmol$^{-1}$ K$^{-1}$ x 10$^{-3}$ | <0.001 |
| c1 | −1.98 ± 0.02 | deg cm$^2$ dmol$^{-1}$ x 10$^{-3}$ | <0.001 |
| d1 | --- | --- | --- |
| a2 | 16.4 ± 0.5 | deg cm$^{-2}$ dmol$^{-1}$ x 10$^{-3}$ | <0.001 |
| b2 | −0.0428 ± 0.0017 | deg cm$^{-2}$ dmol$^{-1}$ K$^{-1}$ x 10$^{-3}$ | <0.001 |
| c2 | −2.09 ± 0.02 | deg cm$^{-2}$ dmol$^{-1}$ x 10$^{-3}$ | <0.001 |
| d2 | --- | --- | --- |
| a3 | 16.5 ± 0.5 | deg cm$^2$ dmol$^{-1}$ x 10$^{-3}$ | <0.001 |
| b3 | −0.0436 ± 0.0017 | deg cm$^2$ dmol$^{-1}$ K$^{-1}$ x 10$^{-3}$ | <0.001 |
| c3 | −2.13 ± 0.03 | deg cm$^{-2}$ dmol$^{-1}$ x 10$^{-3}$ | <0.001 |
| d3 | --- | --- | --- |

$R^2 = 0.9997$
sum residuals$^2$ = 0.2987

For **16/19–11**, when T = 332.02 K,
$\Delta G_f$ = −0.43 ± 0.02 kcal/mol
$\Delta H_f$ = −22.5 ± 0.7 kcal/mol
$-T\Delta S_f$ = 22.1 ± 0.7 kcal/mol

**Figure S3**. (A) CD spectra and (B–D) variable temperature CD data (triplicate) for 50 μM solutions of WW variants **16/19-11** in 20 mM sodium phosphate, pH 7. Fit parameters from equations S1–S3 appear in the table, as do calculated values for $\Delta G_f$, $\Delta H_f$, and $-T\Delta S_f$ at 332 K (the melting temperature of **16/19-00**), with the indicated standard errors.

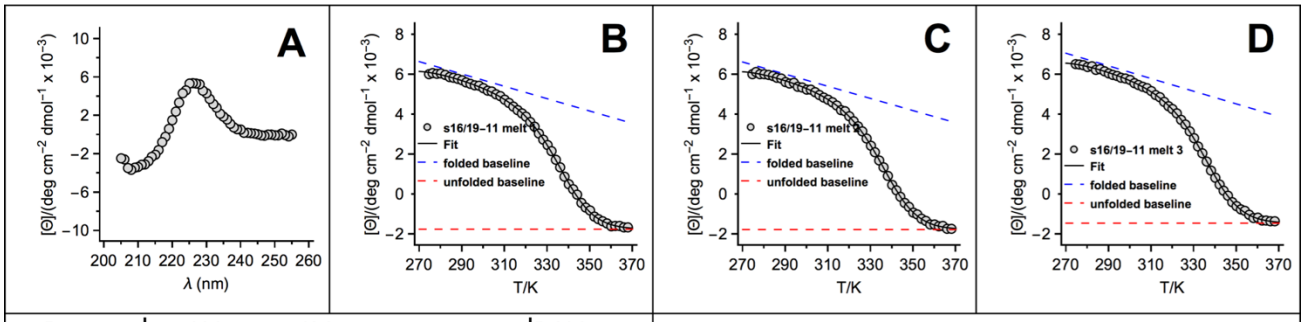


| Parameters | Values | Units | P–Values |
|---|---|---|---|
| $\Delta H_0$ | −25.0 ± 0.3 | kcal/mol | <0.001 |
| $T_m$ | 62.4 ± 0.2 | °C | <0.001 |
| $\Delta C_p$ | −0.49 ± 0.02 | kcal/mol/K | <0.001 |
| a1 | 15.0 ± 0.5 | deg cm$^2$ dmol$^{-1}$ x 10$^{-3}$ | <0.001 |
| b1 | −0.0310 ± 0.0015 | deg cm$^2$ dmol$^{-1}$ K$^{-1}$ x 10$^{-3}$ | <0.001 |
| c1 | −1.76 ± 0.02 | deg cm$^2$ dmol$^{-1}$ x 10$^{-3}$ | <0.001 |
| d1 | --- | --- | --- |
| a2 | 14.8 ± 0.5 | deg cm$^{-2}$ dmol$^{-1}$ x 10$^{-3}$ | <0.001 |
| b2 | −0.0304 ± 0.0015 | deg cm$^{-2}$ dmol$^{-1}$ K$^{-1}$ x 10$^{-3}$ | <0.001 |
| c2 | −1.78 ± 0.02 | deg cm$^{-2}$ dmol$^{-1}$ x 10$^{-3}$ | <0.001 |
| d2 | --- | --- | --- |
| a3 | 15.6 ± 0.5 | deg cm$^2$ dmol$^{-1}$ x 10$^{-3}$ | <0.001 |
| b3 | −0.0317 ± 0.0016 | deg cm$^2$ dmol$^{-1}$ K$^{-1}$ x 10$^{-3}$ | <0.001 |
| c3 | −1.46 ± 0.02 | deg cm$^{-2}$ dmol$^{-1}$ x 10$^{-3}$ | <0.001 |
| d3 | --- | --- | --- |

$R^2 = 0.9999$
sum residuals$^2$ = 0.2268

For **s16/19–11**, when T = 332.02 K,
$\Delta G_f$ = −0.25 ± 0.01 kcal/mol
$\Delta H_f$ = −23.3 ± 0.3 kcal/mol
$-T\Delta S_f$ = 23.0 ± 0.3 kcal/mol

**Figure S4**. (A) CD spectra and (B–D) variable temperature CD data (triplicate) for 50 μM solutions of WW variants s16/19-11 in 20 mM sodium phosphate, pH 7. Fit parameters from equations S1–S3 appear in the table, as do calculated values for ΔGf, ΔHf, and -TΔSf at 332 K (the melting temperature of **16/19-00**), with the indicated standard errors.

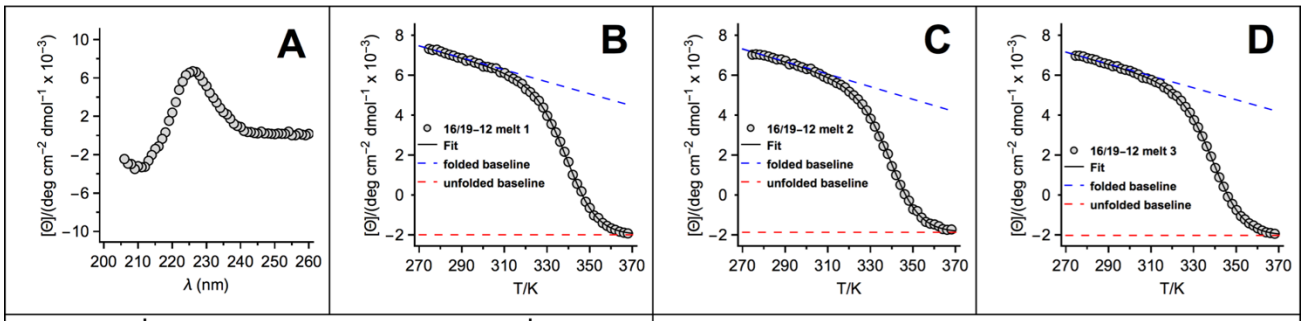


| Parameters | Values | Units | P–Values |
|---|---|---|---|
| $\Delta H_0$ | −31.6 ± 0.3 | kcal/mol | <0.001 |
| $T_m$ | 66.5 ± 0.1 | °C | <0.001 |
| $\Delta C_p$ | −0.34 ± 0.07 | kcal/mol/K | <0.001 |
| a1 | 15.6 ± 0.3 | deg cm$^2$ dmol$^{-1}$ x 10$^{-3}$ | <0.001 |
| b1 | −0.0301 ± 0.0011 | deg cm$^2$ dmol$^{-1}$ K$^{-1}$ x 10$^{-3}$ | <0.001 |
| c1 | −1.99 ± 0.02 | deg cm$^2$ dmol$^{-1}$ x 10$^{-3}$ | <0.001 |
| d1 | --- | --- | --- |
| a2 | 15.8 ± 0.3 | deg cm$^{-2}$ dmol$^{-1}$ x 10$^{-3}$ | <0.001 |
| b2 | −0.0316 ± 0.0011 | deg cm$^{-2}$ dmol$^{-1}$ K$^{-1}$ x 10$^{-3}$ | <0.001 |
| c2 | −1.86 ± 0.02 | deg cm$^{-2}$ dmol$^{-1}$ x 10$^{-3}$ | <0.001 |
| d2 | --- | --- | --- |
| a3 | 15.3 ± 0.3 | deg cm$^2$ dmol$^{-1}$ x 10$^{-3}$ | <0.001 |
| b3 | −0.0299 ± 0.0011 | deg cm$^2$ dmol$^{-1}$ K$^{-1}$ x 10$^{-3}$ | <0.001 |
| c3 | −2.02 ± 0.02 | deg cm$^{-2}$ dmol$^{-1}$ x 10$^{-3}$ | <0.001 |
| d3 | --- | --- | --- |

$R^2 = 0.9999$
sum residuals$^2$ = 0.2274

For **16/19–12**, when T = 332.02 K,
$\Delta G_f$ = −0.68 ± 0.02 kcal/mol
$\Delta H_f$ = −29.0 ± 0.6 kcal/mol
$-T\Delta S_f$ = 28.3 ± 0.6 kcal/mol

**Figure S5**. (A) CD spectra and (B–D) variable temperature CD data (triplicate) for 50 μM solutions of WW variants **16/19-12** in 20 mM sodium phosphate, pH 7. Fit parameters from equations S1–S3 appear in the table, as do calculated values for $\Delta G_f$, $\Delta H_f$, and $-T\Delta S_f$ at 332 K (the melting temperature of **16/19-00**), with the indicated standard errors.

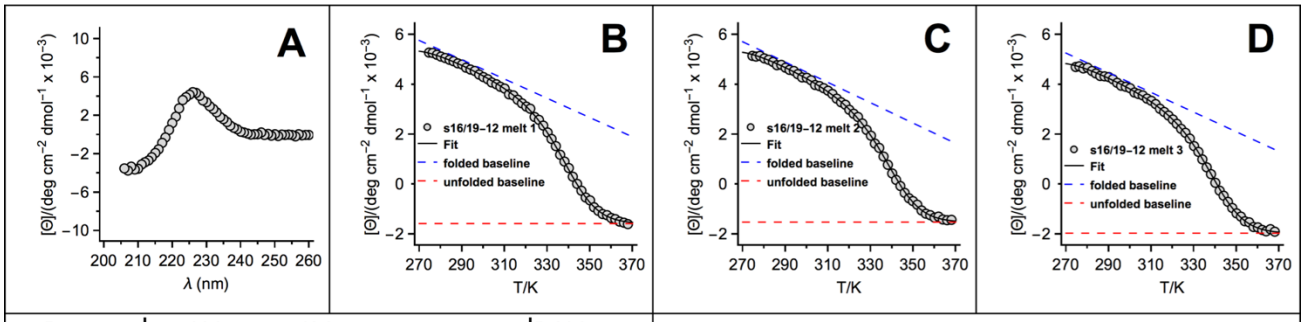


| Parameters | Values | Units | P–Values |
|---|---|---|---|
| $\Delta H_0$ | −26.8 ± 0.5 | kcal/mol | <0.001 |
| $T_m$ | 65.8 ± 0.2 | °C | <0.001 |
| $\Delta C_p$ | −0.52 ± 0.02 | kcal/mol/K | <0.001 |
| a1 | 16.2 ± 0.4 | deg cm$^2$ dmol$^{-1}$ x 10$^{-3}$ | <0.001 |
| b1 | −0.0386 ± 0.0013 | deg cm$^2$ dmol$^{-1}$ K$^{-1}$ x 10$^{-3}$ | <0.001 |
| c1 | −1.58 ± 0.02 | deg cm$^2$ dmol$^{-1}$ x 10$^{-3}$ | <0.001 |
| d1 | --- | --- | --- |
| a2 | 16.7 ± 0.4 | deg cm$^{-2}$ dmol$^{-1}$ x 10$^{-3}$ | <0.001 |
| b2 | −0.0408 ± 0.0012 | deg cm$^{-2}$ dmol$^{-1}$ K$^{-1}$ x 10$^{-3}$ | <0.001 |
| c2 | −1.52 ± 0.02 | deg cm$^{-2}$ dmol$^{-1}$ x 10$^{-3}$ | <0.001 |
| d2 | --- | --- | --- |
| a3 | 15.9 ± 0.4 | deg cm$^2$ dmol$^{-1}$ x 10$^{-3}$ | <0.001 |
| b3 | −0.0395 ± 0.0012 | deg cm$^2$ dmol$^{-1}$ K$^{-1}$ x 10$^{-3}$ | <0.001 |
| c3 | −1.97 ± 0.02 | deg cm$^{-2}$ dmol$^{-1}$ x 10$^{-3}$ | <0.001 |
| d3 | --- | --- | --- |

$R^2 = 0.9999$
sum residuals$^2$ = 0.1983

For **s16/19–12**, when T = 332.02 K,
$\Delta G_f$ = −0.51 ± 0.02 kcal/mol
$\Delta H_f$ = −23.1 ± 0.5 kcal/mol
$-T\Delta S_f$ = 22.6 ± 0.5 kcal/mol

**Figure S6**. (A) CD spectra and (B–D) variable temperature CD data (triplicate) for 50 μM solutions of WW variants **s16/19-12** in 20 mM sodium phosphate, pH 7. Fit parameters from equations S1–S3 appear in the table, as do calculated values for $\Delta G_f$, $\Delta H_f$, and $-T\Delta S_f$ at 332 K (the melting temperature of **16/19-00**), with the indicated standard errors.

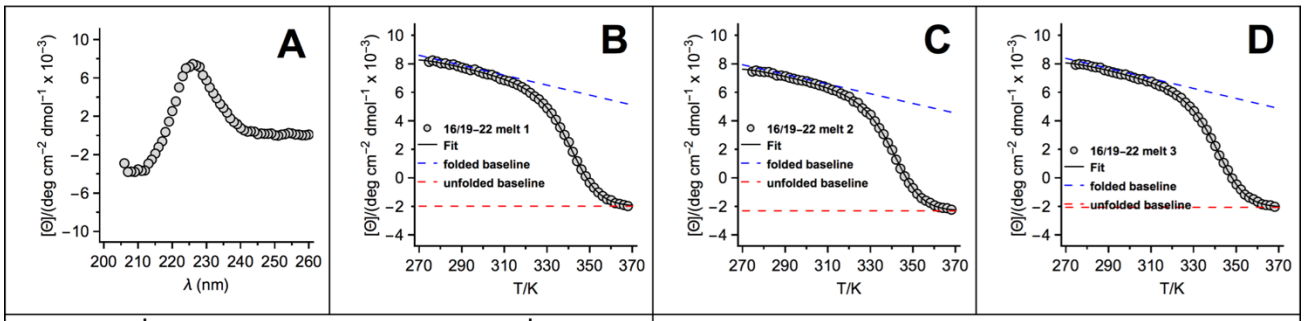


| Parameters | Values | Units | P–Values |
|---|---|---|---|
| $\Delta H_0$ | −32.8 ± 0.3 | kcal/mol | <0.001 |
| $T_m$ | 68.0 ± 0.1 | °C | <0.001 |
| $\Delta C_p$ | −0.62 ± 0.02 | kcal/mol/K | <0.001 |
| a1 | 18.0 ± 0.3 | deg cm$^2$ dmol$^{-1}$ x 10$^{-3}$ | <0.001 |
| b1 | −0.0349 ± 0.0009 | deg cm$^2$ dmol$^{-1}$ K$^{-1}$ x 10$^{-3}$ | <0.001 |
| c1 | −1.98 ± 0.02 | deg cm$^2$ dmol$^{-1}$ x 10$^{-3}$ | <0.001 |
| d1 | --- | --- | --- |
| a2 | 17.1 ± 0.3 | deg cm$^{-2}$ dmol$^{-1}$ x 10$^{-3}$ | <0.001 |
| b2 | −0.0340 ± 0.0009 | deg cm$^{-2}$ dmol$^{-1}$ K$^{-1}$ x 10$^{-3}$ | <0.001 |
| c2 | −2.30 ± 0.02 | deg cm$^{-2}$ dmol$^{-1}$ x 10$^{-3}$ | <0.001 |
| d2 | --- | --- | --- |
| a3 | 17.9 ± 0.3 | deg cm$^2$ dmol$^{-1}$ x 10$^{-3}$ | <0.001 |
| b3 | −0.0352 ± 0.0009 | deg cm$^2$ dmol$^{-1}$ K$^{-1}$ x 10$^{-3}$ | <0.001 |
| c3 | −2.06 ± 0.02 | deg cm$^{-2}$ dmol$^{-1}$ x 10$^{-3}$ | <0.001 |
| d3 | --- | --- | --- |

$R^2 = 0.9999$
sum residuals$^2$ = 0.2538

For **16/19–22**, when T = 332.02 K,
$\Delta G_f$ = −0.80 ± 0.01 kcal/mol
$\Delta H_f$ = −27.1 ± 0.3 kcal/mol
$-T\Delta S_f$ = 26.3 ± 0.3 kcal/mol

**Figure S7**. (A) CD spectra and (B–D) variable temperature CD data (triplicate) for 50 μM solutions of WW variants **16/19-22** in 20 mM sodium phosphate, pH 7. Fit parameters from equations S1–S3 appear in the table, as do calculated values for $\Delta G_f$, $\Delta H_f$, and $-T\Delta S_f$ at 332 K (the melting temperature of **16/19-00**), with the indicated standard errors.

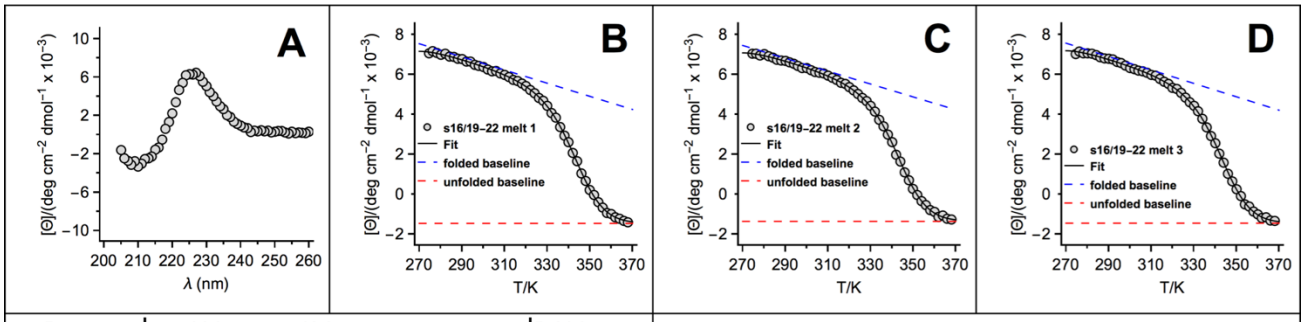


| Parameters | Values | Units | P–Values |
|---|---|---|---|
| $\Delta H_0$ | −32.1 ± 0.4 | kcal/mol | <0.001 |
| $T_m$ | 69.9 ± 0.1 | °C | <0.001 |
| $\Delta C_p$ | −0.62 ± 0.02 | kcal/mol/K | <0.001 |
| a1 | 16.4 ± 0.3 | deg cm$^2$ dmol$^{-1}$ x 10$^{-3}$ | <0.001 |
| b1 | −0.0329 ± 0.0009 | deg cm$^2$ dmol$^{-1}$ K$^{-1}$ x 10$^{-3}$ | <0.001 |
| c1 | −1.47 ± 0.02 | deg cm$^2$ dmol$^{-1}$ x 10$^{-3}$ | <0.001 |
| d1 | --- | --- | --- |
| a2 | 16.2 ± 0.3 | deg cm$^{-2}$ dmol$^{-1}$ x 10$^{-3}$ | <0.001 |
| b2 | −0.0322 ± 0.0009 | deg cm$^{-2}$ dmol$^{-1}$ K$^{-1}$ x 10$^{-3}$ | <0.001 |
| c2 | −1.37 ± 0.02 | deg cm$^{-2}$ dmol$^{-1}$ x 10$^{-3}$ | <0.001 |
| d2 | --- | --- | --- |
| a3 | 16.6 ± 0.3 | deg cm$^2$ dmol$^{-1}$ x 10$^{-3}$ | <0.001 |
| b3 | −0.0336 ± 0.0009 | deg cm$^2$ dmol$^{-1}$ K$^{-1}$ x 10$^{-3}$ | <0.001 |
| c3 | −1.46 ± 0.02 | deg cm$^{-2}$ dmol$^{-1}$ x 10$^{-3}$ | <0.001 |
| d3 | --- | --- | --- |

$R^2 = 0.9999$
sum residuals$^2$ = 0.2478

For **s16/19–22**, when T = 332.02 K,
$\Delta G_f$ = −0.92 ± 0.01 kcal/mol
$\Delta H_f$ = −25.4 ± 0.4 kcal/mol
$-T\Delta S_f$ = 24.4 ± 0.4 kcal/mol

**Figure S8**. (A) CD spectra and (B–D) variable temperature CD data (triplicate) for 50 μM solutions of WW variants **s16/19-22** in 20 mM sodium phosphate, pH 7. Fit parameters from equations S1–S3 appear in the table, as do calculated values for $\Delta G_f$, $\Delta H_f$, and $-T\Delta S_f$ at 332 K (the melting temperature of **16/19-00**), with the indicated standard errors.

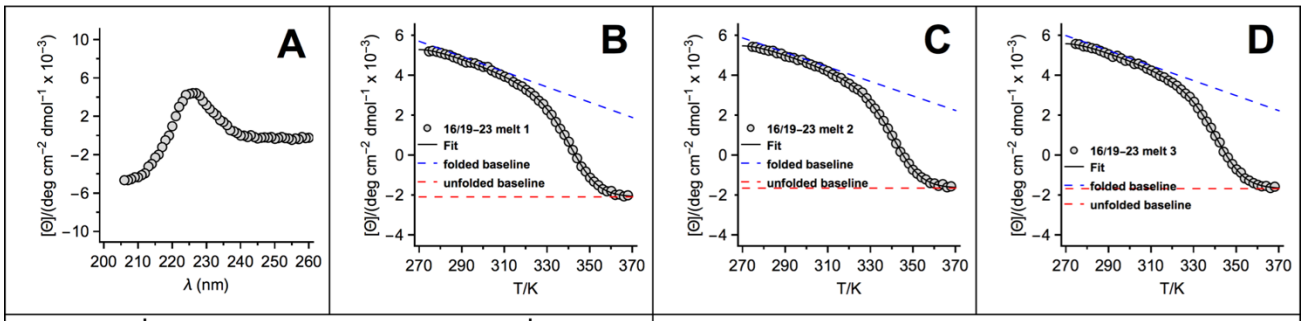


| Parameters | Values | Units | P–Values |
|---|---|---|---|
| $\Delta H_0$ | −31.9 ± 0.4 | kcal/mol | <0.001 |
| $T_m$ | 67.7 ± 0.1 | °C | <0.001 |
| $\Delta C_p$ | −0.64 ± 0.02 | kcal/mol/K | <0.001 |
| a1 | 16.0 ± 0.3 | deg cm$^2$ dmol$^{-1}$ x 10$^{-3}$ | <0.001 |
| b1 | −0.0382 ± 0.0009 | deg cm$^2$ dmol$^{-1}$ K$^{-1}$ x 10$^{-3}$ | <0.001 |
| c1 | −2.09 ± 0.02 | deg cm$^2$ dmol$^{-1}$ x 10$^{-3}$ | <0.001 |
| d1 | --- | --- | --- |
| a2 | 15.7 ± 0.3 | deg cm$^{-2}$ dmol$^{-1}$ x 10$^{-3}$ | <0.001 |
| b2 | −0.0364 ± 0.0009 | deg cm$^{-2}$ dmol$^{-1}$ K$^{-1}$ x 10$^{-3}$ | <0.001 |
| c2 | −1.65 ± 0.02 | deg cm$^{-2}$ dmol$^{-1}$ x 10$^{-3}$ | <0.001 |
| d2 | --- | --- | --- |
| a3 | 16.2 ± 0.3 | deg cm$^2$ dmol$^{-1}$ x 10$^{-3}$ | <0.001 |
| b3 | −0.0376 ± 0.0009 | deg cm$^2$ dmol$^{-1}$ K$^{-1}$ x 10$^{-3}$ | <0.001 |
| c3 | −1.67 ± 0.02 | deg cm$^{-2}$ dmol$^{-1}$ x 10$^{-3}$ | <0.001 |
| d3 | --- | --- | --- |

$R^2 = 0.9999$
sum residuals$^2$ = 0.1811

For **16/19–23**, when T = 332.02 K,
$\Delta G_f$ = −0.75 ± 0.01 kcal/mol
$\Delta H_f$ = −26.2 ± 0.4 kcal/mol
$-T\Delta S_f$ = 25.5 ± 0.4 kcal/mol

**Figure S9**. (A) CD spectra and (B–D) variable temperature CD data (triplicate) for 50 μM solutions of WW variants **16/19-23** in 20 mM sodium phosphate, pH 7. Fit parameters from equations S1–S3 appear in the table, as do calculated values for $\Delta G_f$, $\Delta H_f$, and $-T\Delta S_f$ at 332 K (the melting temperature of **16/19-00**), with the indicated standard errors.

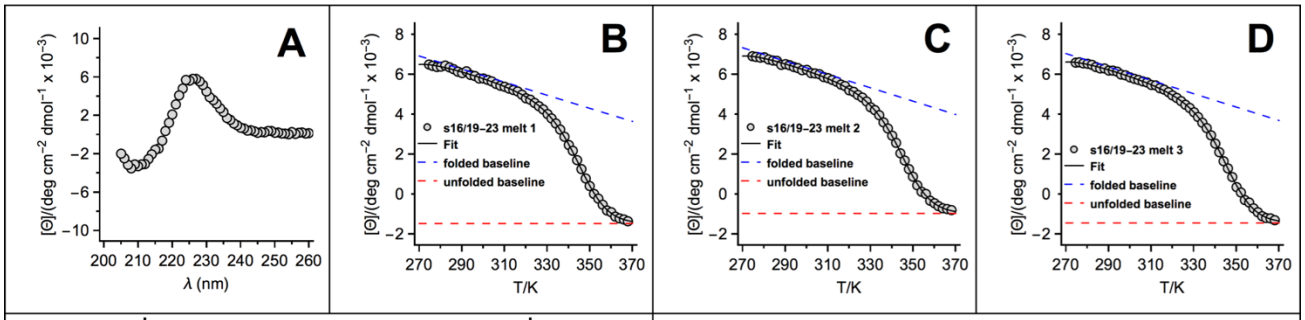


| Parameters | Values | Units | P–Values |
|---|---|---|---|
| $\Delta H_0$ | −32.1 ± 0.4 | kcal/mol | <0.001 |
| $T_m$ | 71.7 ± 0.1 | °C | <0.001 |
| $\Delta C_p$ | −0.61 ± 0.02 | kcal/mol/K | <0.001 |
| a1 | 15.8 ± 0.2 | deg cm$^2$ dmol$^{-1}$ x 10$^{-3}$ | <0.001 |
| b1 | −0.0328 ± 0.0008 | deg cm$^2$ dmol$^{-1}$ K$^{-1}$ x 10$^{-3}$ | <0.001 |
| c1 | −1.47 ± 0.02 | deg cm$^2$ dmol$^{-1}$ x 10$^{-3}$ | <0.001 |
| d1 | --- | --- | --- |
| a2 | 16.4 ± 0.2 | deg cm$^{-2}$ dmol$^{-1}$ x 10$^{-3}$ | <0.001 |
| b2 | −0.0335 ± 0.0008 | deg cm$^{-2}$ dmol$^{-1}$ K$^{-1}$ x 10$^{-3}$ | <0.001 |
| c2 | −0.97 ± 0.02 | deg cm$^{-2}$ dmol$^{-1}$ x 10$^{-3}$ | <0.001 |
| d2 | --- | --- | --- |
| a3 | 16.1 ± 0.2 | deg cm$^2$ dmol$^{-1}$ x 10$^{-3}$ | <0.001 |
| b3 | −0.0335 ± 0.0008 | deg cm$^2$ dmol$^{-1}$ K$^{-1}$ x 10$^{-3}$ | <0.001 |
| c3 | −1.45 ± 0.02 | deg cm$^{-2}$ dmol$^{-1}$ x 10$^{-3}$ | <0.001 |
| d3 | --- | --- | --- |

$R^2$ = 0.9999
sum residuals$^2$ = 0.1877

For **s16/19–23**, when T = 332.02 K,
$\Delta G_f$ = −1.04 ± 0.02 kcal/mol
$\Delta H_f$ = −24.2 ± 0.4 kcal/mol
$-T\Delta S_f$ = 23.2 ± 0.4 kcal/mol

**Figure S10**. (A) CD spectra and (B–D) variable temperature CD data (triplicate) for 50 μM solutions of WW variants **s16/19-23** in 20 mM sodium phosphate, pH 7. Fit parameters from equations S1–S3 appear in the table, as do calculated values for $\Delta G_f$, $\Delta H_f$, and $-T\Delta S_f$ at 332 K (the melting temperature of **16/19-00**), with the indicated standard errors.

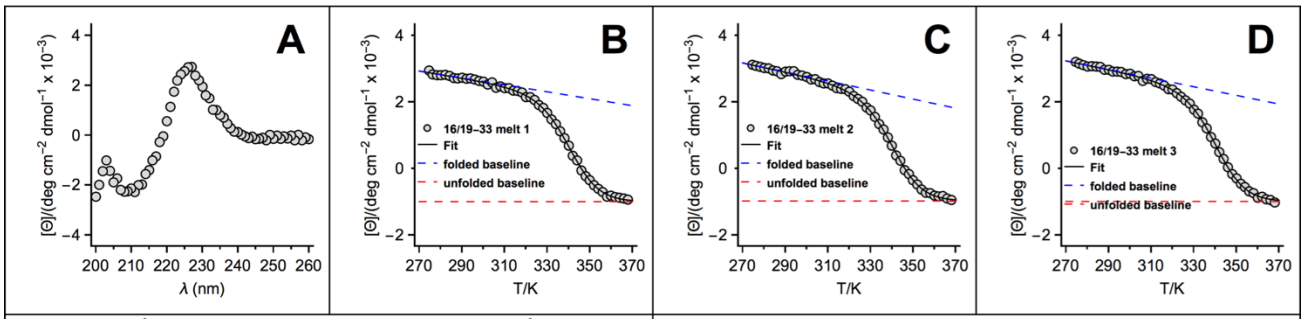


| Parameters | Values | Units | P–Values |
|---|---|---|---|
| $\Delta H_0$ | −32.3 ± 0.5 | kcal/mol | <0.001 |
| $T_m$ | 67.5 ± 0.2 | °C | <0.001 |
| $\Delta C_p$ | −0.39 ± 0.12 | kcal/mol/K | warning! |
| a1 | 5.7 ± 0.2 | deg cm$^2$ dmol$^{-1}$ x 10$^{-3}$ | <0.001 |
| b1 | −0.0104 ± 0.0008 | deg cm$^2$ dmol$^{-1}$ K$^{-1}$ x 10$^{-3}$ | <0.001 |
| c1 | −1.00 ± 0.02 | deg cm$^2$ dmol$^{-1}$ x 10$^{-3}$ | <0.001 |
| d1 | --- | --- | --- |
| a2 | 6.9 ± 0.2 | deg cm$^{-2}$ dmol$^{-1}$ x 10$^{-3}$ | <0.001 |
| b2 | −0.0136 ± 0.0008 | deg cm$^{-2}$ dmol$^{-1}$ K$^{-1}$ x 10$^{-3}$ | <0.001 |
| c2 | −0.98 ± 0.02 | deg cm$^{-2}$ dmol$^{-1}$ x 10$^{-3}$ | <0.001 |
| d2 | --- | --- | --- |
| a3 | 6.8 ± 0.2 | deg cm$^2$ dmol$^{-1}$ x 10$^{-3}$ | <0.001 |
| b3 | −0.0130 ± 0.0008 | deg cm$^2$ dmol$^{-1}$ K$^{-1}$ x 10$^{-3}$ | <0.001 |
| c3 | −0.99 ± 0.02 | deg cm$^{-2}$ dmol$^{-1}$ x 10$^{-3}$ | <0.001 |
| d3 | --- | --- | --- |

$R^2$ = 0.9998
sum residuals$^2$ = 0.1381

For **16/19–33**, when T = 332.02 K,
$\Delta G_f$ = −0.77 ± 0.03 kcal/mol
$\Delta H_f$ = −29.0 ± 1.1 kcal/mol
$-T\Delta S_f$ = 28.2 ± 1.1 kcal/mol

**Figure S11**. (A) CD spectra and (B–D) variable temperature CD data (triplicate) for 50 μM solutions of WW variants **16/19-33** in 20 mM sodium phosphate, pH 7. Fit parameters from equations S1–S3 appear in the table, as do calculated values for $\Delta G_f$, $\Delta H_f$, and $-T\Delta S_f$ at 332 K (the melting temperature of **16/19-00**), with the indicated standard errors.

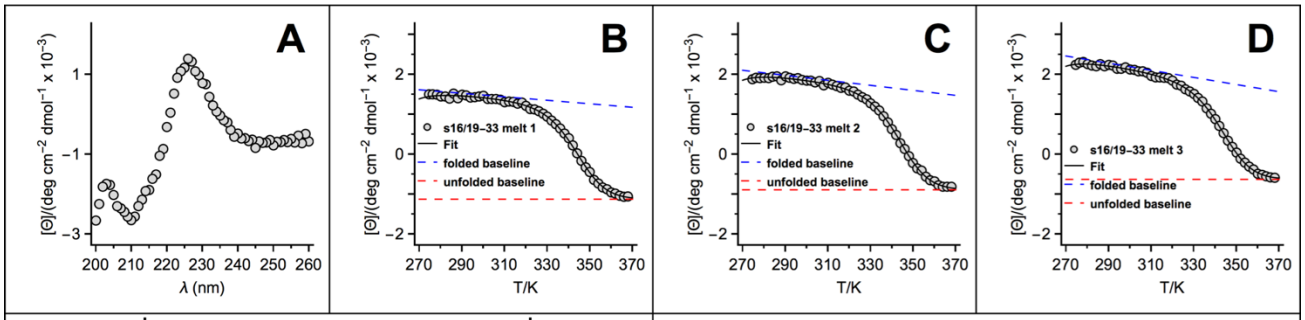


| Parameters | Values | Units | P–Values |
|---|---|---|---|
| $\Delta H_0$ | −31.8 ± 0.6 | kcal/mol | <0.001 |
| $T_m$ | 70.1 ± 0.2 | °C | <0.001 |
| $\Delta C_p$ | −0.65 ± 0.02 | kcal/mol/K | <0.001 |
| a1 | 2.8 ± 0.2 | deg cm$^2$ dmol$^{-1}$ x 10$^{-3}$ | <0.001 |
| b1 | −0.0044 ± 0.0006 | deg cm$^2$ dmol$^{-1}$ K$^{-1}$ x 10$^{-3}$ | <0.001 |
| c1 | −1.13 ± 0.01 | deg cm$^2$ dmol$^{-1}$ x 10$^{-3}$ | <0.001 |
| d1 | --- | --- | --- |
| a2 | 3.8 ± 0.2 | deg cm$^{-2}$ dmol$^{-1}$ x 10$^{-3}$ | <0.001 |
| b2 | −0.0063 ± 0.0006 | deg cm$^{-2}$ dmol$^{-1}$ K$^{-1}$ x 10$^{-3}$ | <0.001 |
| c2 | −0.89 ± 0.01 | deg cm$^{-2}$ dmol$^{-1}$ x 10$^{-3}$ | <0.001 |
| d2 | --- | --- | --- |
| a3 | 4.9 ± 0.2 | deg cm$^2$ dmol$^{-1}$ x 10$^{-3}$ | <0.001 |
| b3 | −0.0089 ± 0.0006 | deg cm$^2$ dmol$^{-1}$ K$^{-1}$ x 10$^{-3}$ | <0.001 |
| c3 | −0.63 ± 0.01 | deg cm$^{-2}$ dmol$^{-1}$ x 10$^{-3}$ | <0.001 |
| d3 | --- | --- | --- |

$R^2 = 0.9997$
sum residuals$^2$ = 0.0969

For **s16/19–33**, when T = 332.02 K,
$\Delta G_f$ = −0.92 ± 0.02 kcal/mol
$\Delta H_f$ = −24.5 ± 0.7 kcal/mol
$-T\Delta S_f$ = 23.6 ± 0.7 kcal/mol

**Figure S12**. (A) CD spectra and (B–D) variable temperature CD data (triplicate) for 50 μM solutions of WW variants **s16/19-33** in 20 mM sodium phosphate, pH 7. Fit parameters from equations S1–S3 appear in the table, as do calculated values for $\Delta G_f$, $\Delta H_f$, and $-T\Delta S_f$ at 332 K (the melting temperature of **16/19-00**), with the indicated standard errors.

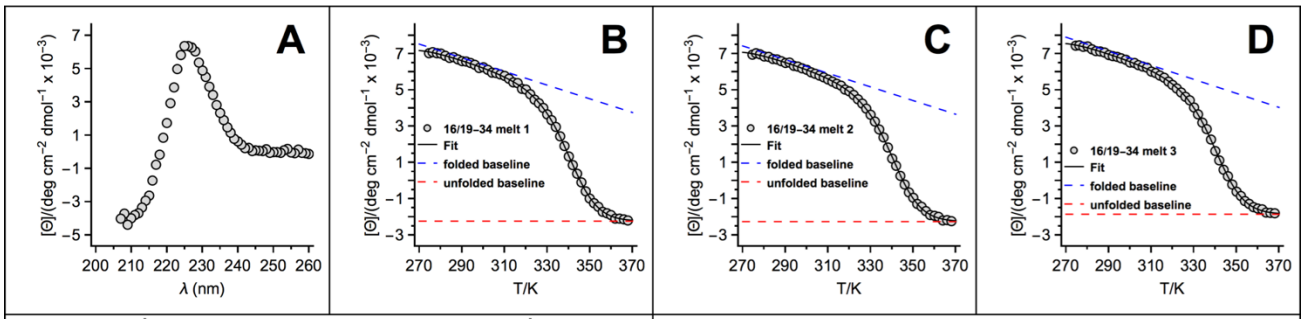


| Parameters | Values | Units | P–Values |
|---|---|---|---|
| $\Delta H_0$ | −32.0 ± 0.3 | kcal/mol | <0.001 |
| $T_m$ | 67.2 ± 0.1 | °C | <0.001 |
| $\Delta C_p$ | −0.62 ± 0.02 | kcal/mol/K | <0.001 |
| a1 | 17.7 ± 0.3 | deg cm$^2$ dmol$^{-1}$ x 10$^{-3}$ | <0.001 |
| b1 | −0.0377 ± 0.0010 | deg cm$^2$ dmol$^{-1}$ K$^{-1}$ x 10$^{-3}$ | <0.001 |
| c1 | −2.24 ± 0.02 | deg cm$^2$ dmol$^{-1}$ x 10$^{-3}$ | <0.001 |
| d1 | --- | --- | --- |
| a2 | 17.6 ± 0.3 | deg cm$^{-2}$ dmol$^{-1}$ x 10$^{-3}$ | <0.001 |
| b2 | −0.0376 ± 0.0010 | deg cm$^{-2}$ dmol$^{-1}$ K$^{-1}$ x 10$^{-3}$ | <0.001 |
| c2 | −2.26 ± 0.02 | deg cm$^{-2}$ dmol$^{-1}$ x 10$^{-3}$ | <0.001 |
| d2 | --- | --- | --- |
| a3 | 18.4 ± 0.3 | deg cm$^2$ dmol$^{-1}$ x 10$^{-3}$ | <0.001 |
| b3 | −0.0387 ± 0.0010 | deg cm$^2$ dmol$^{-1}$ K$^{-1}$ x 10$^{-3}$ | <0.001 |
| c3 | −1.86 ± 0.02 | deg cm$^{-2}$ dmol$^{-1}$ x 10$^{-3}$ | <0.001 |
| d3 | --- | --- | --- |

$R^2 = 0.9999$
sum residuals$^2$ = 0.2513

For **16/19–34**, when T = 332.02 K,
$\Delta G_f$ = −0.72 ± 0.01 kcal/mol
$\Delta H_f$ = −26.9 ± 0.4 kcal/mol
$-T\Delta S_f$ = 26.2 ± 0.4 kcal/mol

**Figure S13**. (A) CD spectra and (B–D) variable temperature CD data (triplicate) for 50 μM solutions of WW variants **16/19-34** in 20 mM sodium phosphate, pH 7. Fit parameters from equations S1–S3 appear in the table, as do calculated values for $\Delta G_f$, $\Delta H_f$, and $-T\Delta S_f$ at 332 K (the melting temperature of **16/19-00**), with the indicated standard errors.

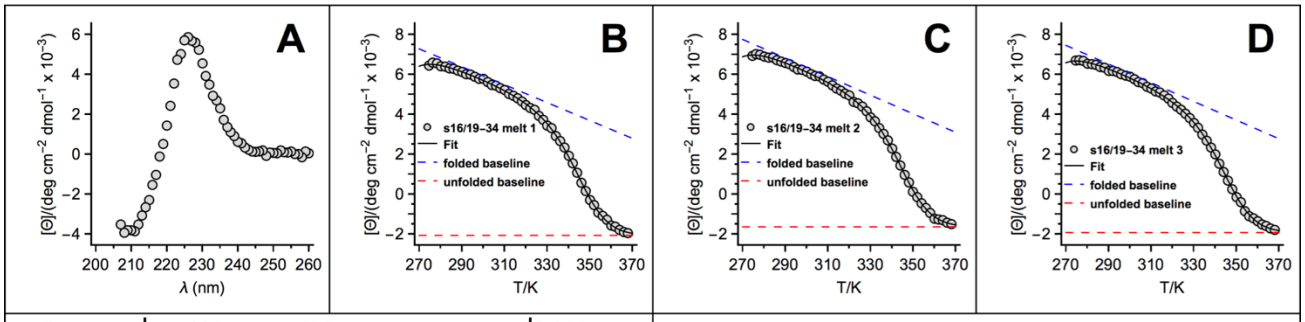


| Parameters | Values | Units | P–Values |
|---|---|---|---|
| $\Delta H_0$ | −30.5 ± 0.5 | kcal/mol | <0.001 |
| $T_m$ | 71.4 ± 0.1 | °C | <0.001 |
| $\Delta C_p$ | −0.62 ± 0.01 | kcal/mol/K | <0.001 |
| a1 | 19.4 ± 0.3 | deg cm$^2$ dmol$^{-1}$ x 10$^{-3}$ | <0.001 |
| b1 | −0.0448 ± 0.0010 | deg cm$^2$ dmol$^{-1}$ K$^{-1}$ x 10$^{-3}$ | <0.001 |
| c1 | −2.07 ± 0.03 | deg cm$^2$ dmol$^{-1}$ x 10$^{-3}$ | <0.001 |
| d1 | --- | --- | --- |
| a2 | 20.3 ± 0.3 | deg cm$^{-2}$ dmol$^{-1}$ x 10$^{-3}$ | <0.001 |
| b2 | −0.0466 ± 0.0010 | deg cm$^{-2}$ dmol$^{-1}$ K$^{-1}$ x 10$^{-3}$ | <0.001 |
| c2 | −1.64 ± 0.02 | deg cm$^{-2}$ dmol$^{-1}$ x 10$^{-3}$ | <0.001 |
| d2 | --- | --- | --- |
| a3 | 20.1 ± 0.3 | deg cm$^2$ dmol$^{-1}$ x 10$^{-3}$ | <0.001 |
| b3 | −0.0468 ± 0.0010 | deg cm$^2$ dmol$^{-1}$ K$^{-1}$ x 10$^{-3}$ | <0.001 |
| c3 | −1.93 ± 0.02 | deg cm$^{-2}$ dmol$^{-1}$ x 10$^{-3}$ | <0.001 |
| d3 | --- | --- | --- |

$R^2 = 0.9999$
sum residuals$^2$ = 0.2578

For **s16/19–34**, when T = 332.02 K,
$\Delta G_f$ = −0.96 ± 0.02 kcal/mol
$\Delta H_f$ = −22.8 ± 0.5 kcal/mol
$-T\Delta S_f$ = 21.8 ± 0.5 kcal/mol

**Figure S14**. (A) CD spectra and (B–D) variable temperature CD data (triplicate) for 50 μM solutions of WW variants **s16/19-34** in 20 mM sodium phosphate, pH 7. Fit parameters from equations S1–S3 appear in the table, as do calculated values for $\Delta G_f$, $\Delta H_f$, and $-T\Delta S_f$ at 332 K (the melting temperature of **16/19-00**), with the indicated standard errors.

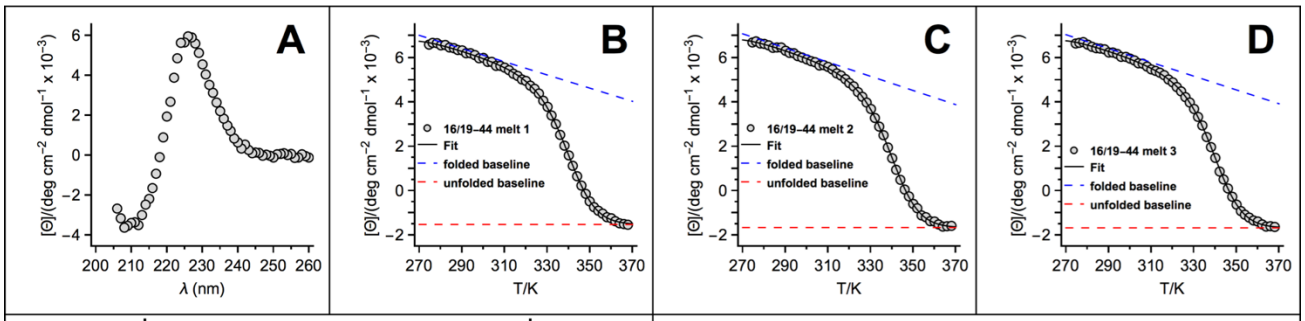


| Parameters | Values | Units | P–Values |
|---|---|---|---|
| $\Delta H_0$ | −32.7 ± 0.3 | kcal/mol | <0.001 |
| $T_m$ | 66.5 ± 0.1 | °C | <0.001 |
| $\Delta C_p$ | −0.63 ± 0.02 | kcal/mol/K | <0.001 |
| a1 | 15.0 ± 0.3 | deg cm$^2$ dmol$^{-1}$ x 10$^{-3}$ | <0.001 |
| b1 | −0.0298 ± 0.0009 | deg cm$^2$ dmol$^{-1}$ K$^{-1}$ x 10$^{-3}$ | <0.001 |
| c1 | −1.52 ± 0.02 | deg cm$^2$ dmol$^{-1}$ x 10$^{-3}$ | <0.001 |
| d1 | --- | --- | --- |
| a2 | 15.7 ± 0.3 | deg cm$^{-2}$ dmol$^{-1}$ x 10$^{-3}$ | <0.001 |
| b2 | −0.0319 ± 0.0009 | deg cm$^{-2}$ dmol$^{-1}$ K$^{-1}$ x 10$^{-3}$ | <0.001 |
| c2 | −1.66 ± 0.02 | deg cm$^{-2}$ dmol$^{-1}$ x 10$^{-3}$ | <0.001 |
| d2 | --- | --- | --- |
| a3 | 15.4 ± 0.3 | deg cm$^2$ dmol$^{-1}$ x 10$^{-3}$ | <0.001 |
| b3 | −0.0311 ± 0.0009 | deg cm$^2$ dmol$^{-1}$ K$^{-1}$ x 10$^{-3}$ | <0.001 |
| c3 | −1.68 ± 0.02 | deg cm$^{-2}$ dmol$^{-1}$ x 10$^{-3}$ | <0.001 |
| d3 | --- | --- | --- |

$R^2 = 0.9999$
sum residuals$^2$ = 0.2086

For **16/19–44**, when T = 332.02 K,
$\Delta G_f$ = −0.68 ± 0.01 kcal/mol
$\Delta H_f$ = −27.8 ± 0.4 kcal/mol
$-T\Delta S_f$ = 27.2 ± 0.4 kcal/mol

**Figure S15**. (A) CD spectra and (B–D) variable temperature CD data (triplicate) for 50 μM solutions of WW variants **16/19-44** in 20 mM sodium phosphate, pH 7. Fit parameters from equations S1–S3 appear in the table, as do calculated values for $\Delta G_f$, $\Delta H_f$, and $-T\Delta S_f$ at 332 K (the melting temperature of **16/19-00**), with the indicated standard errors.

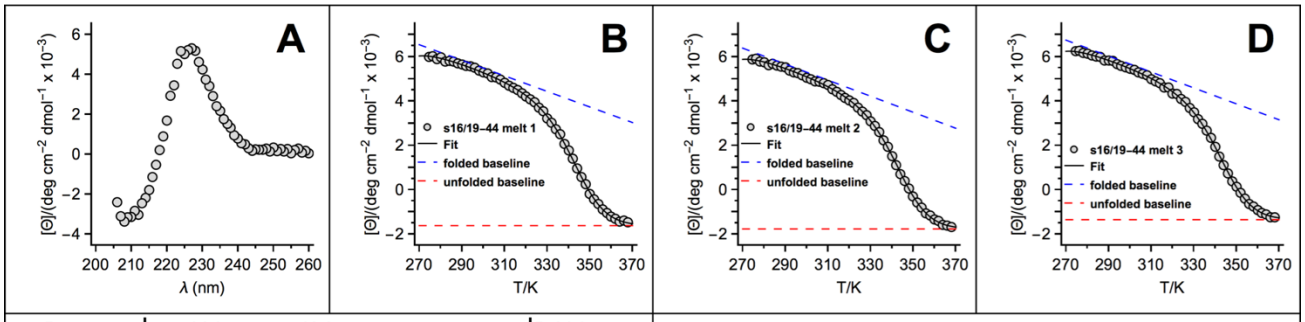


| Parameters | Values | Units | P–Values |
|---|---|---|---|
| $\Delta H_0$ | −29.5 ± 0.4 | kcal/mol | <0.001 |
| $T_m$ | 69.8 ± 0.1 | °C | <0.001 |
| $\Delta C_p$ | −0.58 ± 0.02 | kcal/mol/K | <0.001 |
| a1 | 16.0 ± 0.3 | deg cm$^2$ dmol$^{-1}$ x 10$^{-3}$ | <0.001 |
| b1 | −0.0351 ± 0.0010 | deg cm$^2$ dmol$^{-1}$ K$^{-1}$ x 10$^{-3}$ | <0.001 |
| c1 | −1.62 ± 0.02 | deg cm$^2$ dmol$^{-1}$ x 10$^{-3}$ | <0.001 |
| d1 | --- | --- | --- |
| a2 | 16.1 ± 0.3 | deg cm$^{-2}$ dmol$^{-1}$ x 10$^{-3}$ | <0.001 |
| b2 | −0.0361 ± 0.0010 | deg cm$^{-2}$ dmol$^{-1}$ K$^{-1}$ x 10$^{-3}$ | <0.001 |
| c2 | −1.77 ± 0.02 | deg cm$^{-2}$ dmol$^{-1}$ x 10$^{-3}$ | <0.001 |
| d2 | --- | --- | --- |
| a3 | 16.4 ± 0.3 | deg cm$^2$ dmol$^{-1}$ x 10$^{-3}$ | <0.001 |
| b3 | −0.0359 ± 0.0010 | deg cm$^2$ dmol$^{-1}$ K$^{-1}$ x 10$^{-3}$ | <0.001 |
| c3 | −1.35 ± 0.02 | deg cm$^{-2}$ dmol$^{-1}$ x 10$^{-3}$ | <0.001 |
| d3 | --- | --- | --- |

$R^2$ = 0.9999
sum residuals$^2$ = 0.2081

For **s16/19–44**, when T = 332.02 K,
$\Delta G_f$ = −0.84 ± 0.02 kcal/mol
$\Delta H_f$ = −23.3 ± 0.5 kcal/mol
$-T\Delta S_f$ = 22.4 ± 0.4 kcal/mol

**Figure S16**. (A) CD spectra and (B–D) variable temperature CD data (triplicate) for 50 μM solutions of WW variants **s16/19-44** in 20 mM sodium phosphate, pH 7. Fit parameters from equations S1–S3 appear in the table, as do calculated values for $\Delta G_f$, $\Delta H_f$, and $-T\Delta S_f$ at 332 K (the melting temperature of **16/19-00**), with the indicated standard errors.

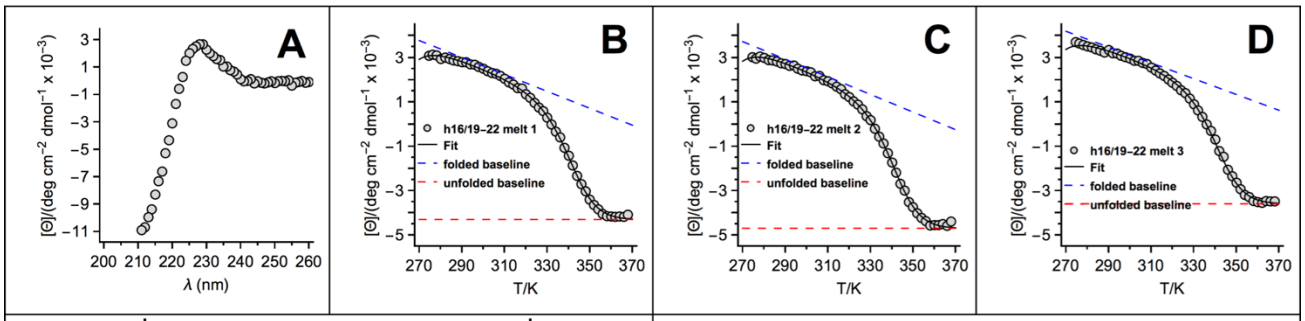


| Parameters | Values | Units | P–Values |
|---|---|---|---|
| $\Delta H_0$ | −33.8 ± 0.7 | kcal/mol | <0.001 |
| $T_m$ | 67.5 ± 0.2 | °C | <0.001 |
| $\Delta C_p$ | −0.74 ± 0.02 | kcal/mol/K | <0.001 |
| a1 | 14.1 ± 0.4 | deg cm$^2$ dmol$^{-1}$ x 10$^{-3}$ | <0.001 |
| b1 | −0.0382 ± 0.0014 | deg cm$^2$ dmol$^{-1}$ K$^{-1}$ x 10$^{-3}$ | <0.001 |
| c1 | −4.30 ± 0.03 | deg cm$^2$ dmol$^{-1}$ x 10$^{-3}$ | <0.001 |
| d1 | --- | --- | --- |
| a2 | 14.5 ± 0.4 | deg cm$^{-2}$ dmol$^{-1}$ x 10$^{-3}$ | <0.001 |
| b2 | −0.0398 ± 0.0015 | deg cm$^{-2}$ dmol$^{-1}$ K$^{-1}$ x 10$^{-3}$ | <0.001 |
| c2 | −4.70 ± 0.03 | deg cm$^{-2}$ dmol$^{-1}$ x 10$^{-3}$ | <0.001 |
| d2 | --- | --- | --- |
| a3 | 13.8 ± 0.4 | deg cm$^2$ dmol$^{-1}$ x 10$^{-3}$ | <0.001 |
| b3 | −0.0356 ± 0.0014 | deg cm$^2$ dmol$^{-1}$ K$^{-1}$ x 10$^{-3}$ | <0.001 |
| c3 | −3.59 ± 0.03 | deg cm$^{-2}$ dmol$^{-1}$ x 10$^{-3}$ | <0.001 |
| d3 | --- | --- | --- |

$R^2$ = 0.9994
sum residuals$^2$ = 0.6169

For **h16/19–22**, when T = 332.02 K,
$\Delta G_f$ = −0.78 ± 0.02 kcal/mol
$\Delta H_f$ = −27.4 ± 0.8 kcal/mol
$-T\Delta S_f$ = 26.6 ± 0.8 kcal/mol

**Figure S17**. (A) CD spectra and (B–D) variable temperature CD data (triplicate) for 50 μM solutions of WW variants **h16/19-22** in 20 mM sodium phosphate, pH 7. Fit parameters from equations S1–S3 appear in the table, as do calculated values for $\Delta G_f$, $\Delta H_f$, and $-T\Delta S_f$ at 332 K (the melting temperature of **16/19-00**), with the indicated standard errors.

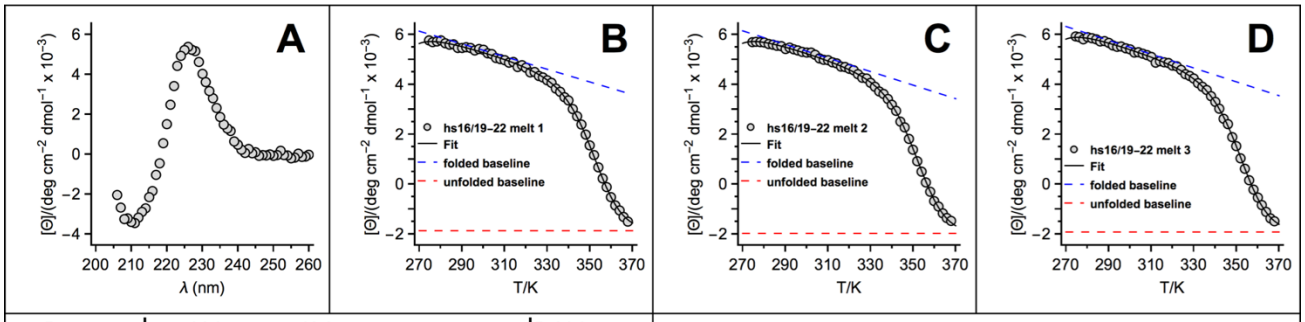


| Parameters | Values | Units | P–Values |
|---|---|---|---|
| $\Delta H_0$ | −34.9 ± 0.6 | kcal/mol | <0.001 |
| $T_m$ | 78.9 ± 0.1 | °C | <0.001 |
| $\Delta C_p$ | −0.64 ± 0.02 | kcal/mol/K | <0.001 |
| a1 | 13.0 ± 0.2 | deg cm$^2$ dmol$^{-1}$ x 10$^{-3}$ | <0.001 |
| b1 | −0.0254 ± 0.0007 | deg cm$^2$ dmol$^{-1}$ K$^{-1}$ x 10$^{-3}$ | <0.001 |
| c1 | −1.87 ± 0.04 | deg cm$^2$ dmol$^{-1}$ x 10$^{-3}$ | <0.001 |
| d1 | --- | --- | --- |
| a2 | 13.5 ± 0.2 | deg cm$^{-2}$ dmol$^{-1}$ x 10$^{-3}$ | <0.001 |
| b2 | −0.0272 ± 0.0007 | deg cm$^{-2}$ dmol$^{-1}$ K$^{-1}$ x 10$^{-3}$ | <0.001 |
| c2 | −1.98 ± 0.04 | deg cm$^{-2}$ dmol$^{-1}$ x 10$^{-3}$ | <0.001 |
| d2 | --- | --- | --- |
| a3 | 13.8 ± 0.2 | deg cm$^2$ dmol$^{-1}$ x 10$^{-3}$ | <0.001 |
| b3 | −0.0277 ± 0.0007 | deg cm$^2$ dmol$^{-1}$ K$^{-1}$ x 10$^{-3}$ | <0.001 |
| c3 | −1.92 ± 0.04 | deg cm$^{-2}$ dmol$^{-1}$ x 10$^{-3}$ | <0.001 |
| d3 | --- | --- | --- |

$R^2 = 0.9999$
sum residuals$^2$ = 0.2730

For **hs16/19–22**, when T = 332.02 K,
$\Delta G_f$ = −1.61 ± 0.03 kcal/mol
$\Delta H_f$ = −22.0 ± 0.7 kcal/mol
$-T\Delta S_f$ = 20.4 ± 0.6 kcal/mol

**Figure S18**. (A) CD spectra and (B–D) variable temperature CD data (triplicate) for 50 μM solutions of WW variants **hs16/19-22** in 20 mM sodium phosphate, pH 7. Fit parameters from equations S1–S3 appear in the table, as do calculated values for $\Delta G_f$, $\Delta H_f$, and $-T\Delta S_f$ at 332 K (the melting temperature of **16/19-00**), with the indicated standard errors.

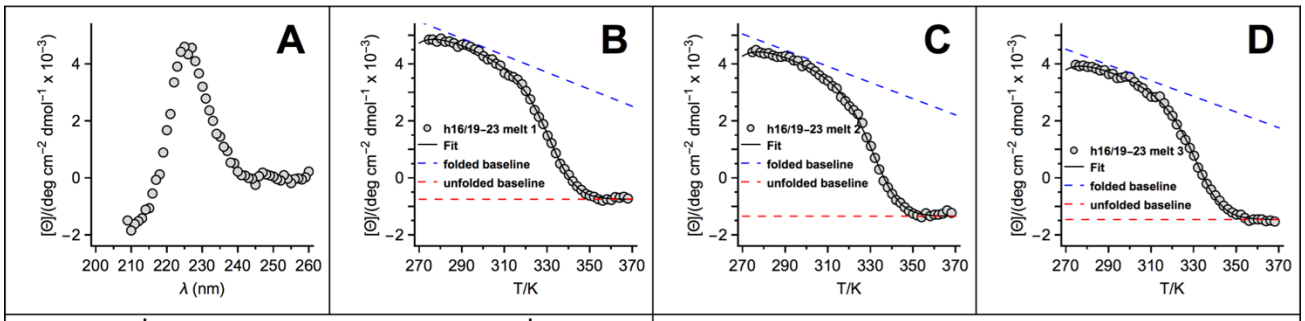


| Parameters | Values | Units | P–Values |
|---|---|---|---|
| $\Delta H_0$ | −30.5 ± 0.8 | kcal/mol | <0.001 |
| $T_m$ | 57.4 ± 0.3 | °C | <0.001 |
| $\Delta C_p$ | −0.76 ± 0.03 | kcal/mol/K | <0.001 |
| a1 | 13.5 ± 0.7 | deg cm$^2$ dmol$^{-1}$ x 10$^{-3}$ | <0.001 |
| b1 | −0.0298 ± 0.0023 | deg cm$^2$ dmol$^{-1}$ K$^{-1}$ x 10$^{-3}$ | <0.001 |
| c1 | −0.75 ± 0.02 | deg cm$^2$ dmol$^{-1}$ x 10$^{-3}$ | <0.001 |
| d1 | --- | --- | --- |
| a2 | 12.7 ± 0.7 | deg cm$^{-2}$ dmol$^{-1}$ x 10$^{-3}$ | <0.001 |
| b2 | −0.0284 ± 0.0024 | deg cm$^{-2}$ dmol$^{-1}$ K$^{-1}$ x 10$^{-3}$ | <0.001 |
| c2 | −1.34 ± 0.02 | deg cm$^{-2}$ dmol$^{-1}$ x 10$^{-3}$ | <0.001 |
| d2 | --- | --- | --- |
| a3 | 12.0 ± 0.7 | deg cm$^2$ dmol$^{-1}$ x 10$^{-3}$ | <0.001 |
| b3 | −0.0276 ± 0.0022 | deg cm$^2$ dmol$^{-1}$ K$^{-1}$ x 10$^{-3}$ | <0.001 |
| c3 | −1.46 ± 0.02 | deg cm$^{-2}$ dmol$^{-1}$ x 10$^{-3}$ | <0.001 |
| d3 | --- | --- | --- |

$R^2 = 0.9995$
sum residuals$^2$ = 0.6167

For **h16/19–23**, when T = 332.02 K,
$\Delta G_f$ = 0.14 ± 0.03 kcal/mol
$\Delta H_f$ = −31.6 ± 0.9 kcal/mol
$-T\Delta S_f$ = 31.8 ± 0.9 kcal/mol

**Figure S19**. (A) CD spectra and (B–D) variable temperature CD data (triplicate) for 50 μM solutions of WW variants **h16/19-23** in 20 mM sodium phosphate, pH 7. Fit parameters from equations S1–S3 appear in the table, as do calculated values for $\Delta G_f$, $\Delta H_f$, and $-T\Delta S_f$ at 332 K (the melting temperature of **16/19-00**), with the indicated standard errors.

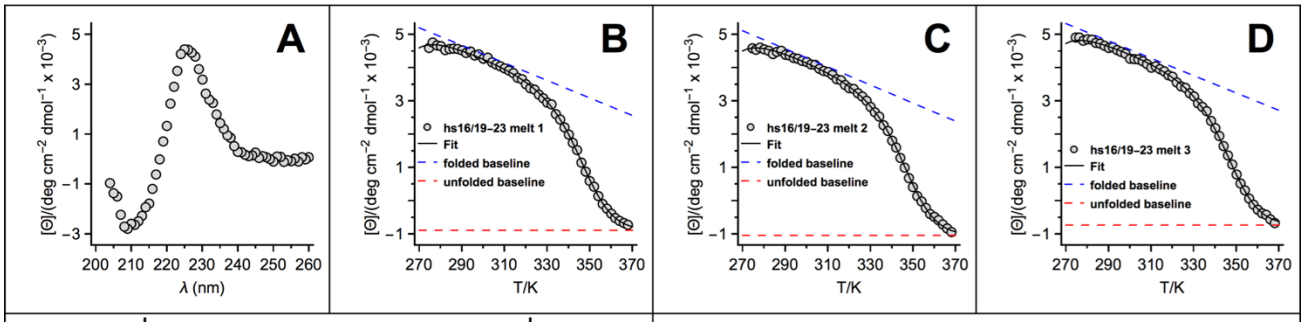


| Parameters | Values | Units | P–Values |
|---|---|---|---|
| $\Delta H_0$ | −30.1 ± 0.7 | kcal/mol | <0.001 |
| $T_m$ | 73.1 ± 0.2 | °C | <0.001 |
| $\Delta C_p$ | −0.60 ± 0.02 | kcal/mol/K | <0.001 |
| a1 | 12.3 ± 0.3 | deg cm$^2$ dmol$^{-1}$ x 10$^{-3}$ | <0.001 |
| b1 | −0.0264 ± 0.0010 | deg cm$^2$ dmol$^{-1}$ K$^{-1}$ x 10$^{-3}$ | <0.001 |
| c1 | −0.89 ± 0.03 | deg cm$^2$ dmol$^{-1}$ x 10$^{-3}$ | <0.001 |
| d1 | --- | --- | --- |
| a2 | 12.5 ± 0.3 | deg cm$^{-2}$ dmol$^{-1}$ x 10$^{-3}$ | <0.001 |
| b2 | −0.0272 ± 0.0010 | deg cm$^{-2}$ dmol$^{-1}$ K$^{-1}$ x 10$^{-3}$ | <0.001 |
| c2 | −1.04 ± 0.03 | deg cm$^{-2}$ dmol$^{-1}$ x 10$^{-3}$ | <0.001 |
| d2 | --- | --- | --- |
| a3 | 12.4 ± 0.3 | deg cm$^2$ dmol$^{-1}$ x 10$^{-3}$ | <0.001 |
| b3 | −0.0261 ± 0.0010 | deg cm$^2$ dmol$^{-1}$ K$^{-1}$ x 10$^{-3}$ | <0.001 |
| c3 | −0.73 ± 0.03 | deg cm$^{-2}$ dmol$^{-1}$ x 10$^{-3}$ | <0.001 |
| d3 | --- | --- | --- |

$R^2 = 0.9998$
sum residuals$^2$ = 0.2764

For **hs16/19–23**, when T = 332.02 K,
$\Delta G_f = -1.06 \pm 0.03$ kcal/mol
$\Delta H_f = -21.6 \pm 0.8$ kcal/mol
$-T\Delta S_f = 20.5 \pm 0.8$ kcal/mol

**Figure S20**. (A) CD spectra and (B–D) variable temperature CD data (triplicate) for 50 μM solutions of WW variants **hs16/19-23** in 20 mM sodium phosphate, pH 7. Fit parameters from equations S1–S3 appear in the table, as do calculated values for $\Delta G_f$, $\Delta H_f$, and $-T\Delta S_f$ at 332 K (the melting temperature of **16/19-00**), with the indicated standard errors.

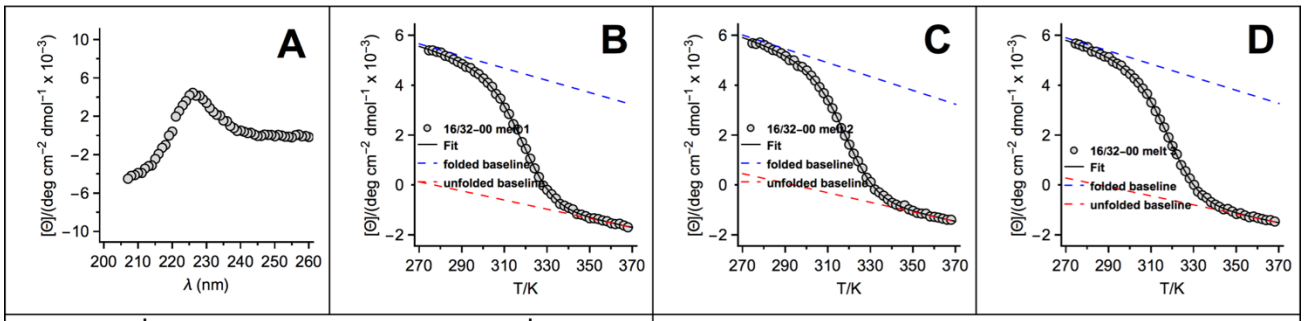


| Parameters | Values | Units | P–Values |
|---|---|---|---|
| $\Delta H_0$ | −25.4 ± 1.0 | kcal/mol | <0.001 |
| $T_m$ | 44.4 ± 0.6 | °C | <0.001 |
| $\Delta C_p$ | −0.44 ± 0.12 | kcal/mol/K | <0.001 |
| a1 | 12.2 ± 0.6 | deg cm$^2$ dmol$^{-1}$ x 10$^{-3}$ | <0.001 |
| b1 | −0.0244 ± 0.0023 | deg cm$^2$ dmol$^{-1}$ K$^{-1}$ x 10$^{-3}$ | <0.001 |
| c1 | 5.08 ± 0.50 | deg cm$^2$ dmol$^{-1}$ x 10$^{-3}$ | <0.001 |
| d1 | −0.0183 ± 0.0014 | deg cm$^2$ dmol$^{-1}$ K$^{-1}$ x 10$^{-3}$ | <0.001 |
| a2 | 13.5 ± 0.6 | deg cm$^{-2}$ dmol$^{-1}$ x 10$^{-3}$ | <0.001 |
| b2 | −0.0277 ± 0.0023 | deg cm$^{-2}$ dmol$^{-1}$ K$^{-1}$ x 10$^{-3}$ | <0.001 |
| c2 | 5.64 ± 0.49 | deg cm$^{-2}$ dmol$^{-1}$ x 10$^{-3}$ | <0.001 |
| d2 | −0.0192 ± 0.0014 | deg cm$^2$ dmol$^{-1}$ K$^{-1}$ x 10$^{-3}$ | <0.001 |
| a3 | 13.0 ± 0.6 | deg cm$^2$ dmol$^{-1}$ x 10$^{-3}$ | <0.001 |
| b3 | −0.0263 ± 0.0023 | deg cm$^2$ dmol$^{-1}$ K$^{-1}$ x 10$^{-3}$ | <0.001 |
| c3 | 5.14 ± 0.49 | deg cm$^{-2}$ dmol$^{-1}$ x 10$^{-3}$ | <0.001 |
| d3 | −0.0180 ± 0.0014 | deg cm$^2$ dmol$^{-1}$ K$^{-1}$ x 10$^{-3}$ | <0.001 |

$R^2 = 0.9999$
sum residuals$^2$ = 0.1657

For **16/32–00**, when T = 317.50 K,
$\Delta G_f = 0.00 \pm 0.05$ kcal/mol
$\Delta H_f = -25.4 \pm 1.0$ kcal/mol
$-T\Delta S_f = 25.4 \pm 1.0$ kcal/mol

**Figure S21**. (A) CD spectra and (B–D) variable temperature CD data (triplicate) for 50 μM solutions of WW variants **16/32-00** in 20 mM sodium phosphate, pH 7. Fit parameters from equations S1–S3 appear in the table, as do calculated values for $\Delta G_f$, $\Delta H_f$, and $-T\Delta S_f$ at 317.5 K (the melting temperature of **16/32-00**), with the indicated standard errors.

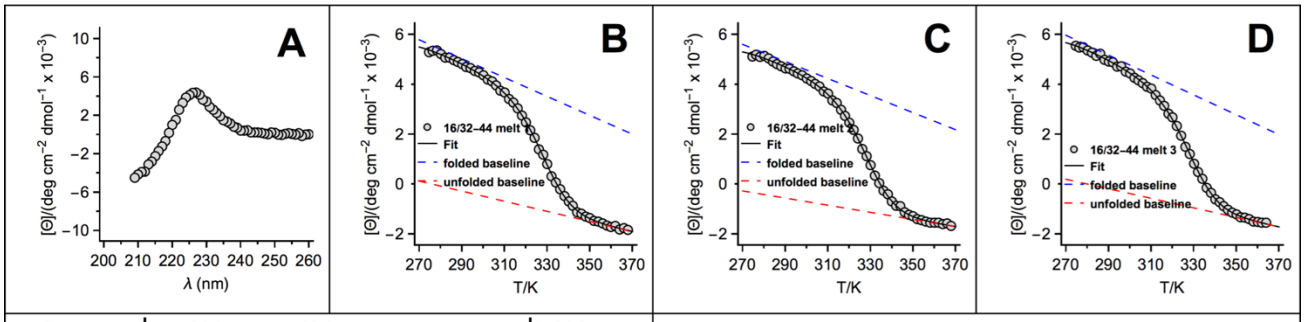


| Parameters | Values | Units | P–Values |
|---|---|---|---|
| $\Delta H_0$ | −28.4 ± 0.6 | kcal/mol | <0.001 |
| $T_m$ | 54.0 ± 0.2 | °C | <0.001 |
| $\Delta C_p$ | −0.64 ± 0.05 | kcal/mol/K | <0.001 |
| a1 | 16.0 ± 0.6 | deg cm$^2$ dmol$^{-1}$ x 10$^{-3}$ | <0.001 |
| b1 | −0.0378 ± 0.0021 | deg cm$^2$ dmol$^{-1}$ K$^{-1}$ x 10$^{-3}$ | <0.001 |
| c1 | 5.60 ± 0.71 | deg cm$^2$ dmol$^{-1}$ x 10$^{-3}$ | <0.001 |
| d1 | −0.0203 ± 0.0020 | deg cm$^2$ dmol$^{-1}$ K$^{-1}$ x 10$^{-3}$ | <0.001 |
| a2 | 14.8 ± 0.6 | deg cm$^{-2}$ dmol$^{-1}$ x 10$^{-3}$ | <0.001 |
| b2 | −0.0342 ± 0.0021 | deg cm$^{-2}$ dmol$^{-1}$ K$^{-1}$ x 10$^{-3}$ | <0.001 |
| c2 | 3.59 ± 0.72 | deg cm$^{-2}$ dmol$^{-1}$ x 10$^{-3}$ | <0.001 |
| d2 | −0.0143 ± 0.0020 | deg cm$^2$ dmol$^{-1}$ K$^{-1}$ x 10$^{-3}$ | <0.001 |
| a3 | 16.7 ± 0.6 | deg cm$^2$ dmol$^{-1}$ x 10$^{-3}$ | <0.001 |
| b3 | −0.0398 ± 0.0021 | deg cm$^2$ dmol$^{-1}$ K$^{-1}$ x 10$^{-3}$ | <0.001 |
| c3 | 5.36 ± 0.81 | deg cm$^{-2}$ dmol$^{-1}$ x 10$^{-3}$ | <0.001 |
| d3 | −0.0191 ± 0.0023 | deg cm$^2$ dmol$^{-1}$ K$^{-1}$ x 10$^{-3}$ | <0.001 |

$R^2$ = 0.9999
sum residuals$^2$ = 0.2261

For **16/32–44**, when T = 317.50 K,
$\Delta G_f$ = −0.74 ± 0.02 kcal/mol
$\Delta H_f$ = −22.2 ± 0.8 kcal/mol
$-T\Delta S_f$ = 22.5 ± 0.8 kcal/mol

**Figure S22**. (A) CD spectra and (B–D) variable temperature CD data (triplicate) for 50 μM solutions of WW variants **16/32-44** in 20 mM sodium phosphate, pH 7. Fit parameters from equations S1–S3 appear in the table, as do calculated values for $\Delta G_f$, $\Delta H_f$, and $-T\Delta S_f$ at 317.5 K (the melting temperature of **16/32-00**), with the indicated standard errors.

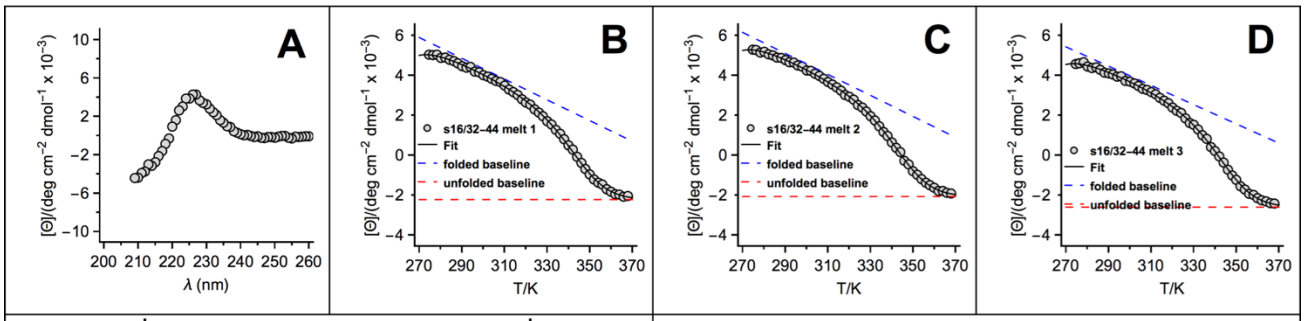


| Parameters | Values | Units | P–Values |
|---|---|---|---|
| $\Delta H_0$ | −26.2 ± 0.6 | kcal/mol | <0.001 |
| $T_m$ | 70.6 ± 0.3 | °C | <0.001 |
| $\Delta C_p$ | −0.53 ± 0.02 | kcal/mol/K | <0.001 |
| a1 | 20.0 ± 0.4 | deg cm$^2$ dmol$^{-1}$ x 10$^{-3}$ | <0.001 |
| b1 | −0.0521 ± 0.0013 | deg cm$^2$ dmol$^{-1}$ K$^{-1}$ x 10$^{-3}$ | <0.001 |
| c1 | −2.22 ± 0.03 | deg cm$^2$ dmol$^{-1}$ x 10$^{-3}$ | <0.001 |
| d1 | --- | --- | --- |
| a2 | 20.4 ± 0.4 | deg cm$^{-2}$ dmol$^{-1}$ x 10$^{-3}$ | <0.001 |
| b2 | −0.0526 ± 0.0013 | deg cm$^{-2}$ dmol$^{-1}$ K$^{-1}$ x 10$^{-3}$ | <0.001 |
| c2 | −2.07 ± 0.03 | deg cm$^{-2}$ dmol$^{-1}$ x 10$^{-3}$ | <0.001 |
| d2 | --- | --- | --- |
| a3 | 18.5 ± 0.4 | deg cm$^2$ dmol$^{-1}$ x 10$^{-3}$ | <0.001 |
| b3 | −0.0483 ± 0.0013 | deg cm$^2$ dmol$^{-1}$ K$^{-1}$ x 10$^{-3}$ | <0.001 |
| c3 | −2.60 ± 0.03 | deg cm$^{-2}$ dmol$^{-1}$ x 10$^{-3}$ | <0.001 |
| d3 | --- | --- | --- |

$R^2$ = 0.9998
sum residuals$^2$ = 0.2596

For **s16/32–44**, when T = 317.50 K,
$\Delta G_f$ = −1.46 ± 0.05 kcal/mol
$\Delta H_f$ = −12.4 ± 0.8 kcal/mol
$-T\Delta S_f$ = 10.9 ± 0.8 kcal/mol

**Figure S23**. (A) CD spectra and (B–D) variable temperature CD data (triplicate) for 50 μM solutions of WW variants **s16/32-44** in 20 mM sodium phosphate, pH 7. Fit parameters from equations S1–S3 appear in the table, as do calculated values for $\Delta G_f$, $\Delta H_f$, and $-T\Delta S_f$ at 317.5 K (the melting temperature of **16/32-00**), with the indicated standard errors.

## 4. ESI-TOF spectra data of WW variants

**Table S1. Summary of the mass spectrum data for the WW variants**

| Name | Molecular Formula | z | Expected [M+z·H]/z | Observed [M+z·H]/z |
|---|---|---|---|---|
| **16/19-00** | $C_{179}H_{270}N_{56}O_{50}S$ | 4 | 1010.009 | 1010.012 |
| **16/19-11** | $C_{189}H_{286}N_{56}O_{52}S$ | 4 | 1052.038 | 1052.034 |
| **s16/19-11** | $C_{187}H_{282}N_{56}O_{52}S$ | 4 | 1045.030 | 1045.037 |
| **16/19-12** | $C_{191}H_{290}N_{56}O_{53}S$ | 4 | 1063.044 | 1063.044 |
| **s16/19-12** | $C_{189}H_{286}N_{56}O_{53}S$ | 4 | 1056.036 | 1056.035 |
| **16/19-22** | $C_{193}H_{294}N_{56}O_{54}S$ | 4 | 1074.051 | 1074.050 |
| **s16/19-22** | $C_{191}H_{290}N_{56}O_{54}S$ | 4 | 1067.043 | 1067.039 |
| **16/19-23** | $C_{195}H_{298}N_{56}O_{55}S$ | 4 | 1085.057 | 1085.055 |
| **s16/19-23** | $C_{193}H_{294}N_{56}O_{55}S$ | 4 | 1078.049 | 1078.046 |
| **16/19-33** | $C_{197}H_{302}N_{56}O_{56}S$ | 4 | 1096.064 | 1096.058 |
| **s16/19-33** | $C_{195}H_{298}N_{56}O_{56}S$ | 4 | 1089.056 | 1089.049 |
| **16/19-34** | $C_{199}H_{306}N_{56}O_{57}S$ | 4 | 1107.070 | 1107.072 |
| **s16/19-34** | $C_{197}H_{302}N_{56}O_{57}S$ | 4 | 1100.062 | 1100.062 |
| **16/19-44** | $C_{201}H_{310}N_{56}O_{58}S$ | 4 | 1118.077 | 1118.070 |
| **s16/19-44** | $C_{199}H_{306}N_{56}O_{58}S$ | 4 | 1111.069 | 1111.061 |
| **h16/19-22** | $C_{197}H_{302}N_{56}O_{50}S$ | 4 | 1072.071 | 1072.072 |
| **hs16/19-22** | $C_{195}H_{298}N_{56}O_{50}S$ | 4 | 1065.064 | 1065.056 |
| **h16/19-23** | $C_{200}H_{308}N_{56}O_{50}S$ | 4 | 1082.583 | 1082.579 |
| **hs16/19-23** | $C_{198}H_{304}N_{56}O_{50}S$ | 4 | 1075.575 | 1075.572 |
| **16/32-00** | $C_{179}H_{270}N_{56}O_{50}S$ | 4 | 1010.009 | 1010.008 |
| **16/32-44** | $C_{201}H_{310}N_{56}O_{58}S$ | 4 | 1118.077 | 1118.072 |
| **s16/32-44** | $C_{199}H_{306}N_{56}O_{58}S$ | 4 | 1111.069 | 1111.068 |

ESI-TOF spectra for WW variant **16/19-00, 16/19-11, s16/19-11, 16/19-12, s16/19-12, 16/19-22, s16/19-22, 16/19-23, s16/19-23, 16/19-33, s16/19-33, 16/19-34, s16/19-34, 16/19-44, s16/19-44, h16/19-22, hs16/19-22, h16/19-23, hs16/19-23, 16/32-00, 16/32-44, s16/32-44** are shown in Figures S25–S46.

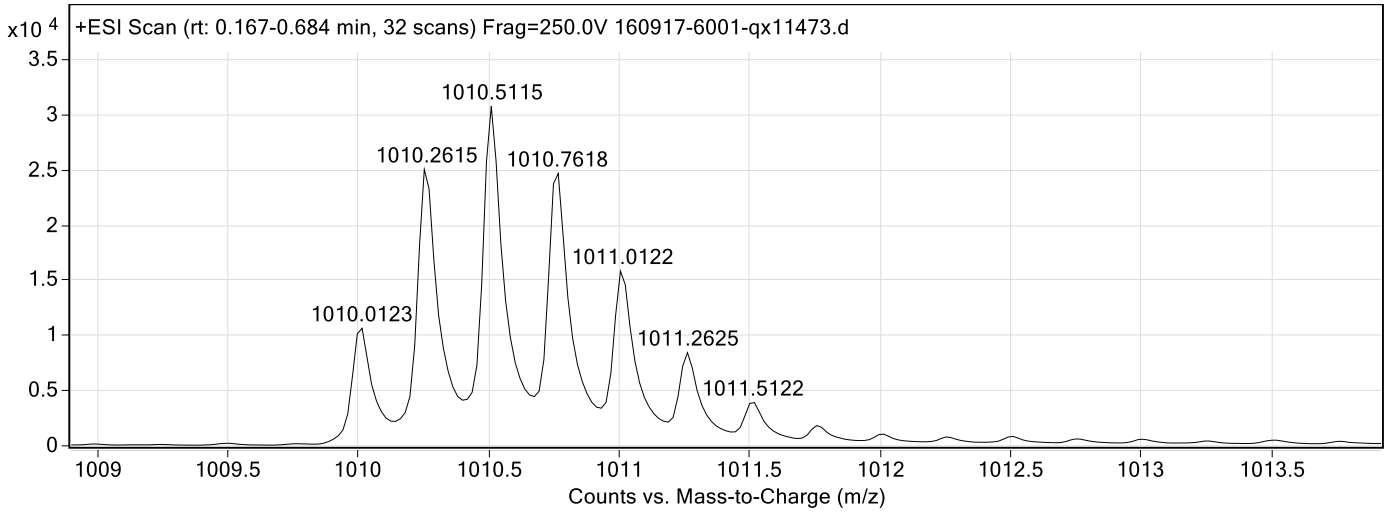


**Figure S24**. ESI-TOF spectrum for WW variant **16/19-00**. Expected $[M+4H^+]/4$ = 1010.009 Da. Obs'd $[M+4H^+]/4$ = 1010.012 Da.

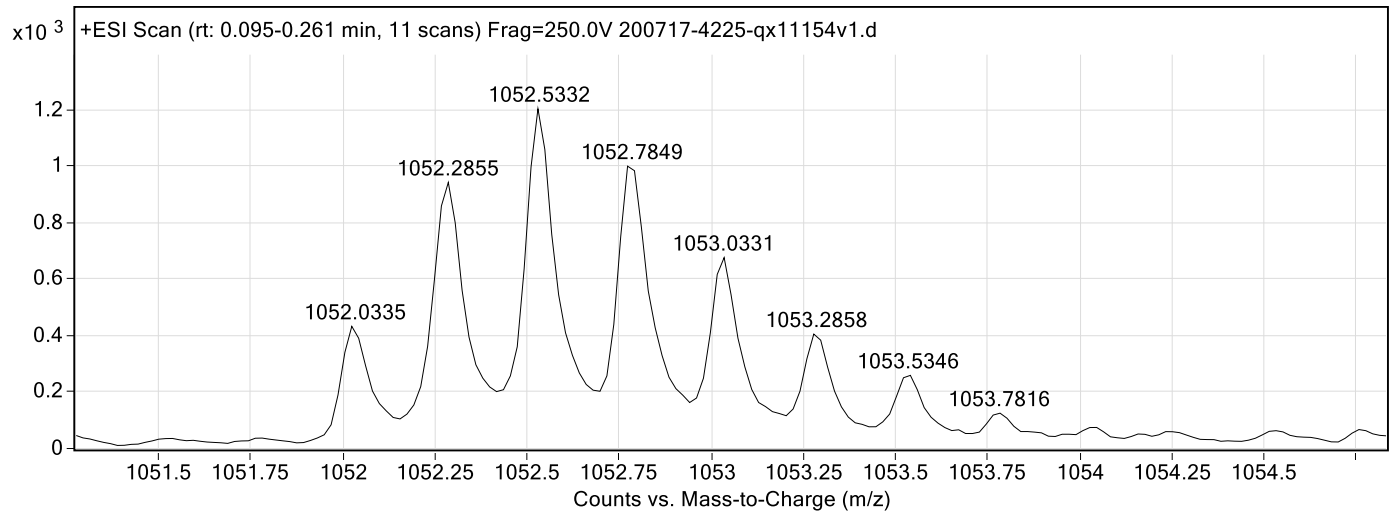


**Figure S25**. ESI-TOF spectrum for WW variant **16/19-11**. Expected [M+4H$^+$]/4 = 1052.038 Da. Obs'd [M+4H$^+$]/4 = 1052.034 Da.

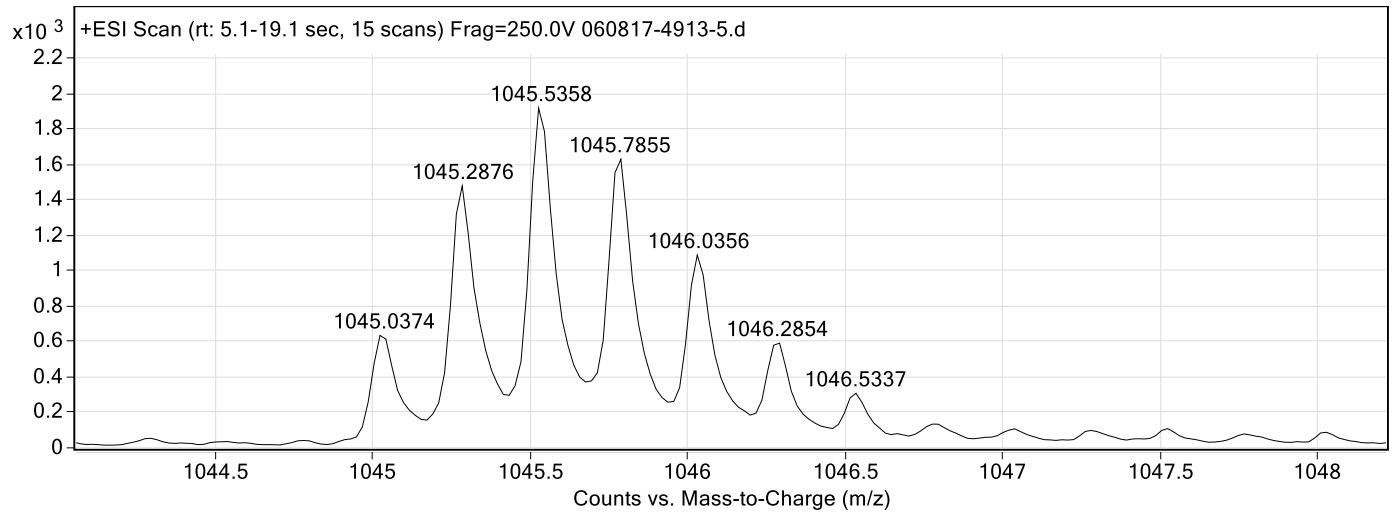


**Figure S26**. ESI-TOF spectrum for WW variant **s16/19-11**. Expected [M+4H$^+$]/4 = 1045.030 Da. Obs'd [M+4H$^+$]/4 = 1045.037 Da.

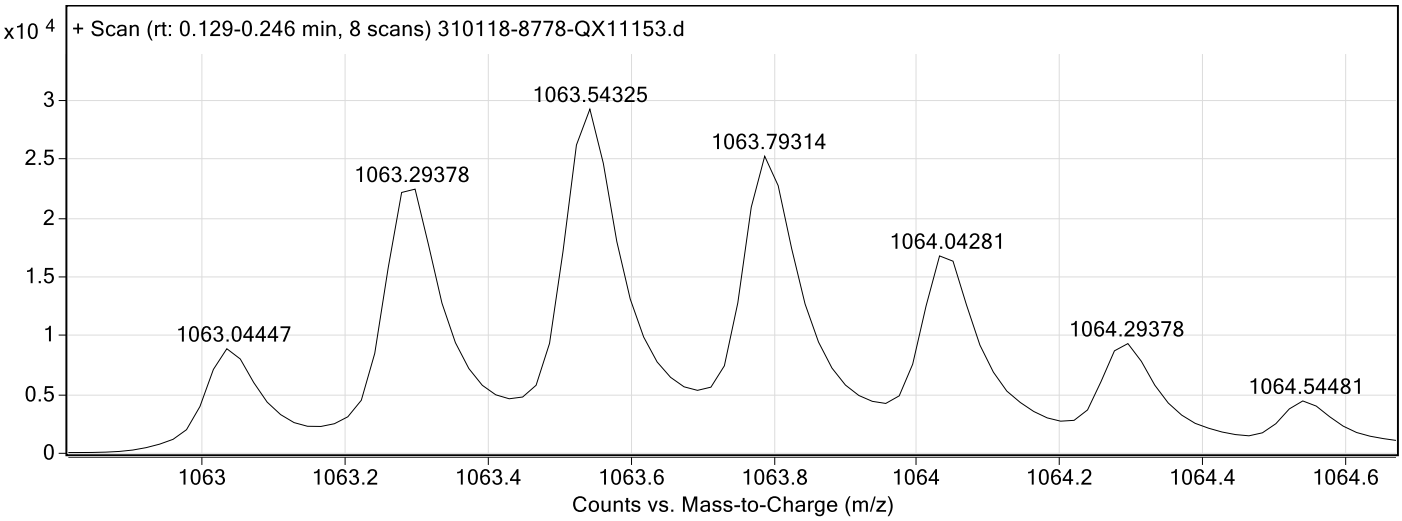


**Figure S27**. ESI-TOF spectrum for WW variant **16/19-12**. Expected [M+4H$^+$]/4 = 1063.044 Da. Obs'd [M+4H$^+$]/4 = 1063.044 Da.

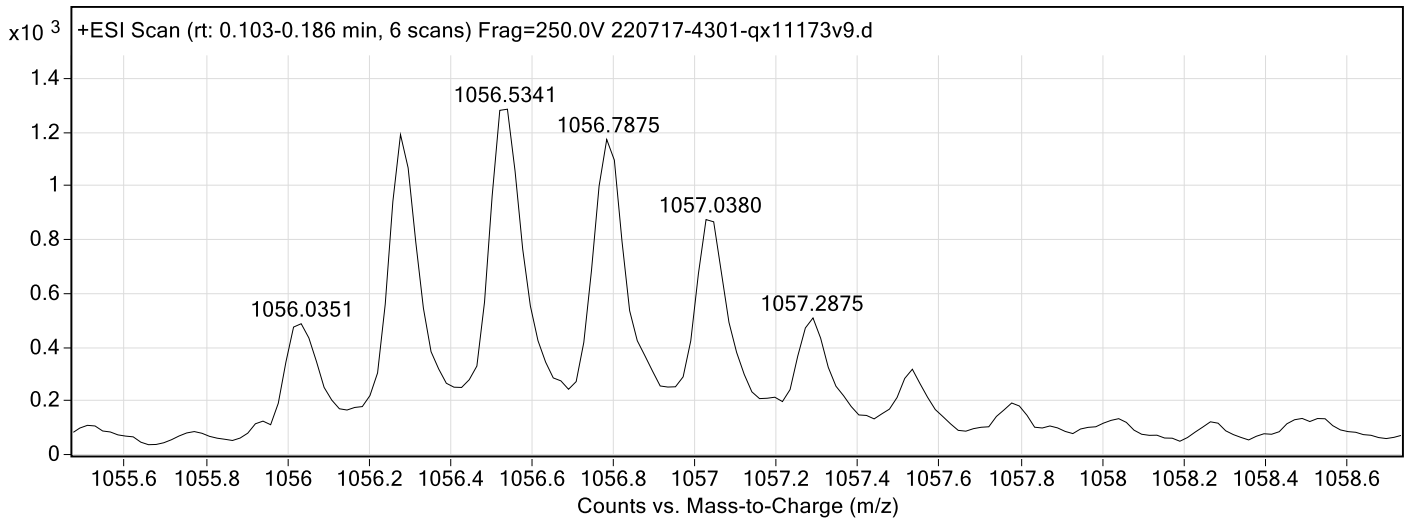


**Figure S28**. ESI-TOF spectrum for WW variant **s16/19-12**. Expected $[M+4H^+]/4$ = 1056.036 Da. Obs'd $[M+4H^+]/4$ = 1056.035 Da

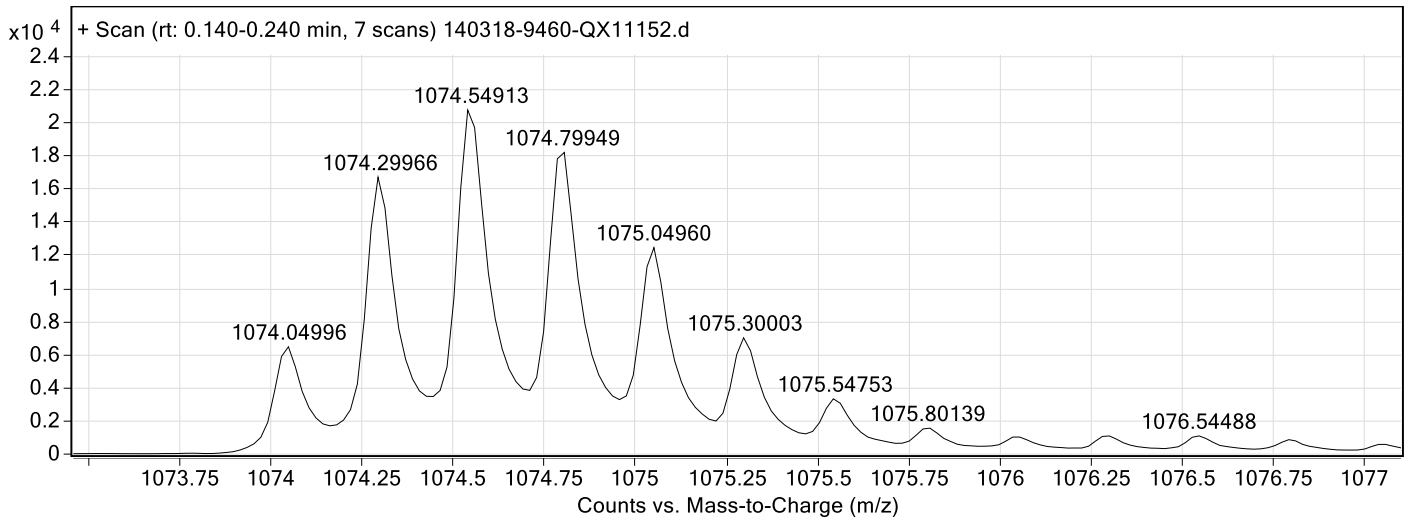


**Figure S29**. ESI-TOF spectrum for WW variant **16/19-22**. Expected $[M+4H^+]/4$ = 1074.051 Da. Obs'd $[M+4H^+]/4$ = 1074.050 Da.

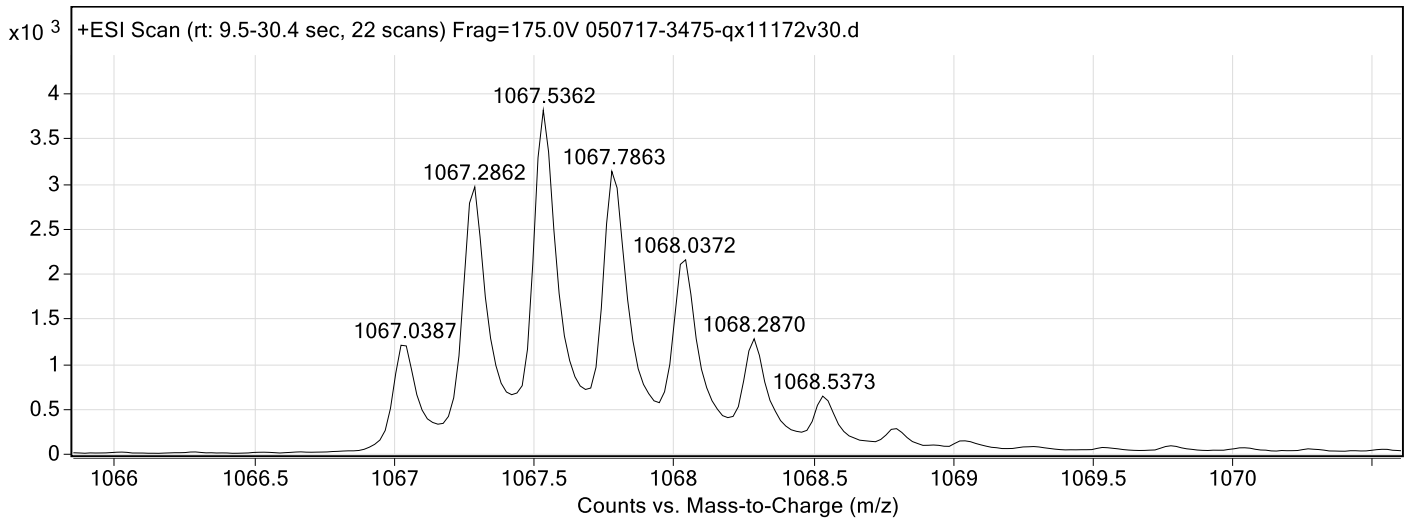


**Figure S30**. ESI-TOF spectrum for WW variant **s16/19-22**. Expected $[M+4H^+]/4$ = 1067.043 Da. Obs'd $[M+4H^+]/4$ = 1067.039 Da.

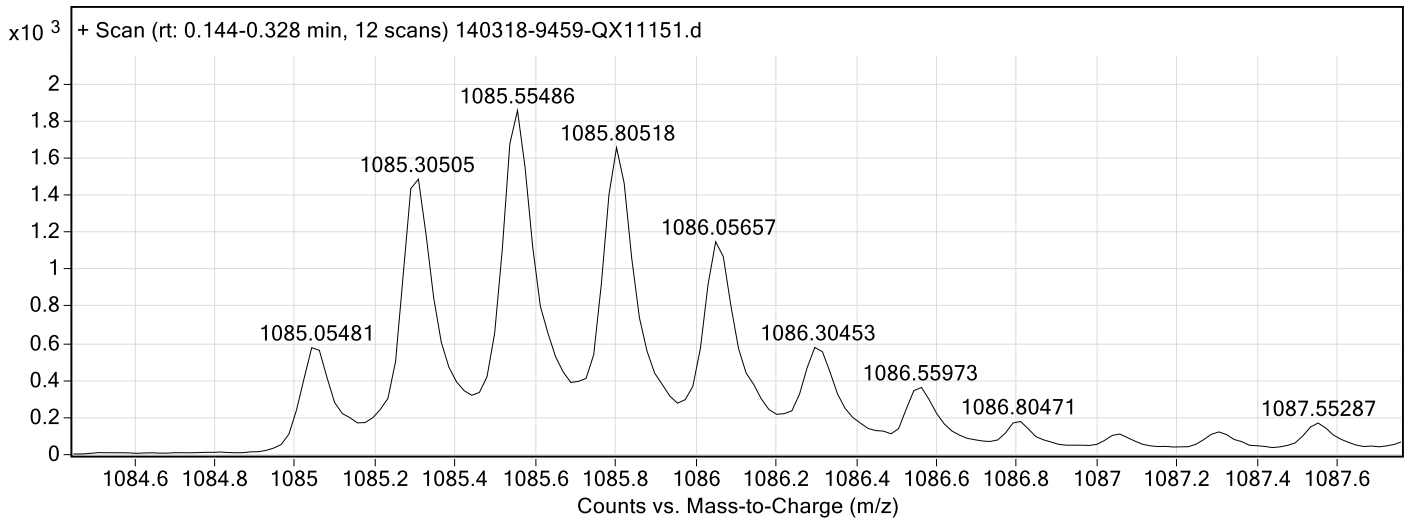


**Figure S31**. ESI-TOF spectrum for WW variant **16/19-23**. Expected [M+4H$^+$]/4 = 1085.057 Da. Obs'd [M+4H$^+$]/4 = 1085.055 Da.

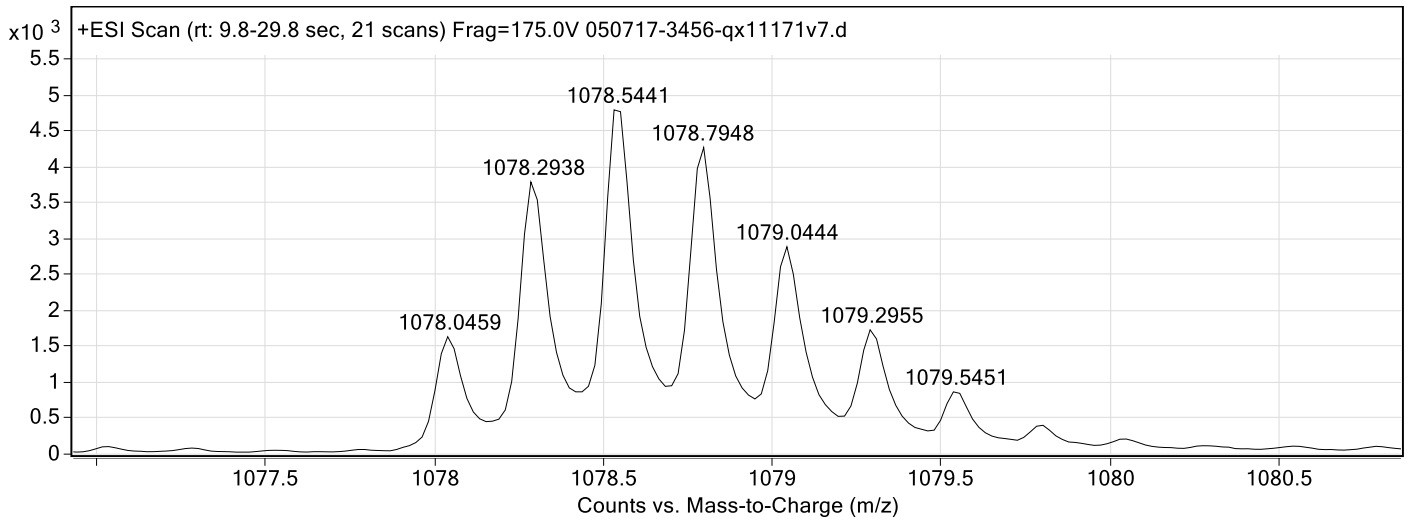


**Figure S32**. ESI-TOF spectrum for WW variant **s16/19-23**. Expected [M+4H$^+$]/4 = 1078.049 Da. Obs'd [M+4H$^+$]/4 = 1078.046 Da.

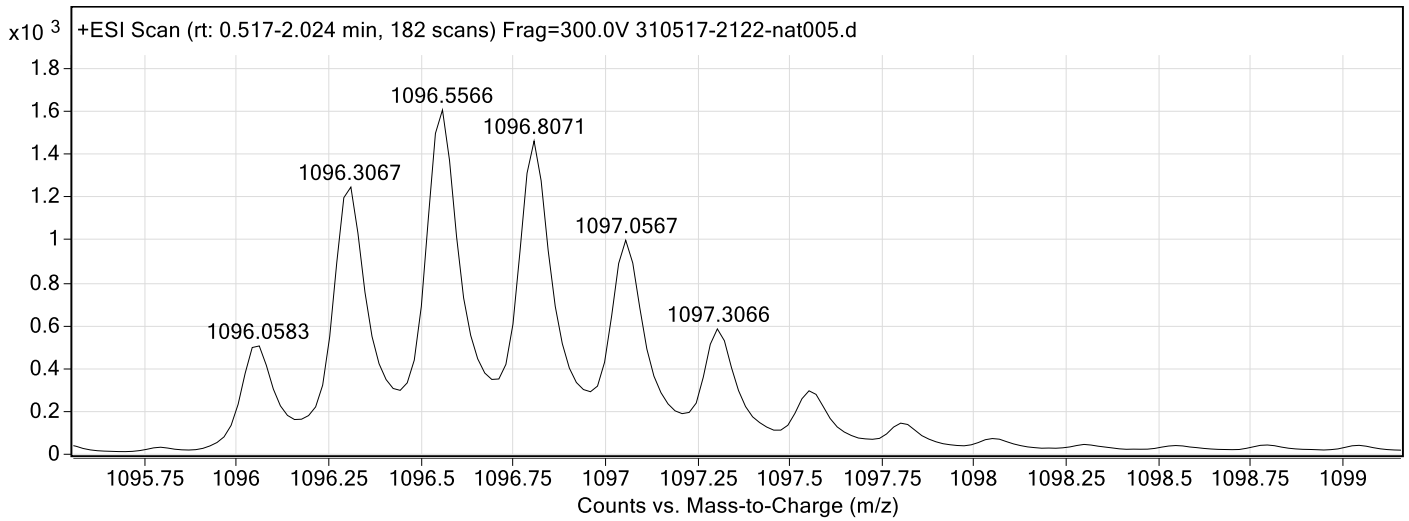


**Figure S33**. ESI-TOF spectrum for WW variant **16/19-33**. Expected [M+4H$^+$]/4 = 1096.064 Da. Obs'd [M+4H$^+$]/4 = 1096.058 Da.

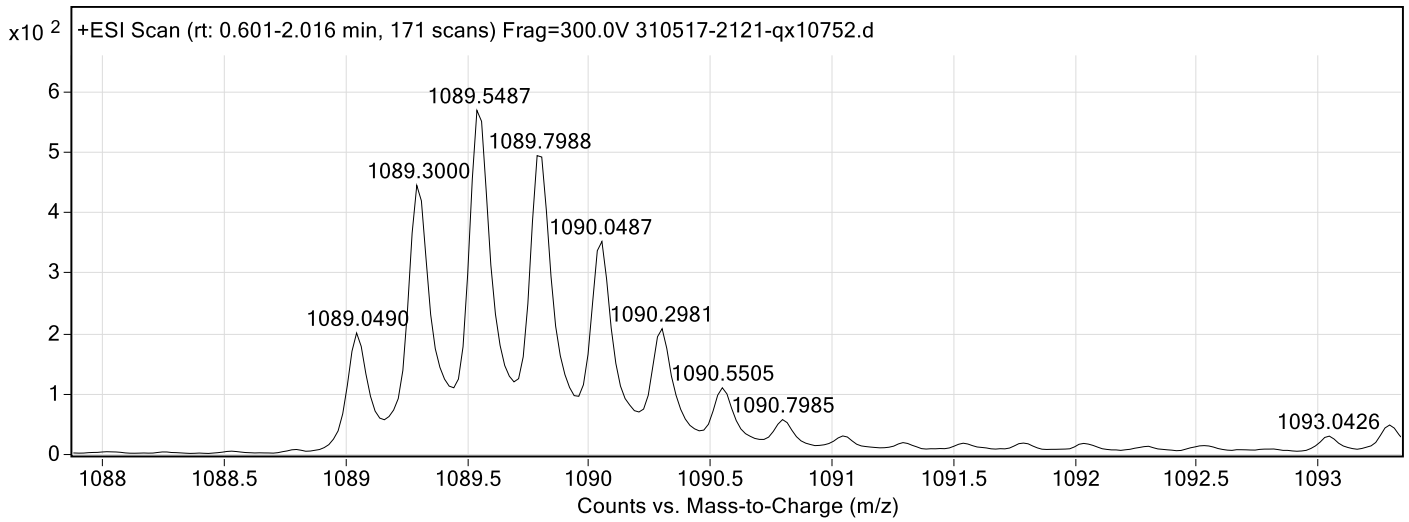


**Figure S34**. ESI-TOF spectrum for WW variant **s16/19-33**. Expected [M+4H$^+$]/4 = 1089.056 Da. Obs'd [M+4H$^+$]/4 = 1089.049 Da.

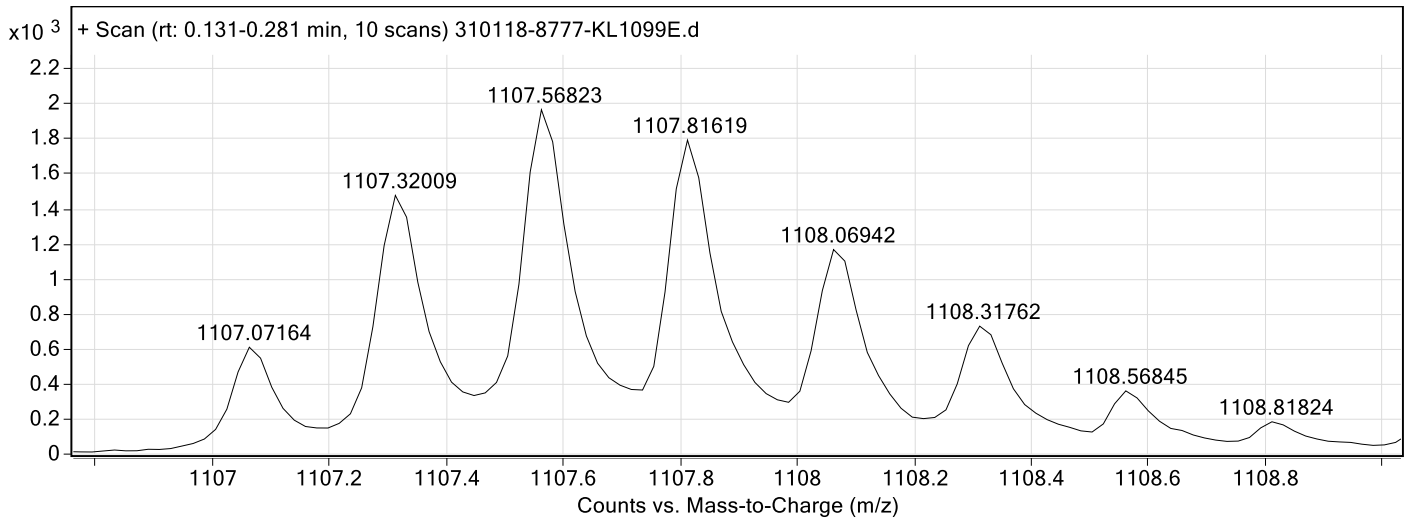


**Figure S35**. ESI-TOF spectrum for WW variant **16/19-34**. Expected [M+4H$^+$]/4 = 1107.070 Da. Obs'd [M+4H$^+$]/4 = 1107.072 Da.

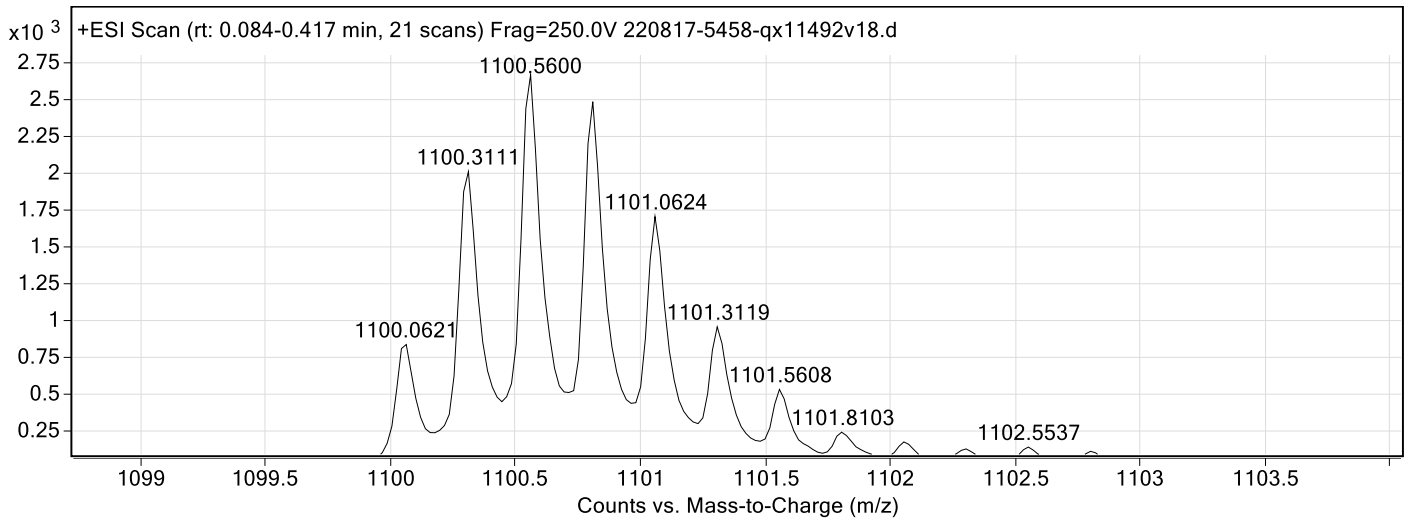


**Figure S36**. ESI-TOF spectrum for WW variant **s16/19-34**. Expected [M+4H$^+$]/4 = 1100.062 Da. Obs'd [M+4H$^+$]/4 = 1100.062 Da.

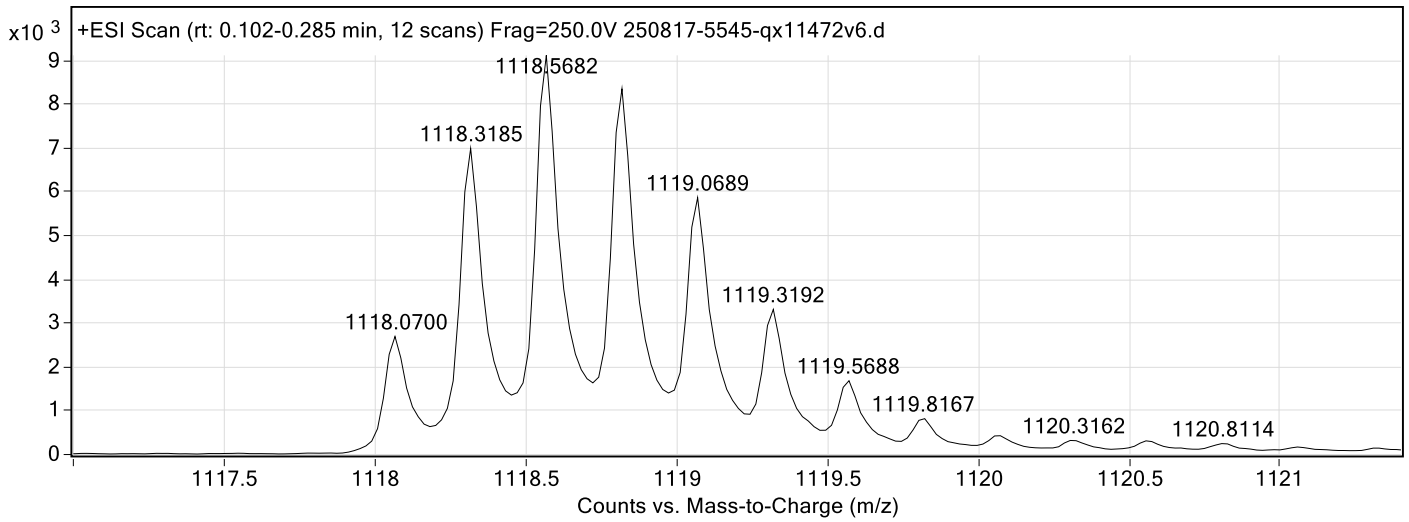


**Figure S37**. ESI-TOF spectrum for WW variant **16/19-44**. Expected [M+4H$^+$]/4 = 1118.077 Da. Observed [M+4H$^+$]/4 = 1118.070 Da.

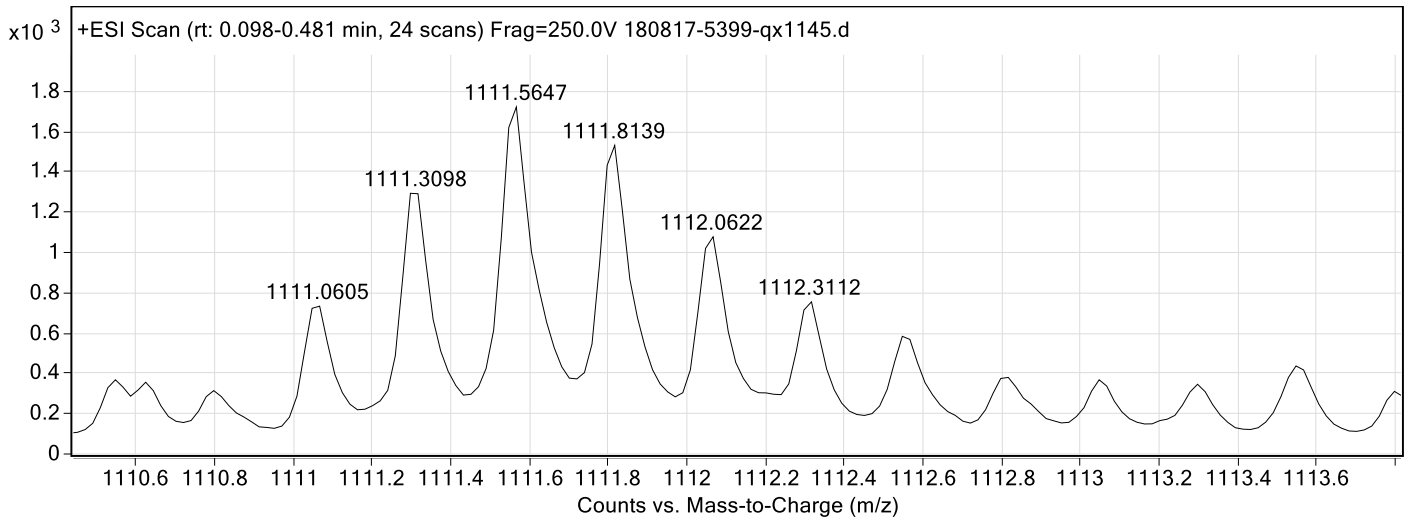


**Figure S38**. ESI-TOF spectrum for WW variant **s16/19-44**. Expected [M+4H$^+$]/4 = 1111.069 Da. Obs'd [M+4H$^+$]/4 = 1111.061 Da.

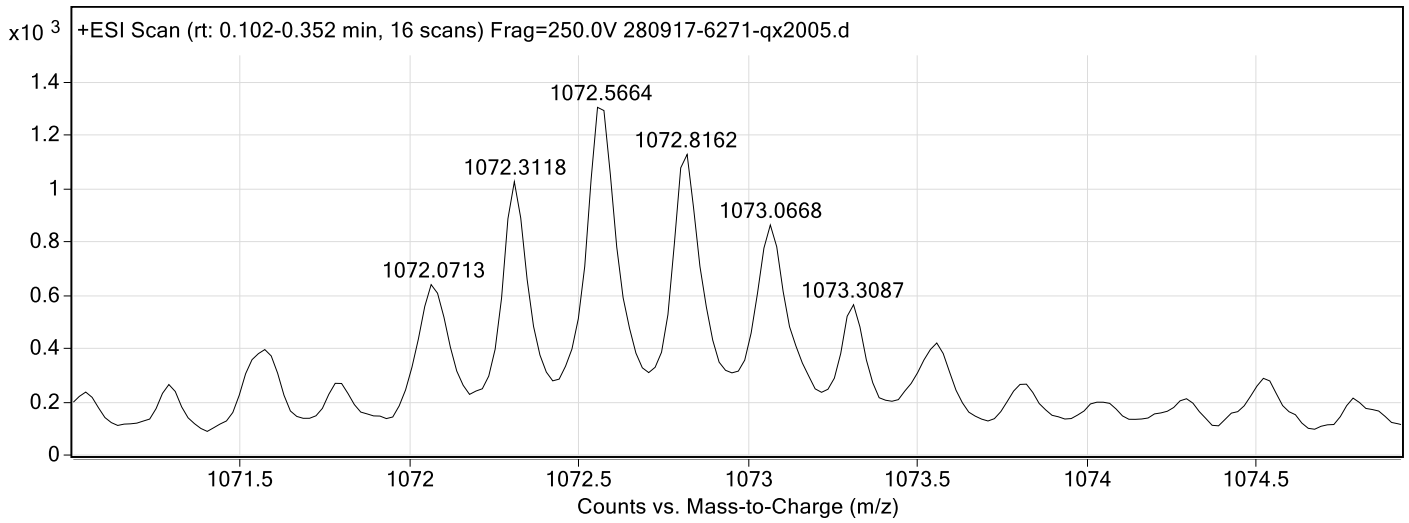


**Figure S39**. ESI-TOF spectrum for WW variant **h16/19-22**. Expected [M+4H$^+$]/4 = 1072.071 Da. Obs'd [M+4H$^+$]/4 = 1072.0718 Da.

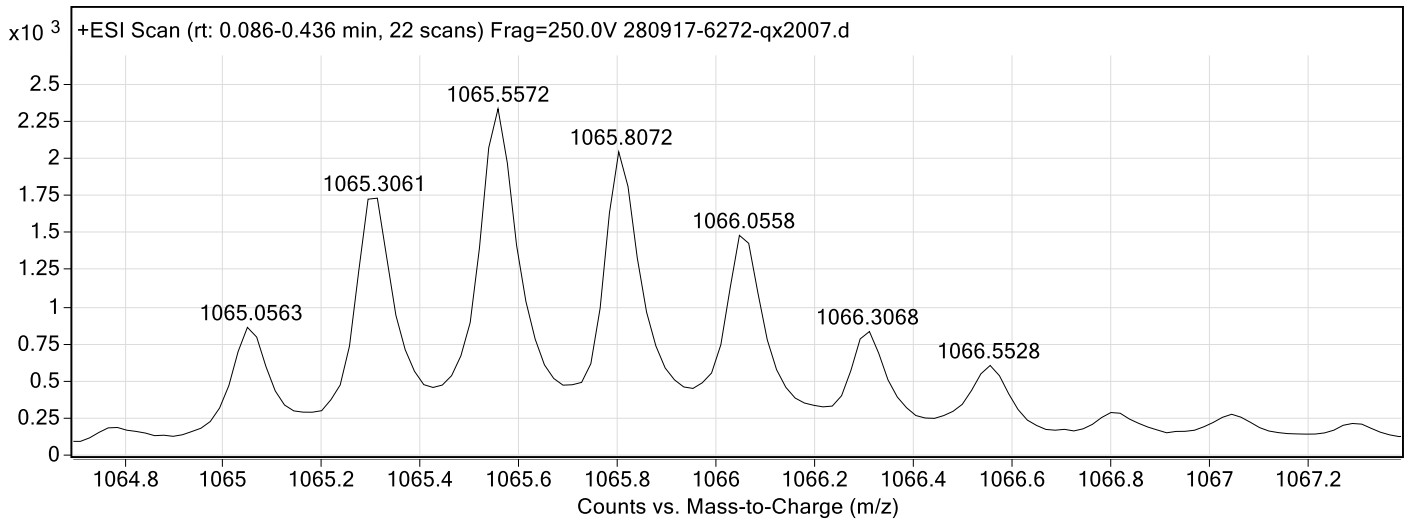


**Figure S40**. ESI-TOF spectrum for WW variant **hs16/19-22**. Expected [M+4H$^+$]/4 = 1065.064 Da. Obs'd [M+4H$^+$]/4 = 1065.056 Da.

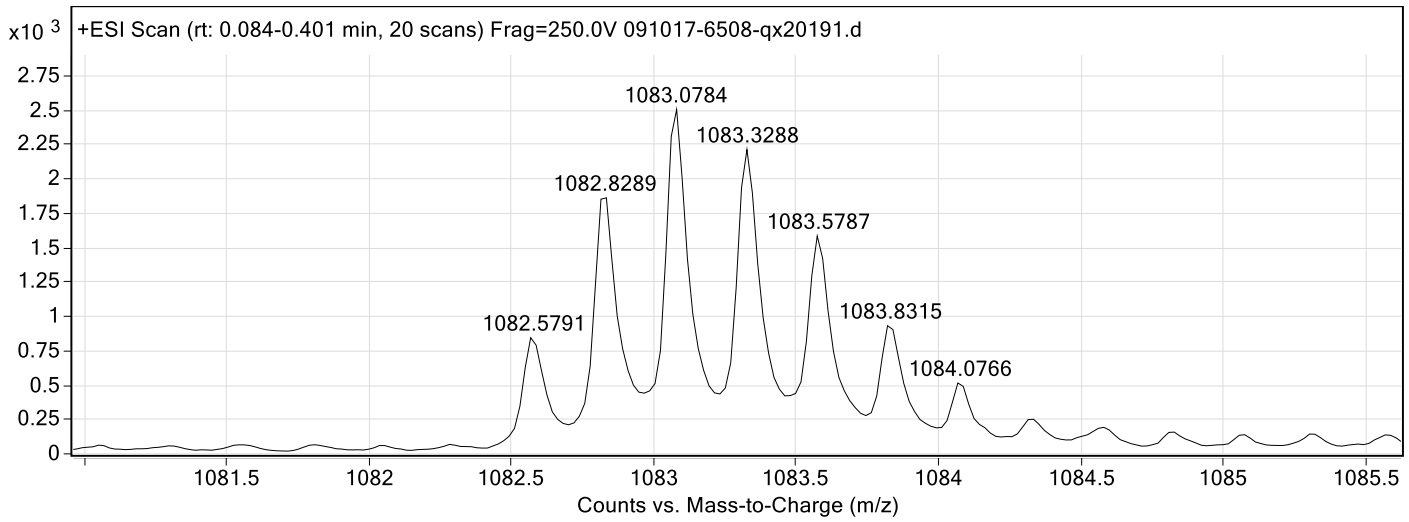


**Figure S41**. ESI-TOF spectrum for WW variant **h16/19-23**. Expected [M+4H$^+$]/4 = 1082.583 Da. Obs'd [M+4H$^+$]/4 = 1082.579 Da.

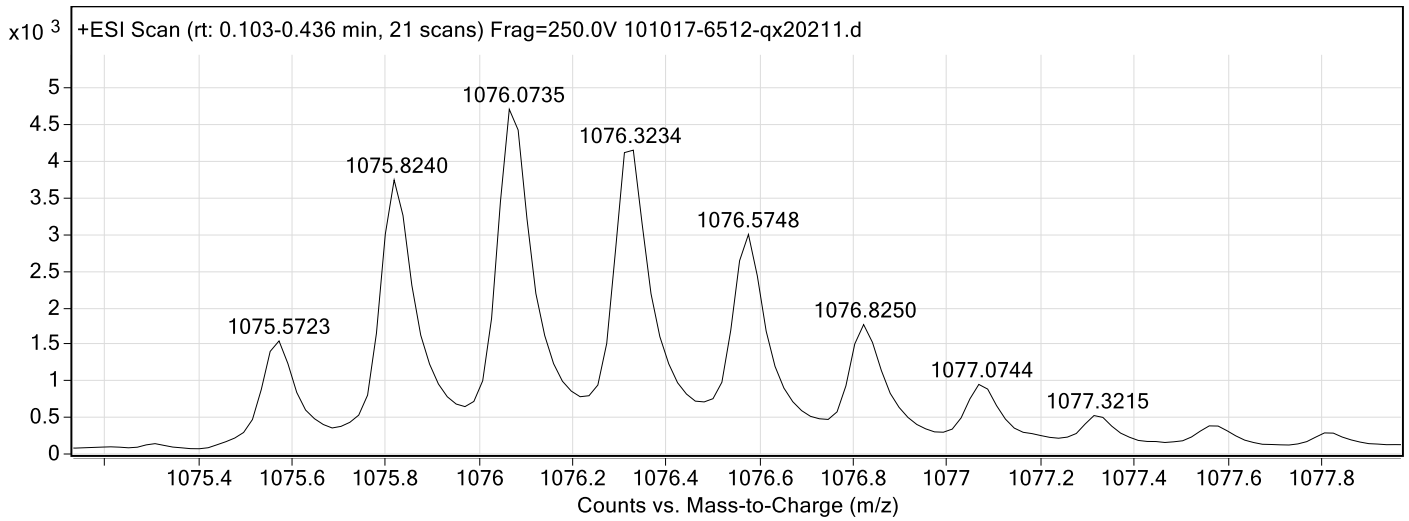


**Figure S42**. ESI-TOF spectrum for WW variant **hs16/19-23**. Expected [M+4H$^+$]/4 = 1075.575 Da. Obs'd [M+4H$^+$]/4 = 1075.572 Da.

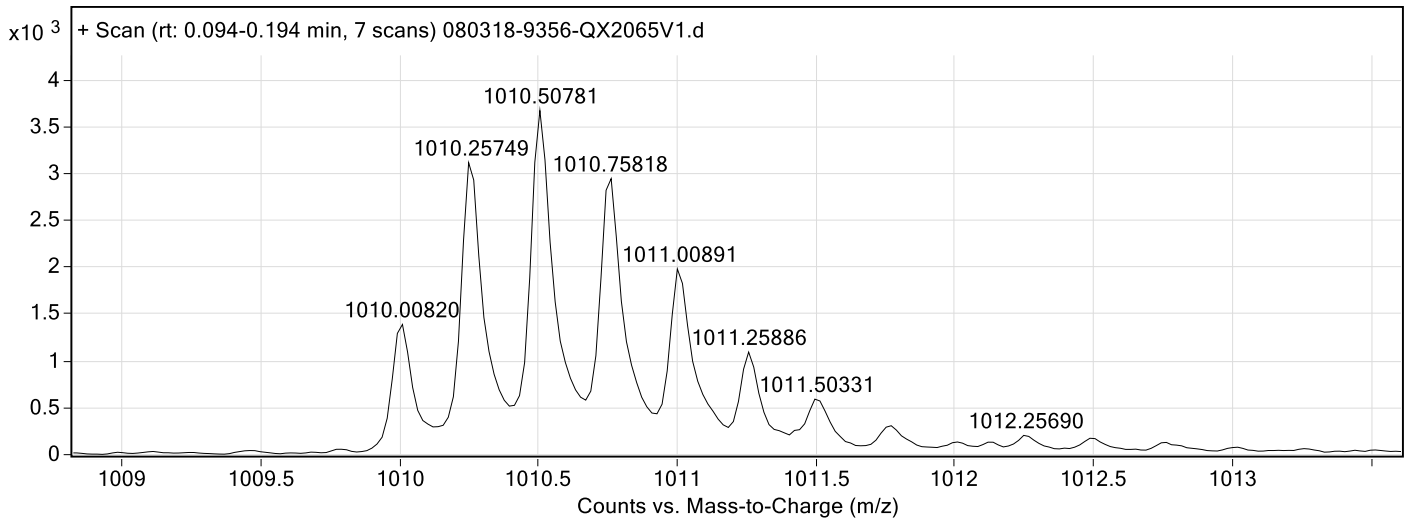


**Figure S43**. ESI-TOF spectrum for WW variant **16/32-00**. Expected $[M+4H^+]/4$ = 1010.009 Da. Obs'd $[M+4H]^+/4$ = 1010.008 Da.

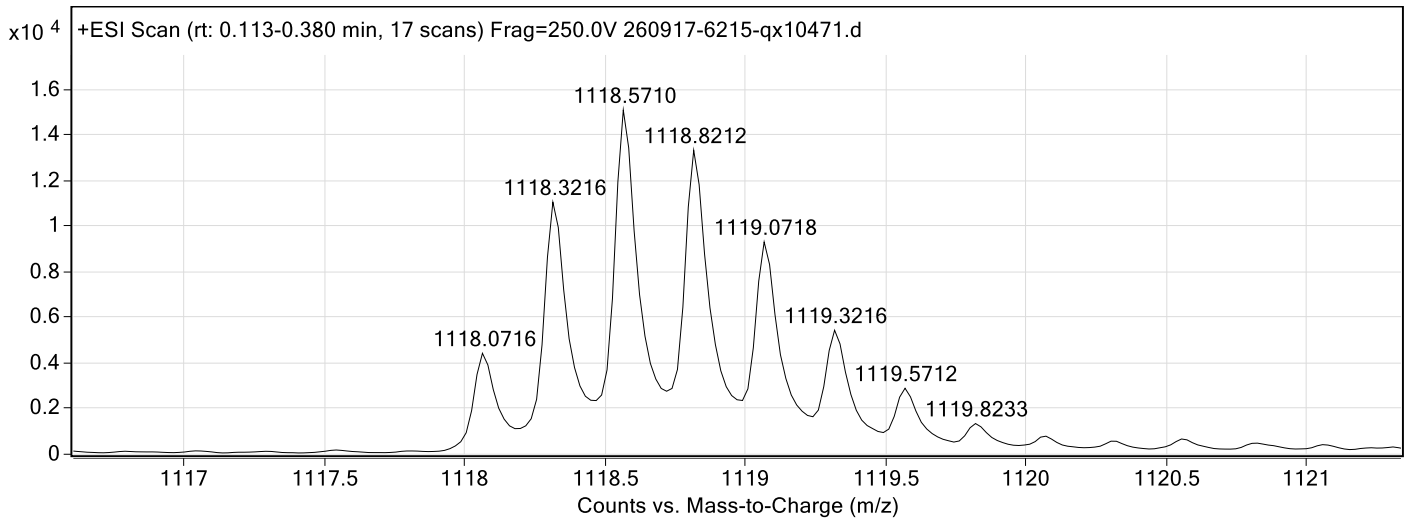


**Figure S44**. ESI-TOF spectrum for WW variant **16/32-44**. Expected $[M+4H^+]/4$ = 1118.077 Da. Obs'd $[M+4H^+]/4$ = 1118.072 Da.

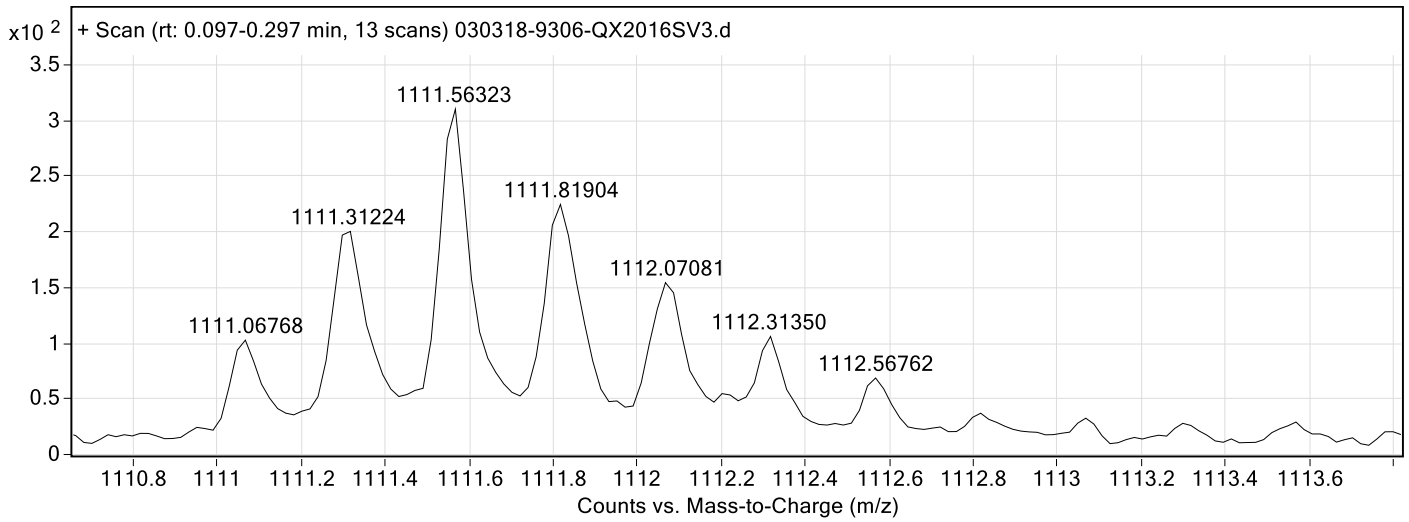


**Figure S45**. ESI-TOF spectrum for WW variant **s16/32-44**. Expected $[M+4H^+]/4$ = 1111.069 Da. Observed $[M+4H^+]/4$ = 1111.068 Da.

## 5. Analytical HPLC data

Analytical HPLC traces for WW variant **16/19-00, 16/19-11, s16/19-11, 16/19-12, s16/19-12, 16/19-22, s16/19-22, 16/19-23, s16/19-23, 16/19-33, s16/19-33, 16/19-34, s16/19-34, 16/19-44, s16/19-44, h16/19-22, hs16/19-22, h16/19-23, hs16/19-23, 16/32-00, 16/32-44, s16/32-44** are shown in Figures S47–S68.

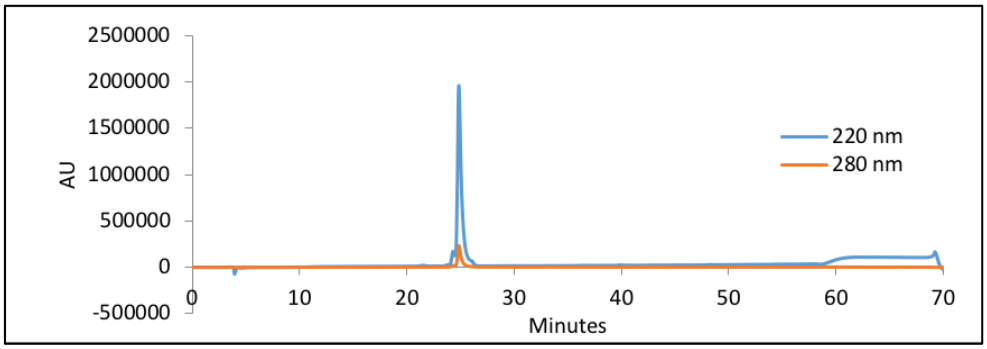


**Figure S46**. Analytical HPLC Data for **WW** variant **16/19-00**. Protein solution was injected onto a C18 analytical column and eluted using a linear gradient of 10-60% B (A = $H_2O$, 0.1% TFA; B = MeCN, 0.1% TFA) over 50 minutes, followed by a 10-minute rinse (95% B), and a 10-minute column re-equilibration.

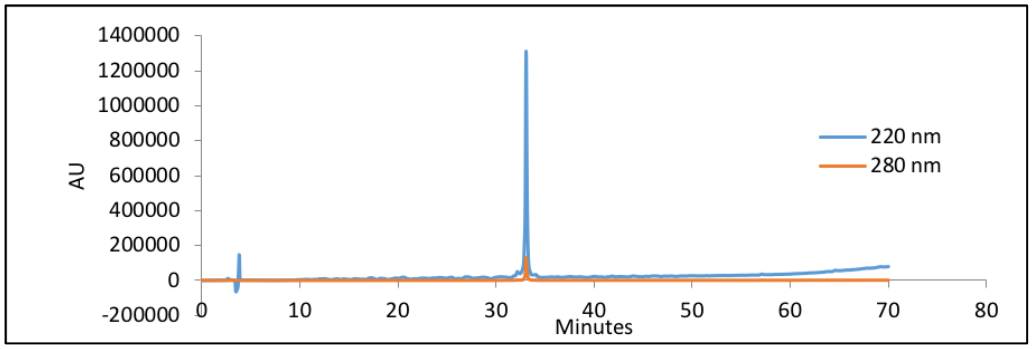


**Figure S47**. Analytical HPLC Data for **WW** variant **16/19-11**. Protein solution was injected onto a C18 analytical column and eluted using a linear gradient of 10-60% B (A = $H_2O$, 0.1% TFA; B= MeCN, 0.1% TFA) over 50 minutes, followed by a 10-minute rinse (95% B), and a 10-minute column re-equilibration.

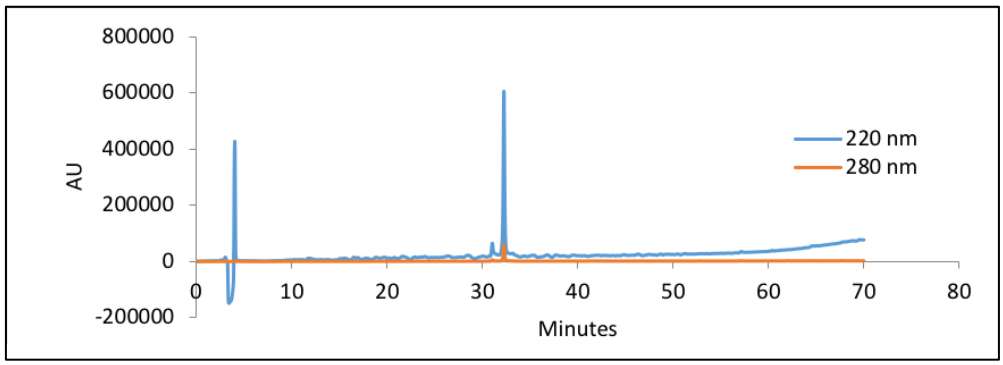


**Figure S48**. Analytical HPLC Data for **WW** variant **s16/19-11**. Protein solution was injected onto a C18 analytical column and eluted using a linear gradient of 10-60% B (A = $H_2O$, 0.1% TFA; B= MeCN, 0.1% TFA) over 50 minutes, followed by a 10-minute rinse (95% B), and a 10-minute column re-equilibration.

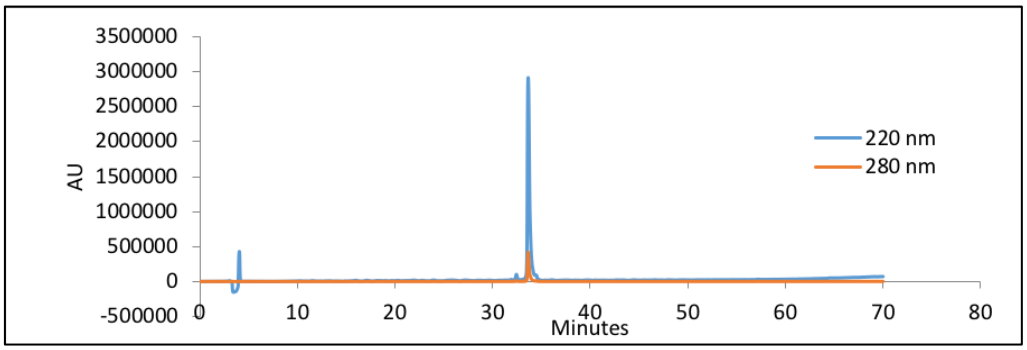


**Figure S49**. Analytical HPLC Data for **WW** variant **16/19-12**. Protein solution was injected onto a C18 analytical column and eluted using a linear gradient of 10-60% B (A = $H_2O$, 0.1% TFA; B= MeCN, 0.1% TFA) over 50 minutes, followed by a 10-minute rinse (95% B), and a 10-minute column re-equilibration.

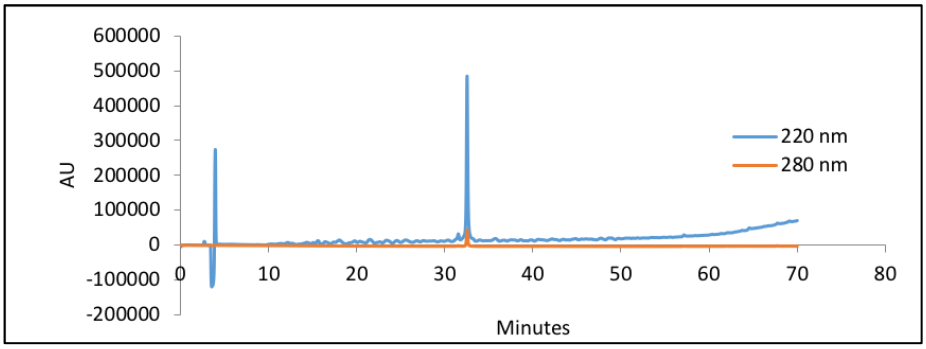


**Figure S50**. Analytical HPLC Data for **WW** variant **s16/19-12**. Protein solution was injected onto a C18 analytical column and eluted using a linear gradient of 10-60% B (A = $H_2O$, 0.1% TFA; B= MeCN, 0.1% TFA) over 50 minutes, followed by a 10-minute rinse (95% B), and a 10-minute column re-equilibration.

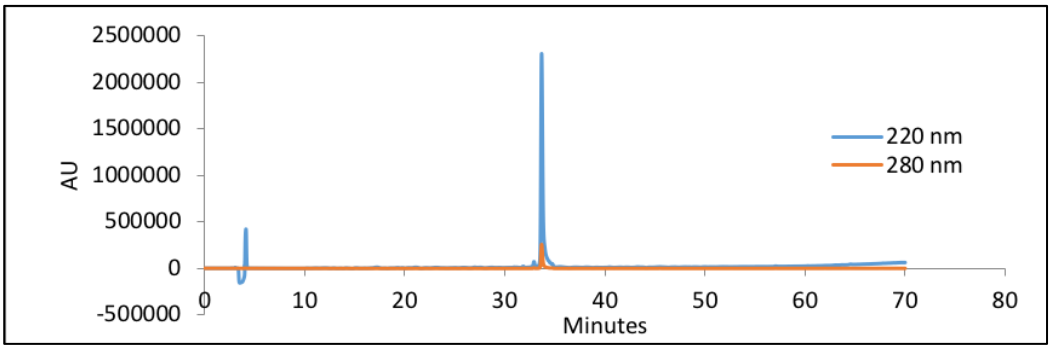


**Figure S51**. Analytical HPLC Data for **WW** variant **16/19-22**. Protein solution was injected onto a C18 analytical column and eluted using a linear gradient of 10-60% B (A = $H_2O$, 0.1% TFA; B= MeCN, 0.1% TFA) over 50 minutes, followed by a 10-minute rinse (95% B), and a 10-minute column re-equilibration.

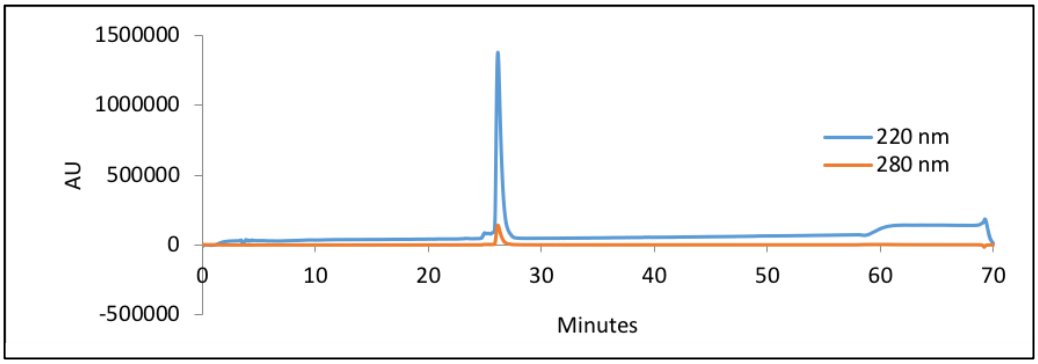

**Figure S52**. Analytical HPLC Data for **WW** variant **s16/19-22**. Protein solution was injected onto a C18 analytical column and eluted using a linear gradient of 10-60% B (A = $H_2O$, 0.1% TFA; B= MeCN, 0.1% TFA) over 50 minutes, followed by a 10-minute rinse (95% B), and a 10-minute column re-equilibration.

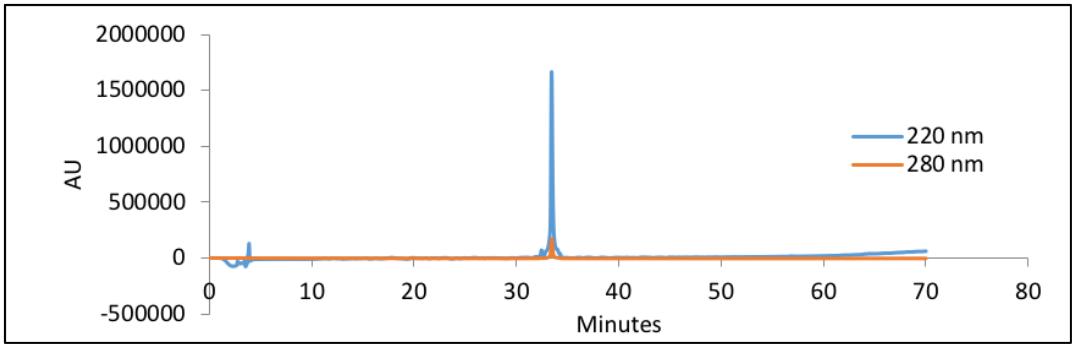


**Figure S53**. Analytical HPLC Data for **WW** variant **16/19-23**. Protein solution was injected onto a C18 analytical column and eluted using a linear gradient of 10-60% B (A = $H_2O$, 0.1% TFA; B= MeCN, 0.1% TFA) over 50 minutes, followed by a 10-minute rinse (95% B), and a 10-minute column re-equilibration.

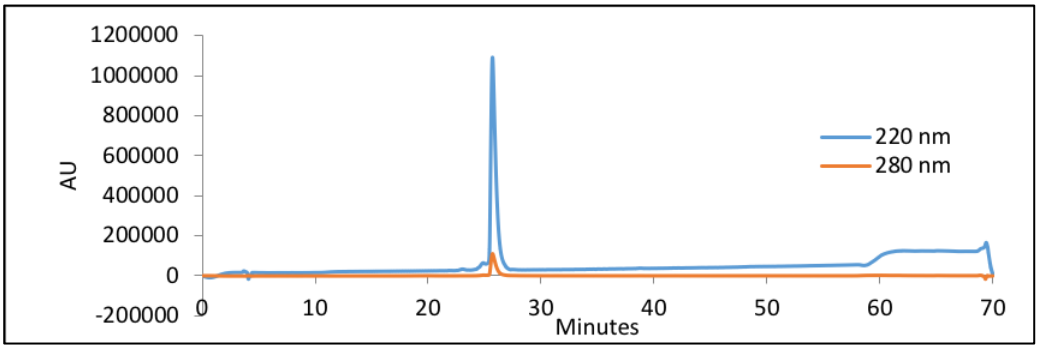


**Figure S54**. Analytical HPLC Data for **WW** variant **s16/19-23**. Protein solution was injected onto a C18 analytical column and eluted using a linear gradient of 10-60% B (A = $H_2O$, 0.1% TFA; B= MeCN, 0.1% TFA) over 50 minutes, followed by a 10-minute rinse (95% B), and a 10-minute column re-equilibration.

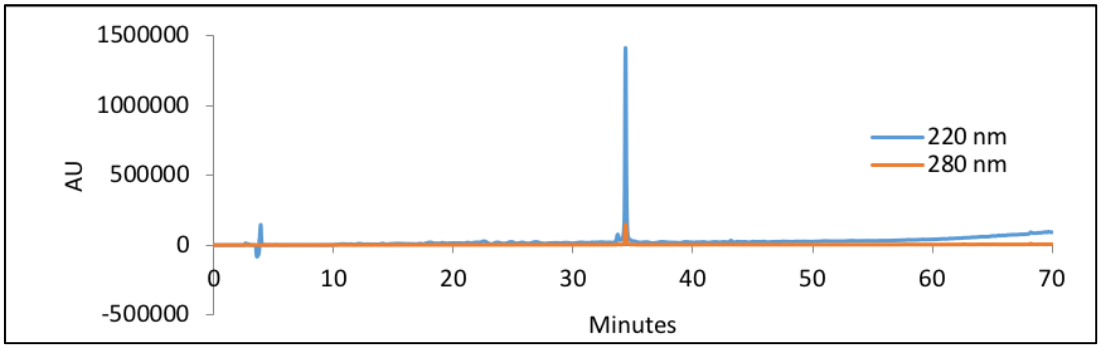


**Figure S55**. Analytical HPLC Data for **WW** variant **16/19-33**. Protein solution was injected onto a C18 analytical column and eluted using a linear gradient of 10-60% B (A = $H_2O$, 0.1% TFA; B= MeCN, 0.1% TFA) over 50 minutes, followed by a 10-minute rinse (95% B), and a 10-minute column re-equilibration.

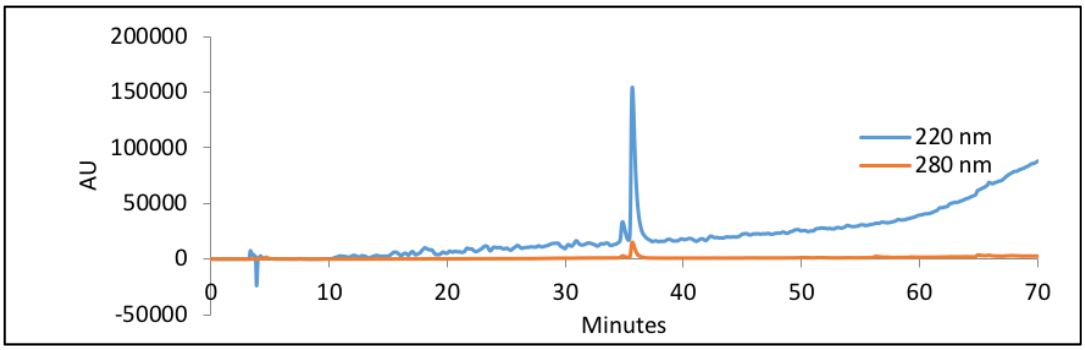


**Figure S56**. Analytical HPLC Data for **WW** variant **s16/19-33**. Protein solution was injected onto a C18 analytical column and eluted using a linear gradient of 10-60% B (A = $H_2O$, 0.1% TFA; B= MeCN, 0.1% TFA) over 50 minutes, followed by a 10-minute rinse (95% B), and a 10-minute column re-equilibration.

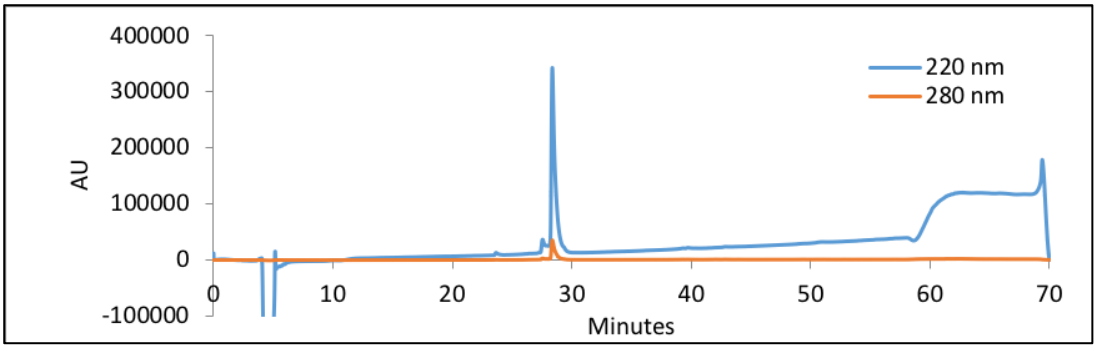


**Figure S57**. Analytical HPLC Data for **WW** variant **16/19-34**. Protein solution was injected onto a C18 analytical column and eluted using a linear gradient of 10-60% B (A = $H_2O$, 0.1% TFA; B= MeCN, 0.1% TFA) over 50 minutes, followed by a 10-minute rinse (95% B), and a 10-minute column re-equilibration.

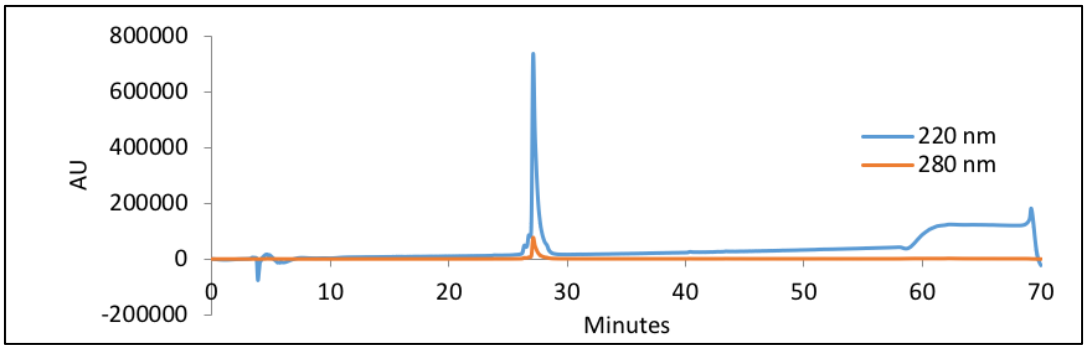


**Figure S58**. Analytical HPLC Data for **WW** variant **s16/19-34**. Protein solution was injected onto a C18 analytical column and eluted using a linear gradient of 10-60% B (A = $H_2O$, 0.1% TFA; B= MeCN, 0.1% TFA) over 50 minutes, followed by a 10-minute rinse (95% B), and a 10-minute column re-equilibration.

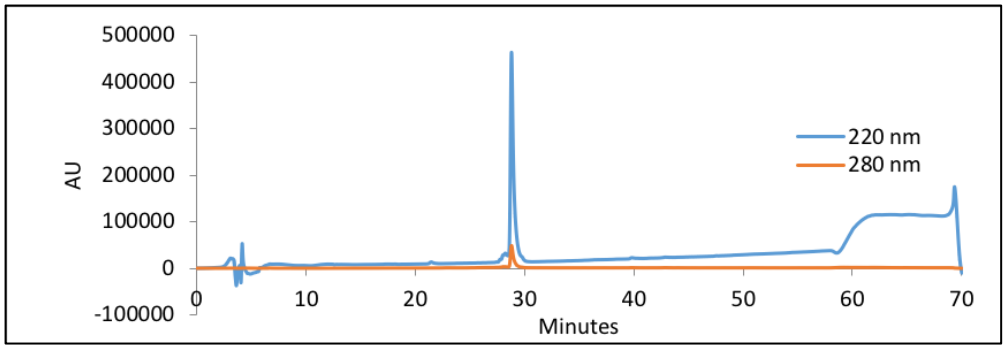

**Figure S59**. Analytical HPLC Data for **WW** variant **16/19-44**. Protein solution was injected onto a C18 analytical column and eluted using a linear gradient of 10-60% B (A = $H_2O$, 0.1% TFA; B = MeCN, 0.1% TFA) over 50 minutes, followed by a 10-minute rinse (95% B), and a 10-minute column re-equilibration.

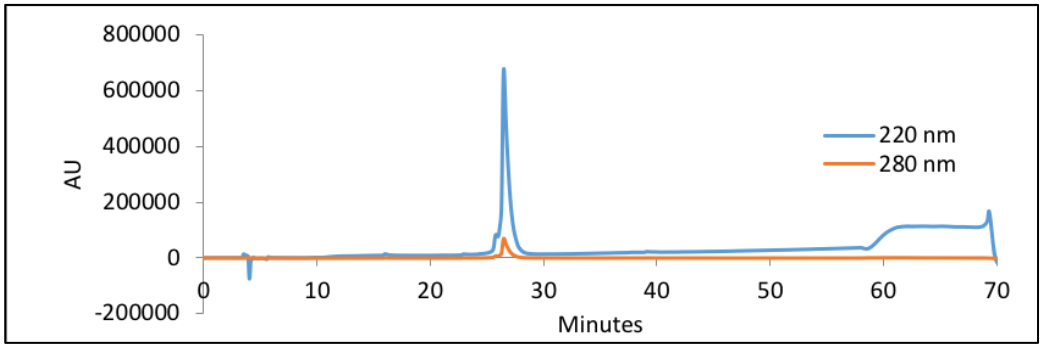


**Figure S60**. Analytical HPLC Data for **WW** variant **s16/19-44**. Protein solution was injected onto a C18 analytical column and eluted using a linear gradient of 10-60% B (A = $H_2O$, 0.1% TFA; B= MeCN, 0.1% TFA) over 50 minutes, followed by a 10-minute rinse (95% B), and a 10-minute column re-equilibration.

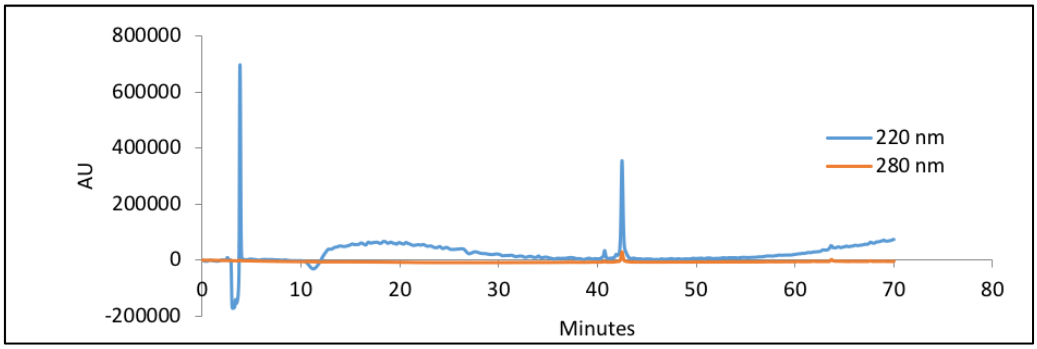


**Figure S61**. Analytical HPLC Data for **WW** variant **h16/19-22**. Protein solution was injected onto a C18 analytical column and eluted using a linear gradient of 10-60% B (A = $H_2O$, 0.1% TFA; B= MeCN, 0.1% TFA) over 50 minutes, followed by a 10-minute rinse (95% B), and a 10-minute column re-equilibration.

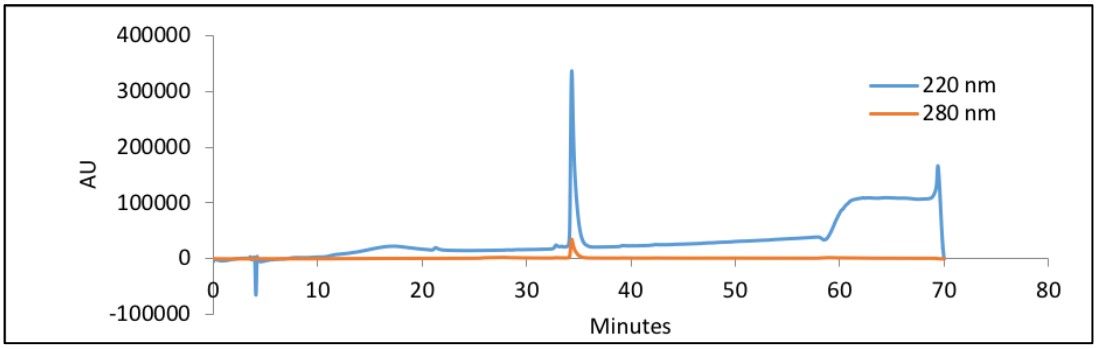


**Figure S62**. Analytical HPLC Data for **WW** variant **hs16/19-22**. Protein solution was injected onto a C18 analytical column and eluted using a linear gradient of 10-60% B (A = $H_2O$, 0.1% TFA; B= MeCN, 0.1% TFA) over 50 minutes, followed by a 10-minute rinse (95% B), and a 10-minute column re-equilibration.

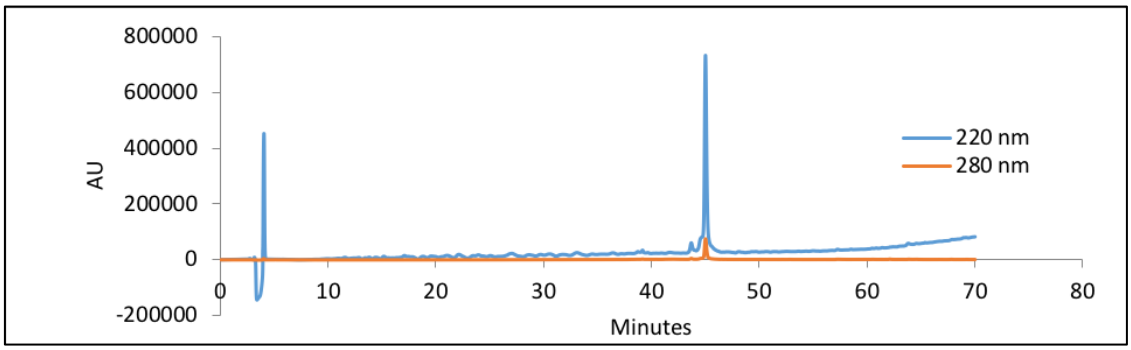


**Figure S63**. Analytical HPLC Data for **WW** variant **h16/19-23.** Protein solution was injected onto a C18 analytical column and eluted using a linear gradient of 10-60% B (A = $H_2O$, 0.1% TFA; B= MeCN, 0.1% TFA) over 50 minutes, followed by a 10-minute rinse (95% B), and a 10-minute column re-equilibration.

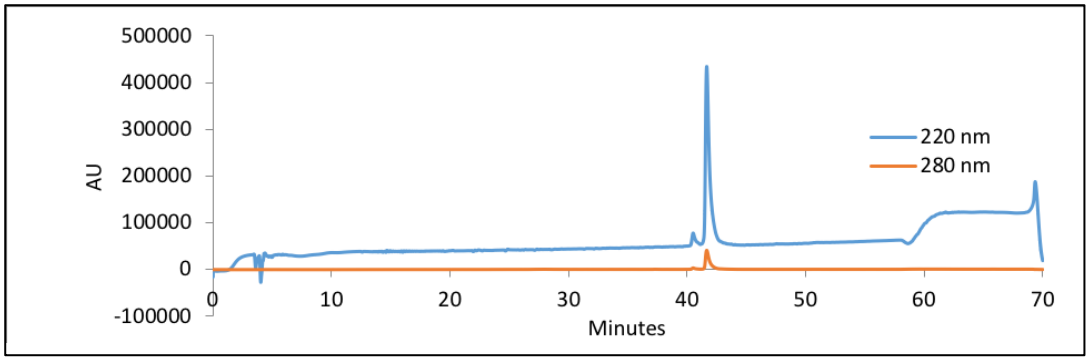


**Figure S64**. Analytical HPLC Data for **WW** variant **sh16/19-23.** Protein solution was injected onto a C18 analytical column and eluted using a linear gradient of 10-60% B (A = $H_2O$, 0.1% TFA; B= MeCN, 0.1% TFA) over 50 minutes, followed by a 10-minute rinse (95% B), and a 10-minute column re-equilibration.

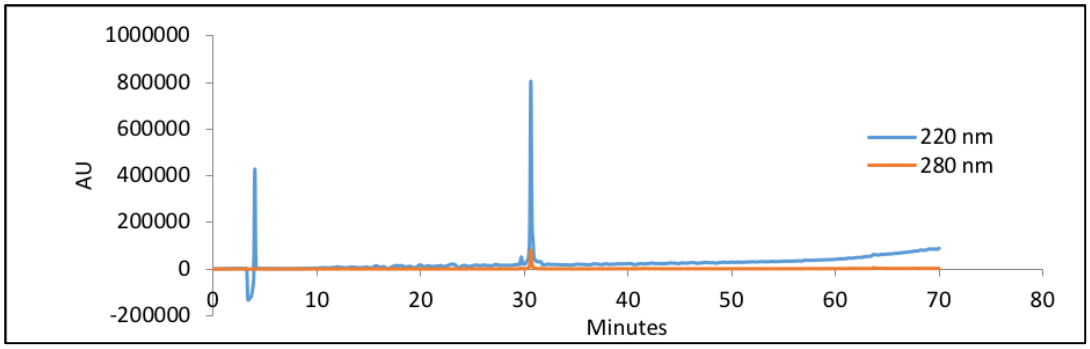


**Figure S65**. Analytical HPLC Data for **WW** variant **16/32-00**. Protein solution was injected onto a C18 analytical column and eluted using a linear gradient of 10-60% B (A = $H_2O$, 0.1% TFA; B= MeCN, 0.1% TFA) over 50 minutes, followed by a 10-minute rinse (95% B), and a 10-minute column re-equilibration.

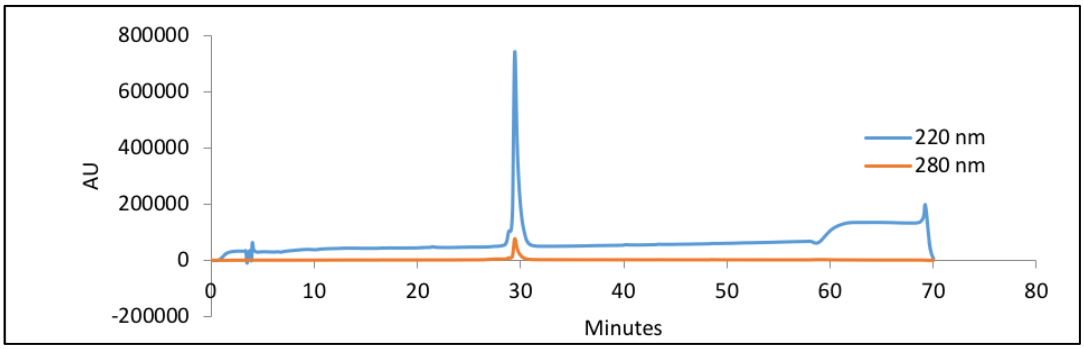

**Figure S66**. Analytical HPLC Data for **WW** variant **16/32-44**. Protein solution was injected onto a C18 analytical column and eluted using a linear gradient of 10-60% B (A = $H_2O$, 0.1% TFA; B= MeCN, 0.1% TFA) over 50 minutes, followed by a 10-minute rinse (95% B), and a 10-minute column re-equilibration.

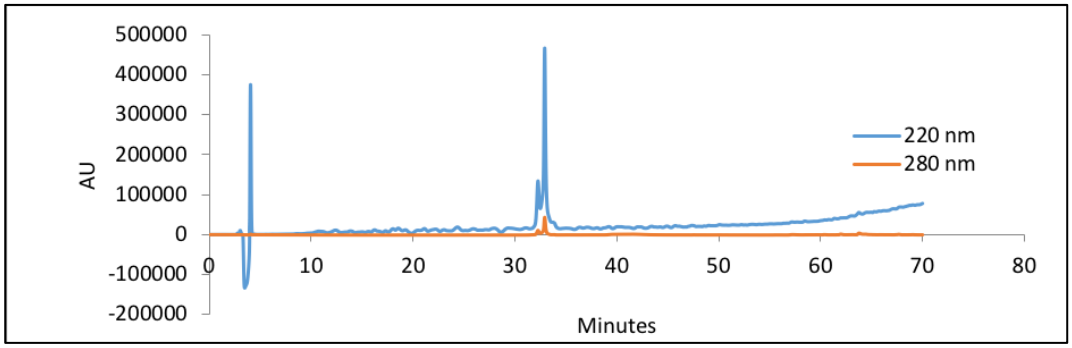


**Figure S67**. Analytical HPLC Data for **WW** variant **s16/32-44**. Protein solution was injected onto a C18 analytical column and eluted using a linear gradient of 10-60% B (A = $H_2O$, 0.1% TFA; B= MeCN, 0.1% TFA) over 50 minutes, followed by a 10-minute rinse (95% B), and a 10-minute column re-equilibration.

## 6. Turbidity experiments to assess aggregation kinetics

Analytical HPLC experiments suggest that **hs16/19-23** is substantially more hydrophobic than **s16/19-23**. We wondered whether PEG-stapled WW variants might be more resistant to aggregation than hydrocarbon-stapled WW variants. To explore this possibility, we monitored the turbidity (absorbance at 405 nm) of 1.5 mg/mL solutions of **16/19-00**, of **s16/19-23**, and of **hs16/19-23** in phosphate buffered saline at 50 °C as a function of time. Though **hs16/19-23** shows an initially higher level of turbidity than **s16/19-23**, the solutions are indistinguishable at the end of the experiment, suggesting that PEG stapling and hydrocarbon stapling provide similar protection from aggregation. This result agrees with the similar stability of **s16/19-23** and **hs16/19-23** (compare $T_m$ values in main text Table 1).

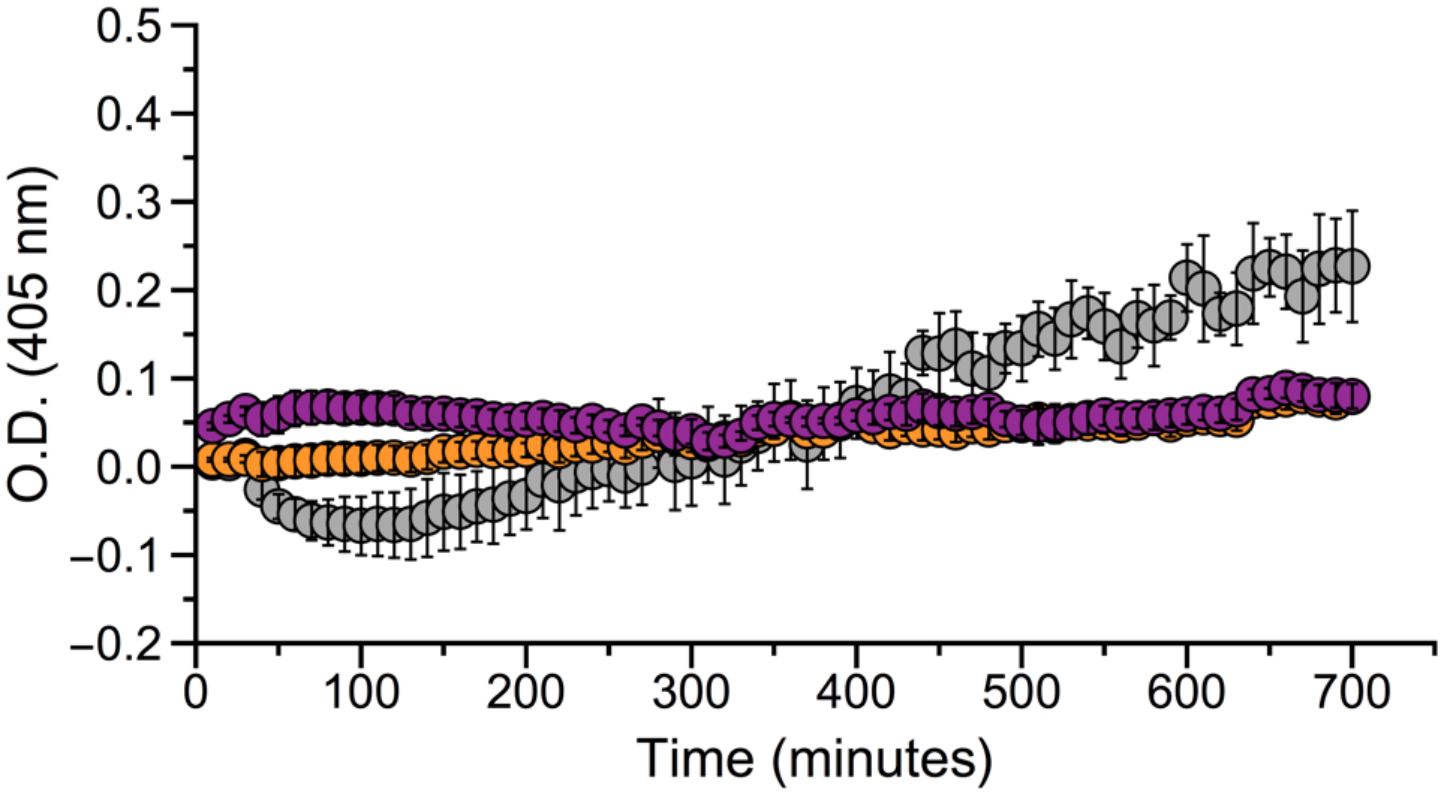


**Figure S68**. Absorbance at 405 nm of 1.5 mg/mL solutions of **16/19-00** (gray circles), of **s16/19-23** (orange circles), or of **hs16/19-23** (purple circles) in phosphate buffered saline at 50 °C as a function of time. Experiment performed in triplicate, with standard error as shown above.

## 7. Synthesis and characterization of PEGylated Asn derivatives

### 2-(2-(2-azidoethoxy)ethoxy)ethan-1-ol (QX1011)

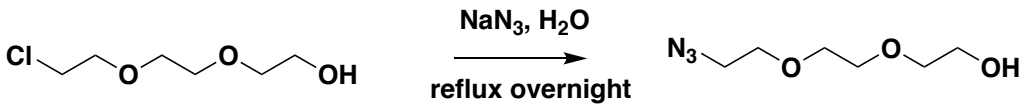


**QX1011**

To a solution of $NaN_3$ (3.85 g, 59.30 mmol) in water (200 mL) was added 2-(2-(2-chloroethoxy)ethoxy)ethan-1-ol (5.00 g, 29.65 mmol) at room temperature. The reaction mixture was then refluxed overnight. The crude mixture was extracted with DCM for 3 times after the reaction was completed. The combined organic phases were washed with saturated brine and dried over anhydrous sodium sulfate, evaporated to dryness to obtain QX1011 as colorless oil without further purification. Yield quantitative. MS(ESI-TOF) m/z calc. for $C_6H_{13}N_3O_3Na^+$ 198.08, found 198.08 [M+$Na^+$]. $^1$H NMR (500 MHz, Chloroform-*d*) δ 3.76 – 3.73 (m, 2H), 3.71 – 3.67 (m, 6H), 3.63 – 3.62 (m, 2H), 3.41 (t, *J* = 5.0 Hz, 2H). $^{13}$C NMR (126 MHz, Chloroform-*d*) δ 72.47, 70.66, 70.39, 70.07, 61.77, 50.64.

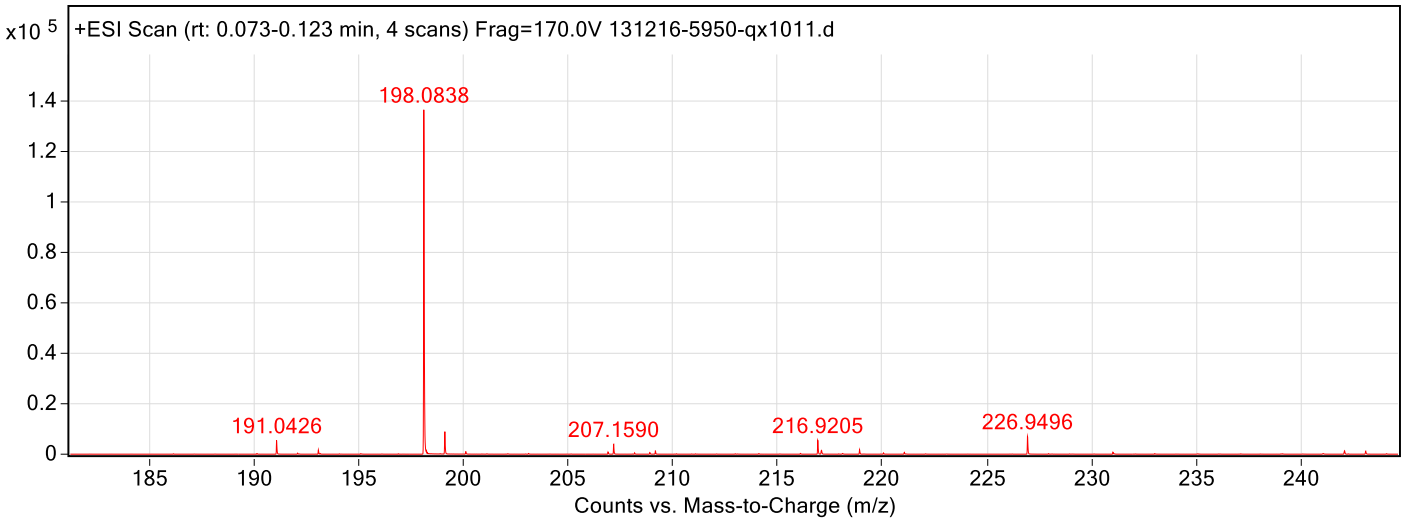


**Figure S69**. ESI-TOF MS data for compound **QX1011**.

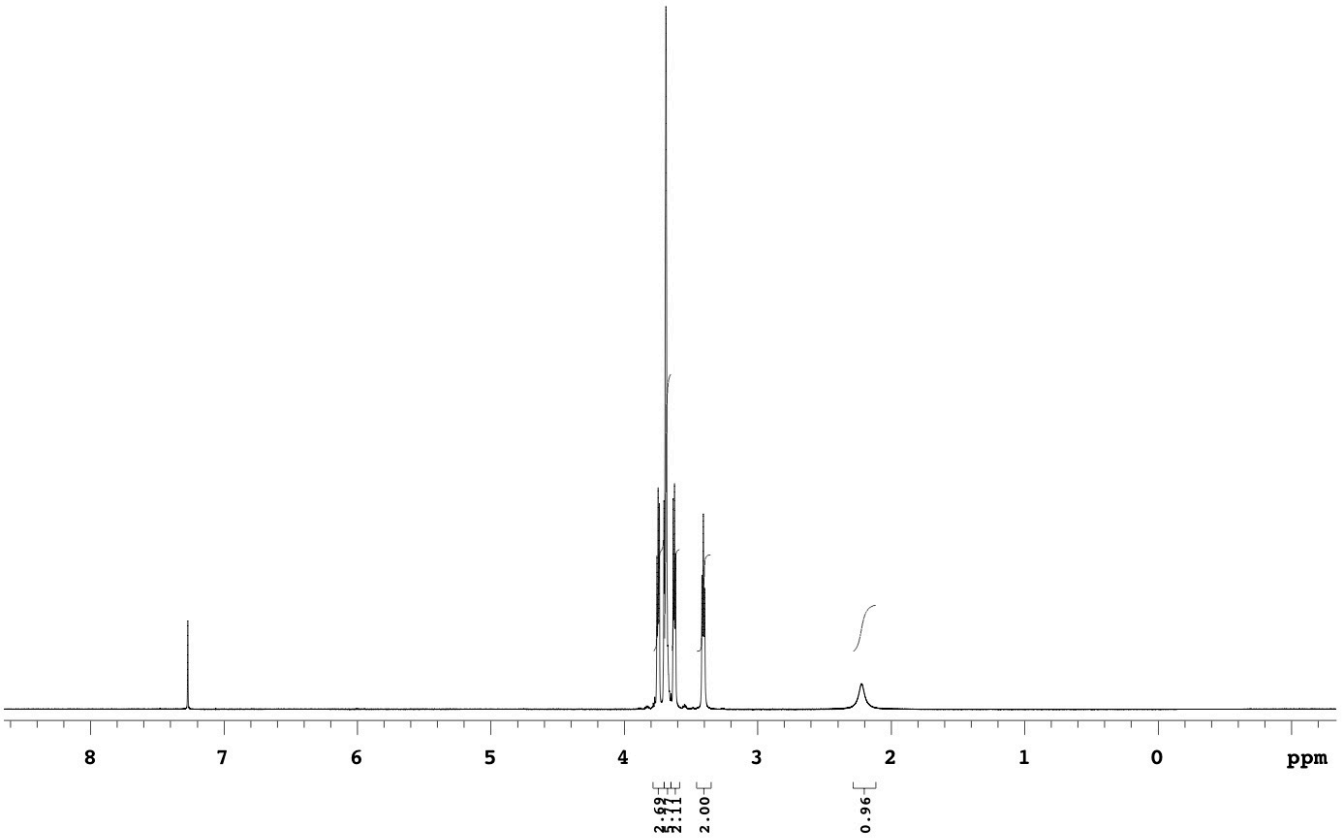


**Figure S70.** $^{1}$H NMR for compound QX1011.

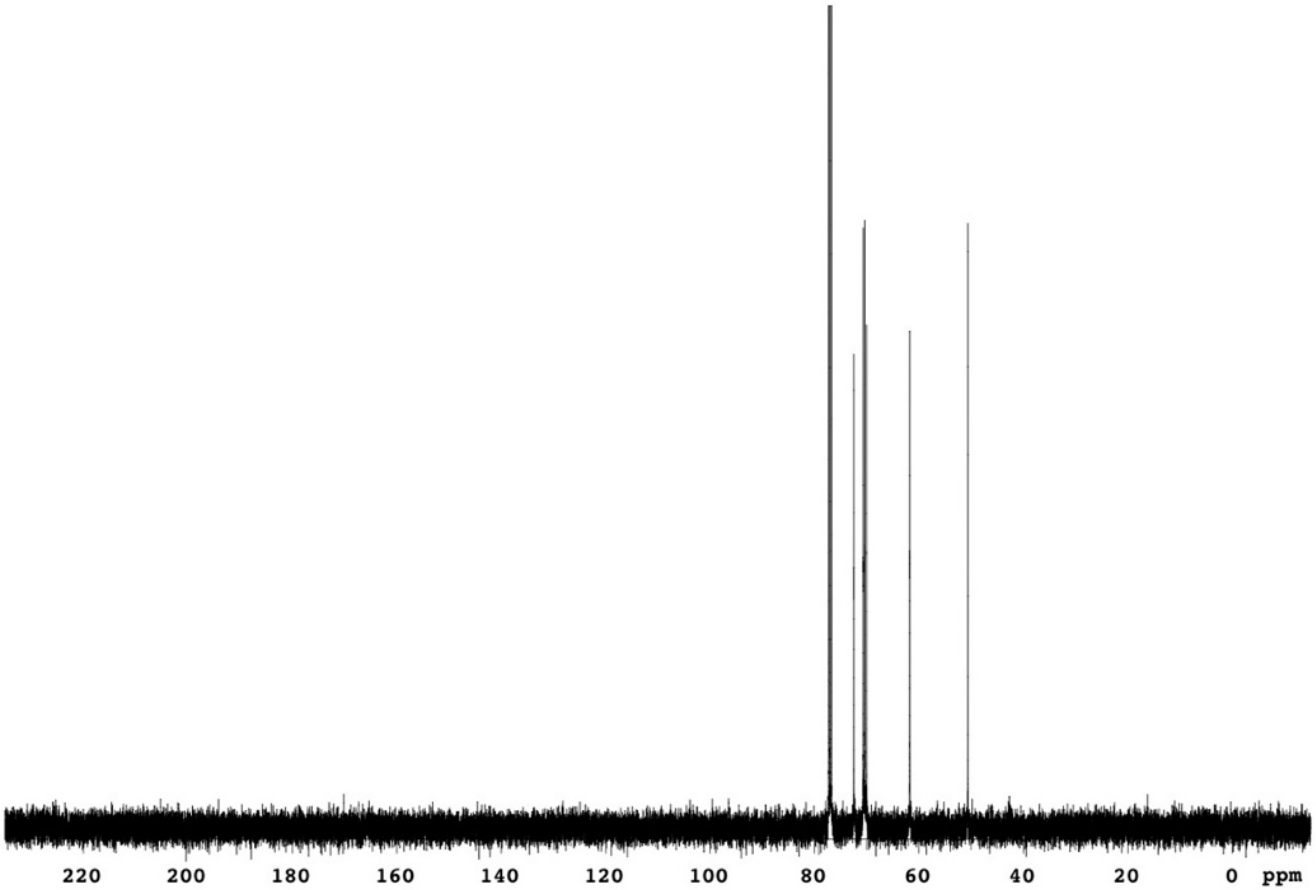

**Figure S71.** $^{13}C$ NMR for compound **QX1011**.

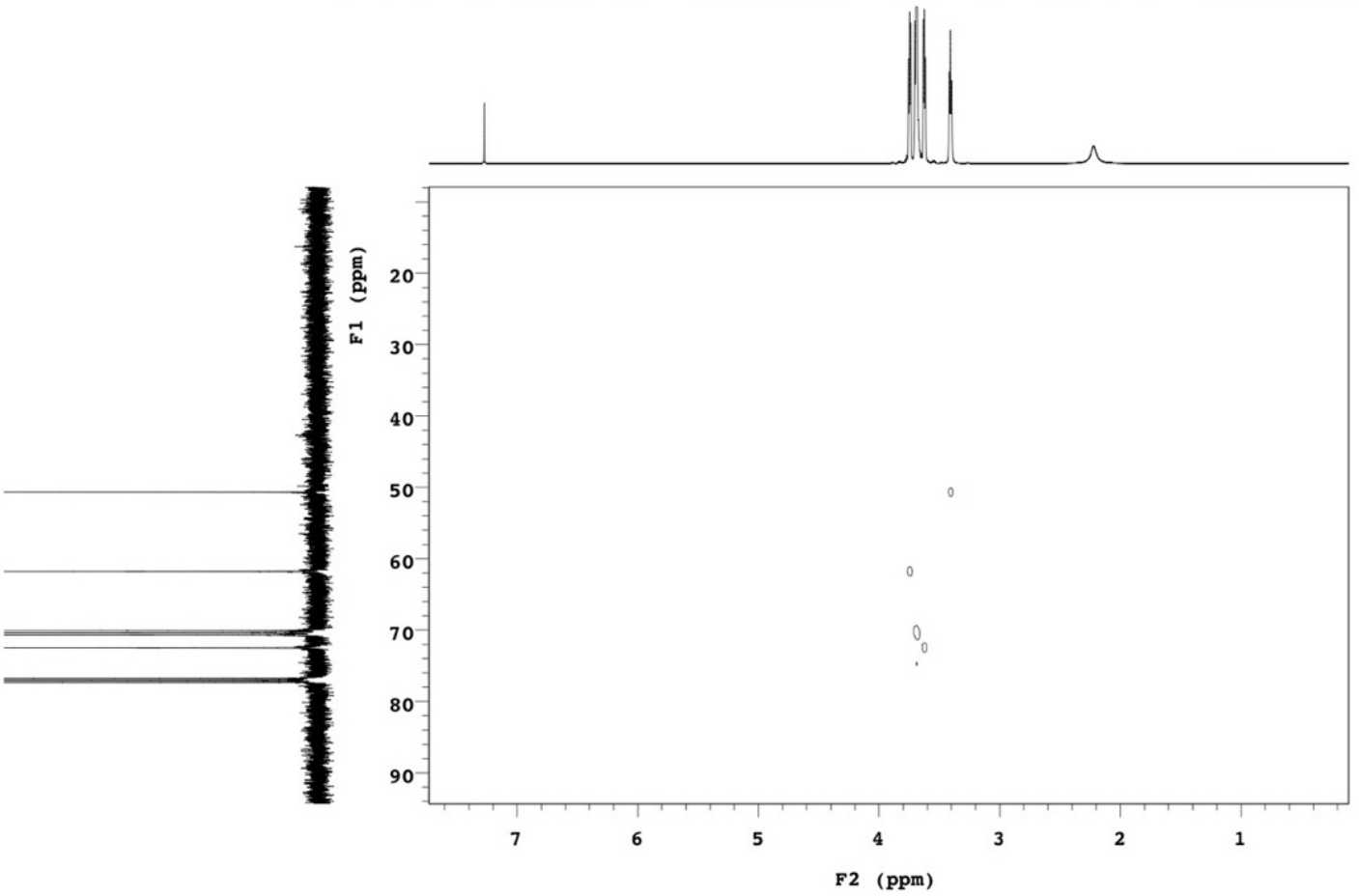


**Figure S72.** HSQC data for compounds **QX1011**.

**3-(2-(2-(2-azidoethoxy)ethoxy)ethoxy)prop-1-ene (QX1013)**

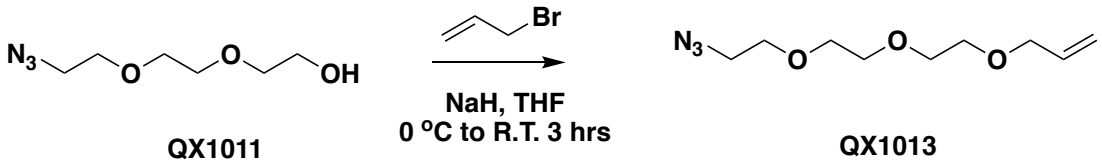


QX1011 QX1013

To NaH (60 % in mineral oil, 1.3 g, 32.30 mmol, washed with dry hexane) in THF (50 mL) was added QX1011 (2.83 g, 16.15 mmol) at 0°C under argon. The reaction mixture was stirred at 0°C for 1 hour, allyl bromide (3.9 g, 32.30 mmol) in THF (10 mL) was added slowly at 0°C and stirring was continued for another 2 hours at room temperature. The reaction mixture was poured into cold saturated ammonium chloride solution (40 mL) and extracted with ethyl acetate. The combined organic phases were washed with saturated brine and dried over anhydrous sodium sulfate, evaporated to dryness. The products were separated by flash column chromatography to obtain the desired product QX1013 as colorless oil. Yield 67.5%; MS(ESI-TOF) m/z calc. for $C_9H_{17}N_3O_3NH_4^+$ 223.16, found 233.16 [M+$NH_4^+$]; $^1$H NMR (500 MHz, Chloroform-*d*) δ 5.86 (ddt, *J* = 16.4, 10.8, 5.7 Hz, 1H), 5.2 (dd, *J* = 17.2, 1.0 Hz, 1H), 5.12 (dd, *J* = 10.4, 1.7 Hz, 1H), 3.97 (d, *J* = 5.5 Hz, 2H), 3.63 – 3.61 (m, 8H), 3.56 – 3.54 (m, 2H), 3.33 (t, *J* = 5.1 Hz, 2H). $^{13}$C NMR (126 MHz, Chloroform-*d*) δ 134.72, 116.97, 72.13, 70.64, 69.97, 69.97, 69.36, 50.60, 50.60.

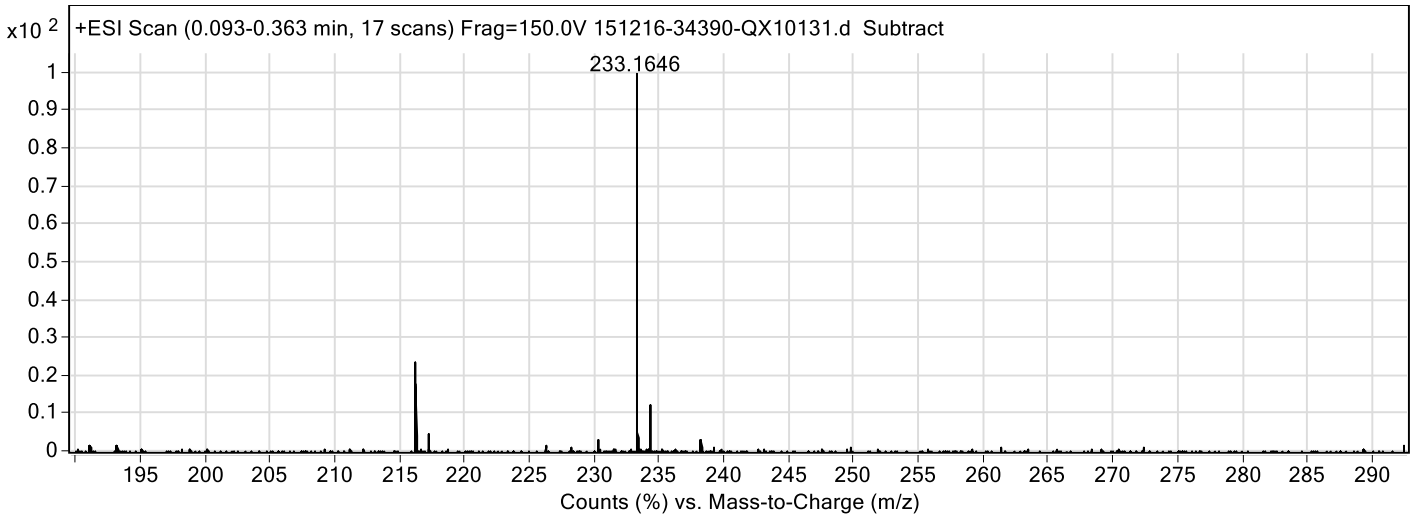


**Figure S73.** ESI-TOF MS data for compounds **QX1013**.

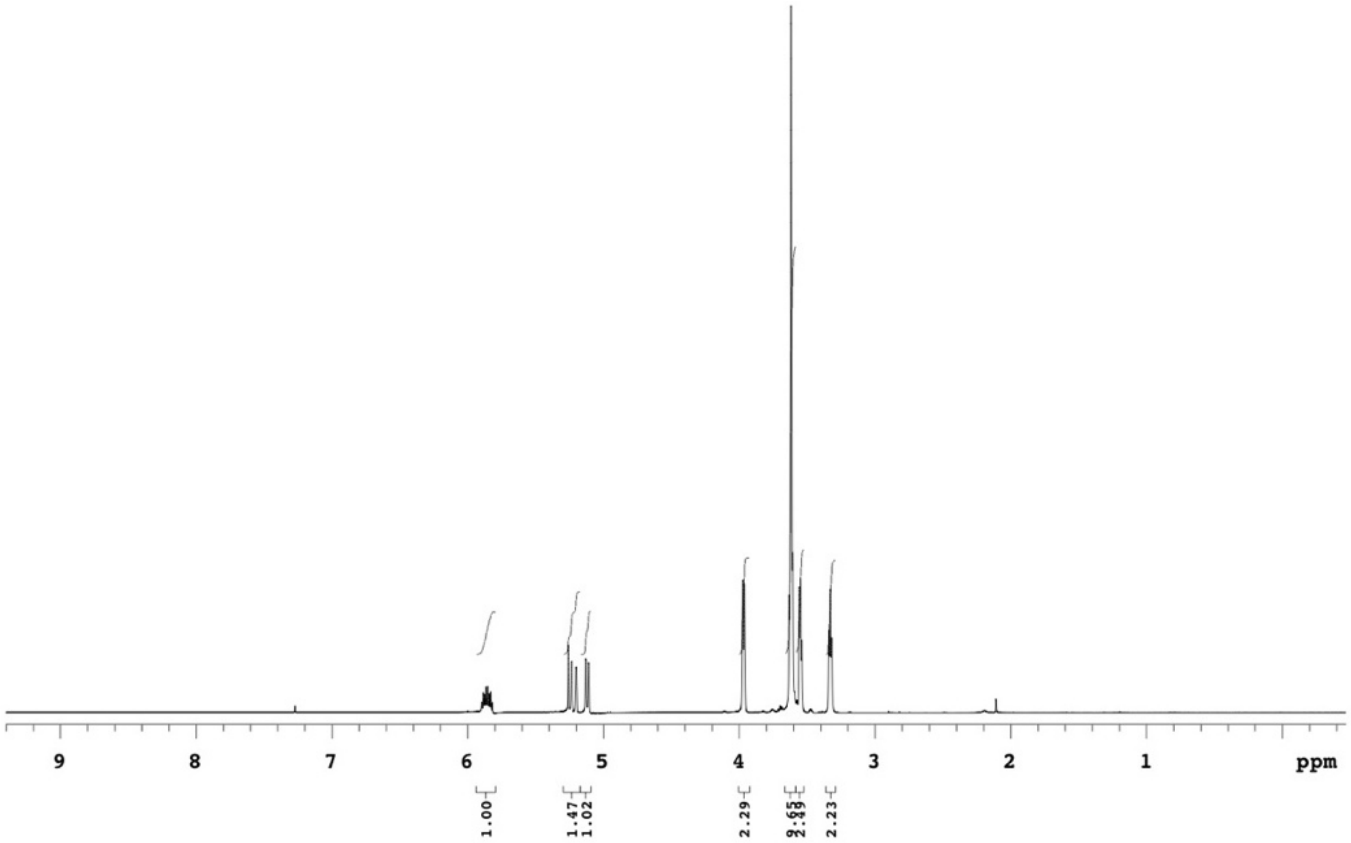


**Figure S74.** $^{1}$H NMR data for compound **QX1013**.

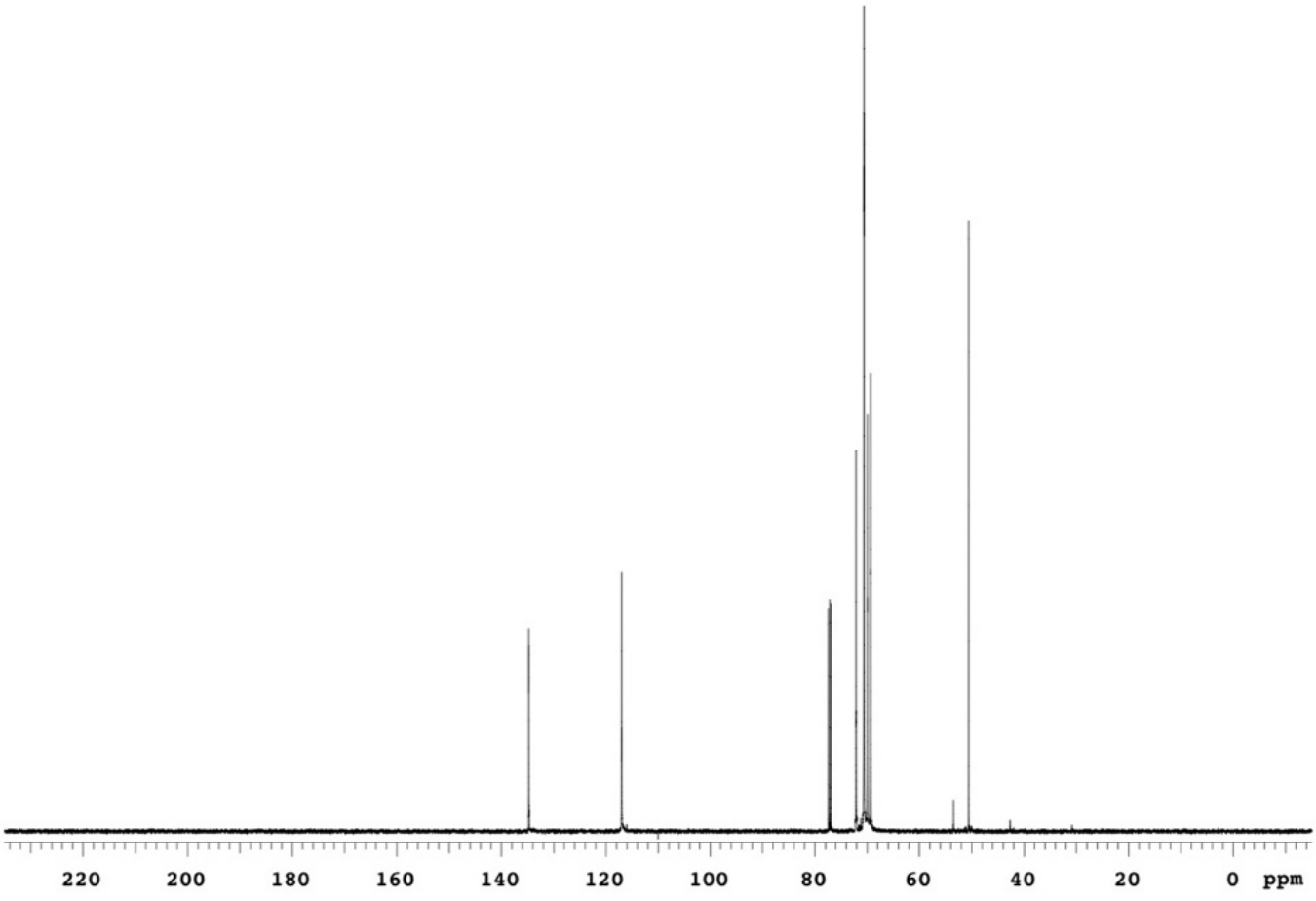

**Figure S75.** $^{13}C$ NMR data for compound **QX1013**.

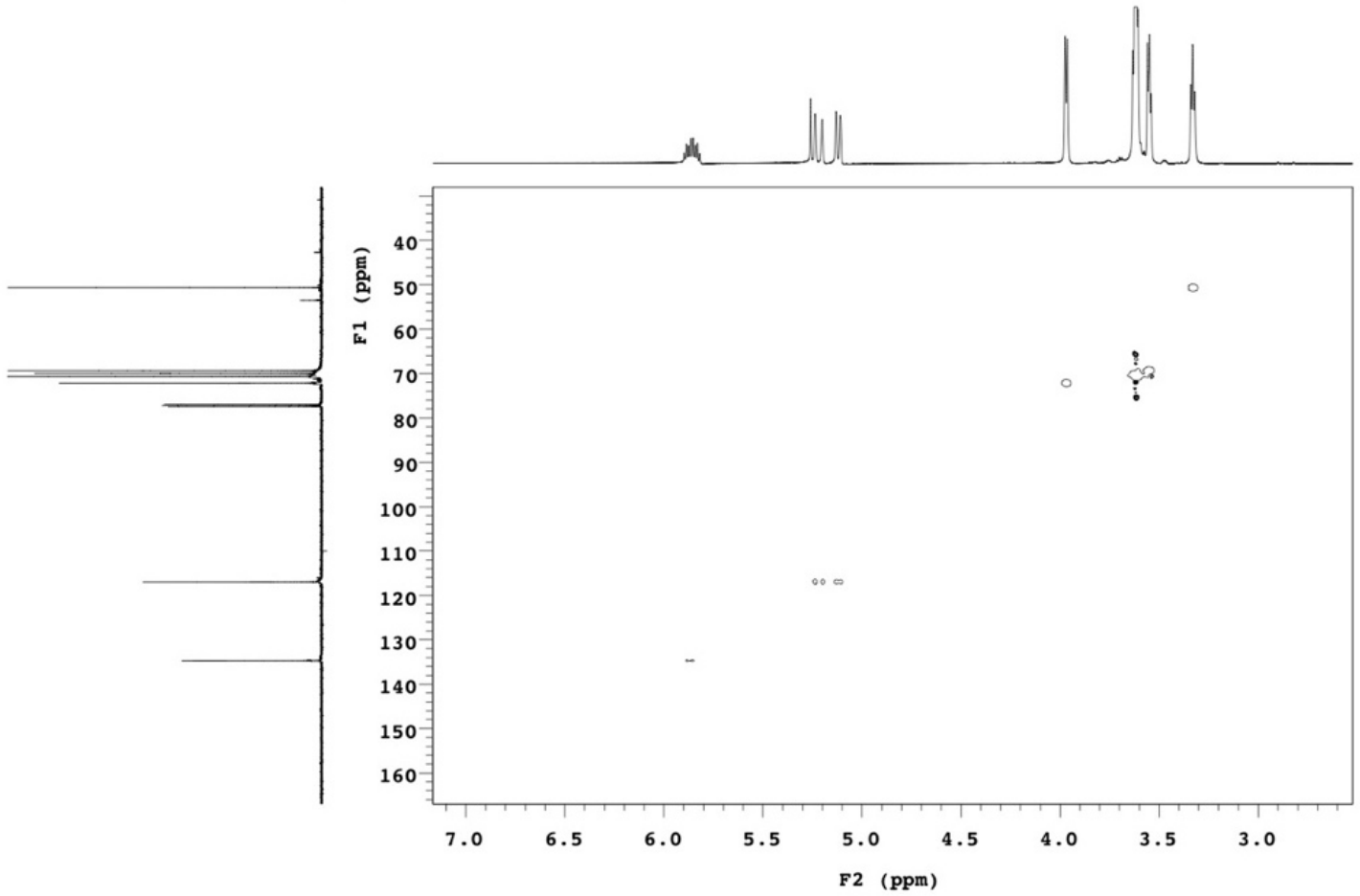


**Figure S76.** HSQC NMR data for compound **QX1013**.

**2-(2-(2-(allyloxy)ethoxy)ethoxy)ethan-1-amine (QX1015)**

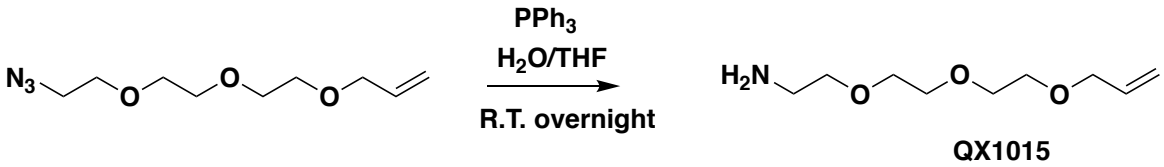


QX1013 QX1015

Compound QX1013 (2.35g, 10.90 mmol) and $PPh_3$ (5.73 g, 21.80 mmol) in a mixture of THF (40 mL) and water (1 mL) were stirred at room temperature overnight. 1M HCl (60 mL) was added and extracted 3 times with diethyl ether. The aqueous phase was lyophilized to obtain compound 9 as colorless oil without further purification. Isolated yield 72%; MS(ESI-TOF) m/z calc. for $C_9H_{19}NO_3H^+$ 190.14, found 190.15 [$M+H^+$]. $^1$H NMR (500 MHz, Chloroform-*d*) δ 8.25 (s, 2H), 5.94 (ddt, *J* = 16.4, 11.2, 5.8 Hz, 1H), 5.30 (dd, *J* = 17.2, 1.2 Hz, 1H), 5.23 (d, *J* = 10.4 Hz, 1H), 4.07 (d, *J* = 5.8 Hz, 2H), 3.90 – 3.83 (m, 2H), 3.74 – 3.66 (m, 8H), 3.62 (dd, *J* = 5.6, 2.9 Hz, 2H). $^{13}$C NMR (126 MHz, Chloroform-*d*) δ 134.42, 117.92, 109.98, 72.17, 70.22, 70.02, 68.95, 67.58, 66.65.

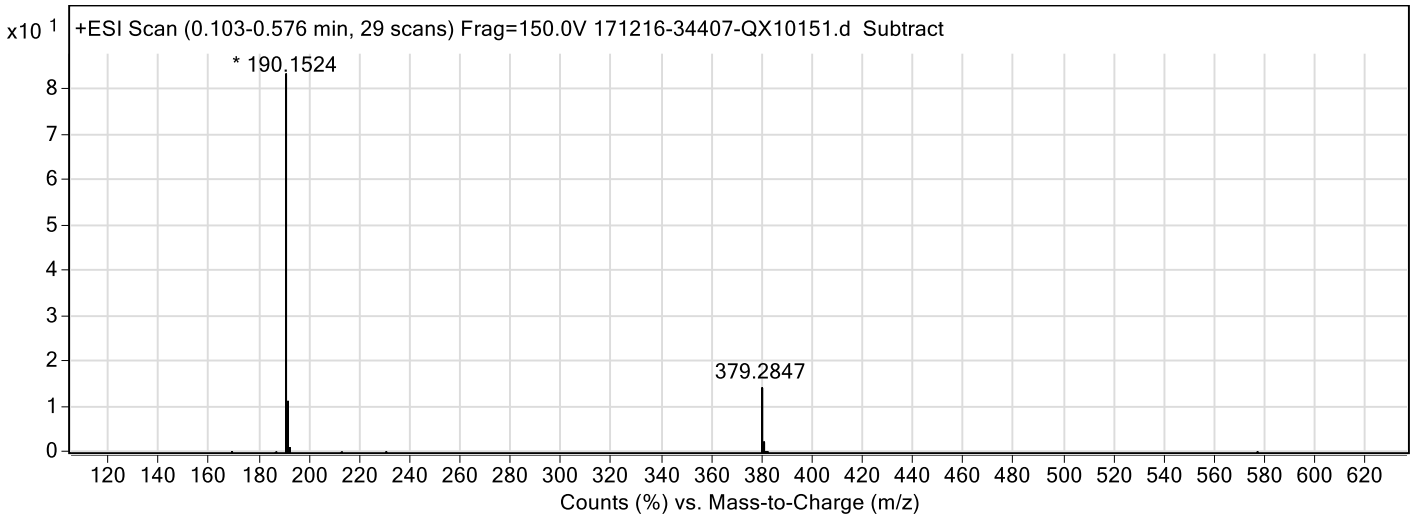


**Figure S77.** ESI-TOF MS data for compound **QX1015**.

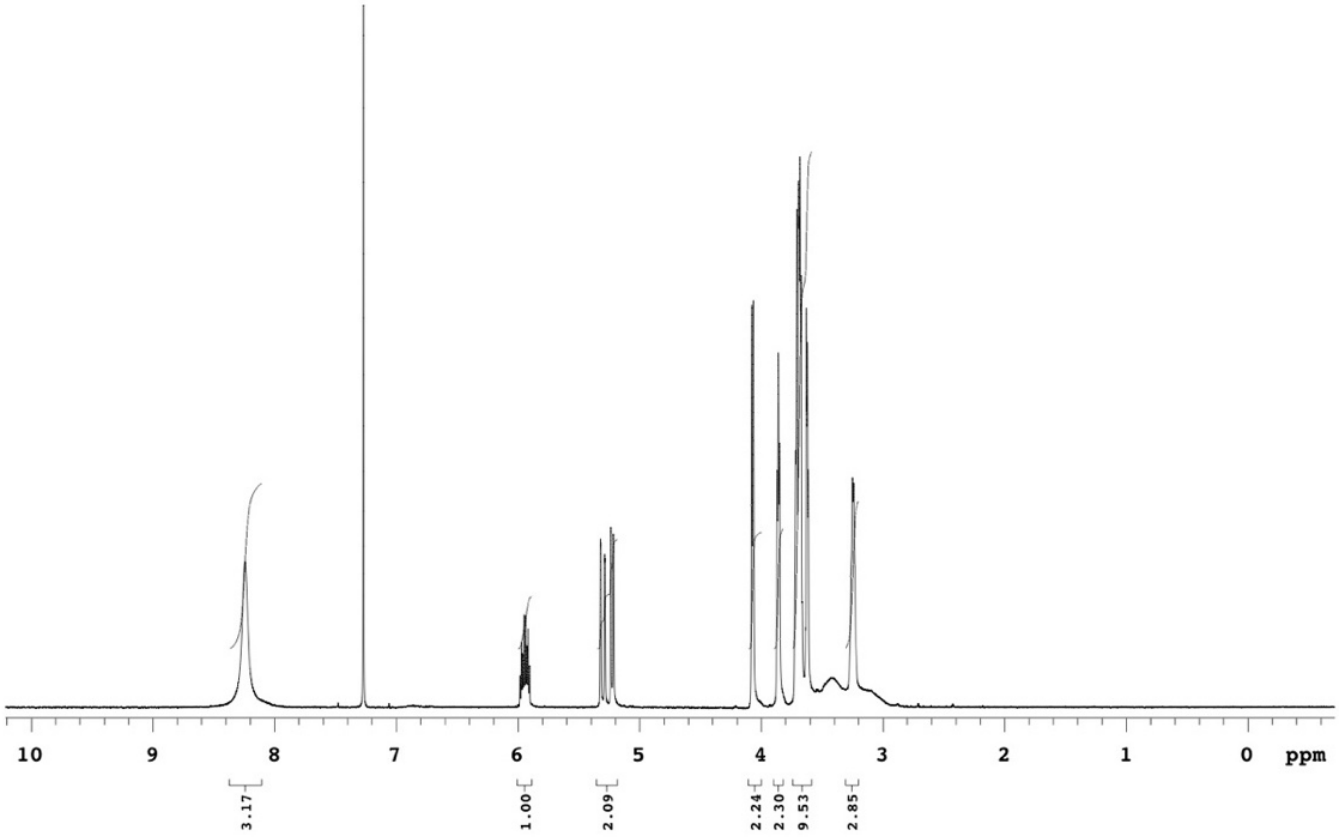


**Figure S78.** [1]H NMR data for compound **QX1015**.

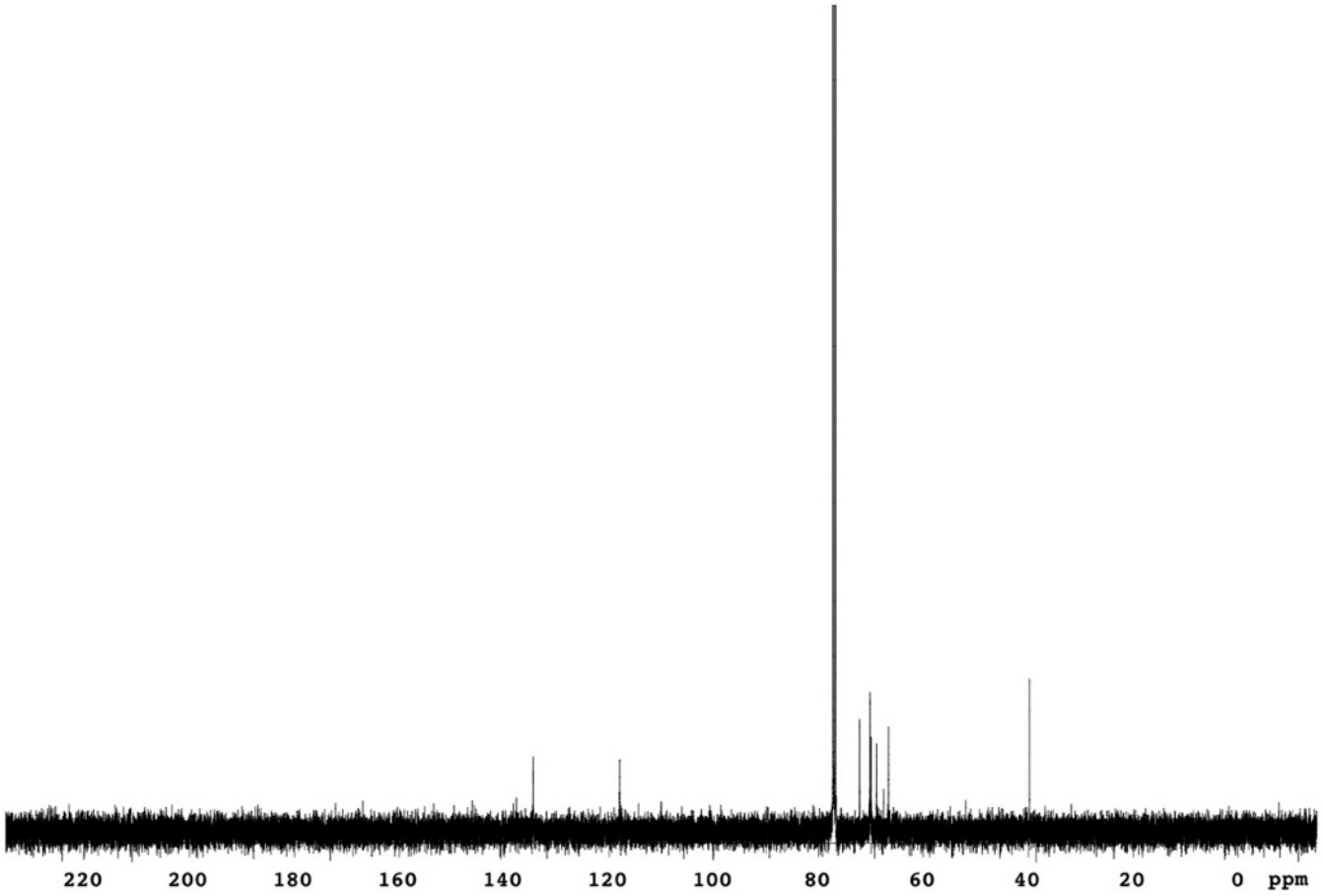

**Figure S79.** $^{13}C$ NMR data for compound **QX1015**.

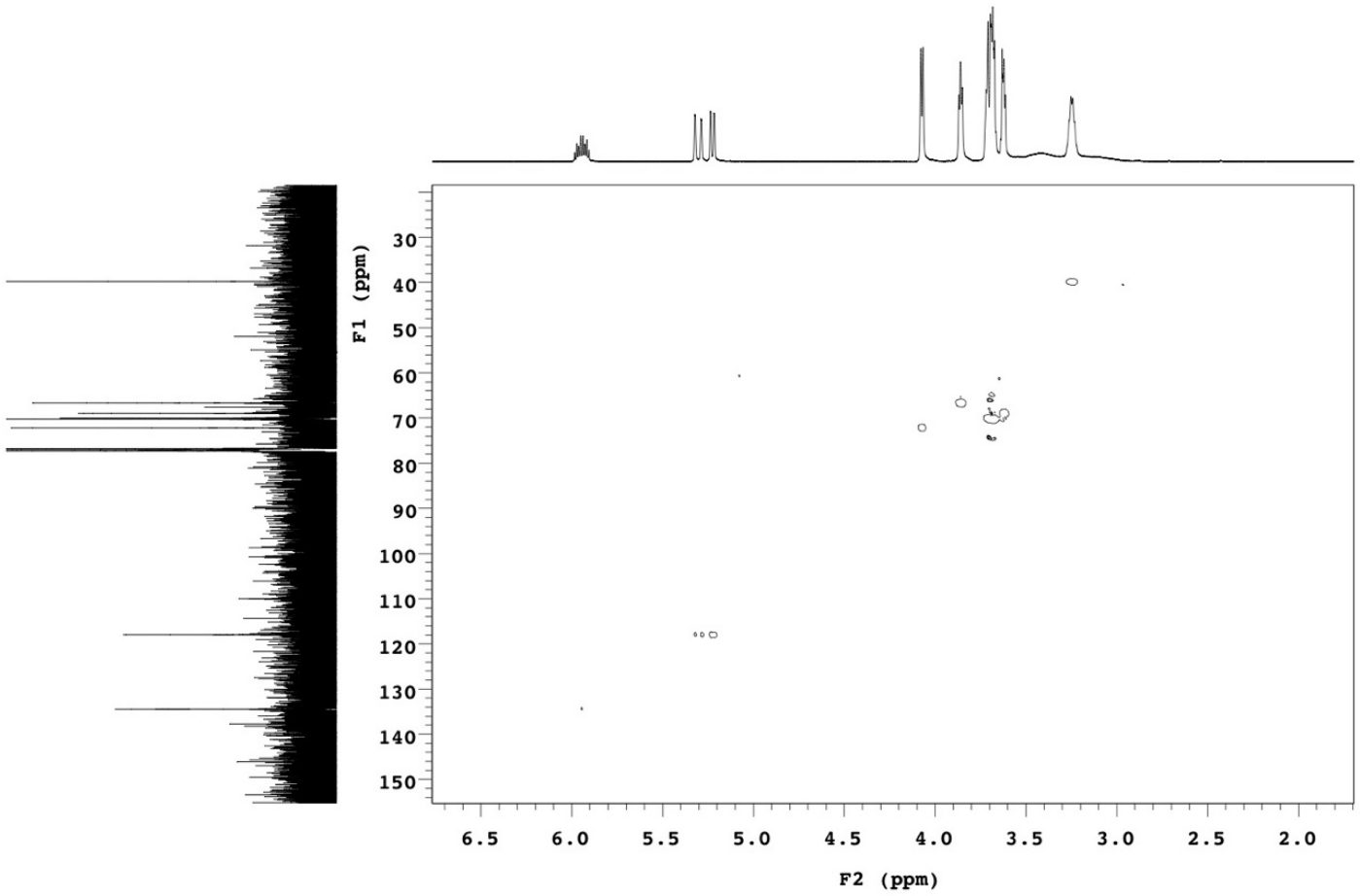


**Figure S80.** HSQC data for compound **QX1015**.

***tert*-butyl (*S*)-16-((((9*H*-fluoren-9-yl)methoxy)carbonyl)amino)-14-oxo-4,7,10-trioxa-13-azaheptadec-1-en-17-oate (QX1017)**

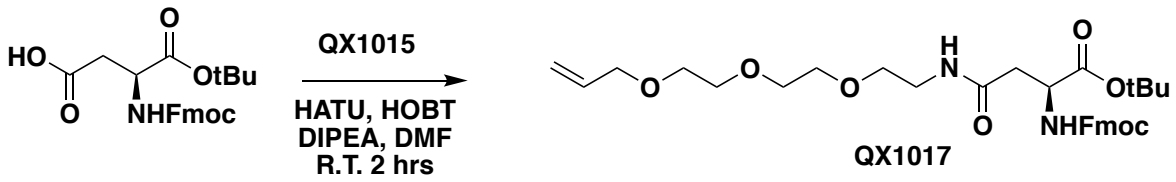


To Fmoc-Asp-tBu (1.65 g, 4.0 mmol) dissolved in dry DMF (25 ml) was added HATU (2.5 g, 6.0 mmol), HOBT (920 mg, 6.0 mmol), DIPEA (2 ml, 12.0 mmol). Then the mixture was stirred for 15 minutes at room temperature. Then compound QX1015 (dissolved in 5 ml DMF) was added to the mixture and the system was stirred for another 2 hours at room temperature. Upon completion of the reaction monitored by TLC, 30 ml water was added to the flask and extracted 3 times with ethylacetate. The organic phases were combined, washed with saturated brine and evaporated to dryness. The crude was then applied to flash column chromatography to obtain the product QX1017 as white solid. Yield 78%; MS(ESI-TOF) m/z calc. for $C_{32}H_{42}N_2O_8H^+$ 583.30, $C_{32}H_{42}N_2O_8NH_4^+$ 600.33, $C_{32}H_{42}N_2O_8Na^+$ 605.28, found 583.30 [M+H$^+$], 600.33 [M+NH$_4^+$], 605.28 [M+Na$^+$]. $^1$H NMR (500 MHz, Chloroform-*d*) δ 7.77 (d, *J* = 7.6 Hz, 2H), 7.62 (dd, *J* = 7.6, 3.5 Hz, 2H), 7.40 (t, *J* = 7.4 Hz, 2H), 7.32 (t, *J* = 7.4 Hz, 2H), 6.31 (s, 1H), 6.07 (d, *J* = 8.5 Hz, 1H), 5.91 (ddt, *J* = 16.5, 11.0, 5.8 Hz, 1H), 5.28 (dd, *J* = 17.2, 1.6 Hz, 1H), 5.20 (d, *J* = 10.3 Hz, 1H), 4.49 (dt, *J* = 8.9, 4.6 Hz, 1H), j 4.02 (d, *J* = 5.8 Hz, 2H), 3.66 – 3.52 (m, 12H), 2.86 (dd, *J* = 15.5, 4.4 Hz, 1H), 2.69 (dd, *J* = 15.5, 4.4 Hz, 1H), 1.48 (s, 9H).

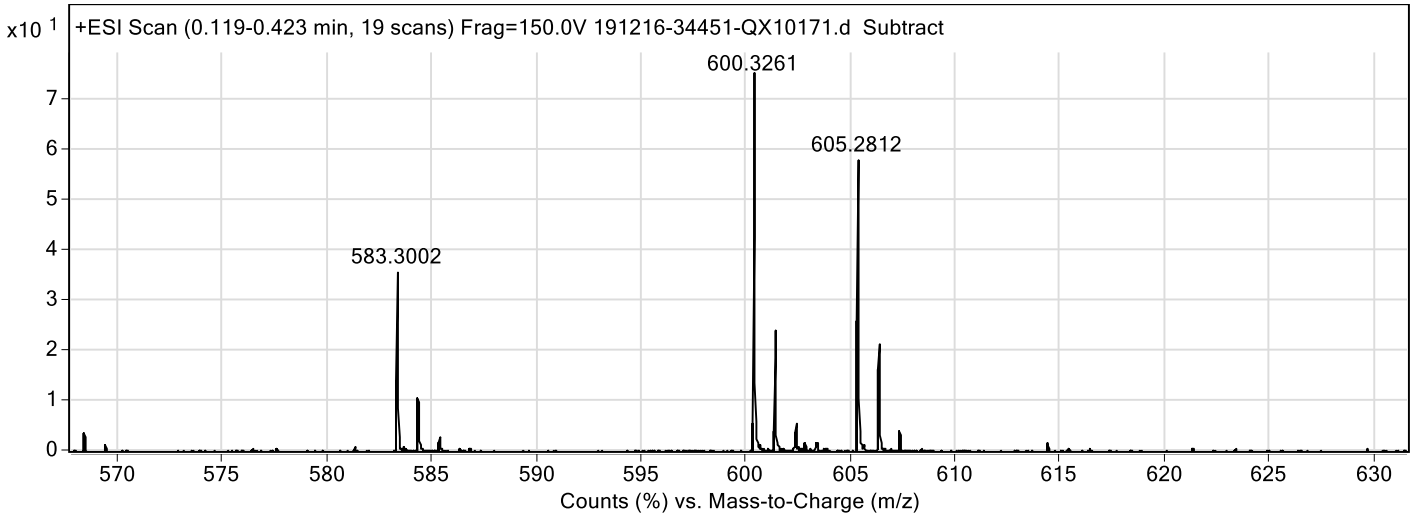


**Figure S81.** ESI-TOF MS data for compound **QX1017**.

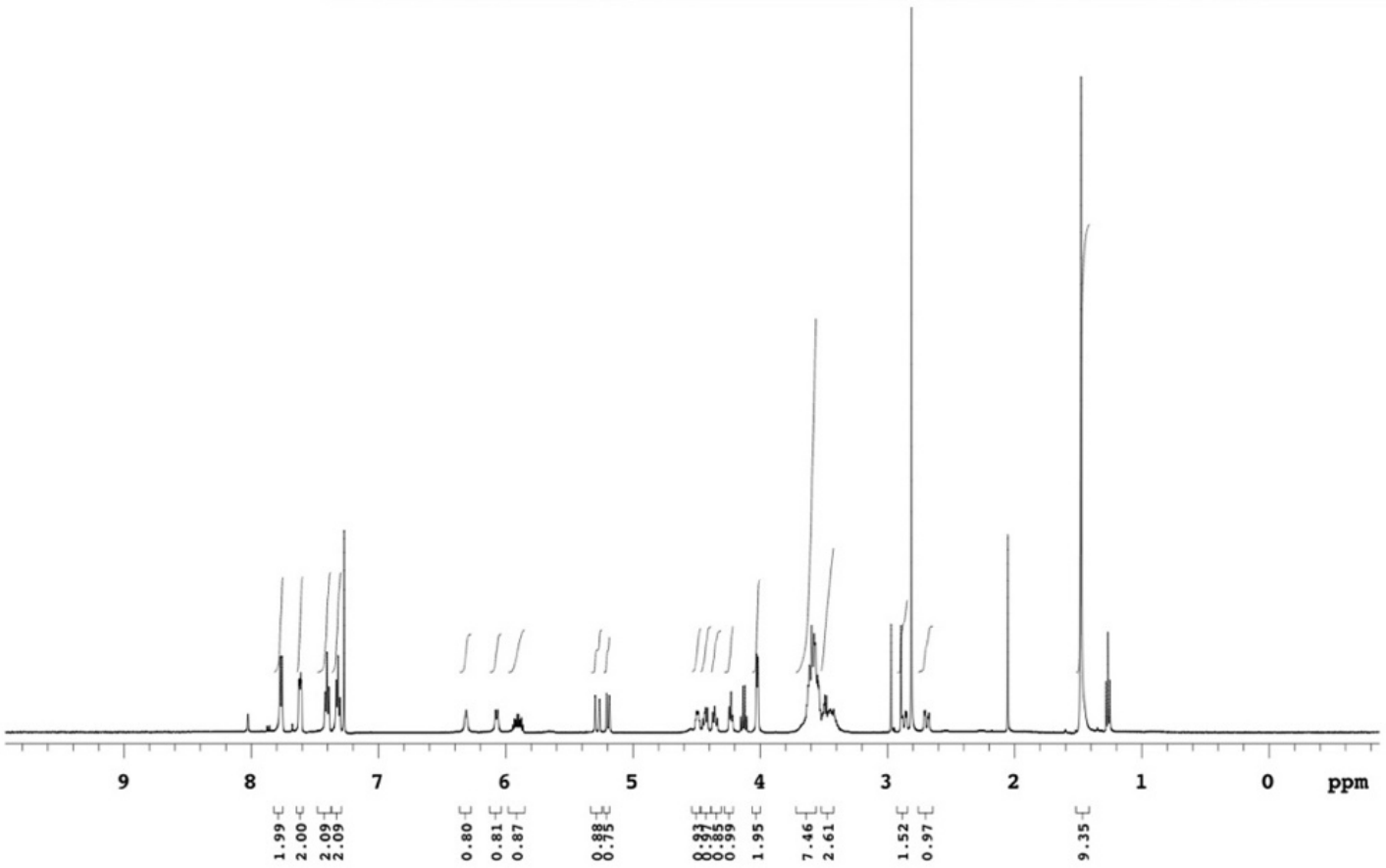


**Figure S82.** $^{1}$H NMR data for compound **QX1017**.

**(*S*)-16-((((9*H*-fluoren-9-yl)methoxy)carbonyl)amino)-14-oxo-4,7,10-trioxa-13-azaheptadec-1-en-17-oic acid (QX1019)**

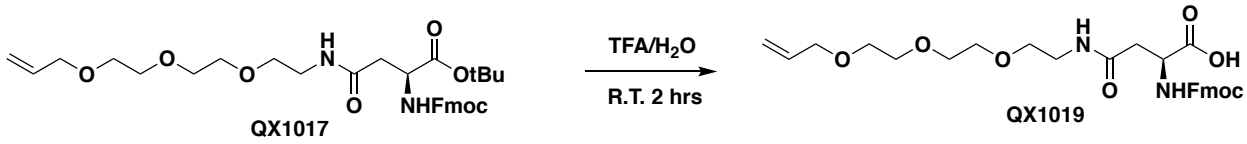


QX1017 QX1019

Compound **QX1017** (953 mg, 1.80 mmol) was dissolved in a mixture of TFA (3 ml) and water (150 uL). Then the reaction mixture was stirred at room temperature for 2 hours. After completion of the reaction, TFA and water were removed by rotavapor. Yield quantitative; MS(ESI-TOF) m/z calc. for $C_{28}H_{34}N_2O_8H^+$ 527.23, found 527.24 [M+H$^+$]; $^1$H NMR (500 MHz, Chloroform-d) δ 10.59 (s, 1H), 7.76 (d, *J* = 7.5 Hz, 2H), 7.60 (d, *J* = 7.3 Hz, 2H), 7.40 (t, *J* = 7.4 Hz, 2H), 7.32 (d, *J* = 7.4 Hz, 2H), 7.06 (s, 1H), 6.28 (d, *J* = 7.4 Hz, 1H), 5.84 (ddt, *J* = 16.6, 11.0, 5.9 Hz, 1H), 5.24 (d, *J* = 17.2 Hz, 1H), 5.18 (d, *J* = 10.3 Hz, 1H), 4.63 – 4.57 (m, 1H), 4.39 (d, *J* = 7.2 Hz, 2H), 4.22 (t, *J* = 7.1 Hz, 1H), 3.99 (d, *J* = 5.9 Hz, 2H), 3.62 – 3.50 (m, 12H), 2.92 (dd, *J* = 15.5, 3.9 Hz, 1H), 2.77 (dd, *J* = 15.3, 6.4 Hz, 1H). $^{13}$C NMR (75 MHz, Chloroform-*d*) δ 173.29, 171.91, 159.97, 159.42, 158.87, 158.33, 156.70, 143.39, 141.27, 133.35, 127.83, 127.15, 125.11, 119.99, 118.66, 116.73, 112.94, 72.23, 70.25, 70.03, 69.76, 69.02, 68.75, 67.82, 46.91, 39.77, 38.94, 37.82.

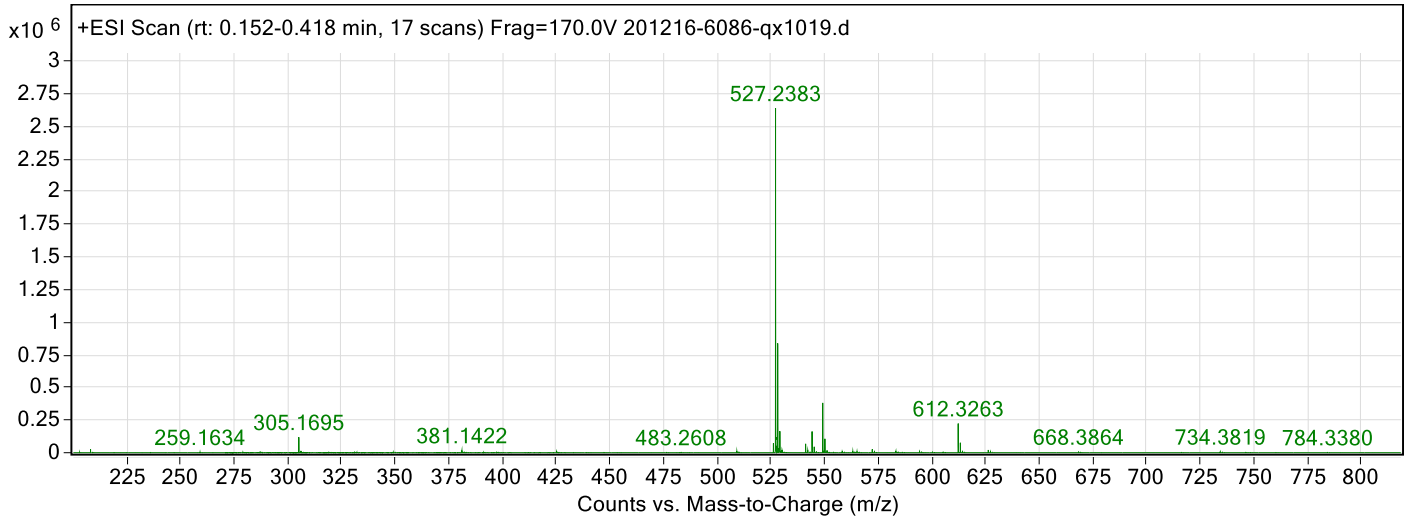


**Figure S83**. ESI-TOF MS data for compound **QX1019**.

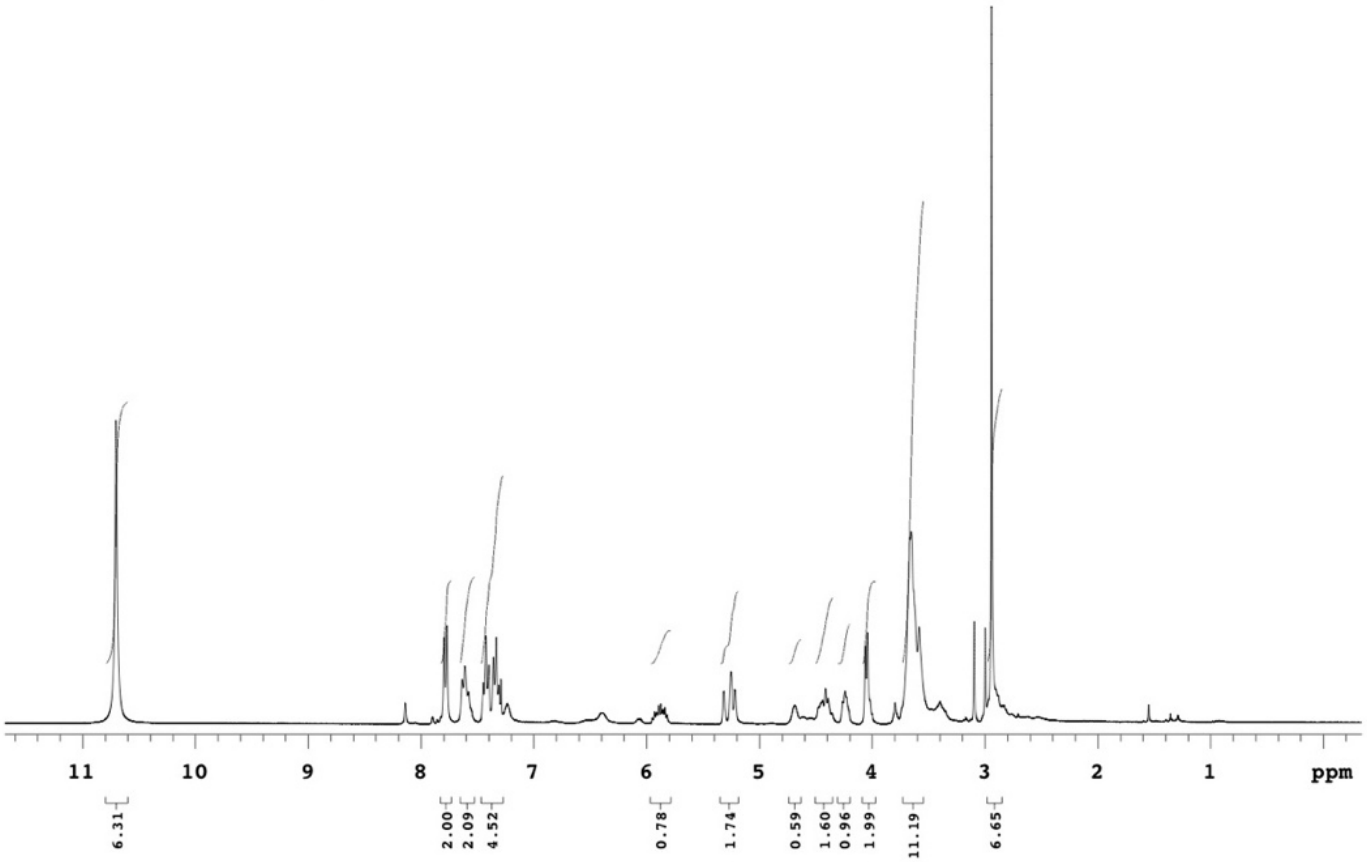


**Figure S84.** [1]H NMR data for compound **QX1019**.

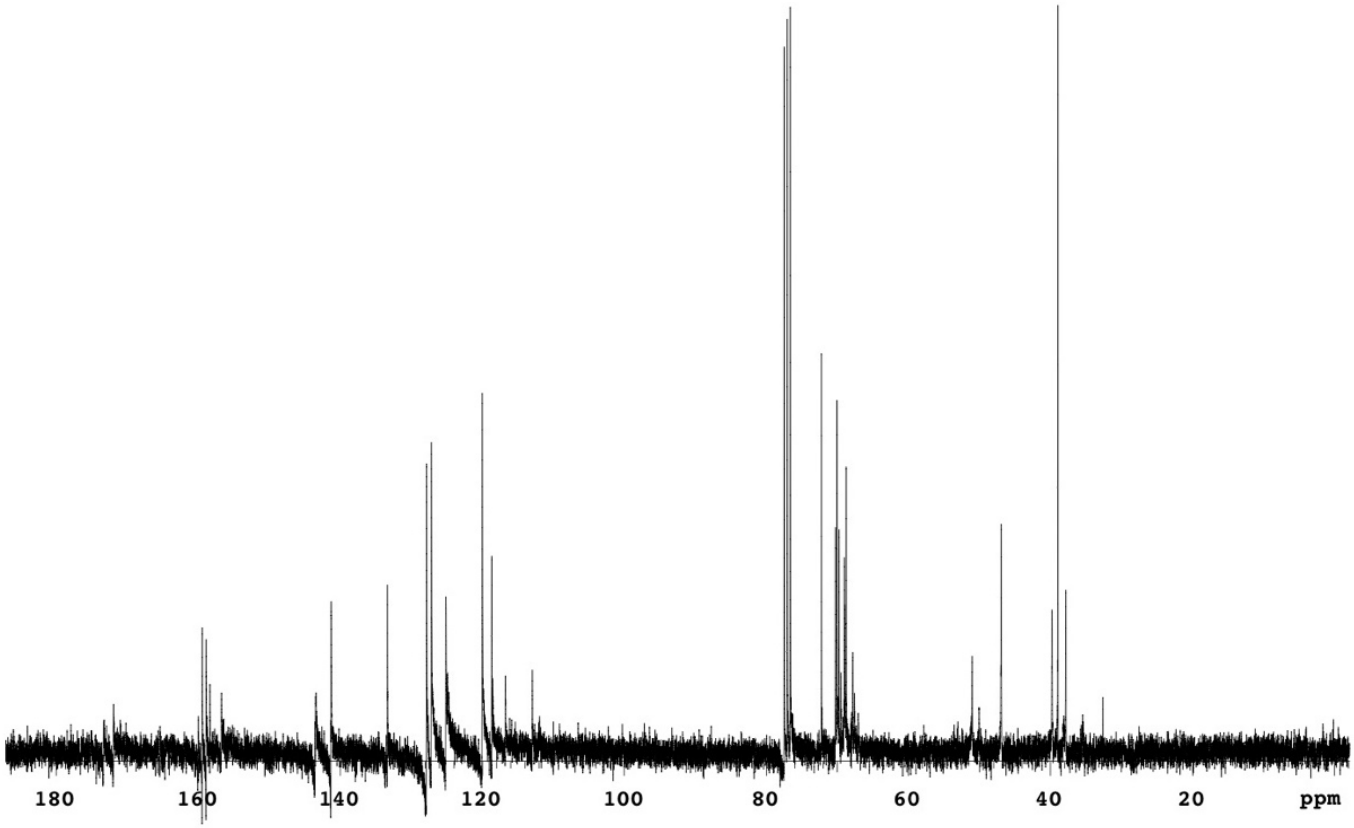


**Figure S85.** [13]C NMR data for compound **QX1019**.

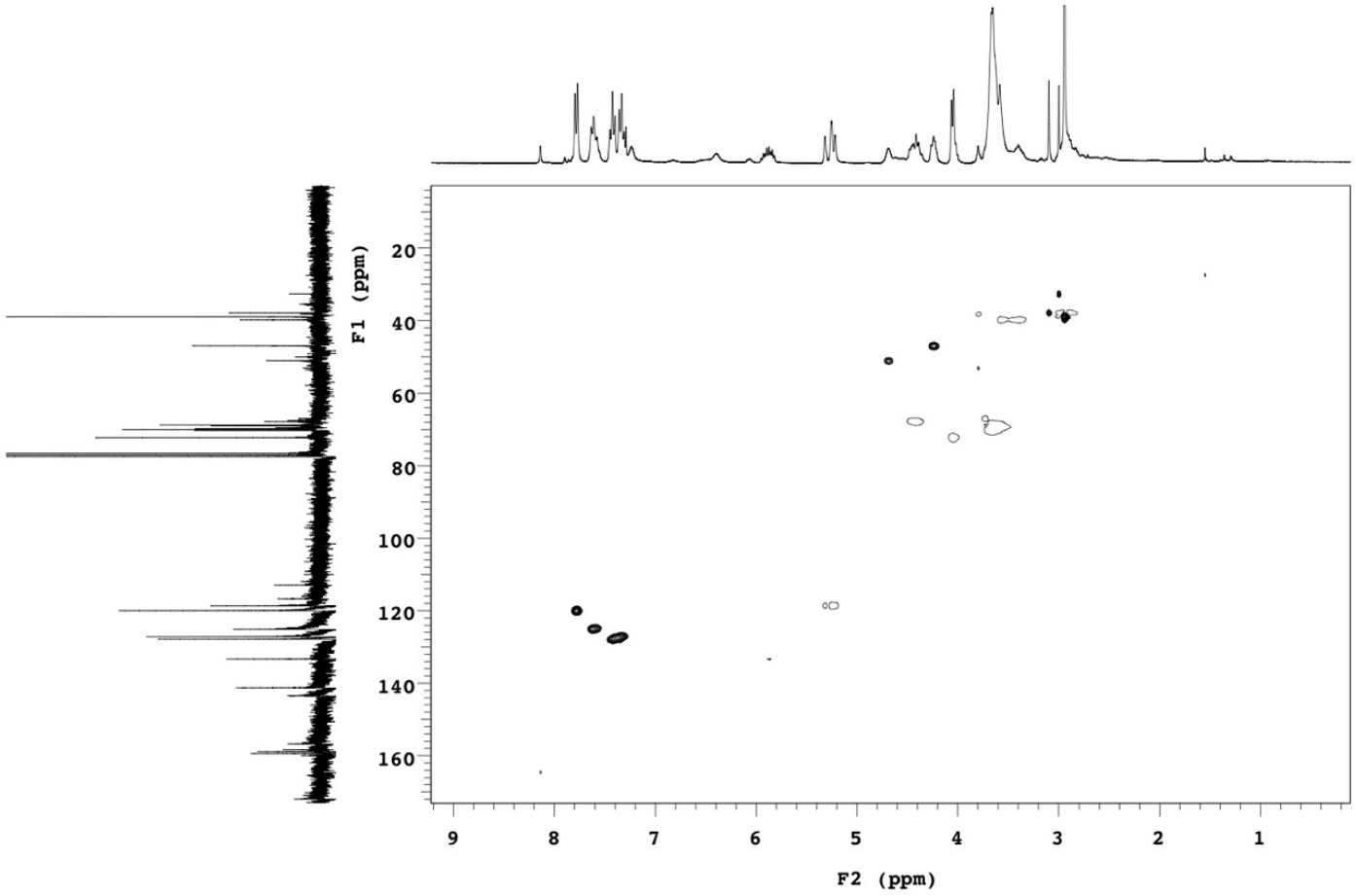


**Figure S86.** HSQC data for compound **QX1019**.

**2-(2-azidoethoxy)ethan-1-ol (QX1083)**

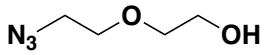


**QX1083**

Procedure was performed as described above for compound **QX1011** but using 2-(2-chloroethoxy)ethan-1-ol as starting material. Yield: 44.3% MS(ESI-TOF) m/z calc. for $C_4H_9N_3O_2H^+$ 132.08, found 132.08 [M+H$^+$]; $^1$H NMR (300 MHz, Chloroform-*d*) δ 3.77 (dd, *J* = 5.3, 3.7 Hz, 2H), 3.74 – 3.69 (m, 2H), 3.63 (dd, *J* = 5.2, 3.7 Hz, 2H), 3.43 (t, *J* = 5.0 Hz, 2H), 2.24 (b.r.s, 1H). $^{13}$C NMR (75 MHz, Chloroform-*d*) δ 72.44, 70.07, 61.79, 50.74.

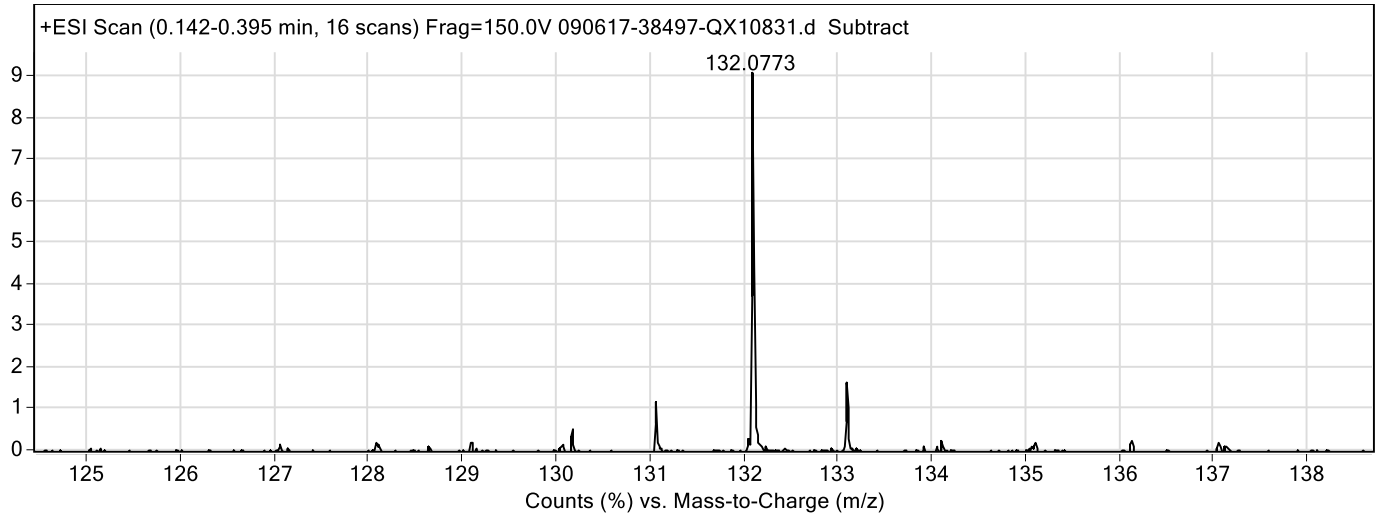


**Figure S87**. ESI-TOF MS data for compound **QX1083**.

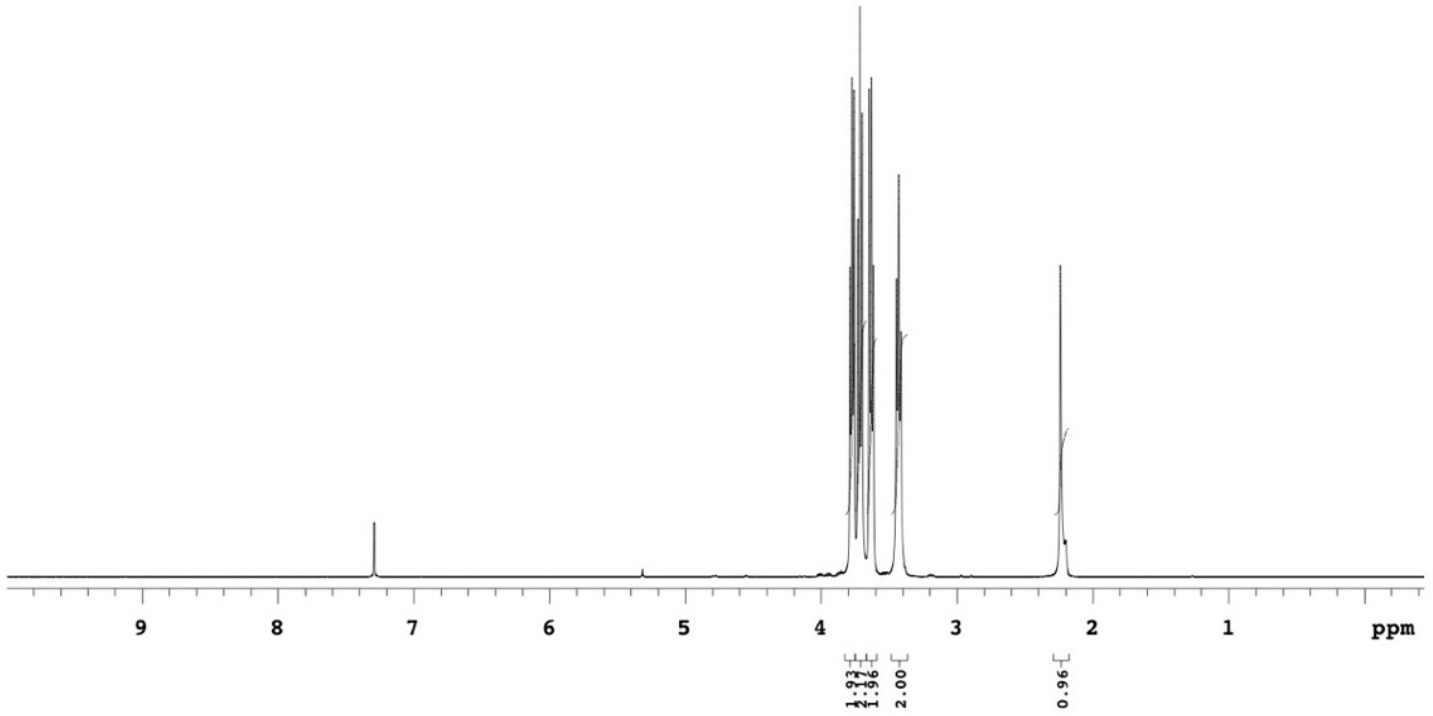


**Figure S88.** $^1$H NMR data for compound **QX1083**.

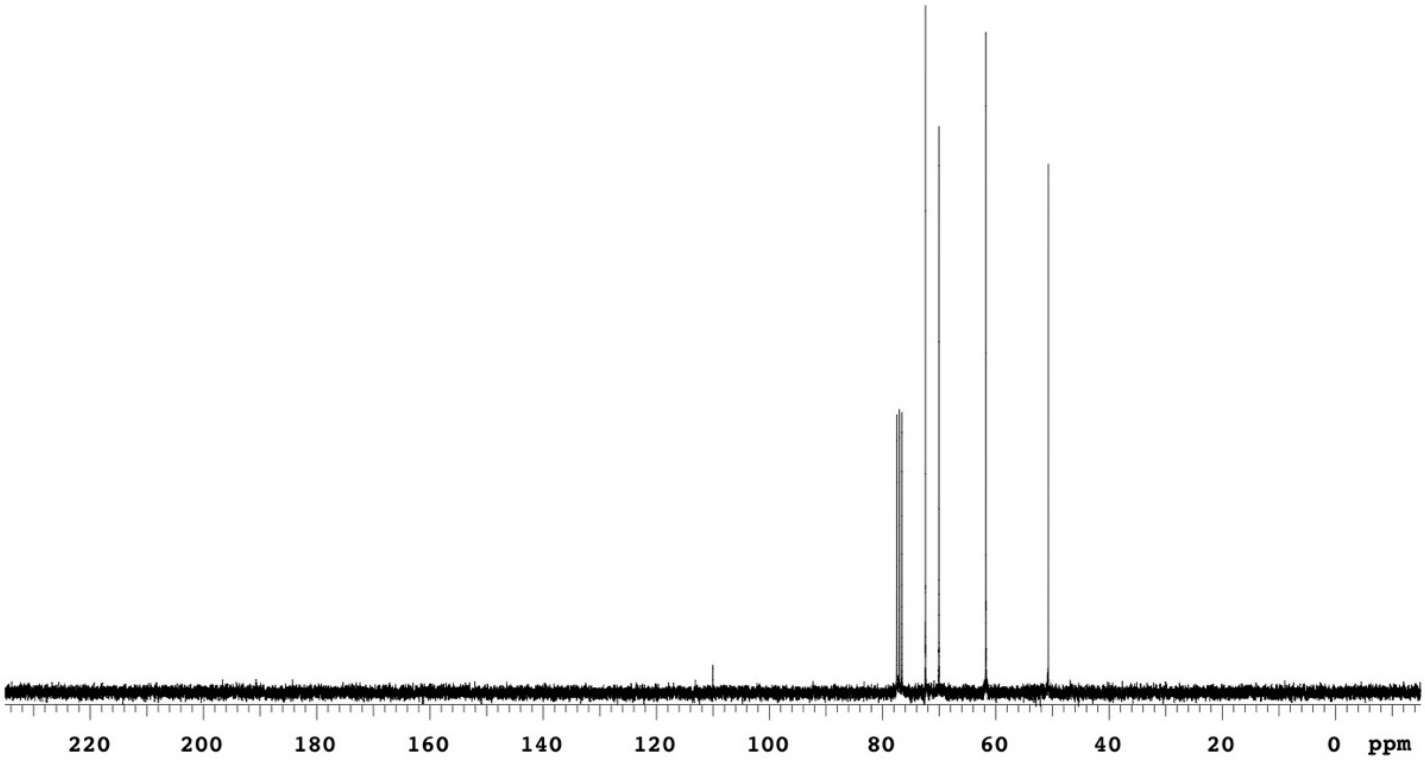


**Figure S89.** $^{13}C$ NMR data for compound **QX1083**.

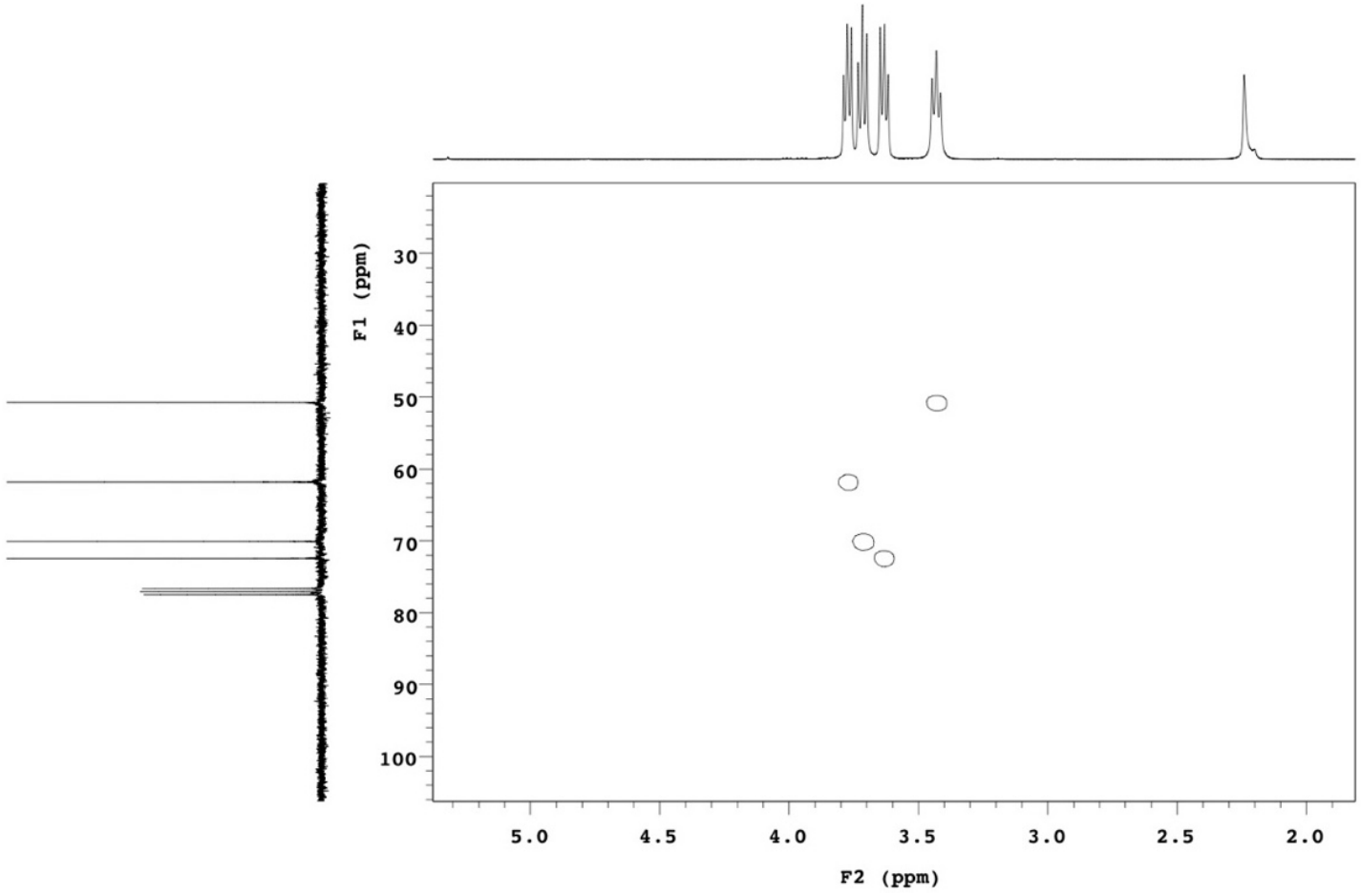


**Figure S90**. HSQC data for compound **QX1083**.

**3-(2-(2-azidoethoxy)ethoxy)prop-1-ene (QX1085)**

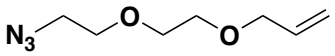

**QX1085**

Procedure was performed as described above for compound QX1013 but using QX1083 as starting material. Desired product not visible by mass spectrometry, though detectable by NMR. Yield: 82.7%; $^{1}$H NMR (500 MHz, Chloroform-*d*) δ 5.92 (ddt, *J* = 17.3, 10.3, 5.7 Hz, 1H), 5.28 (dd, *J* = 17.3, 1.7 Hz, 1H), 5.19 (dd, *J* = 10.4, 1.6 Hz, 1H), 4.04 (dt, *J* = 5.7, 1.5 Hz, 2H), 3.72 – 3.64 (m, 4H), 3.65 – 3.59 (m, 2H), 3.40 (t, *J* = 5.1 Hz, 2H). $^{13}$C NMR (126 MHz, Chloroform-*d*) δ 134.66, 117.15, 72.29, 70.73, 70.06, 69.45, 50.68.

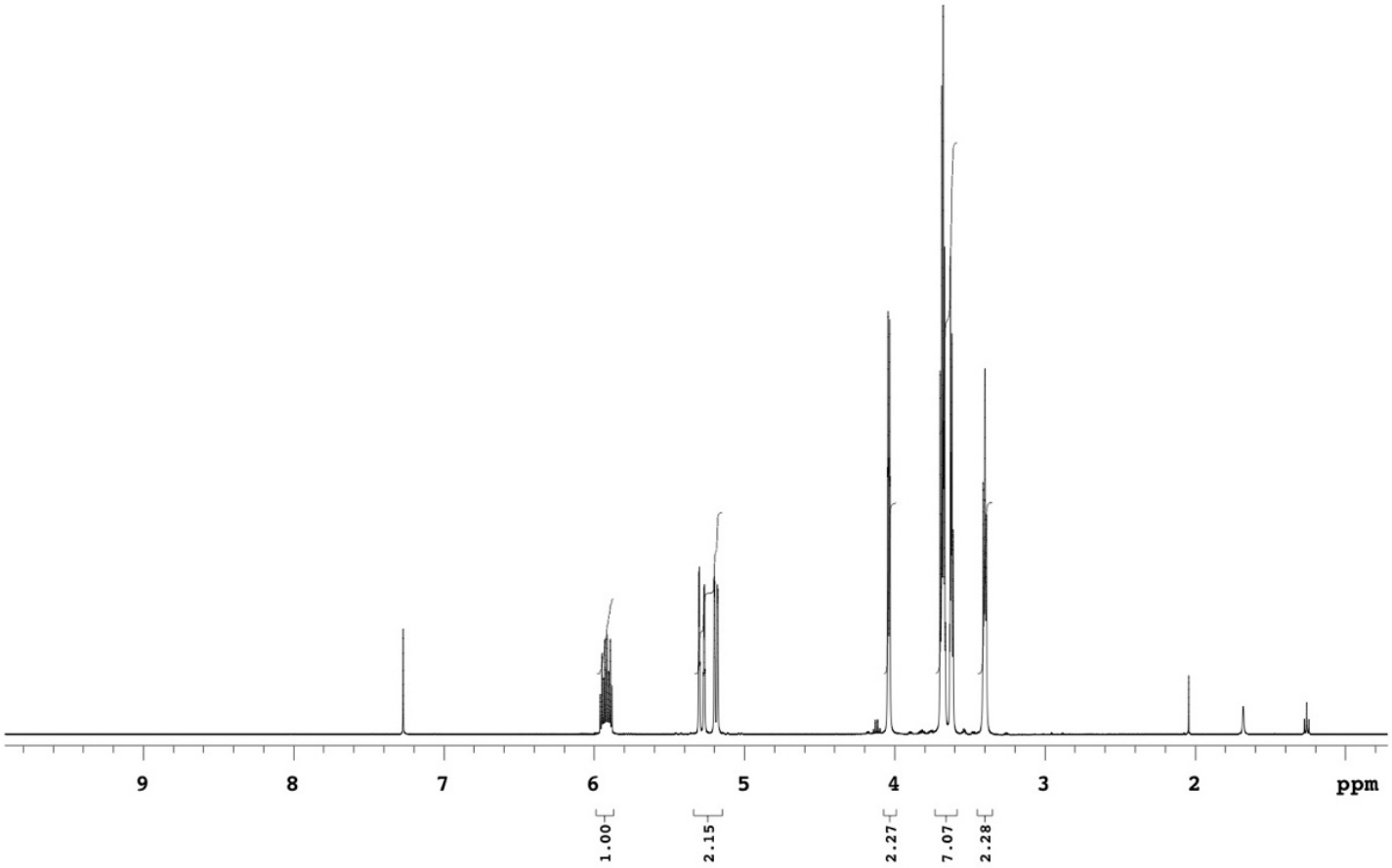


**Figure S91**. $^{1}$H NMR data for compound **QX1085**.

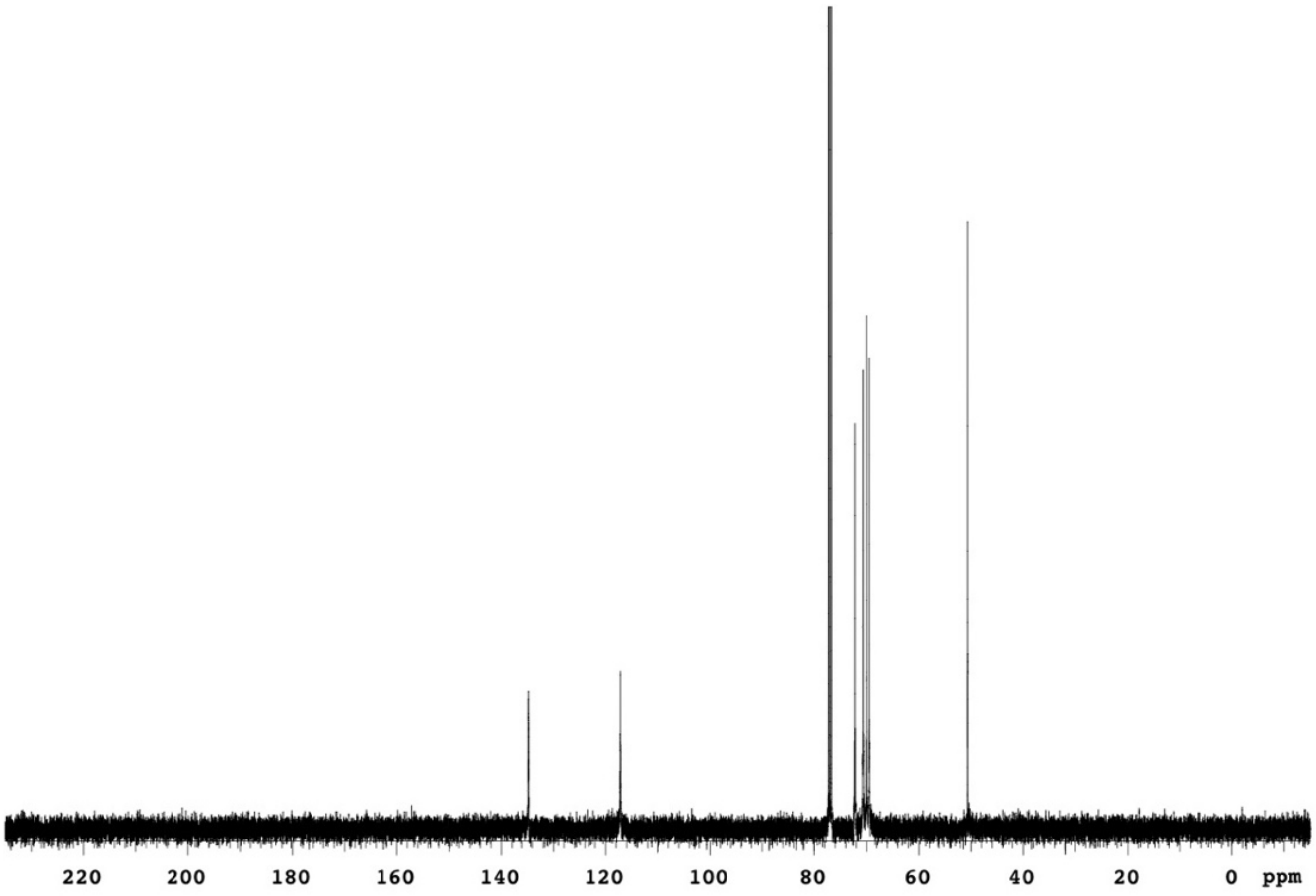


**Figure S92**. $^{13}C$ NMR data for compound **QX1085**.

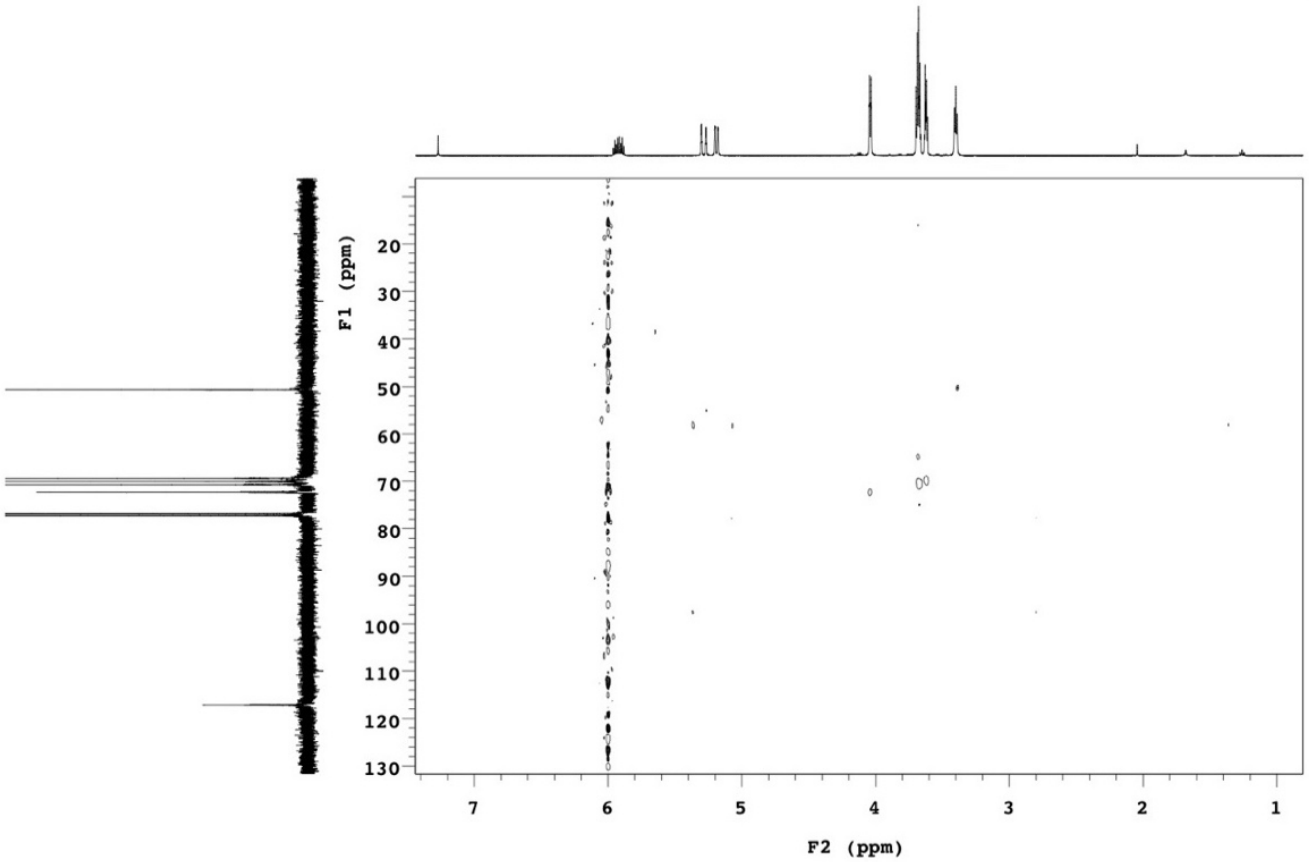

**Figure S93**. HSQC data for compound **QX1085**.

## 2-(2-(allyloxy)ethoxy)ethan-1-amine (QX1095)

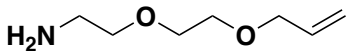

**QX1095**

Procedure was performed as described above for compound QX1015 but using QX1085 as starting material. Yield: quantitative; MS(ESI-TOF) m/z calc. for $C_7H_{15}NO_2H^+$ 146.12, found 146.12 [M+H$^+$]; $^1$H NMR (500 MHz, Chloroform-*d*) δ 8.14 (b.r.s, 2H), 5.91 (ddt, *J* = 17.3, 10.4, 5.8 Hz, 1H), 5.29 (dd, *J* = 17.2, 1.5 Hz, 1H), 5.20 (dd, *J* = 10.3, 1.2 Hz, 2H), 4.04 (d, *J* = 5.8 Hz, 1H), 3.83 (t, *J* = 5.1 Hz, 2H), 3.73 – 3.68 (m, 2H), 3.66 – 3.61 (m, 2H), 3.28 (q, *J* = 5.4 Hz, 2H). $^{13}$C NMR (126 MHz, Chloroform-*d*) δ 134.25, 117.94, 72.13, 70.21, 69.13, 66.69, 39.73.

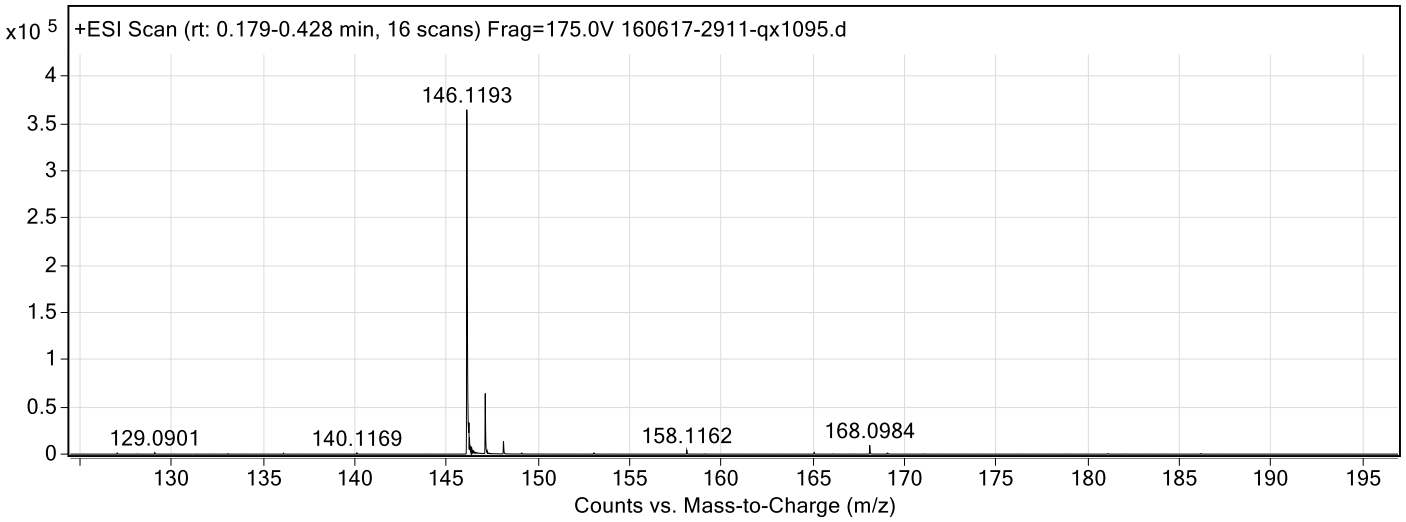


**Figure S94**. ESI-TOF MS data for compound **QX1095**.

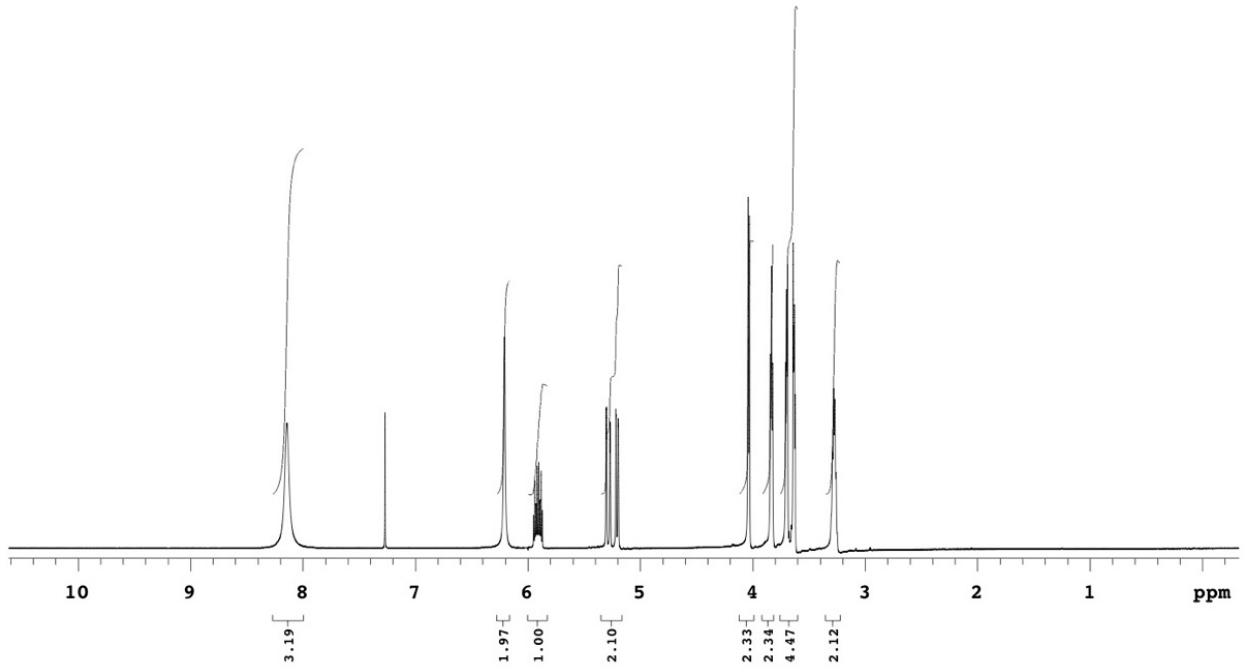


**Figure S95**. [1]H NMR data for compound **QX1095**.

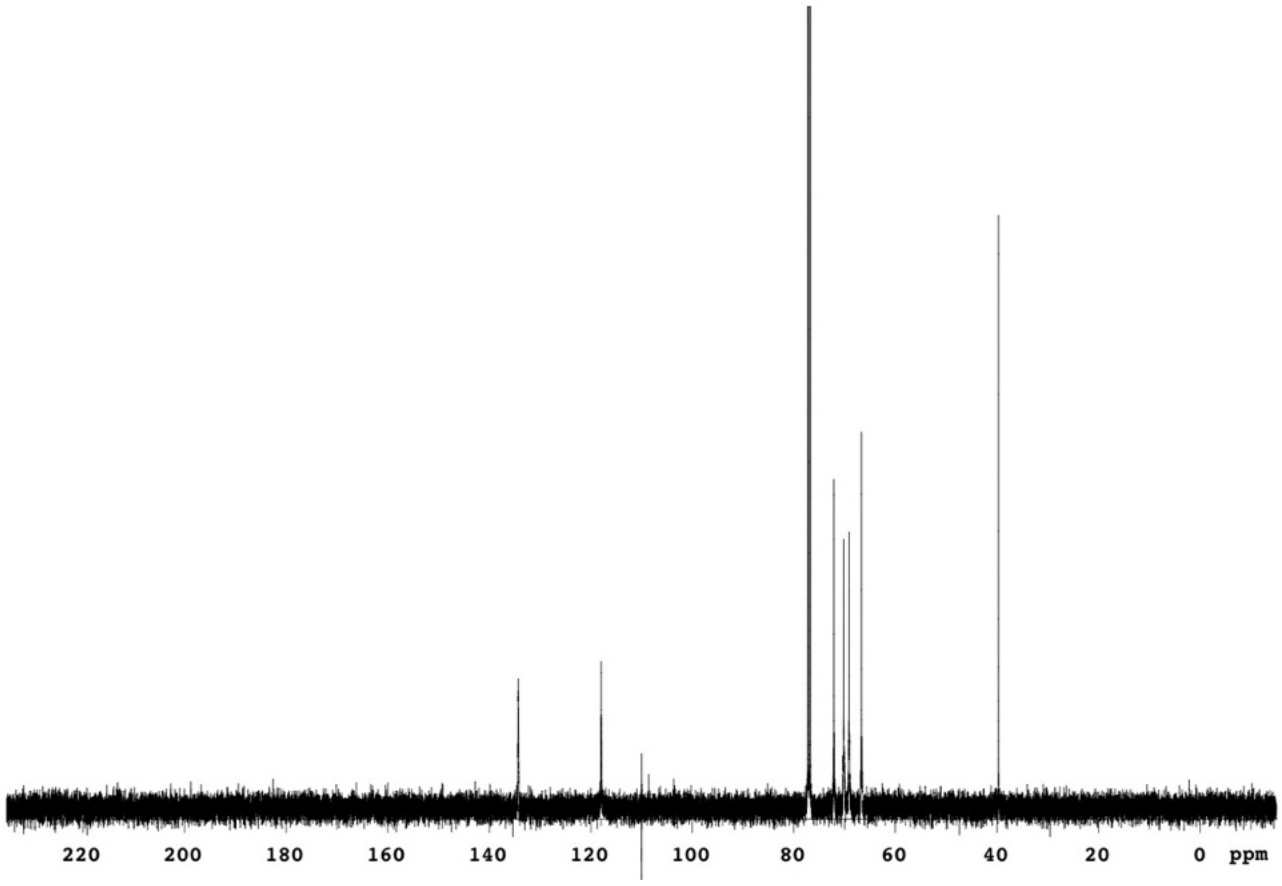


**Figure S96**. [13]C NMR data for compound **QX1095**.

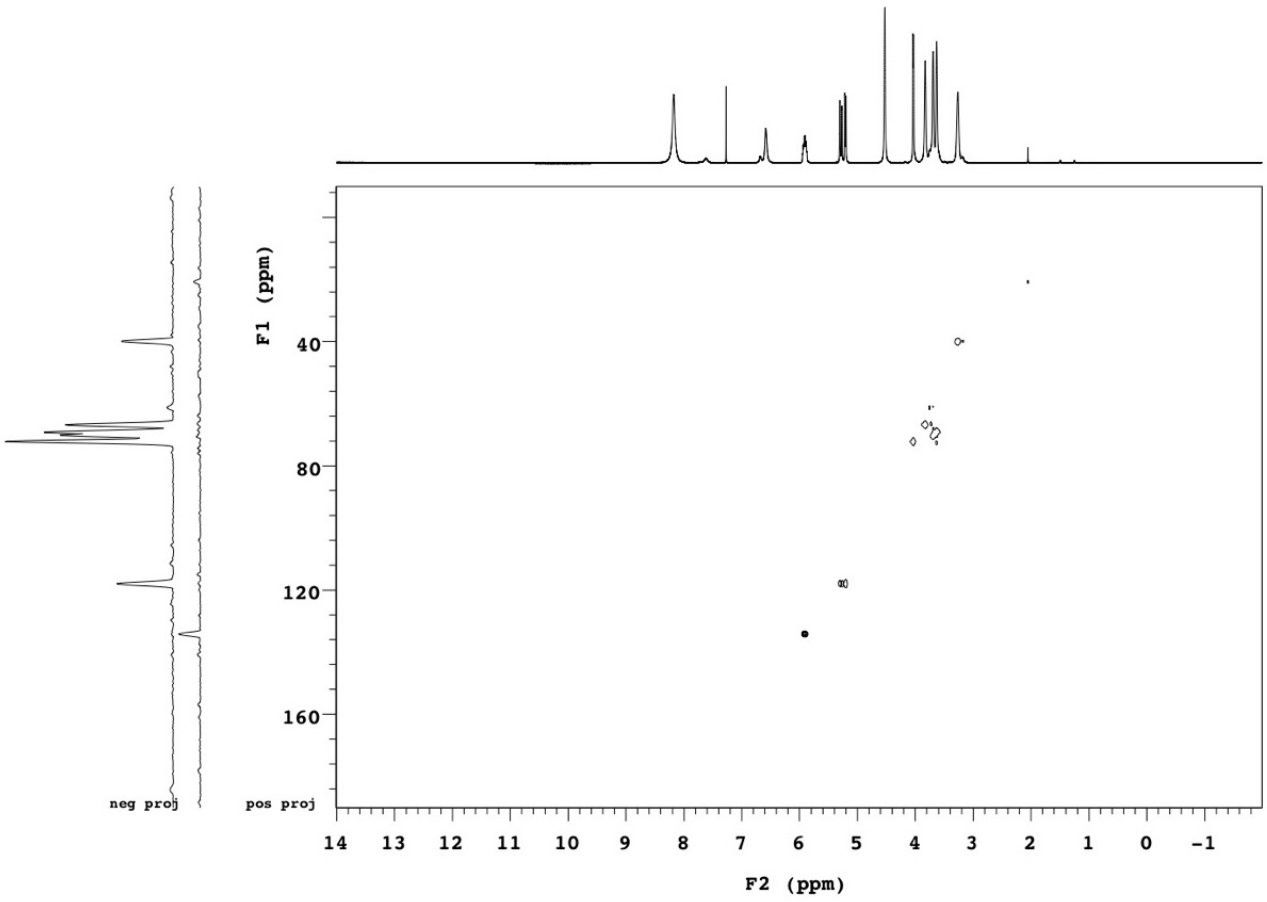


**Figure S97**. HSQC data for compound **QX1095**.

***tert*-butyl $N^2$-(((9*H*-fluoren-9-yl)methoxy)carbonyl)-$N^4$-(2-(2-(allyloxy)ethoxy)ethyl)-*L*-asparaginate (QX1099)**

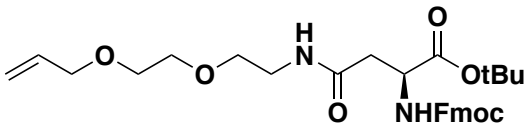


**QX1099**

Procedure was performed as described above for compound QX1017 but using QX1095 as starting material. Yield: 85.8%; MS(ESI-TOF) m/z calc. for $C_{30}H_{38}N2O_7H^+$ 539.28, found 539.28 [M+H$^+$]; $^1$H NMR (300 MHz, Chloroform-*d*) δ 7.78 (d, *J* = 7.5 Hz, 2H), 7.63 (d, *J* = 7.2 Hz, 2H), 7.41 (t, *J* = 7.3 Hz, 2H), 7.33 (t, *J* = 7.4 Hz, 2H), 6.26 (t, *J* = 6.0 Hz, 1H), 6.11 (d, *J* = 8.4 Hz, 1H), 5.92 (ddt, *J* = 16.4, 10.9, 5.7 Hz, 1H), 5.29 (dd, *J* = 17.2, 1.7 Hz, 1H), 5.21 (dd, *J* = 10.4, 1.5 Hz, 1H), 4.50 (dt, *J* = 8.9, 4.7 Hz, 1H), 4.43 (dd, *J* = 10.3, 7.4 Hz, 1H), 4.33 (t, *J* = 8.8 Hz, 1H), 4.25 (dd, *J* = 10.3, 7.1 Hz, 1H), 4.03 (d, *J* = 5.7 Hz, 2H), 3.58 (dt, *J* = 9.4, 3.5 Hz, 6H), 3.47 (q, *J* = 5.3 Hz, 2H), 2.91 (dd, *J* = 15.6, 4.5 Hz, 1H), 2.72 (dd, *J* = 15.6, 4.5 Hz, 1H), 1.49 (s, 9H). $^{13}$C NMR (75 MHz, Chloroform-*d*) δ 170.02, 169.83, 162.57, 156.19, 143.96, 141.26, 134.48, 127.67, 127.06, 125.20, 119.93, 117.45, 109.99, 82.22, 72.23, 70.30, 69.68, 69.33, 67.11, 51.43, 47.15, 39.23, 38.62, 37.92, 36.50, 31.45, 27.93.

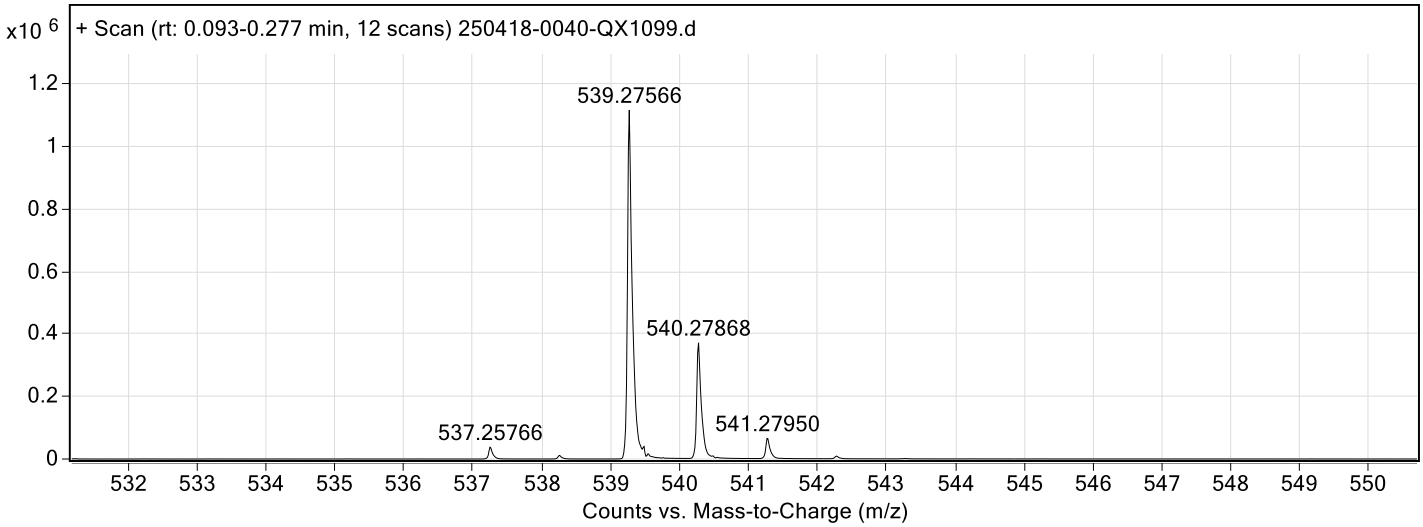


**Figure S98**. ESI-TOF data for compound **QX1099**.

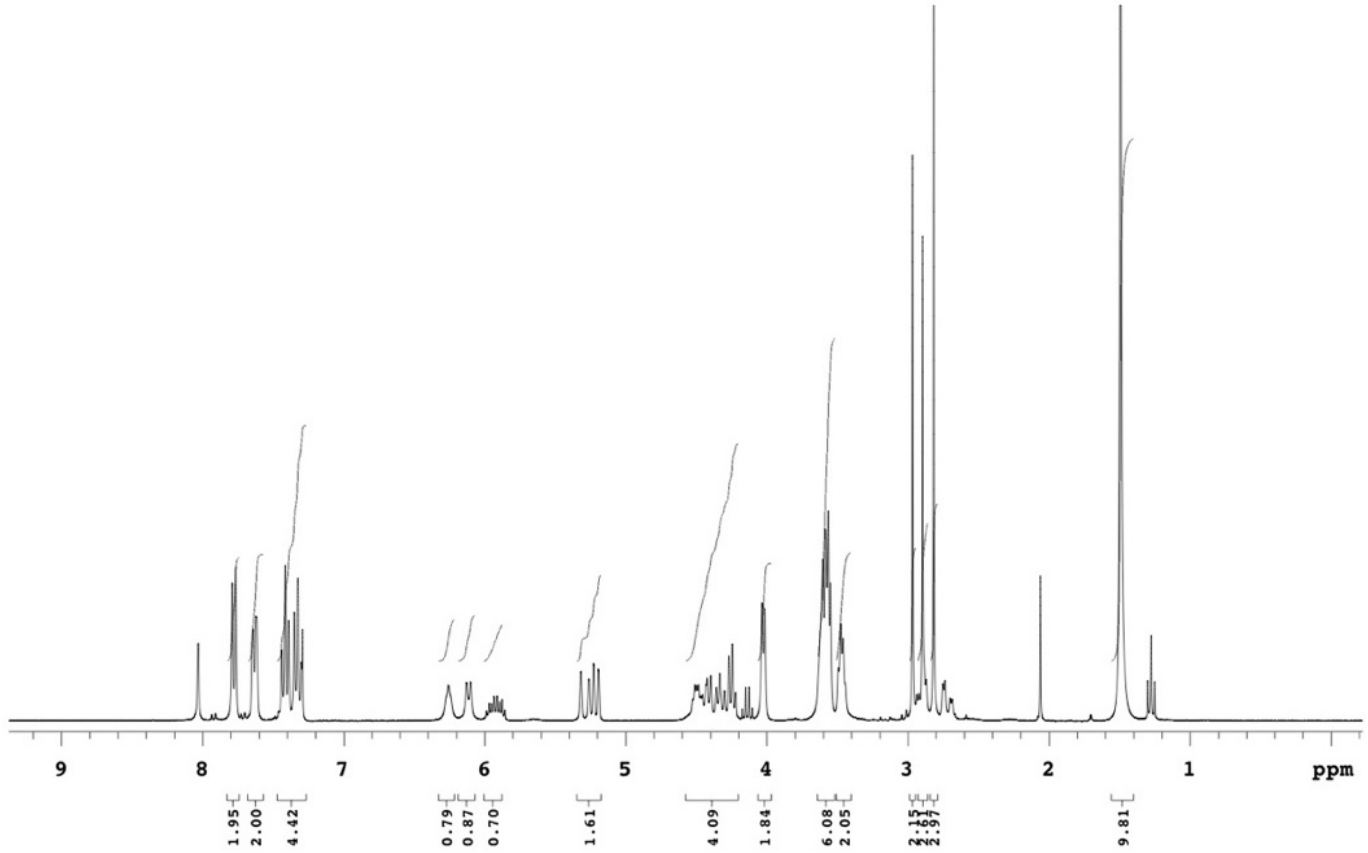


**Figure S99**. $^{1}$H NMR data for compound **QX1099**.

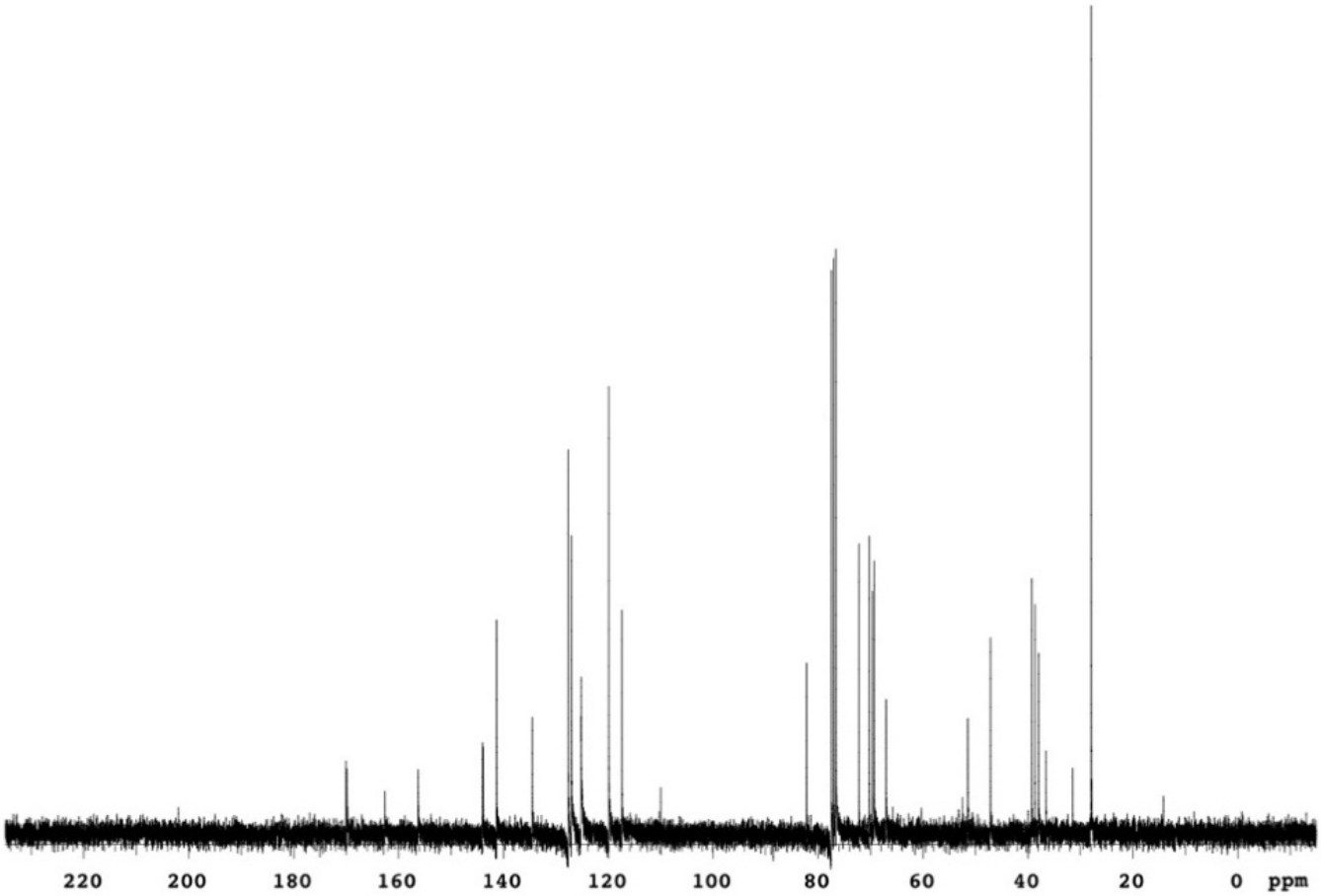


**Figure S100**. $^{13}C$ NMR data for compound **QX1099**.

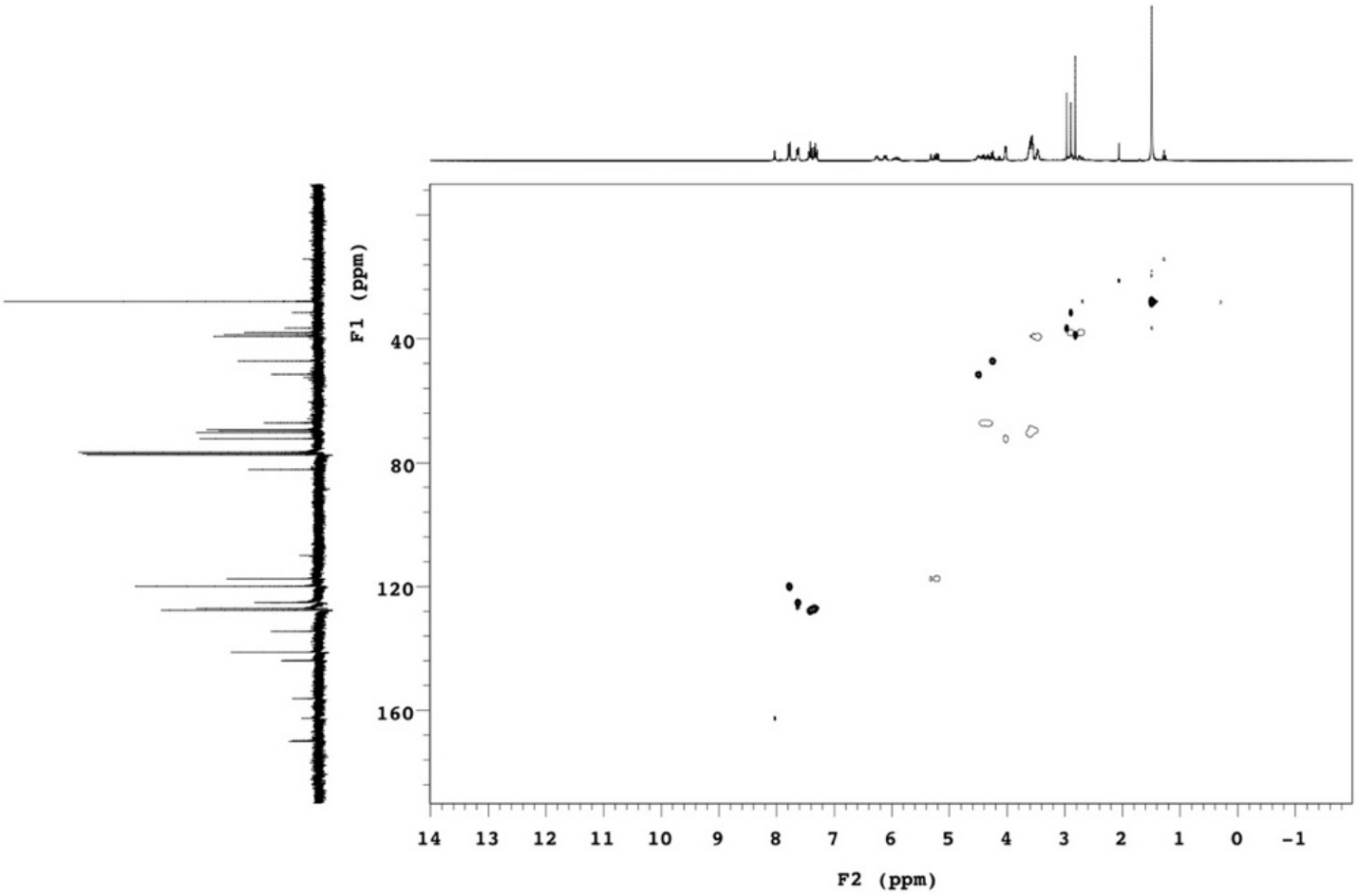


**Figure S101**. HSQC data for compound **QX1099**.

## $N^2$-(((9*H*-fluoren-9-yl)methoxy)carbonyl)-$N^4$-(2-(2-(allyloxy)ethoxy)ethyl)-*L*-asparagine (QX1101)

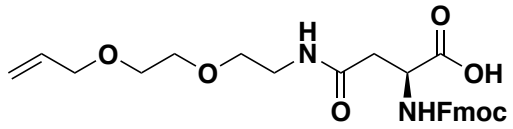

QX1101

Procedure was performed as described above for compound QX1019 but using QX1099 as starting material. Yield: quantitative; MS(ESI-TOF) m/z calc. for $C_{26}H_{30}N_2O_7H^+$ 482.22, found 482.23. [M+H$^+$]; $^1$H NMR (300 MHz, Chloroform-*d*) δ 10.94 (b.r.s, 1H), 7.79 (d, *J* = 7.5 Hz, 2H), 7.61 (dd, *J* = 12.4, 7.4 Hz, 2H), 7.43 (t, *J* = 7.4 Hz, 2H), 7.34 (t, *J* = 7.4 Hz, 2H), 6.98 (s, 1H), 6.30 (d, *J* = 7.5 Hz, 1H), 5.89 (ddt, *J* = 16.4, 11.7, 6.1 Hz, 1H), 5.39 – 5.16 (m, 2H), 4.74 – 4.33 (m, 2H), 4.24 (q, *J* = 6.3 Hz, 1H), 4.07 (dd, *J* = 16.4, 5.9 Hz, 2H), 3.84 – 3.54 (m, 8H), 2.90 (dd, *J* = 18.3, 5.4 Hz, 1H), 2.77 (dd, *J* = 18.3, 5.4 Hz, 1H).

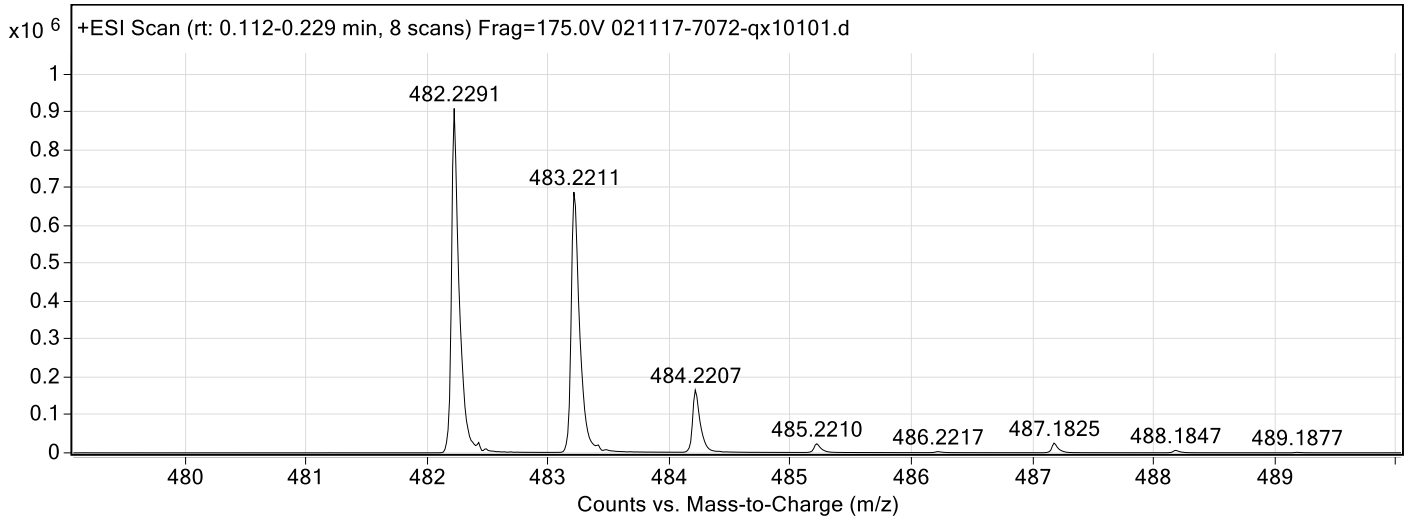


**Figure S102**. ESI-TOF MS data for compound **QX1101**.

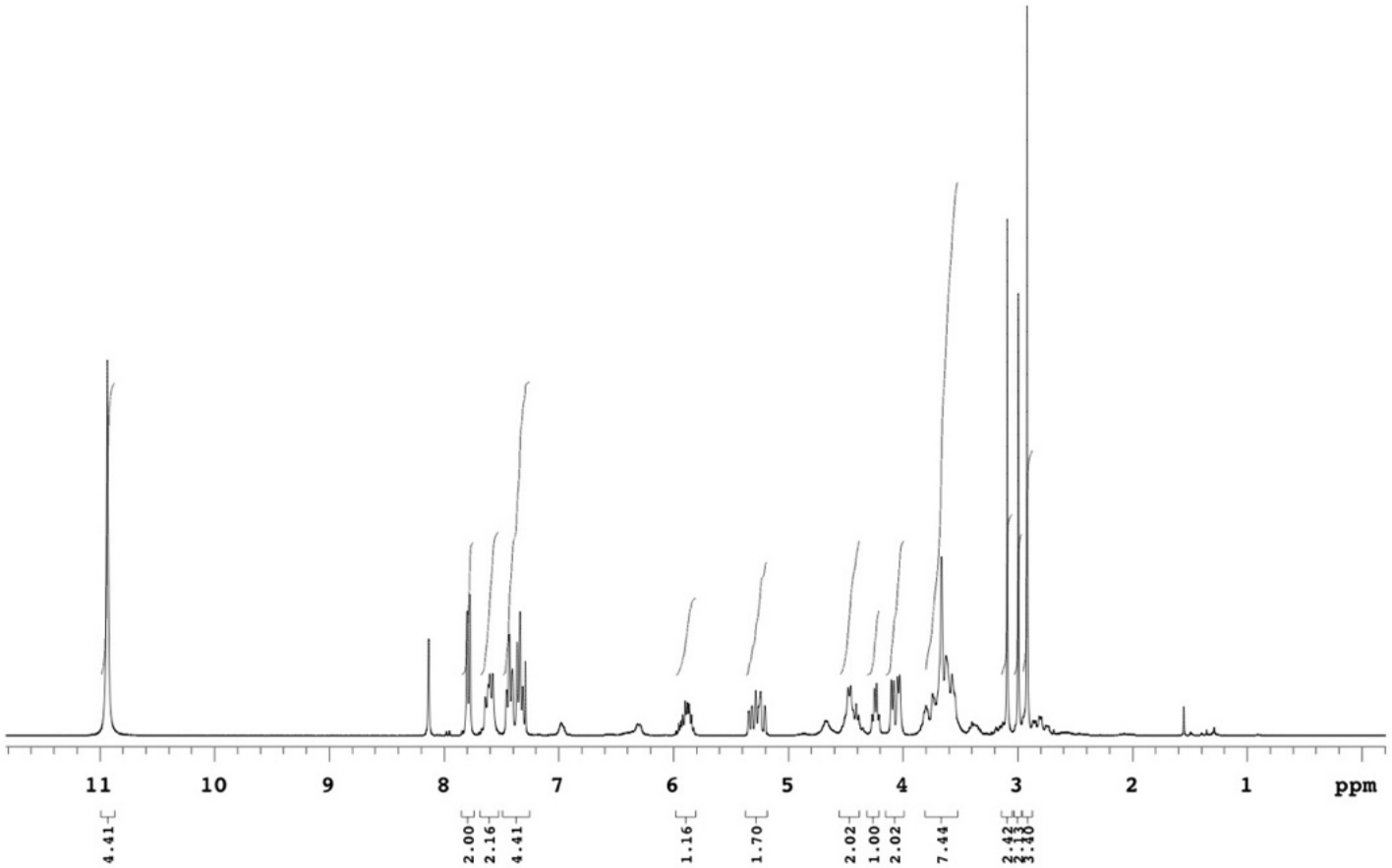


**Figure S103**. [1]H NMR data for compound **QX1101**.

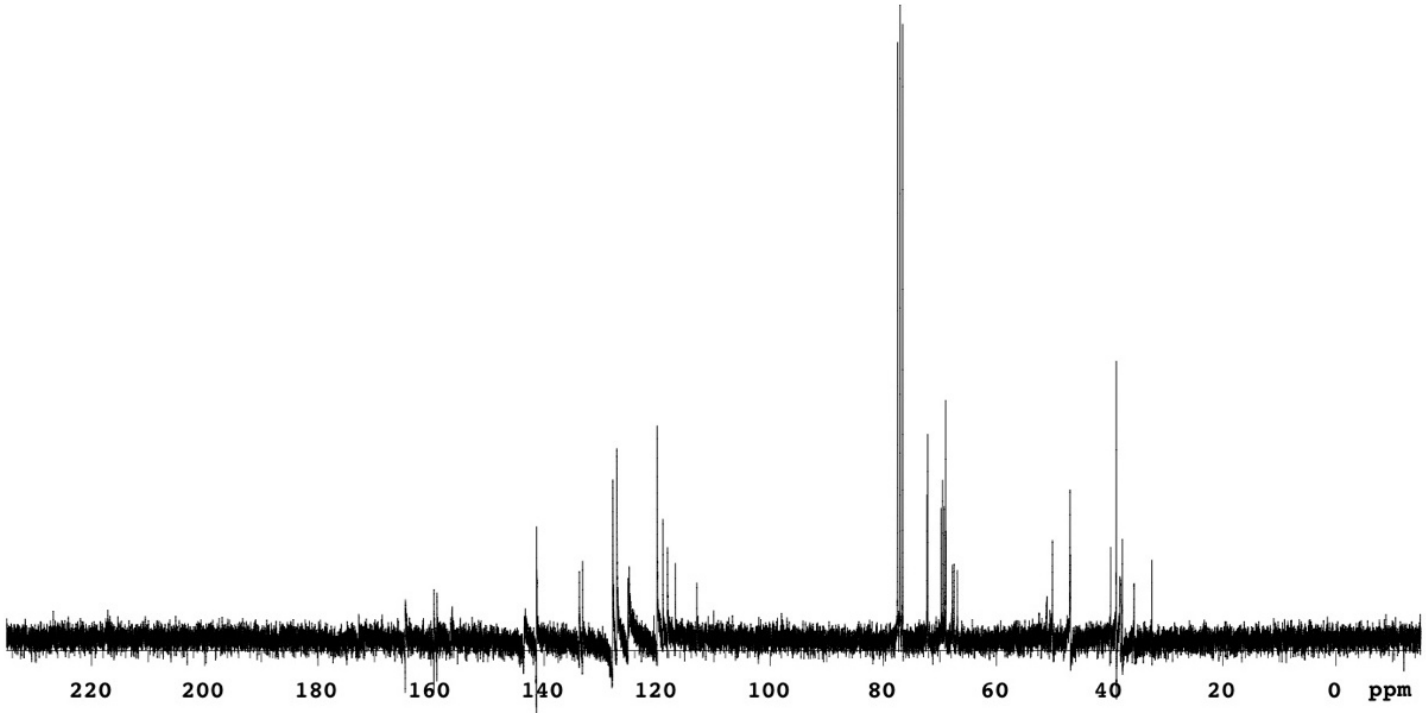


**Figure S104**. [13]C NMR data for compound **QX1101**.

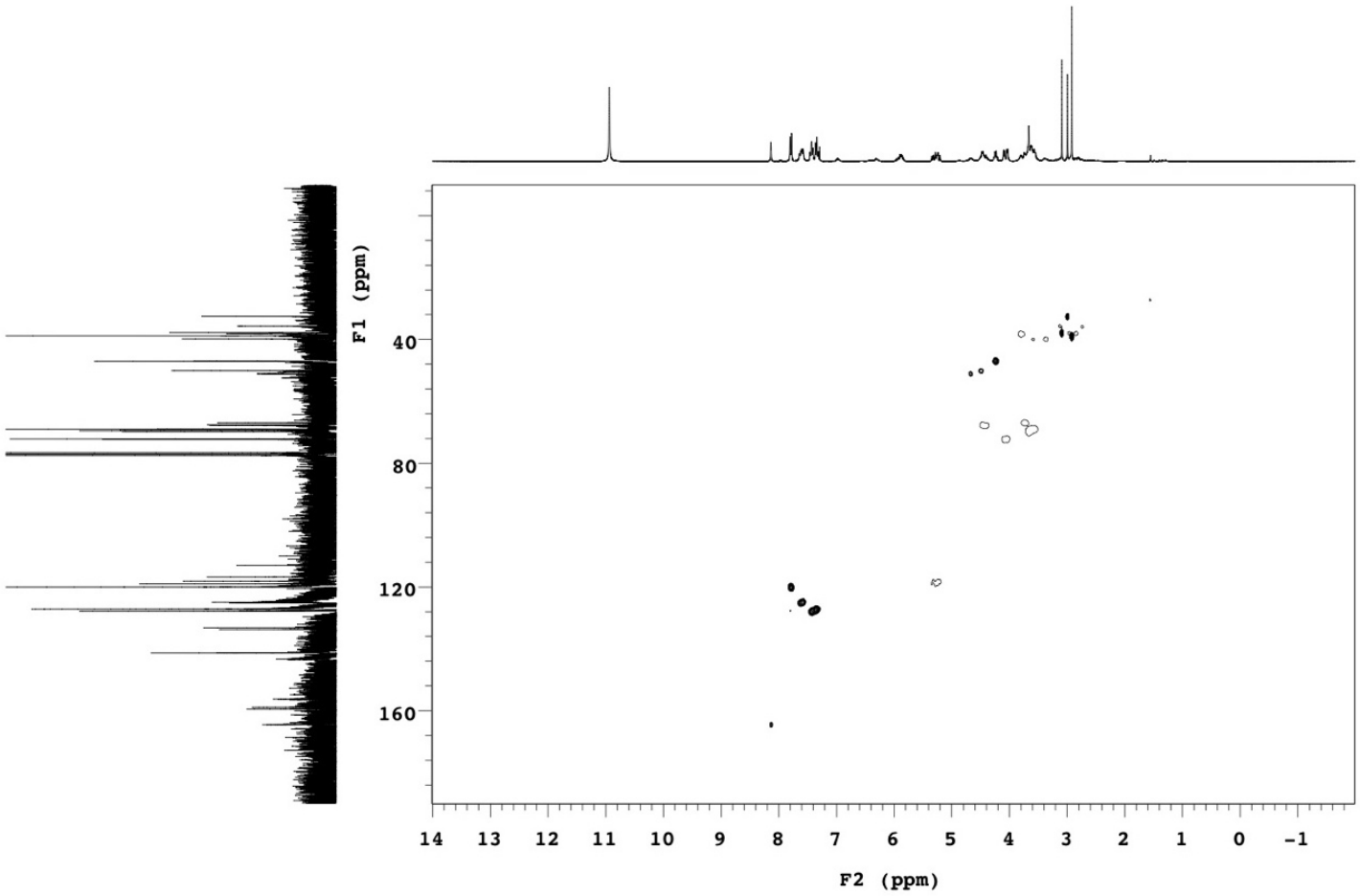


**Figure S105**. HSQC data for compound **QX1101**.

**2-(allyloxy)ethan-1-amine (QX1107)**

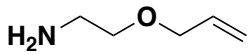

**QX1107**

Procedure was performed as described above for compound QX1015 but using 2-azidoethan-1-ol as starting material. Yield: 90.7%; MS(ESI-TOF) m/z calc. for $C_5H_{11}NOH^+$ 102.09, found 102.09 [M+H$^+$]; $^1$H NMR (300 MHz, Chloroform-*d*) δ 8.24 (s, 2H), 5.95 (ddt, *J* = 16.4, 10.9, 5.6 Hz, 1H), 5.34 (dd, *J* = 17.3, 1.7 Hz, 1H), 5.23 (d, *J* = 10.4 Hz, 1H), 4.09 (d, *J* = 5.6 Hz, 2H), 3.78 (t, *J* = 5.1 Hz, 2H), 3.28 (q, *J* = 5.4 Hz, 2H). $^{13}$C NMR (75 MHz, Chloroform-*d*) δ 134.07, 117.93, 72.12, 65.41, 39.68.

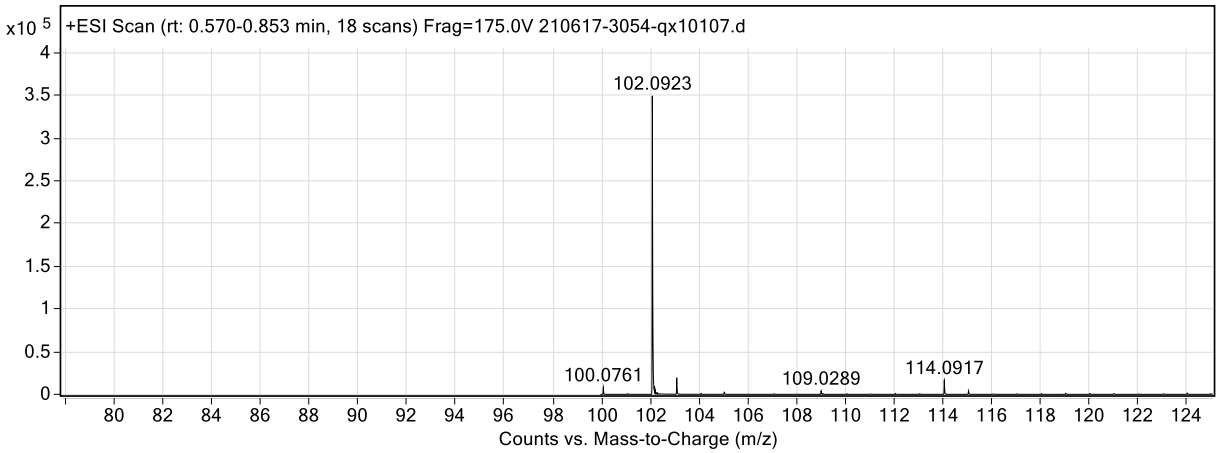


**Figure S106**. ESI-TOF MS data for compound **QX1107**.

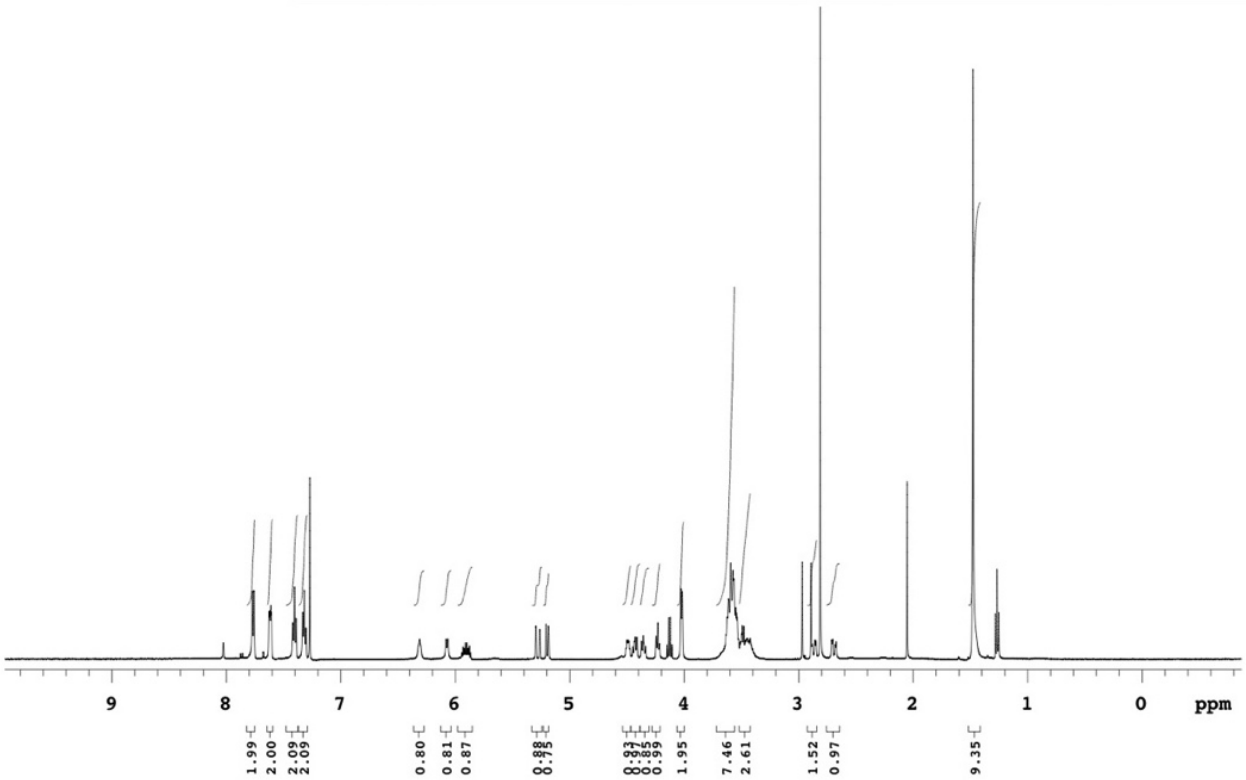

**Figure S107**. $^{1}H$ NMR data for compound **QX1107**.

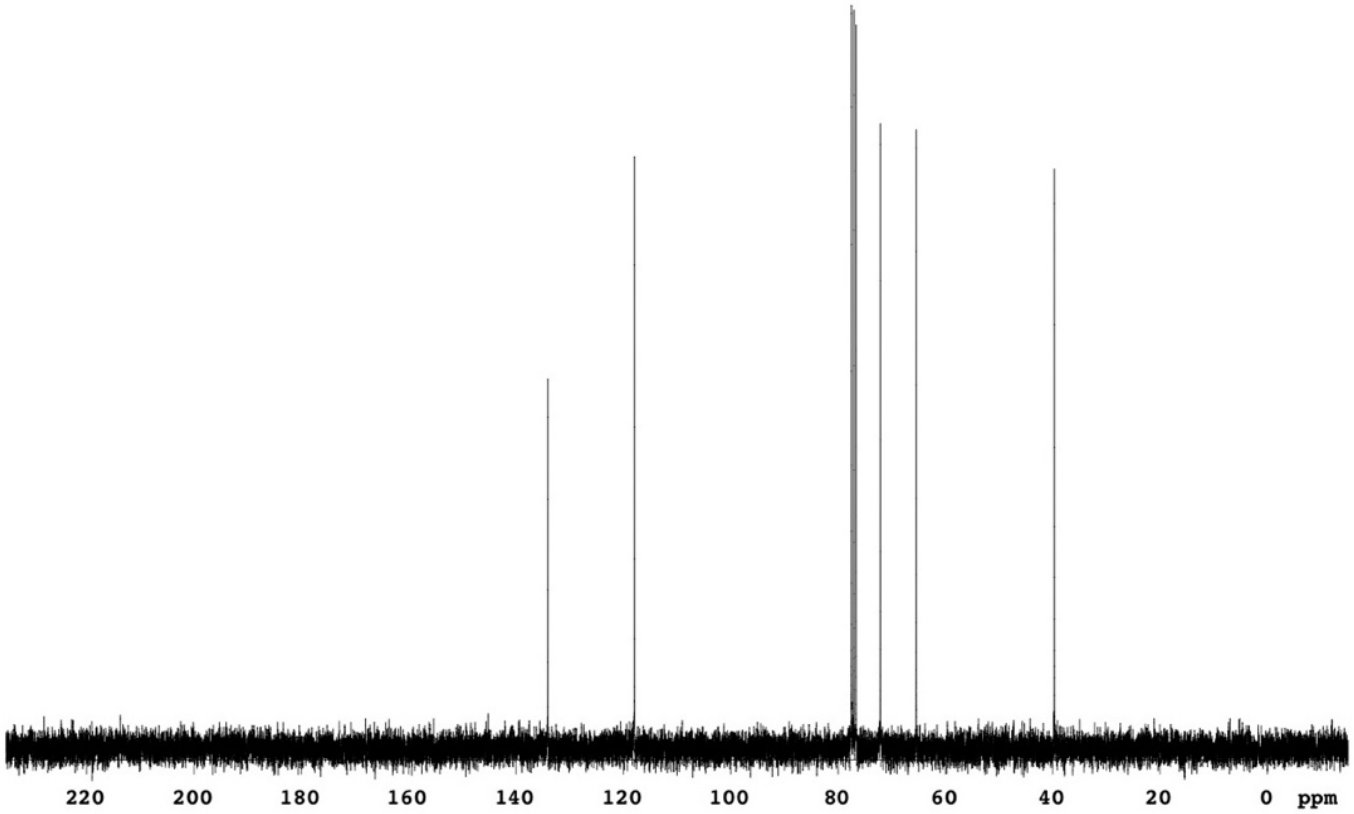


**Figure S108**. $^{13}C$ NMR data for compound **QX1107**.

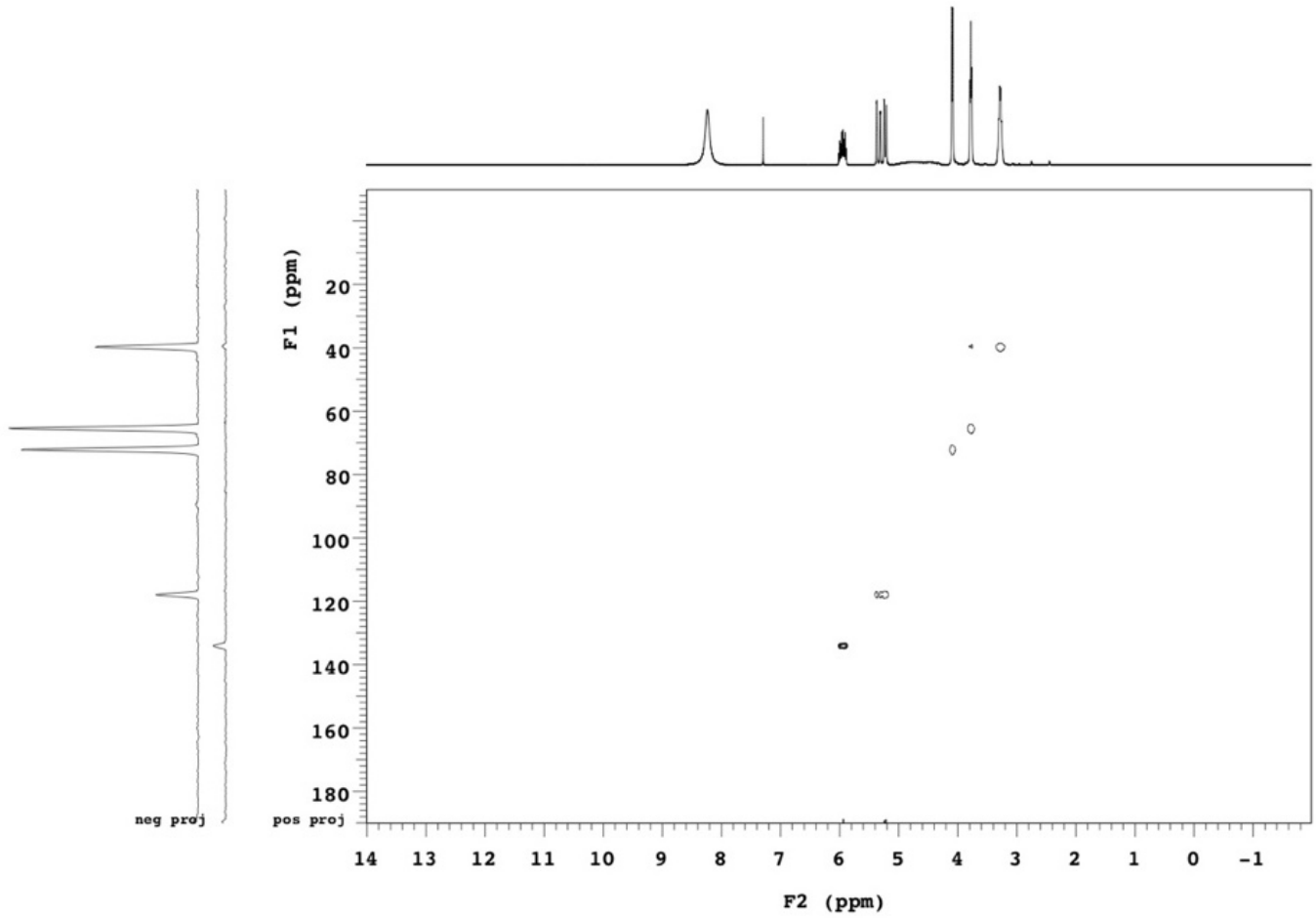


**Figure S109**. HSQC data for compound **QX1107**.

## *N*$^2$-(((9*H*-fluoren-9-yl)methoxy)carbonyl)-*N*$^4$-(2-(allyloxy)ethyl)-*L*-asparagine (QX1111)

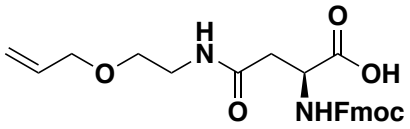


QX1111

Procedure was performed as described above for compound QX1019 but using QX1107 as starting material. Yield: quantitative; MS(ESI-TOF) m/z calc. for $C_{24}H_{26}N_2O_6H^+$ 439.19, found 439.18 [M+H$^+$]; $^1$H NMR (300 MHz, Chloroform-*d*) δ 9.38 (s, 1H), 7.79 (d, *J* = 7.5 Hz, 2H), 7.62 (d, *J* = 7.7 Hz, 2H), 7.43 (t, *J* = 7.4 Hz, 2H), 7.34 (t, *J* = 7.4 Hz, 2H), 6.88 (s, 1H), 6.38 (d, *J* = 7.1 Hz, 1H), 5.88 (ddt, *J* = 16.5, 11.1, 5.8 Hz, 1H), 5.29 (d, *J* = 16.3 Hz, 1H), 5.25 (d, *J* = 9.9 Hz, 1H), 4.69 – 4.60 (m, 1H), 4.42 (qd, *J* = 10.5, 6.8 Hz, 2H), 4.31 – 4.14 (m, 1H), 4.02 (d, *J* = 6.0 Hz, 2H), 3.62 – 3.39 (m, 4H), 3.05 (dd, *J* = 17.9, 5.7 Hz, 1H), 2.90 (dd, *J* = 15.9, 6.6 Hz, 1H). $^{13}$C NMR (75 MHz, Chloroform-*d*) δ 174.13, 171.82, 159.62, 159.07, 156.79, 143.34, 141.32, 133.32, 127.89, 127.17, 125.08, 120.07, 118.68, 116.54, 112.76, 109.98, 72.11, 67.92, 67.83, 50.62, 46.92, 39.84, 37.63.

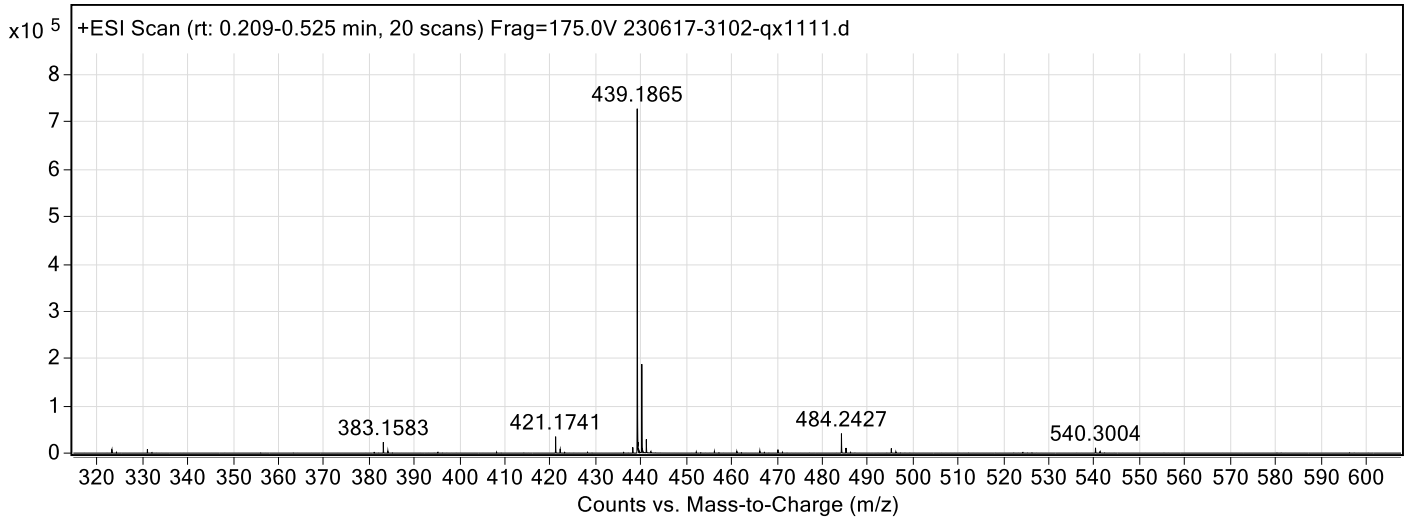


**Figure S110**. ESI-TOF MS data for compound **QX1111**.

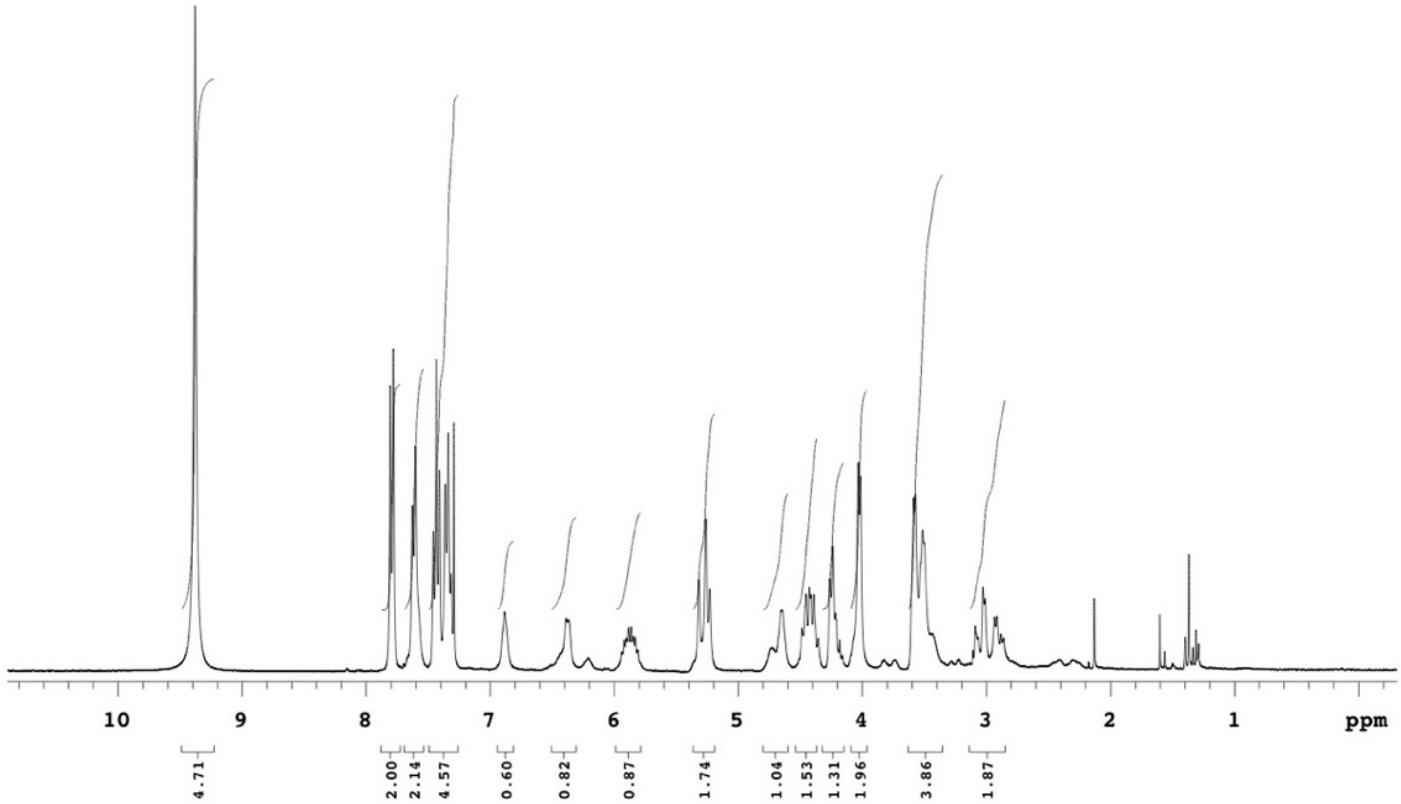


**Figure S111**. $^{1}$H NMR data for compound **QX1111**.

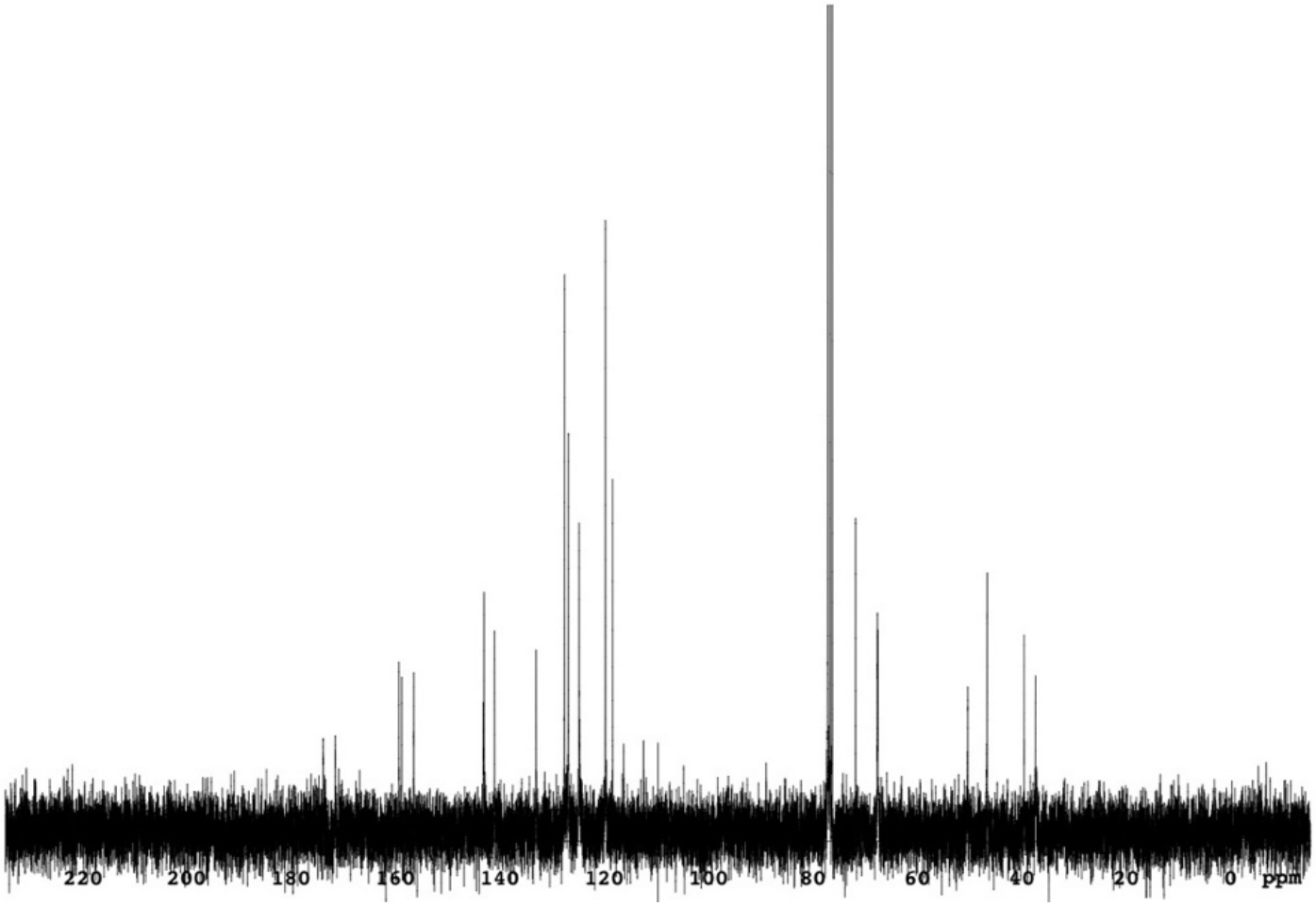


**Figure S112**. $^{13}C$ NMR data for compound **QX1111**.

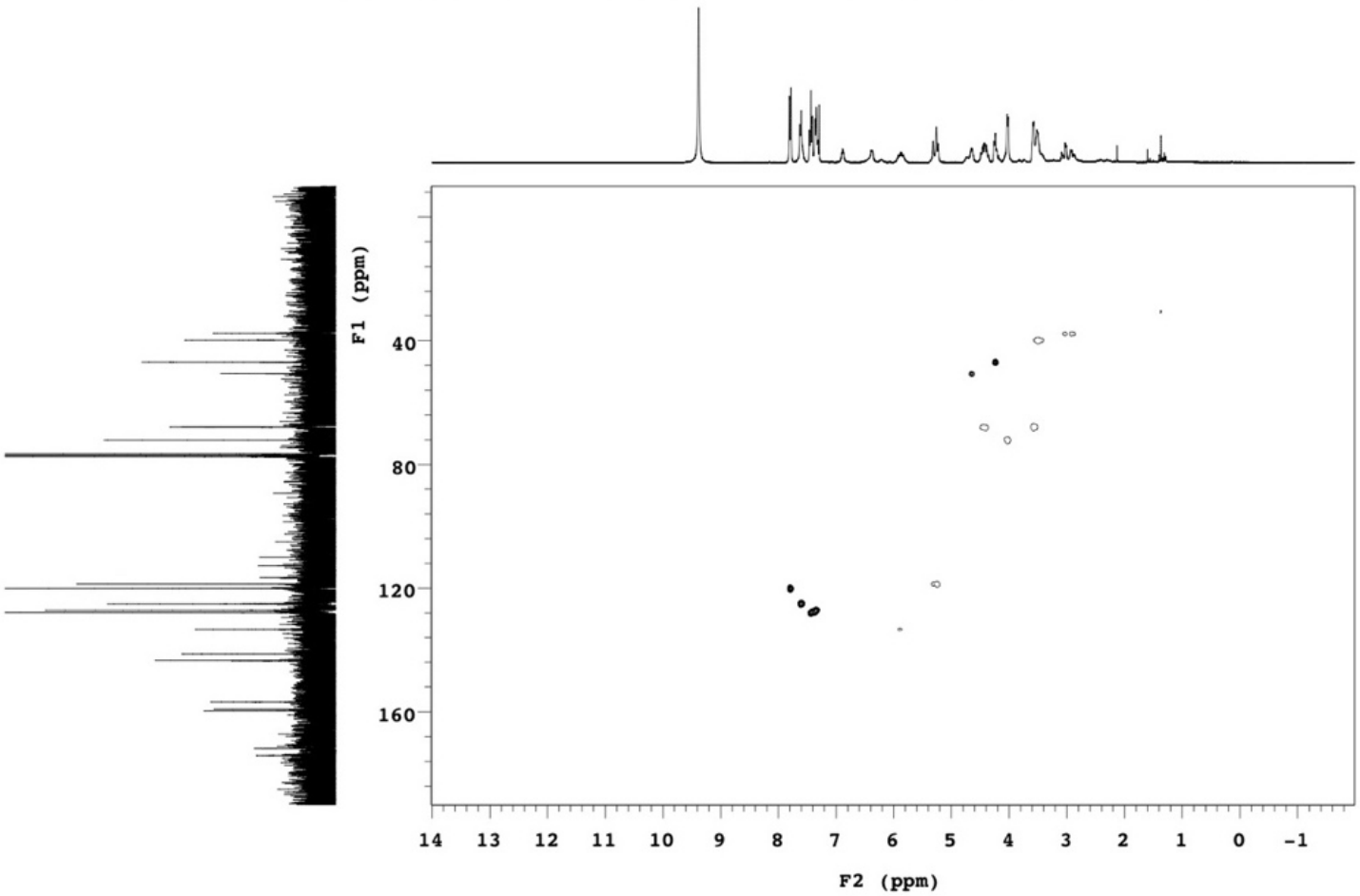


**Figure S113**. HSQC data for compound **QX1111**.

**3,6,9,12-tetraoxapentadec-14-en-1-ol (QX1127)**

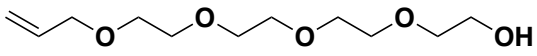

**QX1127**

Procedure was performed as described above for compound QX1013 but using 2,2'-((oxybis(ethane-2,1-diyl))bis(oxy))bis(ethan-1-ol) as starting material. Yield: 33.10% MS(ESI-TOF) m/z calc. for $C_{11}H_{22}O_5H^+$ 235.15, found 235.15 [M+H$^+$]; $^1$H NMR (500 MHz, Chloroform-*d*) δ 5.92 (ddt, *J* = 17.3, 10.3, 5.7 Hz, 1H), 5.28 (dd, *J* = 17.3, 1.7 Hz, 1H), 5.19 (dd, *J* = 10.4, 1.5 Hz, 1H), 4.03 (dt, *J* = 5.7, 1.4 Hz, 2H), 3.75 – 3.72 (m, 2H), 3.70 – 3.65 (m, 10H), 3.63 – 3.60 (m, 4H).

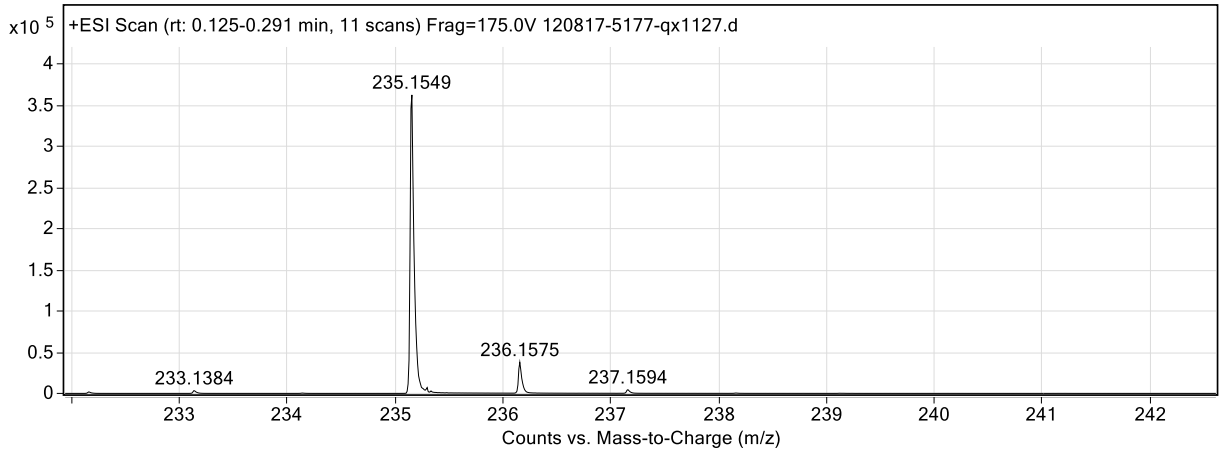


**Figure S114**. ESI-TOF MS data for compound **QX1127**.

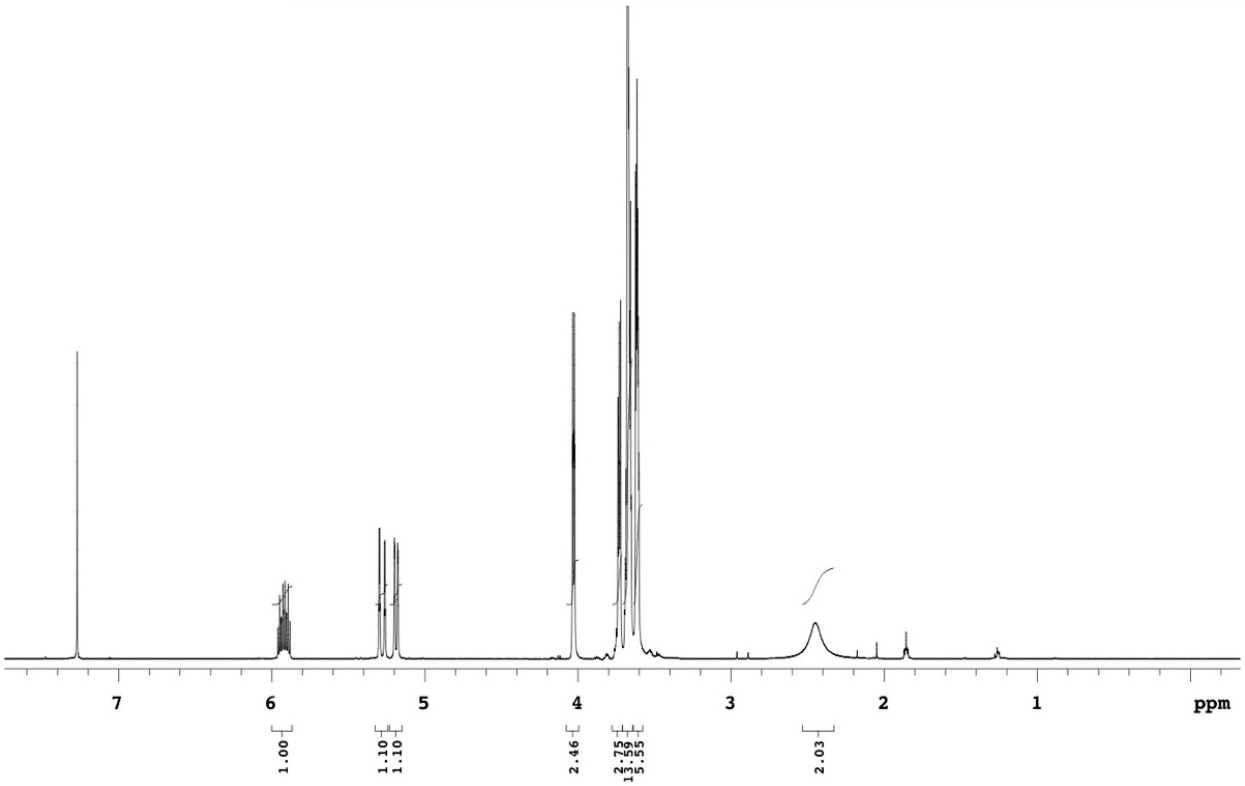

**Figure S115**. $^{1}$H NMR data for compound **QX1127**.

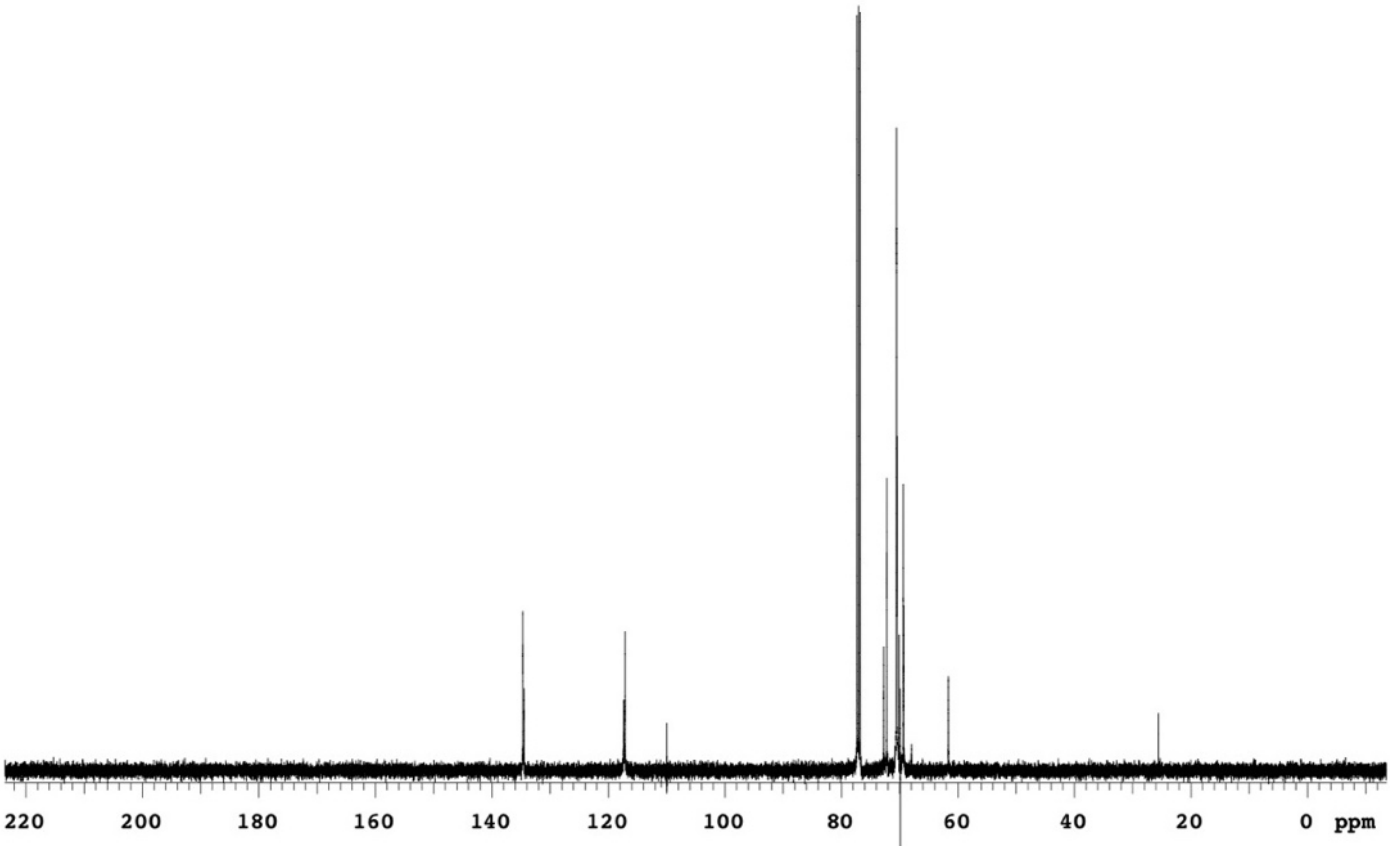


**Figure S116**. $^{13}$C NMR data for compound **QX1127**.

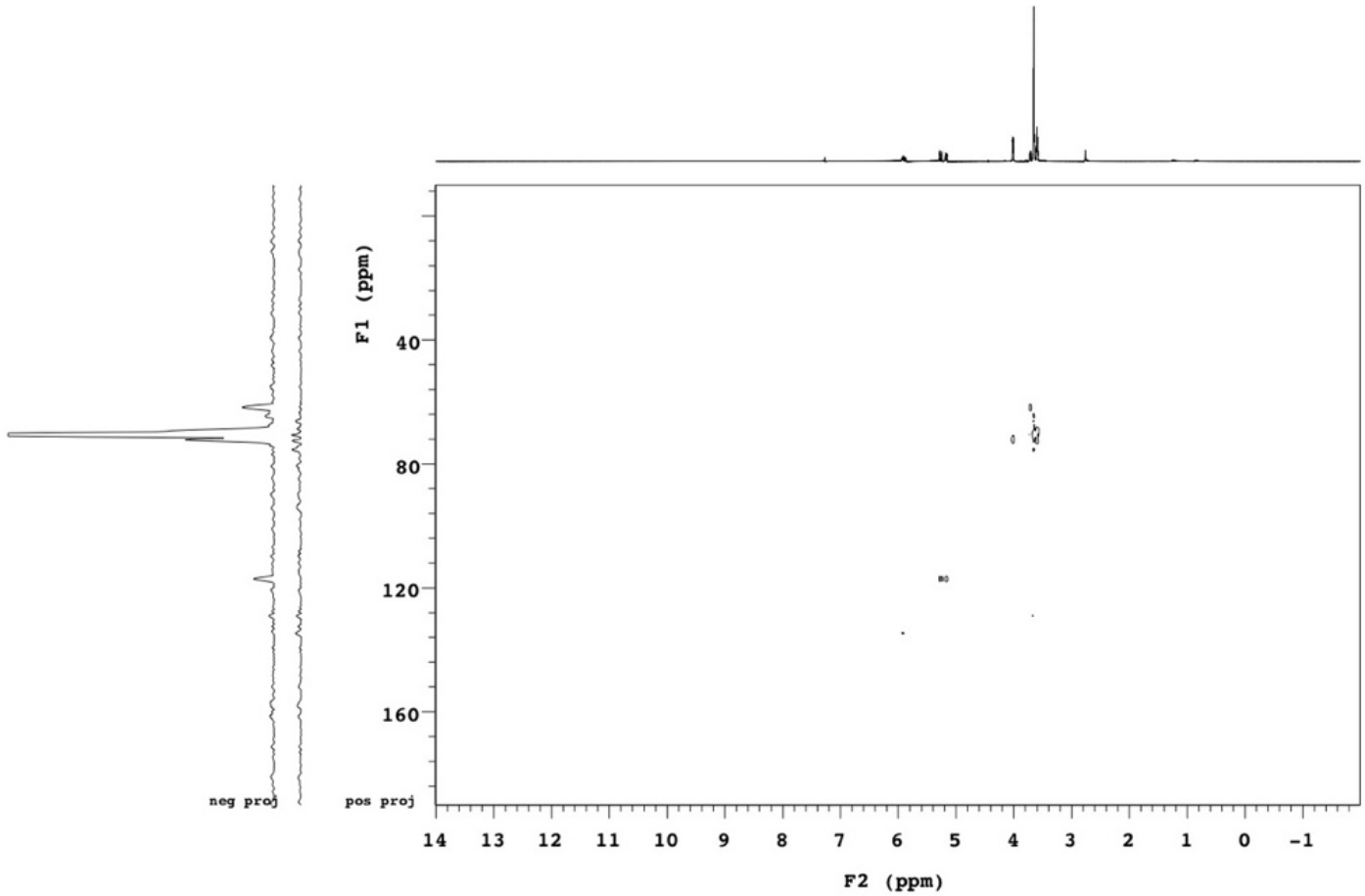


**Figure S117**. HSQC data for compound **QX1127**.

## 3,6,9,12-tetraoxapentadec-14-en-1-amine (QX1139)

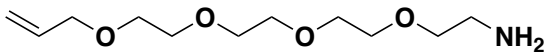


**QX1139**

Procedure was performed as described above for compound QX1015 but using 1-azido-3,6,9,12-tetraoxapentadec-14-ene as starting material. Yield: quantitative. MS(ESI-TOF) m/z calc. for $C_{11}H_{23}NO_4H^+$ 234.17, found 234.17 [M+H$^+$]; $^1$H NMR (500 MHz, DMSO-$d_6$) δ 8.02 (s, 2H), 5.87 (ddt, $J$ = 17.3, 10.6, 5.4 Hz, 1H), 5.24 (dd, $J$ = 17.3, 1.8 Hz, 1H), 5.13 (dd, $J$ = 10.5, 1.8 Hz, 1H), 3.94 (dt, $J$ = 5.4, 1.6 Hz, 2H), 3.60 (t, $J$ = 5.3 Hz, 2H), 3.57 – 3.46 (m, 12H), 2.94 (q, $J$ = 5.6 Hz, 2H).

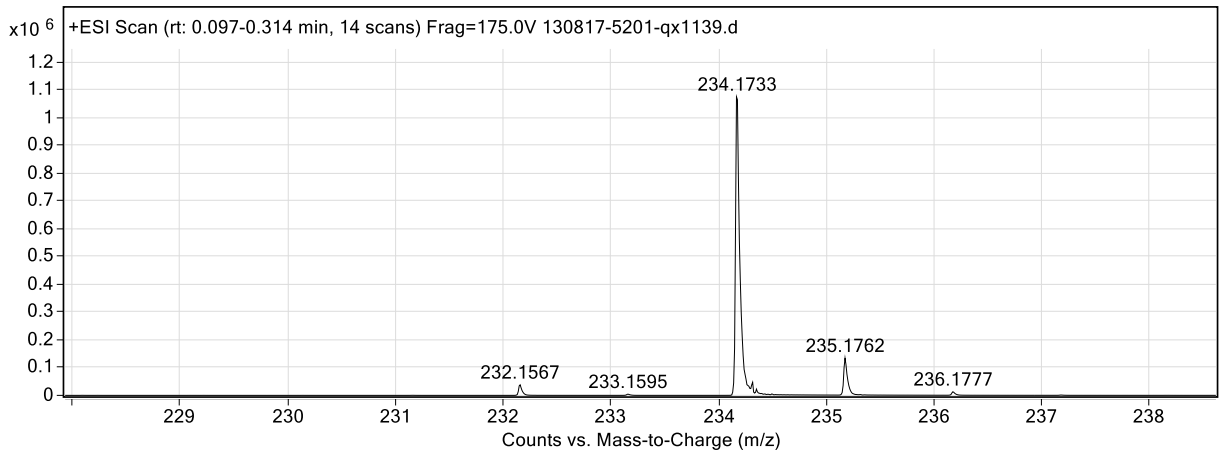


**Figure S118**. ESI-TOF MS data for compound **QX1139**.

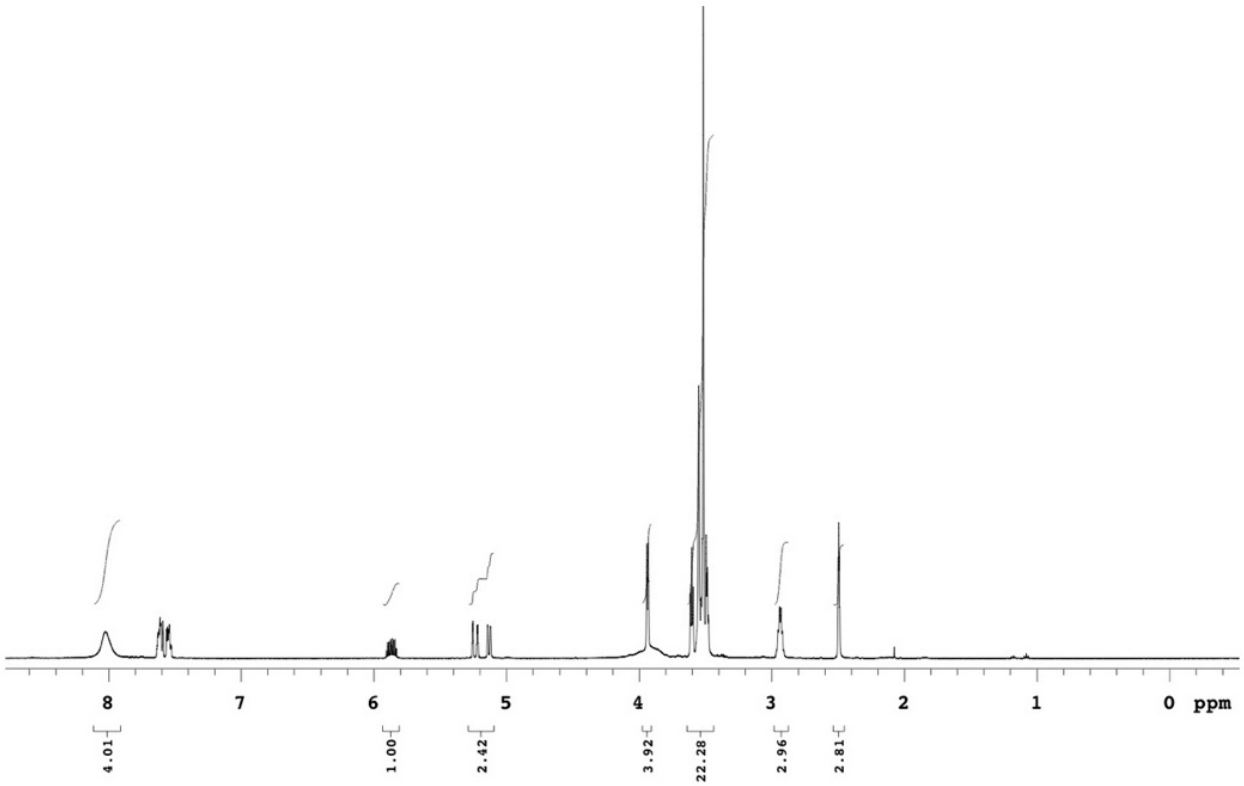


**Figure S119**. $^{1}$H NMR data for compound **QX1139**.

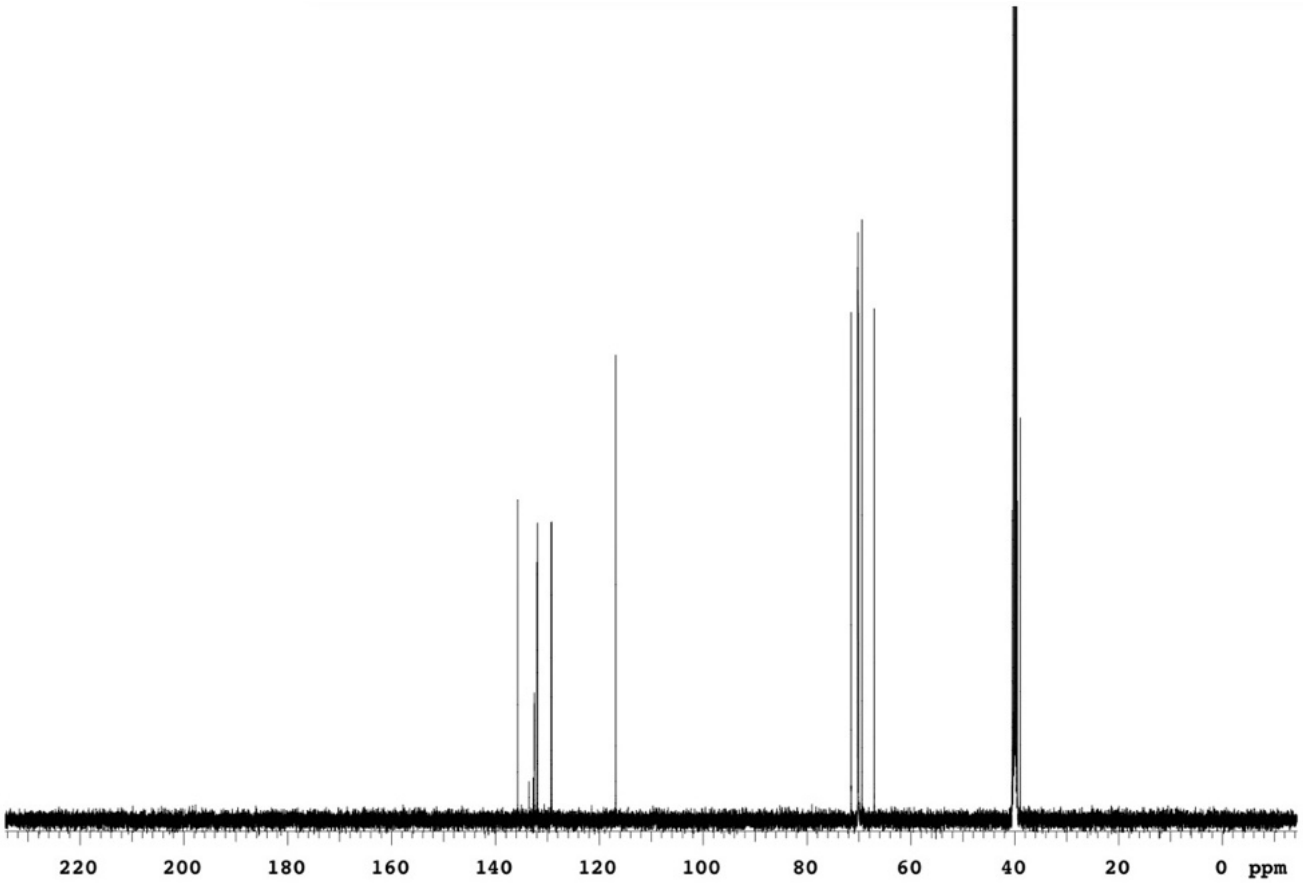


**Figure S120**. $^{13}C$ NMR data for compound **QX1139**.

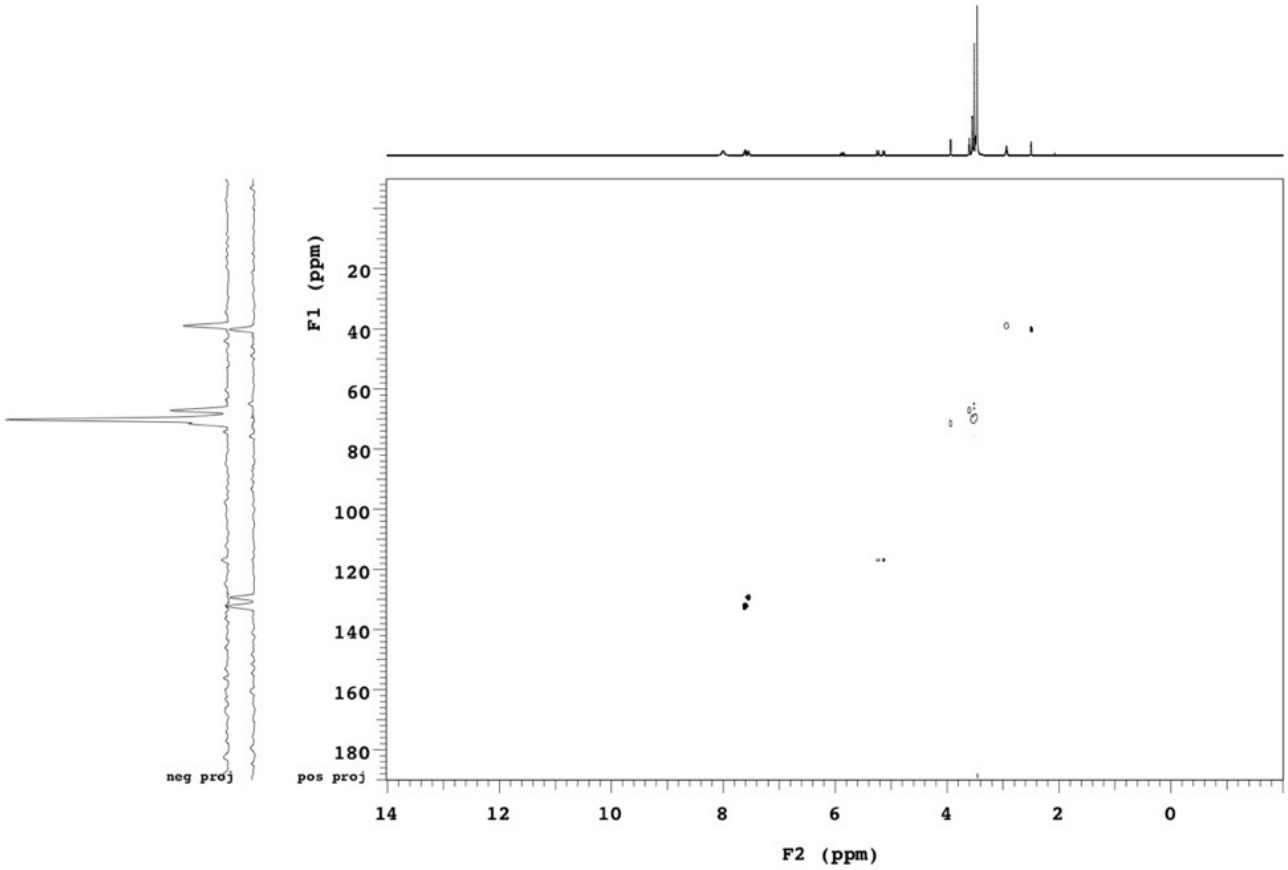

**Figure S121**. HSQC data for compound **QX1139**.

***tert*-butyl (*S*)-19-((((9*H*-fluoren-9-yl)methoxy)carbonyl)amino)-17-oxo-4,7,10,13-tetraoxa-16-aza-icos-1-en-20-oate (QX1141)**

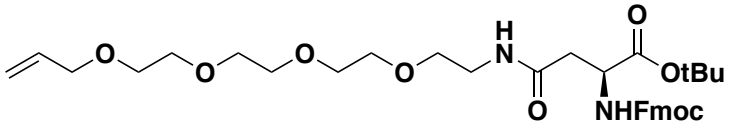


**QX1141**

Procedure was performed as described above for compound QX1017 but using QX1139 as starting material. Yield: 67.2%; MS(ESI-TOF) m/z calc. for $C_{34}H_{46}N_2O_9H^+$ 627.32, found 627.32 [M+H$^+$]; $^1$H NMR (500 MHz, Chloroform-*d*) δ 7.75 (d, *J* = 7.5 Hz, 2H), 7.60 (dd, *J* = 7.3, 4.9 Hz, 2H), 7.38 (t, *J* = 7.4 Hz, 2H), 7.30 (t, *J* = 7.5 Hz, 2H), 6.48 (t, *J* = 5.5 Hz, 1H), 6.15 (d, *J* = 8.5 Hz, 1H), 5.89 (ddt, *J* = 16.1, 11.2, 5.7 Hz, 1H), 5.25 (dd, *J* = 17.2, 1.5 Hz, 1H), 5.16 (d, *J* = 10.4 Hz, 1H), 4.48 (dt, *J* = 8.8, 4.6 Hz, 1H), 4.41 (dd, *J* = 10.5, 7.2 Hz, 1H), 4.30 (dd, *J* = 10.6, 7.4 Hz, 1H), 4.22 (t, *J* = 7.2 Hz, 1H), 3.99 (d, *J* = 5.7 Hz, 2H), 3.67 – 3.49 (m, 16H), 2.88 (dd, *J* = 15.7, 4.9 Hz, 1H), 2.70 (dd, *J* = 15.6, 4.4 Hz, 1H), 1.47 (s, 9H). $^{13}$C NMR (126 MHz, Chloroform-*d*) δ 170.16, 169.93, 156.20, 143.97, 143.83, 141.23, 134.62, 132.08, 132.00, 128.58, 128.49, 127.65, 127.07, 125.25, 125.18, 119.91, 117.20, 82.07, 72.19, 70.53, 70.51, 70.43, 70.23, 69.65, 69.35, 67.02, 51.45, 47.12, 39.32, 38.61, 37.75, 27.92.

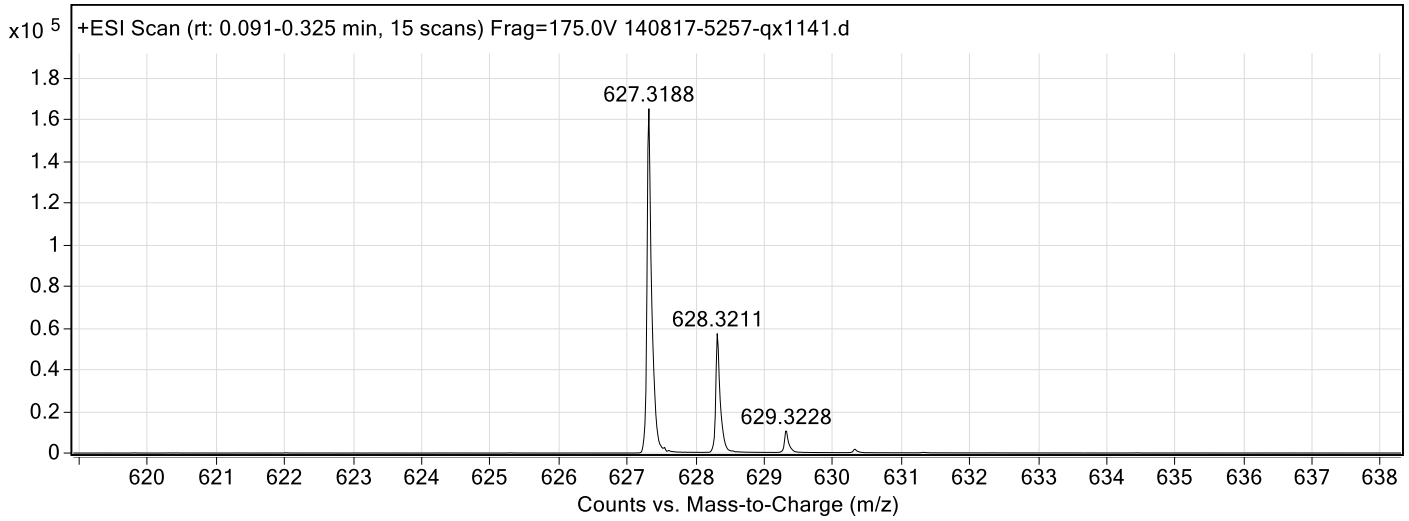


**Figure S122**. ESI-TOF data for compound **QX1141**.

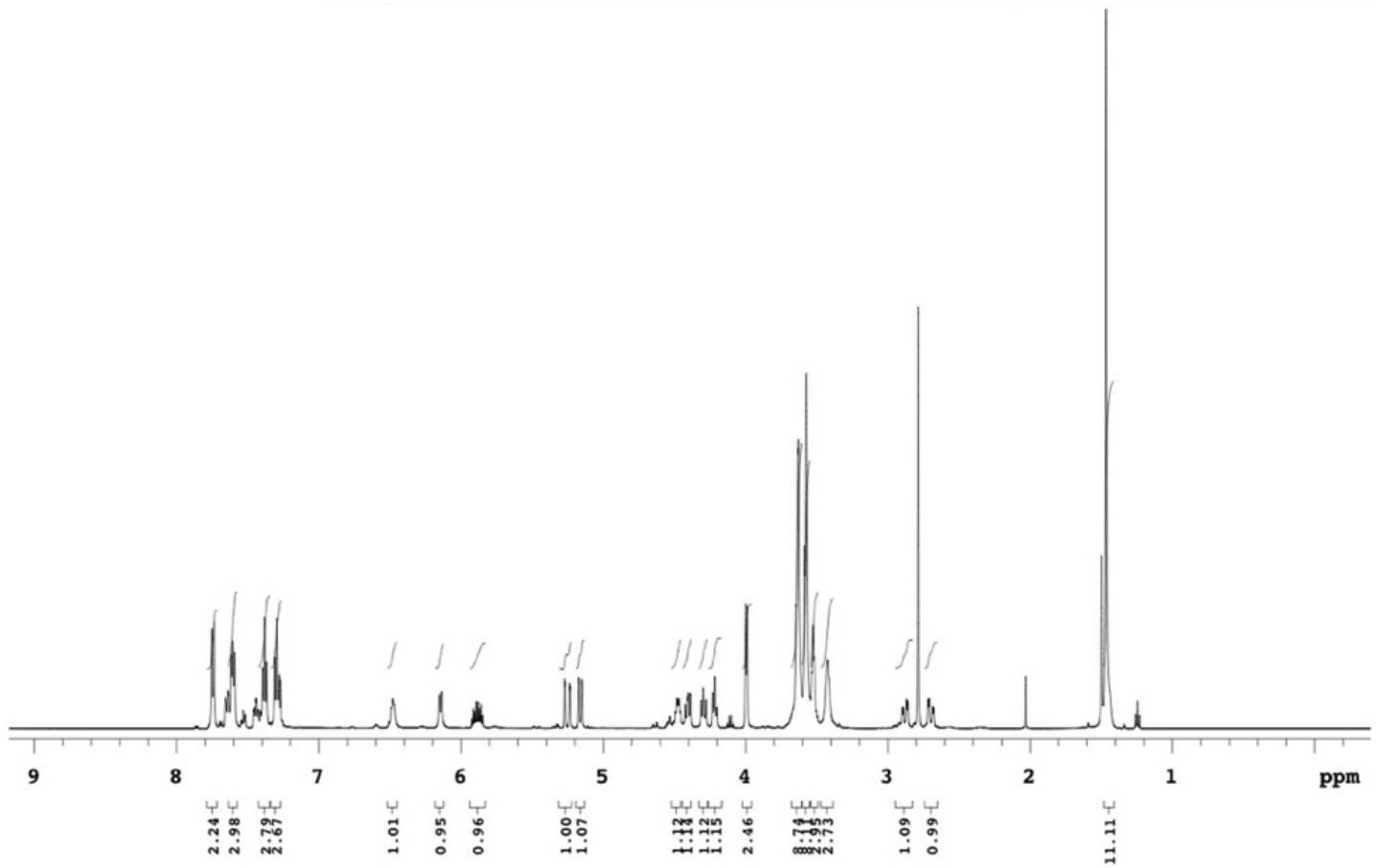


**Figure S123**. [1]H NMR data for compound **QX1141**.

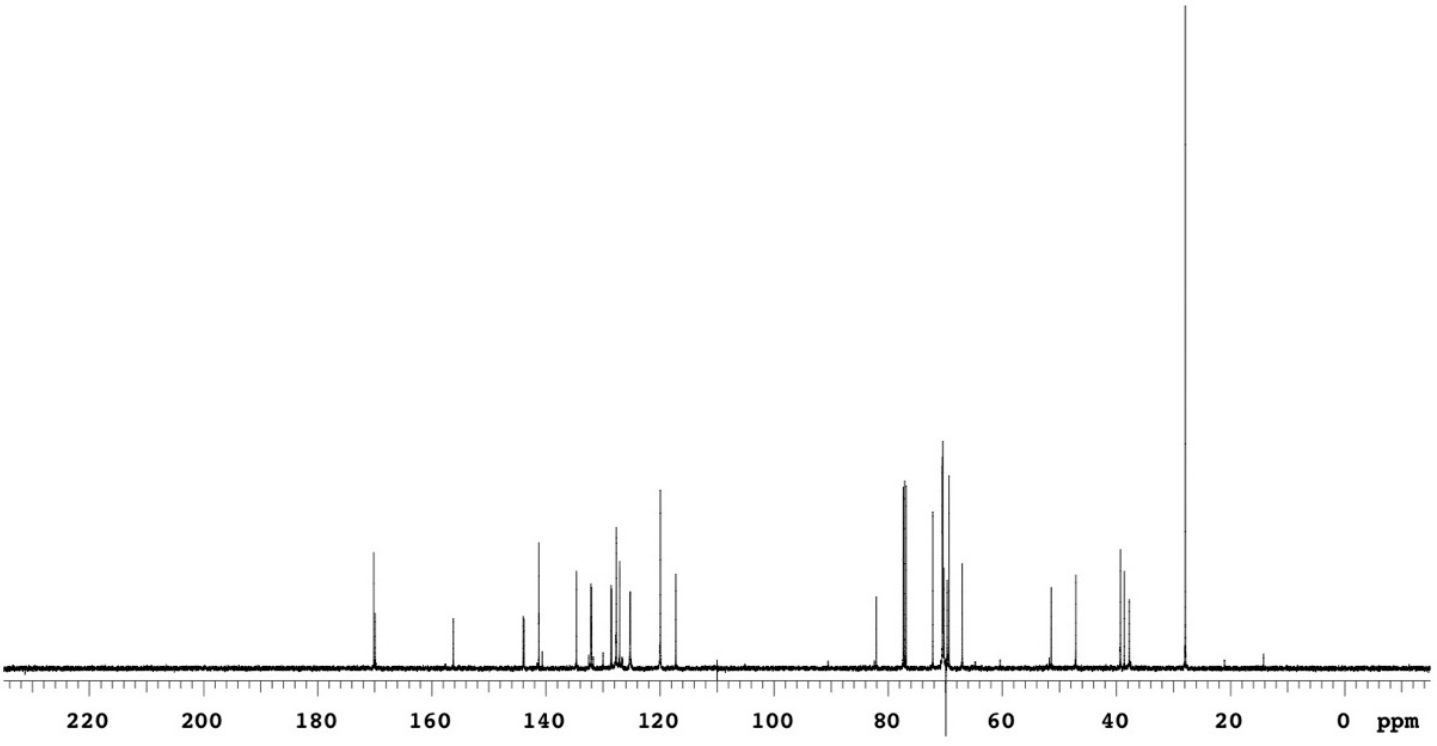


**Figure S124**. [13]C NMR data for compound **QX1141**.

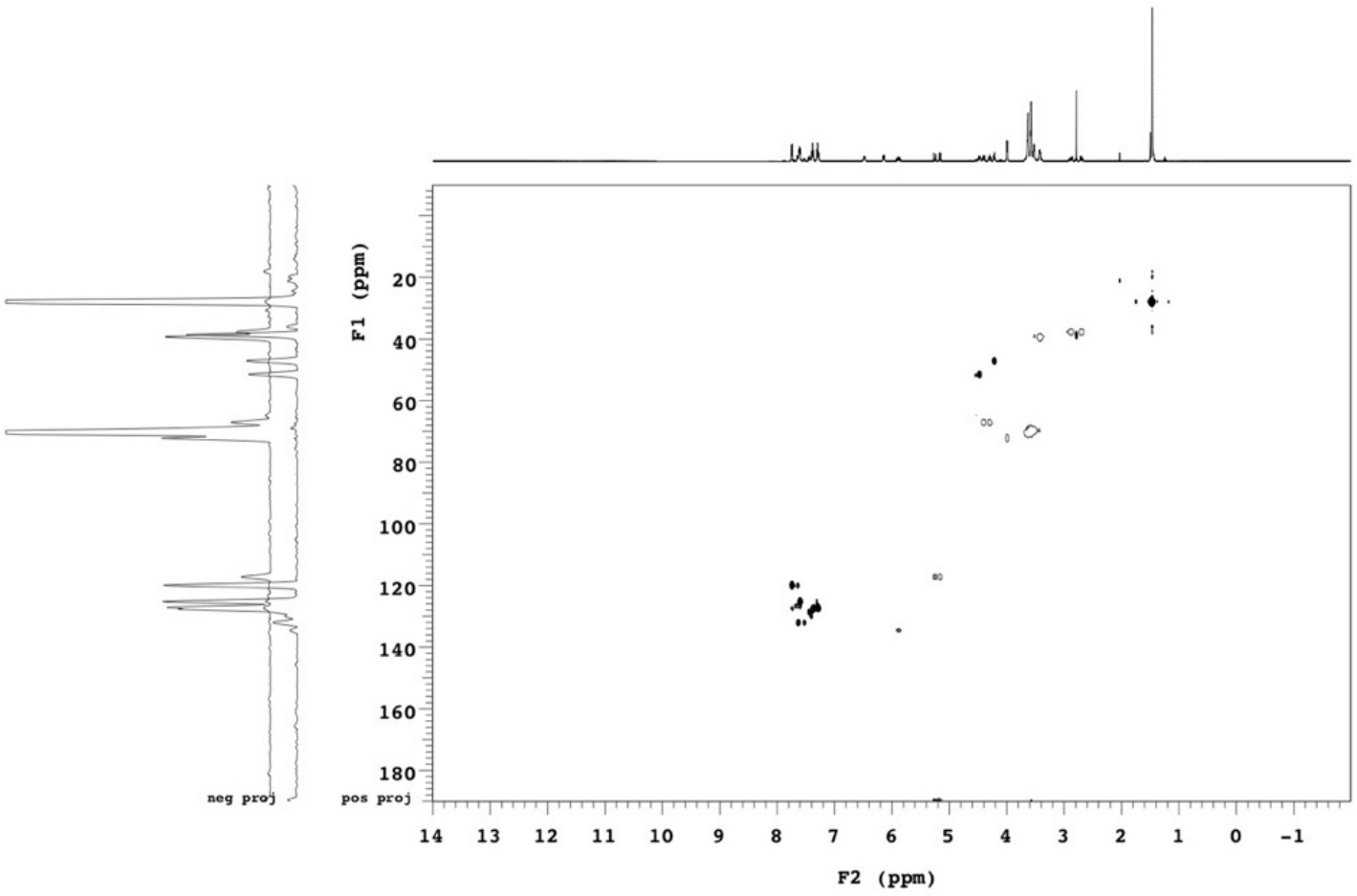


**Figure S125**. HSQC data for compound **QX1141**.

**(*S*)-19-((((9*H*-fluoren-9-yl)methoxy)carbonyl)amino)-17-oxo-4,7,10,13-tetraoxa-16-azaicos-1-en-20-oic acid (QX1143)**

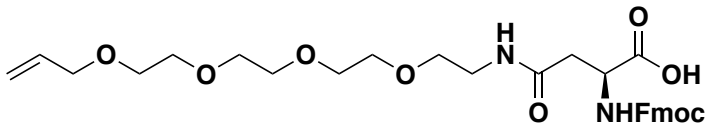


**QX1143**

Procedure was performed as described above for compound QX1019 but using QX1141 as starting material. Yield: quantitative; MS(ESI-TOF) m/z calc. for $C_{30}H_{38}N_2O_9H^+$ 571.26, found 571.26 [M+H$^+$]; $^1$H NMR (500 MHz, Chloroform-*d*) δ 7.75 (d, *J* = 7.5 Hz, 2H), 7.60 (t, *J* = 8.0 Hz, 2H), 7.38 (t, *J* = 7.4 Hz, 2H), 7.30 (t, *J* = 7.4 Hz, 2H), 6.29 (d, *J* = 7.2 Hz, 1H), 5.87 (ddt, *J* = 16.4, 10.9, 5.7 Hz, 1H), 5.24 (dd, *J* = 17.3, 1.8 Hz, 1H), 5.16 (d, *J* = 10.3 Hz, 1H), 4.58 (s, 1H), 4.38 (dd, *J* = 10.5, 7.3 Hz, 1H), 4.31 (dd, *J* = 10.5, 7.3 Hz, 1H), 4.21 (t, *J* = 7.3 Hz, 1H), 3.99 (d, *J* = 5.7 Hz, 2H), 3.67 – 3.50 (m, 16H), 2.78 (d, *J* = 6.3 Hz, 1H), 2.75 (d, *J* = 6.1 Hz, 1H). $^{13}$C NMR (126 MHz, Chloroform-*d*) δ 172.63, 171.34, 163.06, 156.04, 143.89, 143.74, 141.23, 138.90, 134.39, 127.69, 127.10, 125.24, 125.18, 119.92, 117.50, 114.31, 72.17, 70.51, 70.39, 70.32, 70.30, 69.97, 69.34, 69.19, 67.20, 47.05, 39.61, 37.83, 36.73.

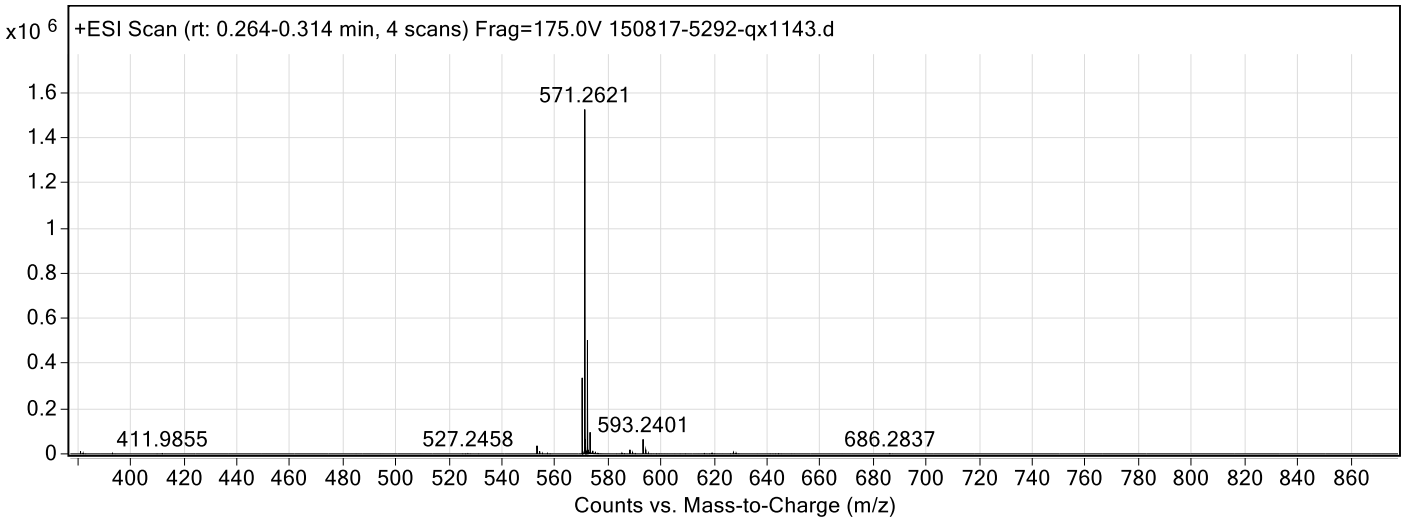


**Figure S126**. ESI-TOF MS data for compound **QX1143**.

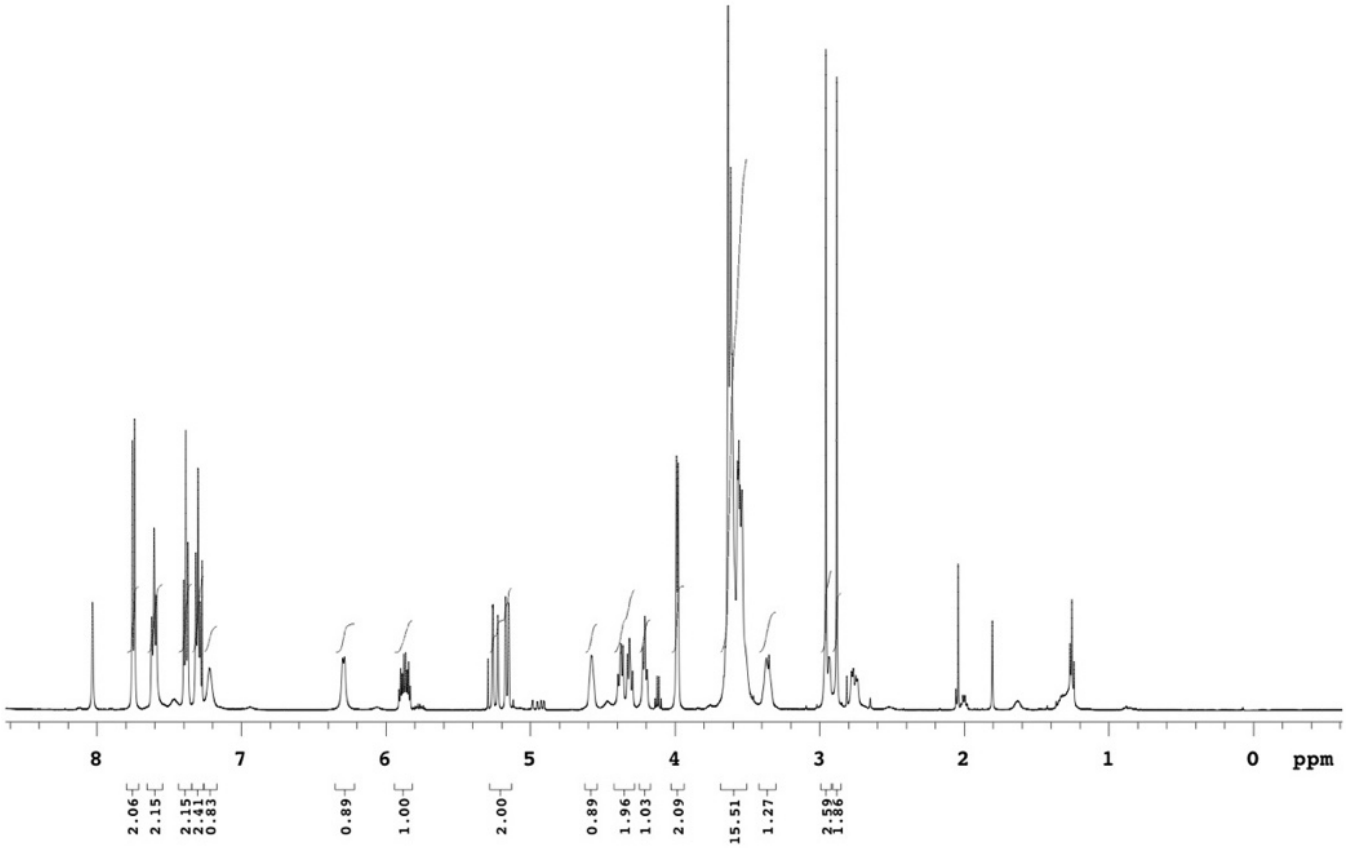


**Figure S127**. [1]H NMR data for compound **QX1143**.

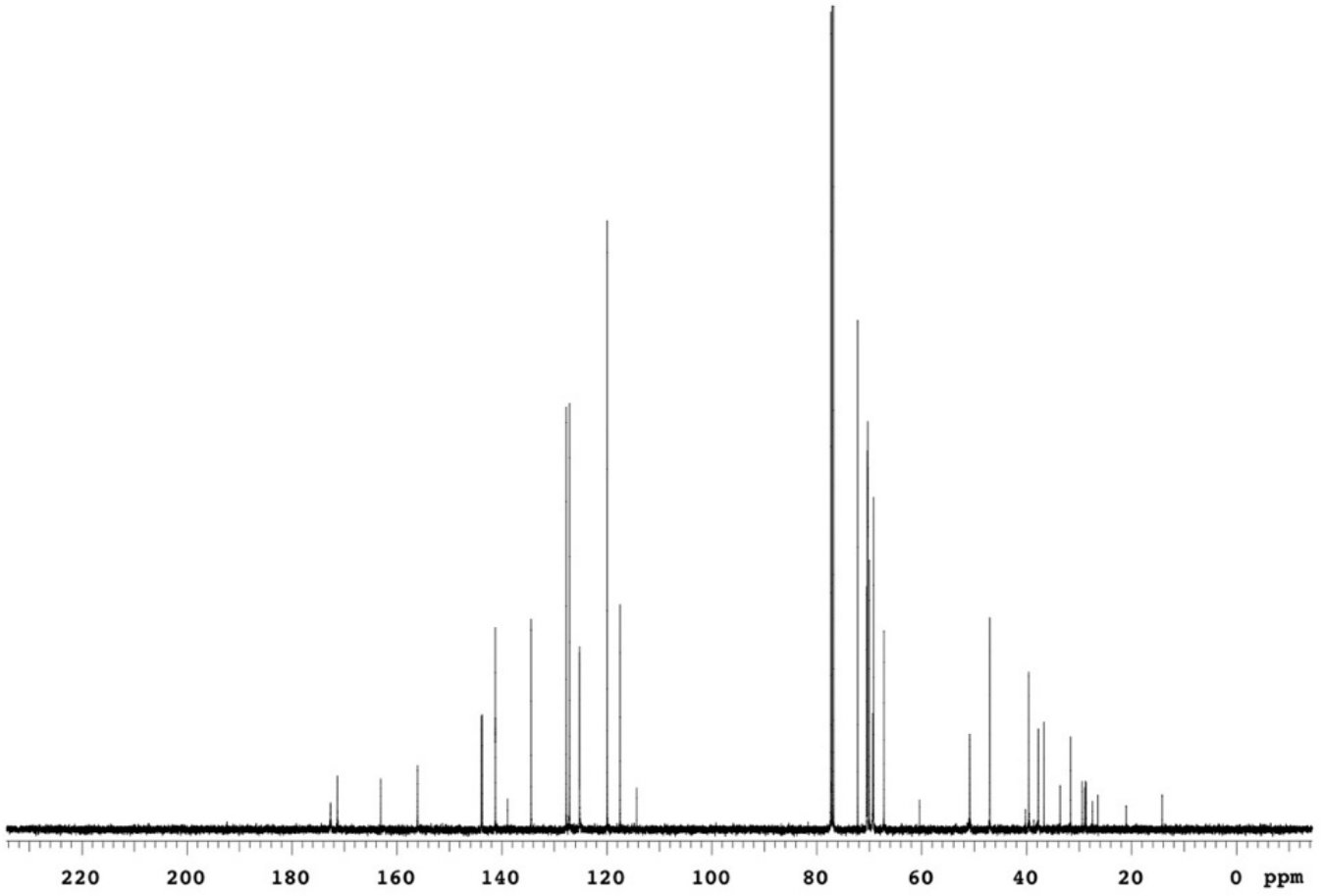

**Figure S128**. $^{13}C$ NMR data for compound **QX1143**.

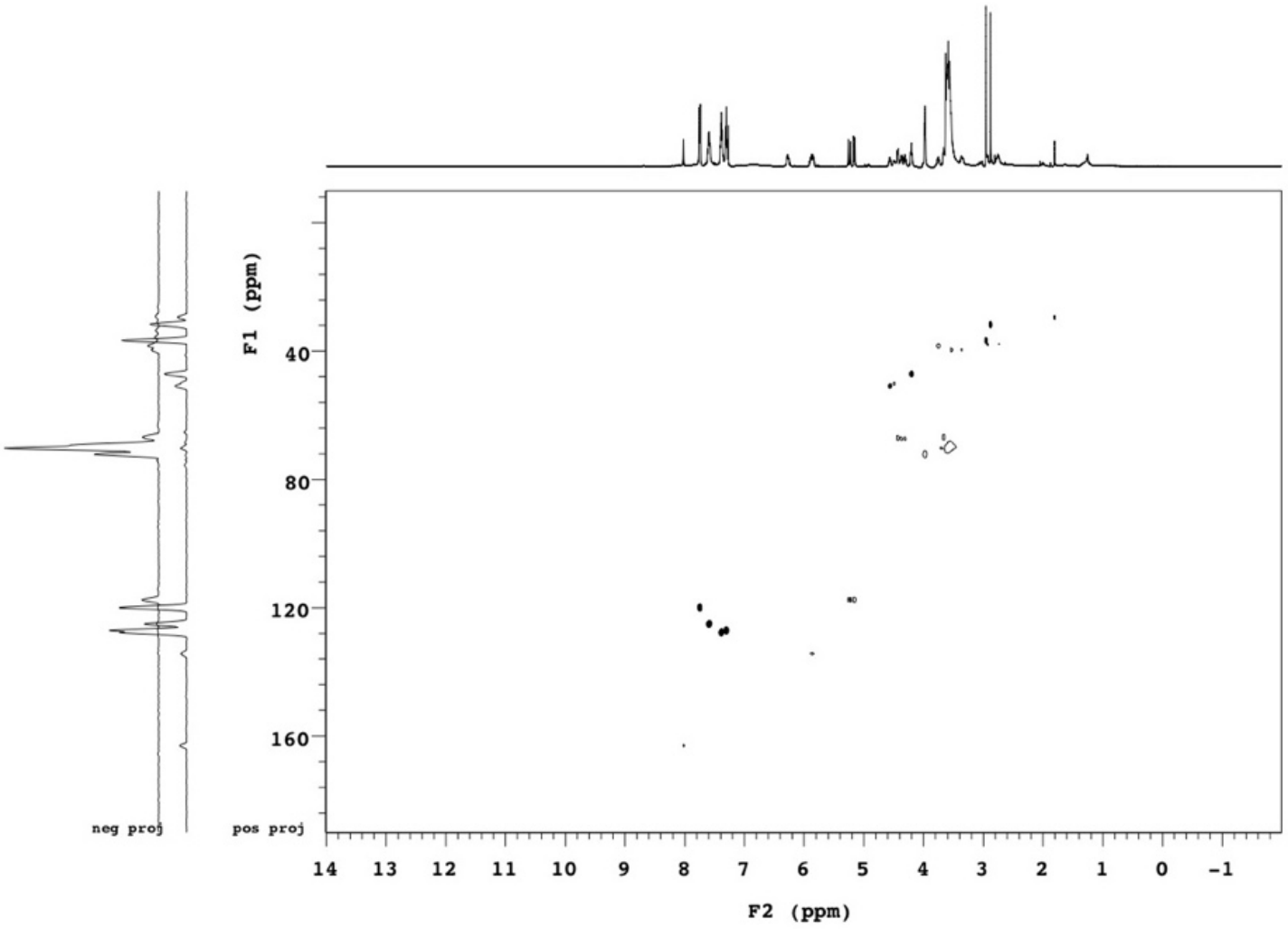


**Figure S129**. HSQC data for compound **QX1143**.

**9-azidonon-1-ene (QX1151)**


QX1151

To a solution of $NaN_3$ (650 mg, 10 mmol) in DMSO (20 mL) was added 9-Bromo-1-nonene (1 ml, 5 mmol) at room temperature. The reaction mixture was heated up to 100 $^{O}$C for 8 hours. The crude mixture was extracted with ethyl ether for 3 times after the reaction was completed. The combined organic phases were washed with saturated brine and dried over anhydrous sodium sulfate, evaporated to dryness to obtain QX1151 as colorless oil. Desired product not visible by mass spectrometry, though detectable by NMR. Yield quantitative. $^{1}$H NMR (300 MHz, Chloroform-*d*) δ 5.83 (ddt, *J* = 16.9, 10.1, 6.6 Hz, 1H), 5.02 (dd, *J* = 17.1, 1.9 Hz, 1H), 4.96 (dd, *J* = 10.2, 2.0 Hz, 1H), 3.28 (t, *J* = 6.9 Hz, 2H), 1.61 (q, *J* = 7.1 Hz, 2H), 1.43 – 1.33 (m, 10H).

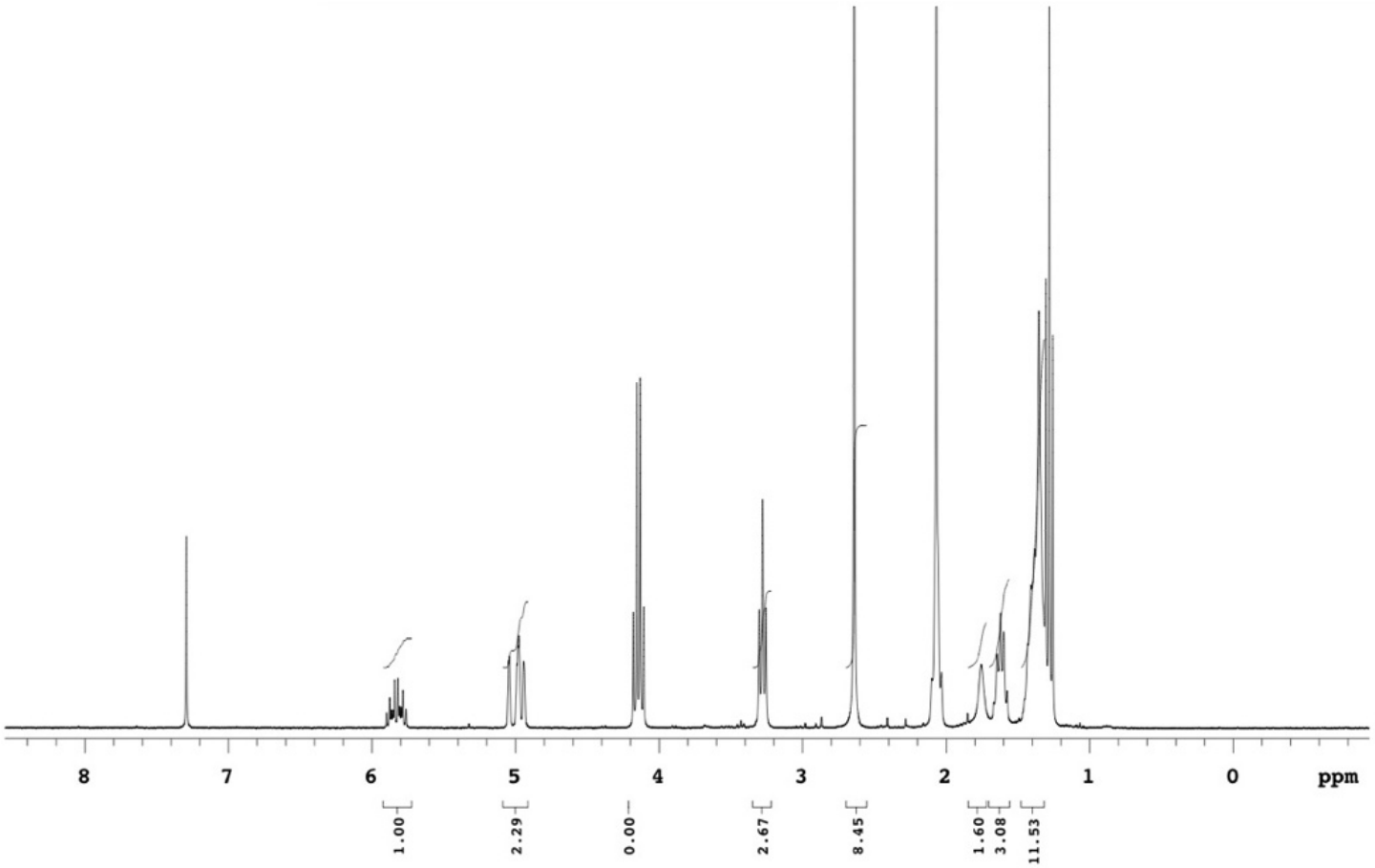


**Figure S130**. $^{1}$H NMR data for compound **QX1151**.

**non-8-en-1-amine (QX1153)**

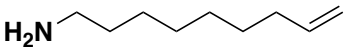

**QX1153**

Procedure was performed as described above for compound QX1015 but using QX1151 as starting material. Yield: 54.5% MS(ESI-TOF) m/z calc. for $C_9H_{19}NH^+$ 142.16, found 142.16 [M+H$^+$]; $^1$H NMR (300 MHz, Chloroform-*d*) δ 8.16 (b.r.s, 2H), 5.82 (ddt, *J* = 16.9, 10.2, 6.6 Hz, 1H), 5.02 (dd, *J* = 17.1, 1.9 Hz, 1H), 4.96 (dd, *J* = 10.1, 1.9 Hz, 1H), 3.08 – 2.93 (m, 2H), 2.06 (q, *J* = 6.8 Hz, 2H), 1.48 – 1.29 (m, 10H).

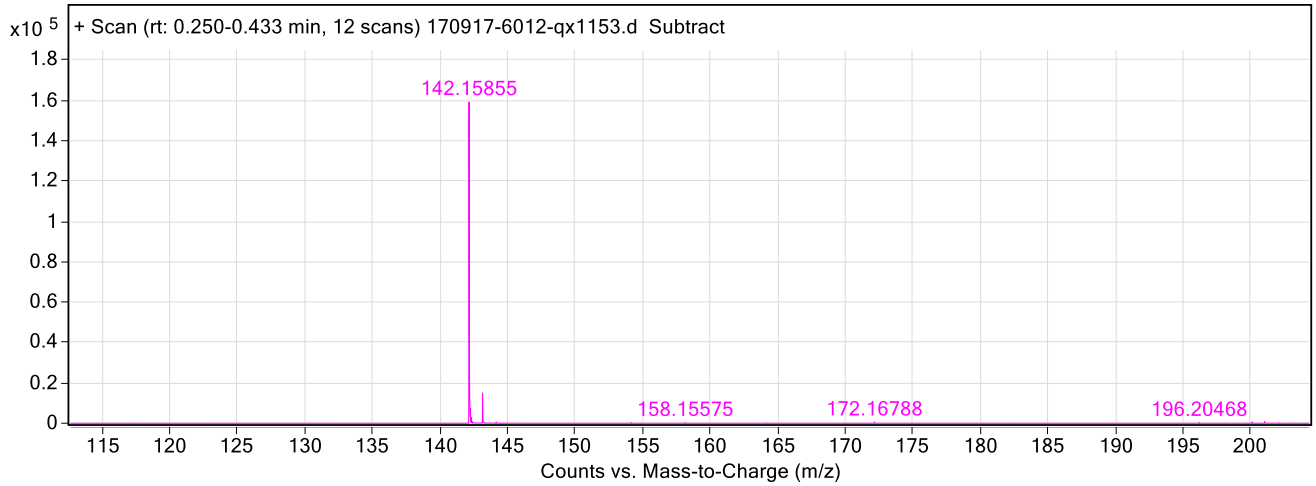


**Figure S131**. ESI-TOF MS data for compound **QX1153**.

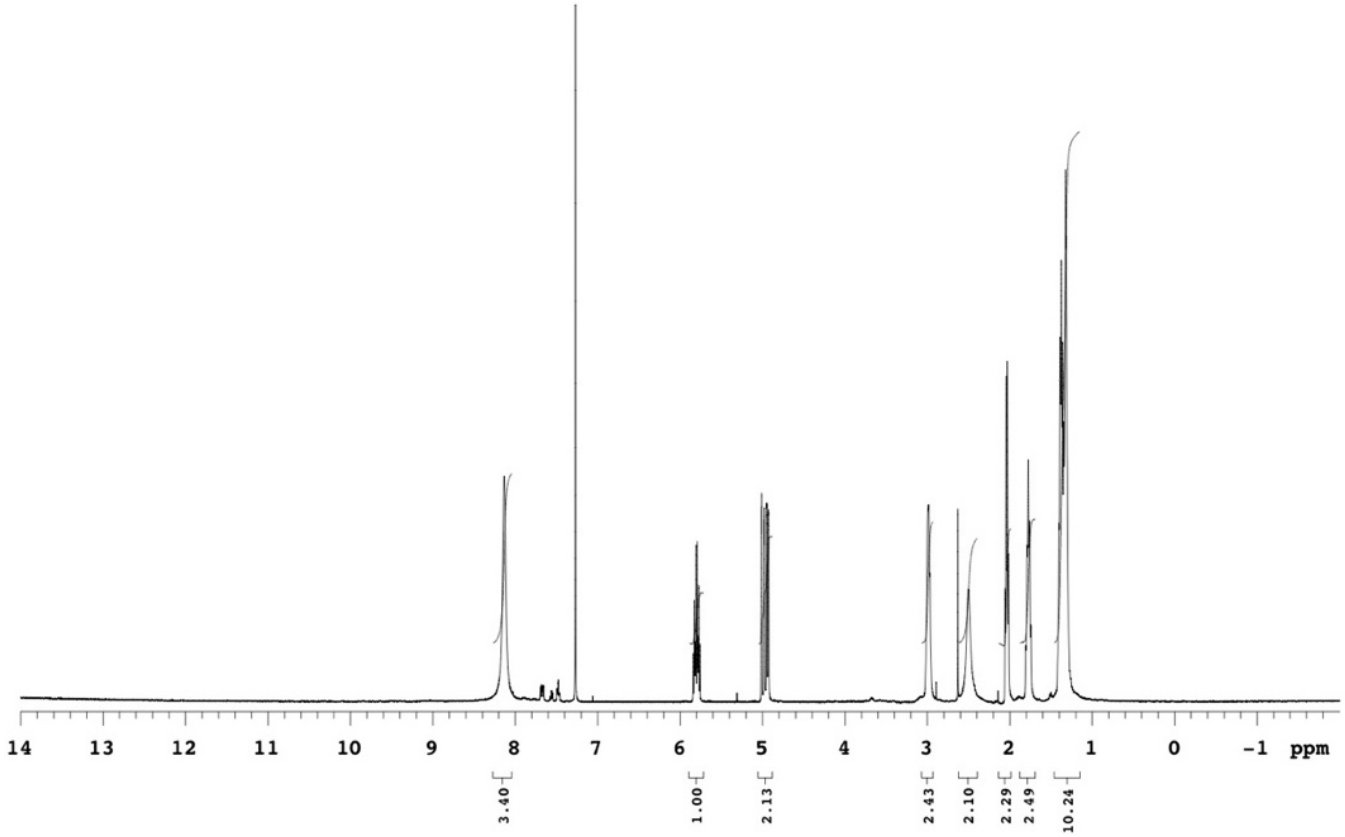

**Figure S132**. $^{1}$H NMR data for compound **QX1153**.

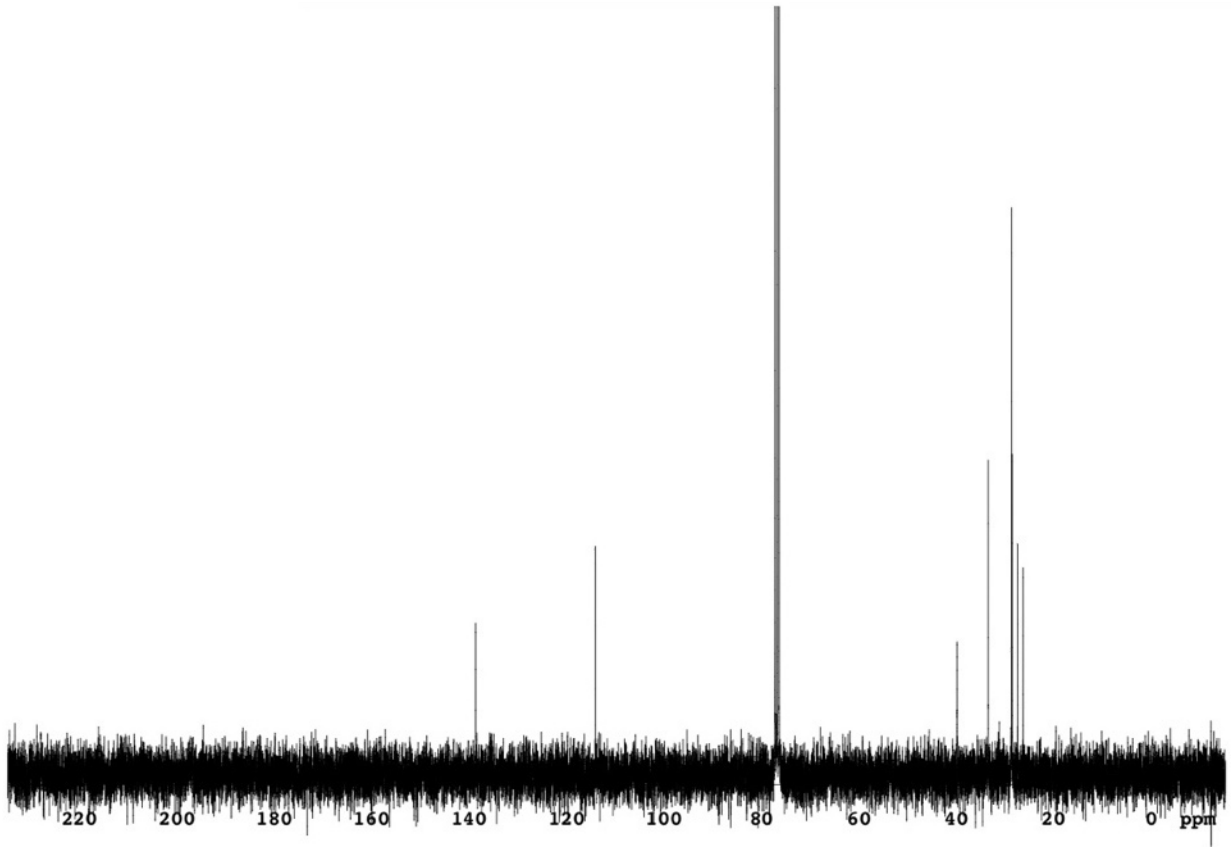


**Figure S133**. $^{13}$C NMR data for compound **QX1153**.

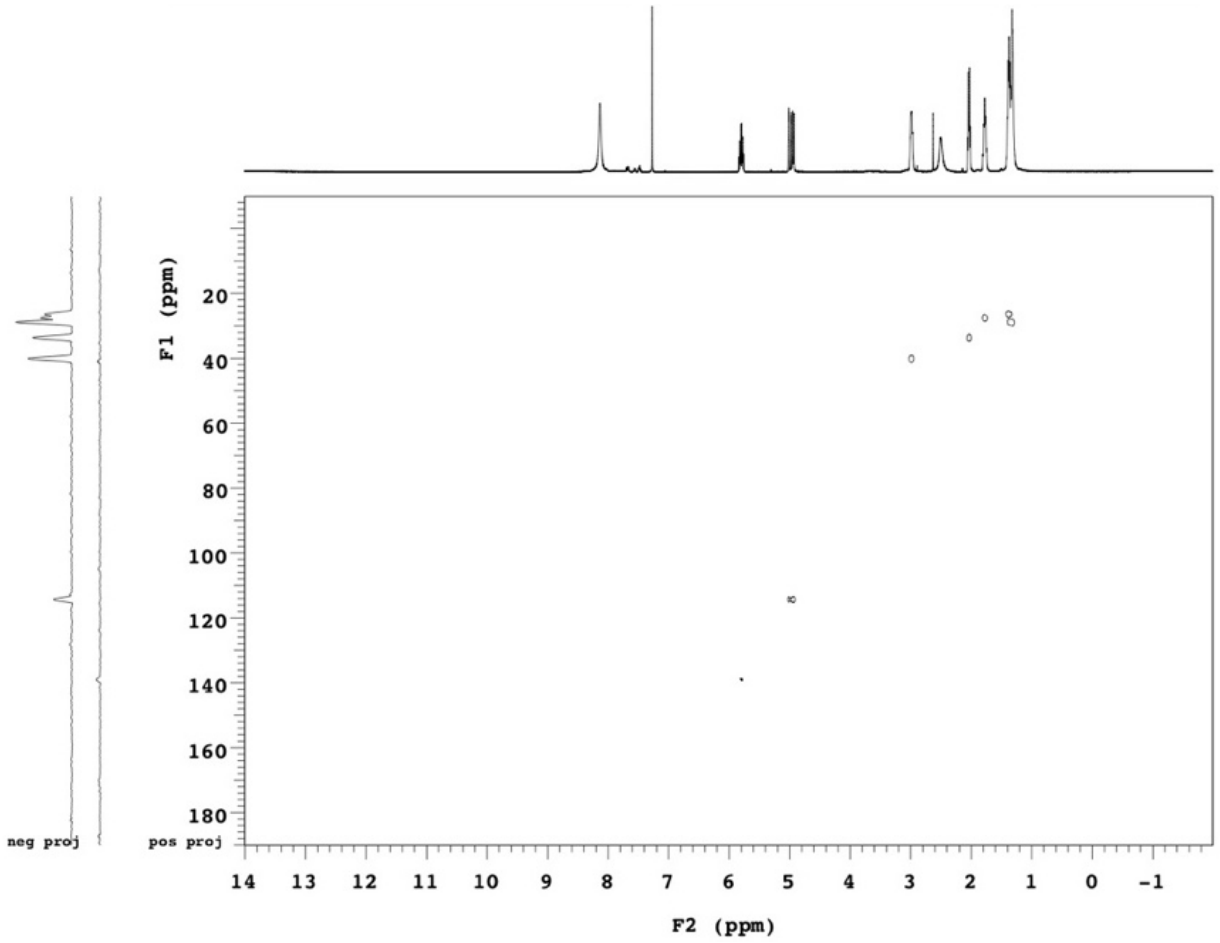


**Figure S134**. HSQC data for compound **QX1153**.

---

## ***tert*-butyl $N^2$-(((9*H*-fluoren-9-yl)methoxy)carbonyl)-$N^4$-(non-8-en-1-yl)-*L*-asparaginate (QX2001)**

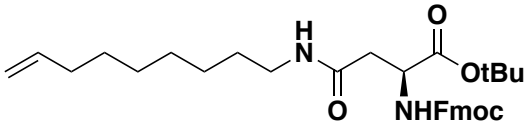


QX2001

Procedure was performed as described above for compound QX1017 but using QX1153 as starting material. Yield: 42.4% MS(ESI-TOF) m/z calc. for $C_{32}H_{42}N_2O_5H^+$ 535.31, found 535.31 [M+H$^+$]; $^1$H NMR (300 MHz, Chloroform-*d*) δ 7.79 (d, *J* = 7.5 Hz, 2H), 7.64 (dd, *J* = 7.5, 2.2 Hz, 2H), 7.43 (t, *J* = 7.4 Hz, 2H), 7.33 (t, *J* = 7.4 Hz, 2H), 6.16 (d, *J* = 8.2 Hz, 1H), 5.82 (ddt, *J* = 17.1, 10.3, 6.8 Hz, 1H), 5.78 (s, 1H), 5.01 (d, *J* = 17.8 Hz, 1H), 4.96 (d, *J* = 11.1 Hz, 2H), 4.50 (dt, *J* = 8.7, 4.6 Hz, 1H), 4.43 (dd, *J* = 10.3, 7.5 Hz, 1H), 4.34 (t, *J* = 8.8 Hz, 1H), 4.25 (t, *J* = 7.1 Hz, 1H), 3.25 (q, *J* = 7.2 Hz, 2H), 2.89 (dd, *J* = 15.6, 4.8 Hz, 1H), 2.73 (dd, *J* = 15.6, 4.5 Hz, 1H), 2.04 (q, *J* = 7.1, 6.3 Hz, 2H), 1.51 (s, 9H), 1.41 – 1.25 (m, 10H). $^{13}$C NMR (75 MHz, Chloroform-*d*) δ 170.08, 169.72, 156.28, 143.92, 143.80, 141.27, 139.06, 127.72, 127.72, 127.11, 127.09, 125.25, 125.21, 119.98, 119.98, 114.27, 82.37, 67.20, 51.49, 47.13, 39.65, 38.07, 33.75, 29.60, 29.13, 29.01, 28.83, 27.95, 27.95, 27.95, 26.87.

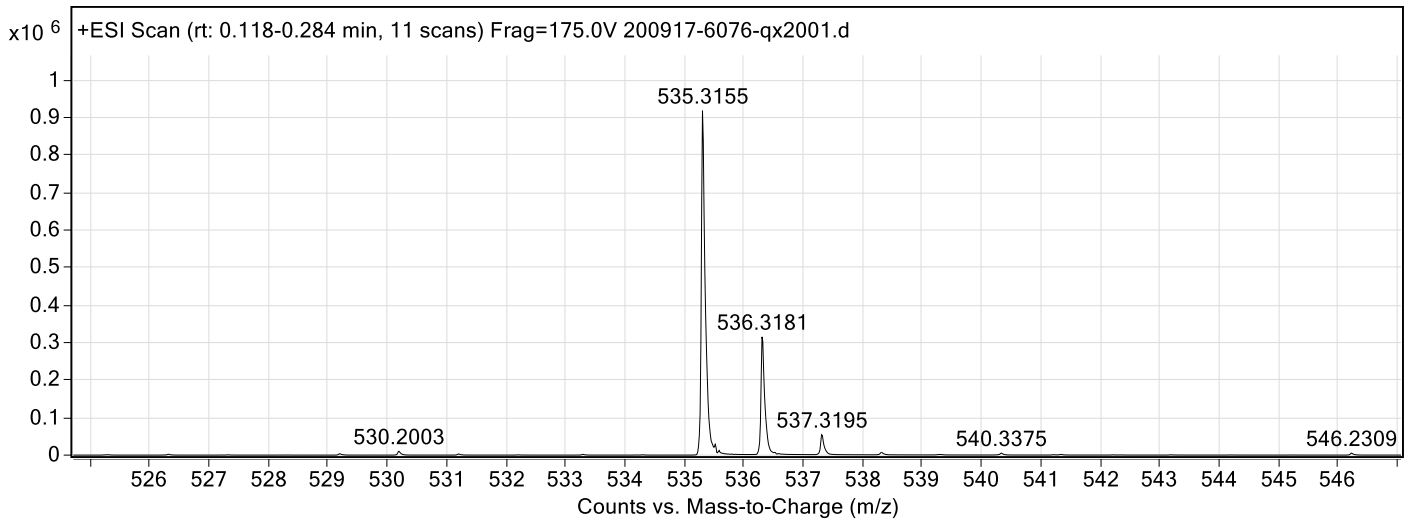


**Figure S135**. ESI-TOF MS data for compound **QX2001**.

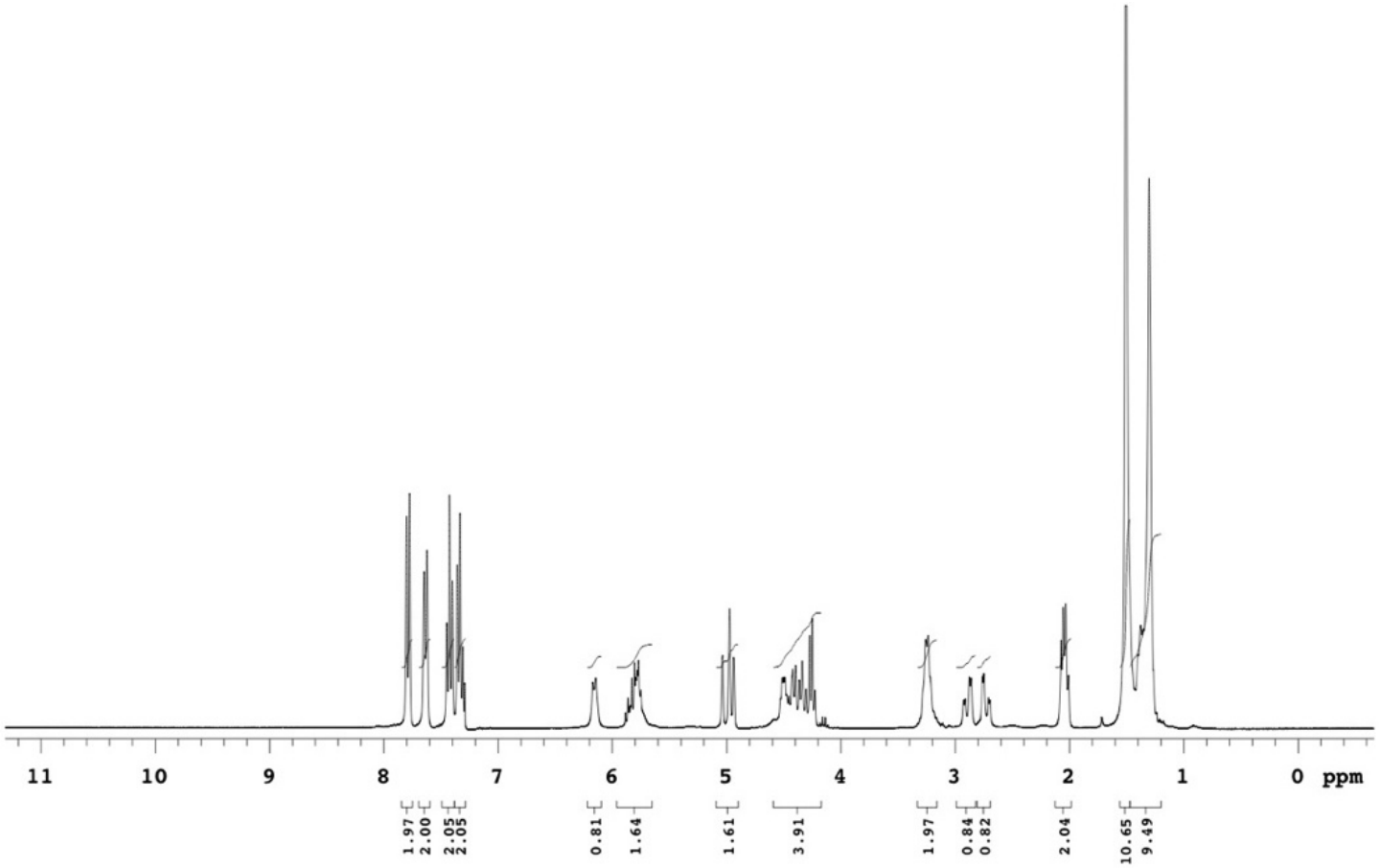


**Figure S136**. $^{1}$H NMR data for compound **QX2001**.

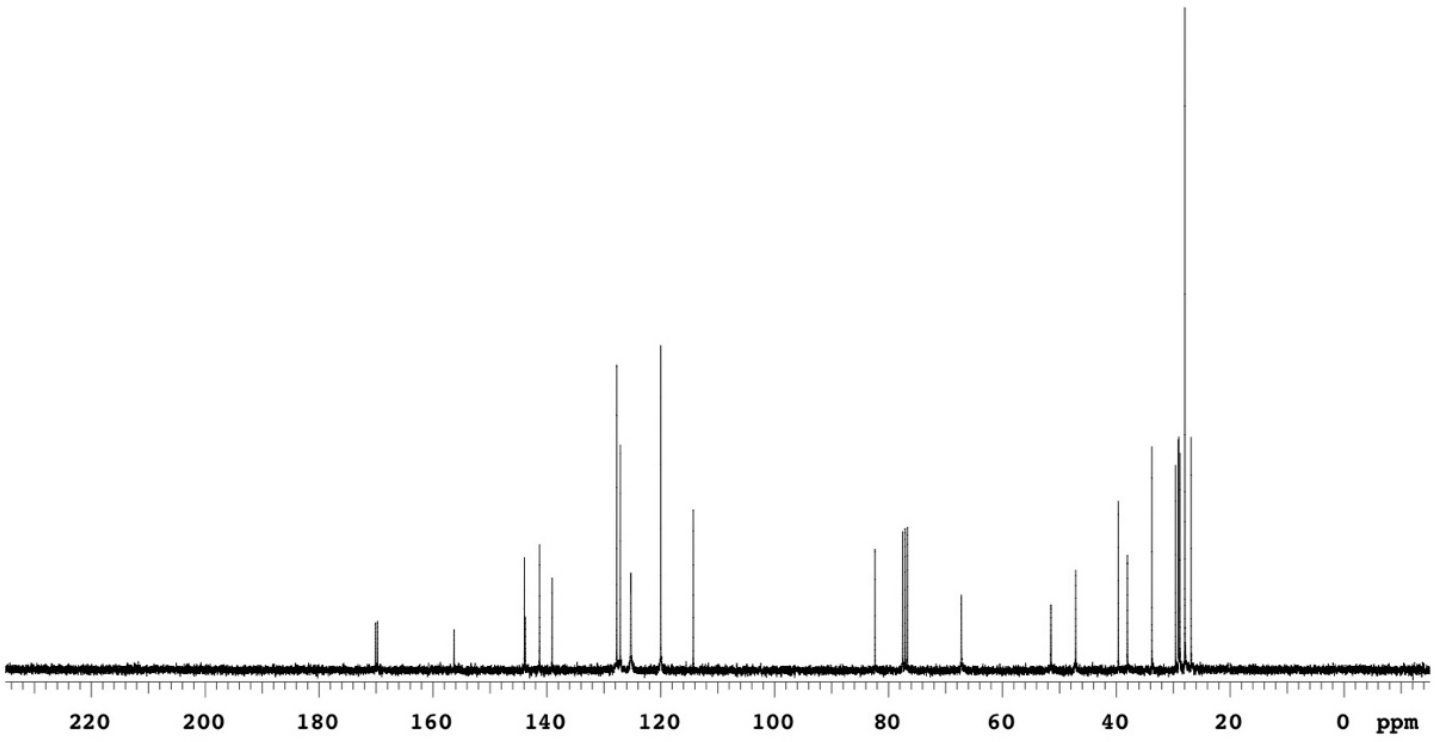


**Figure S137**. $^{13}C$ NMR data for compound **QX2001**.

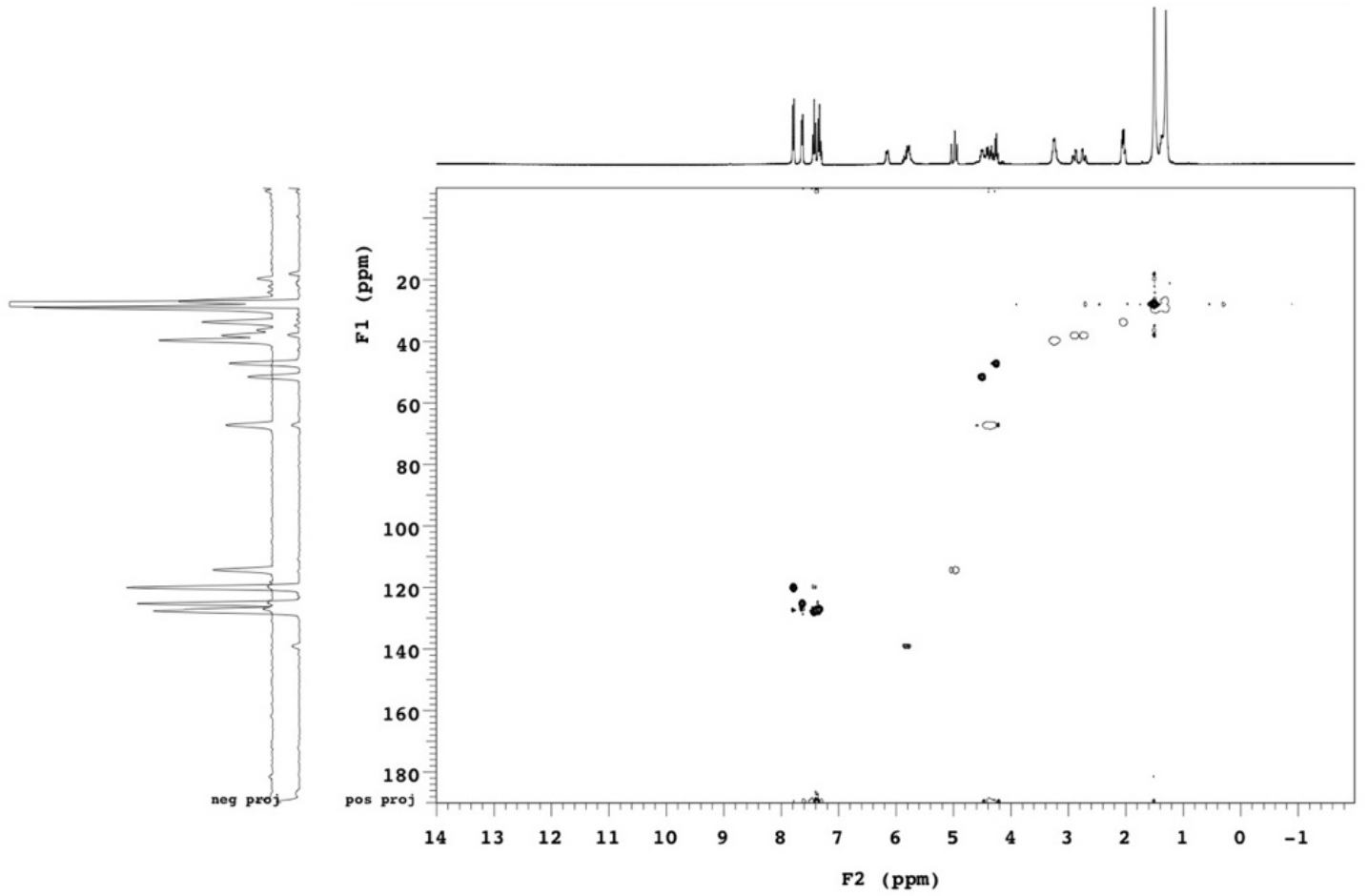


**Figure S138**. HSQC data for compound **QX2001**.

## $N^2$-(((9*H*-fluoren-9-yl)methoxy)carbonyl)-$N^4$-(non-8-en-1-yl)-*L*-asparagine (QX2003)

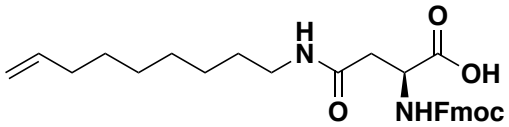


**QX2003**

Procedure was performed as described above for compound QX1019 but using QX2001 as starting material. Yield: quantitative; MS(ESI-TOF) m/z calc. for $C_{28}H_{34}N_2O_5H^+$ 479.25, found 479.25 [M+H$^+$]; $^1$H NMR (500 MHz, Chloroform-*d*) δ 10.86 (b.r.s, 1H), 7.77 (d, *J* = 7.5 Hz, 2H), 7.59 (dd, *J* = 7.7, 3.5 Hz, 2H), 7.41 (t, *J* = 7.4 Hz, 2H), 7.36 – 7.29 (m, 2H), 6.59 (s, 1H), 6.44 (s, 1H), 5.79 (ddt, *J* = 17.0, 12.3, 6.3 Hz, 1H), 4.99 (d, *J* = 17.3 Hz, 1H), 4.94 (d, *J* = 10.1 Hz, 1H), 4.58 (s, 1H), 4.43 – 4.30 (m, 1H), 4.21 (t, *J* = 7.2 Hz, 2H), 3.27 – 3.20 (m, 2H), 2.98 (dd, *J* = 15.6, 4.7 Hz, 1H), 2.88 (dd, *J* = 15.6, 4.7 Hz, 1H), 2.02 (q, *J* = 7.1 Hz, 2H), 1.55 – 1.17 (m, 10H). $^{13}$C NMR (126 MHz, Chloroform-*d*) δ 173.93, 173.81, 171.67, 159.73, 156.81, 143.40, 143.26, 141.27, 138.99, 127.90, 127.90, 127.16, 125.08, 125.05, 120.07, 120.07, 114.25, 67.97, 46.85, 40.48, 37.60, 35.26, 33.68, 28.97, 28.89, 28.89, 28.75, 26.68.

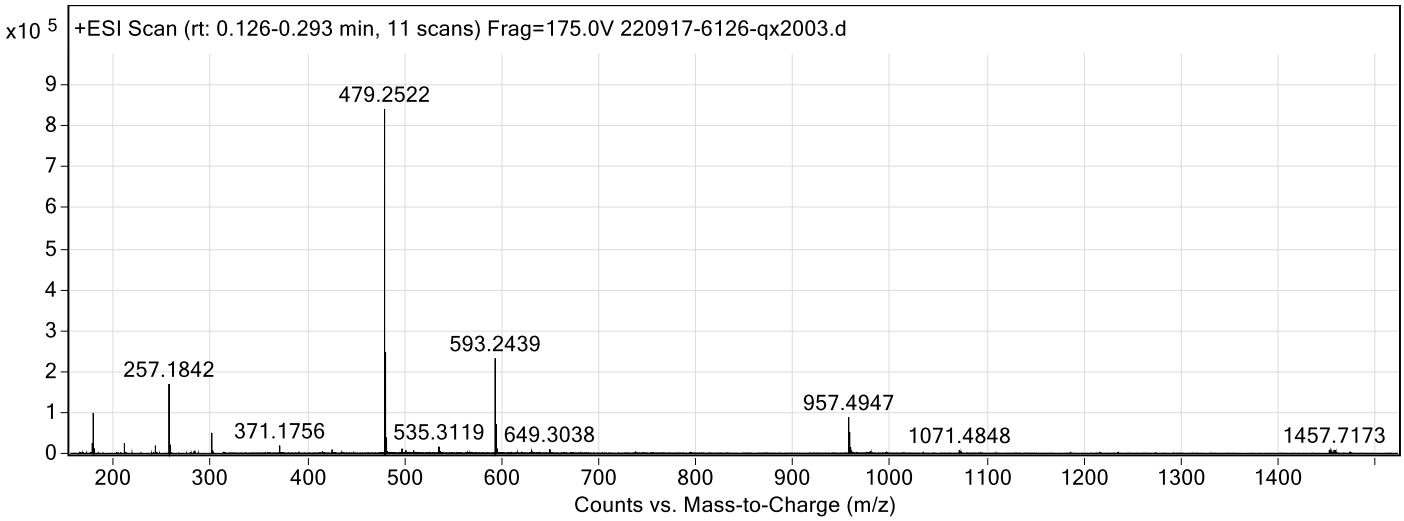


**Figure S139**. ESI-TOF MS data for compound **QX2003**.

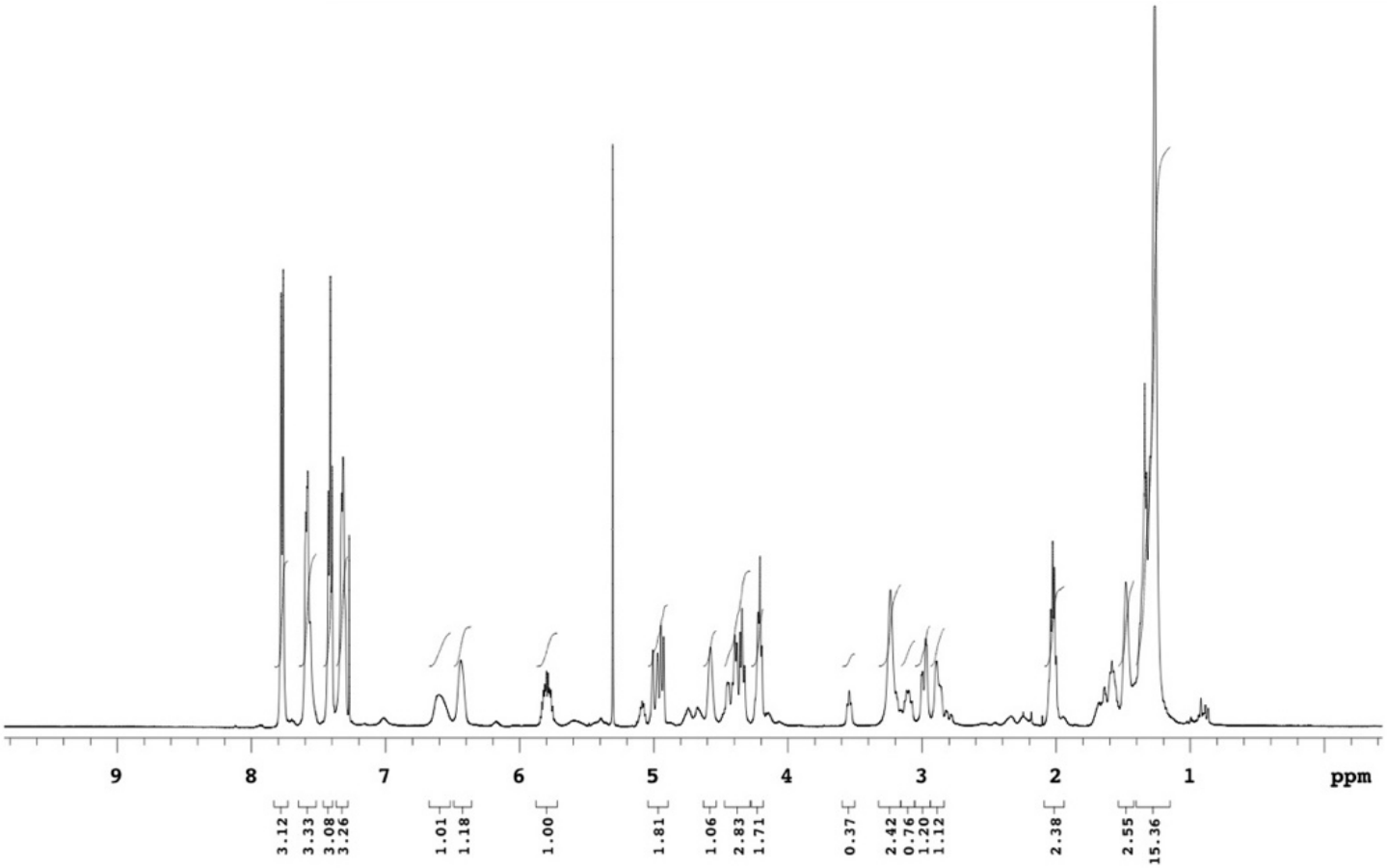


**Figure S140**. ESI-TOF MS data for compound **QX2003**.

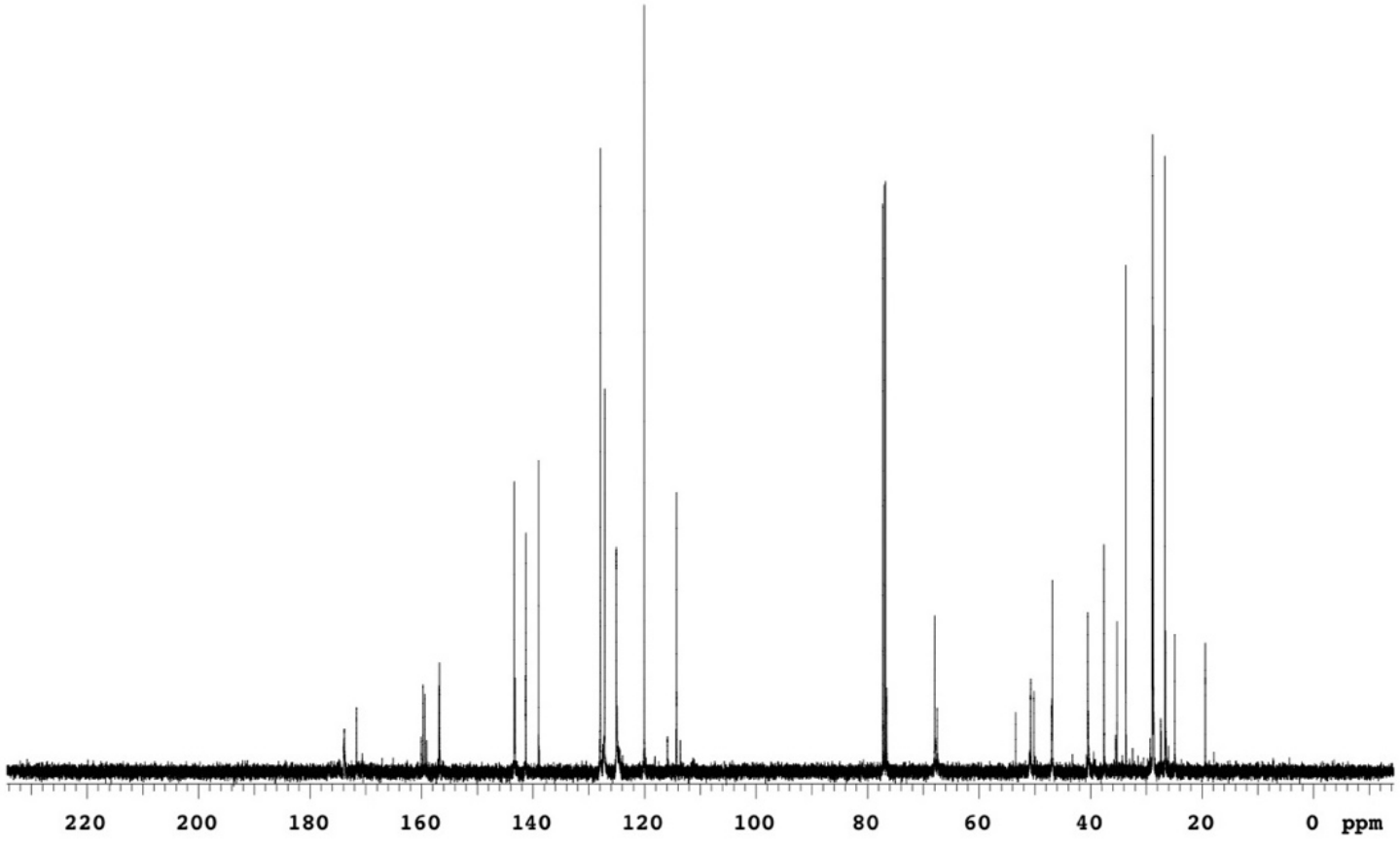

**Figure S141**. $^{13}C$ NMR data for compound **QX2003**.

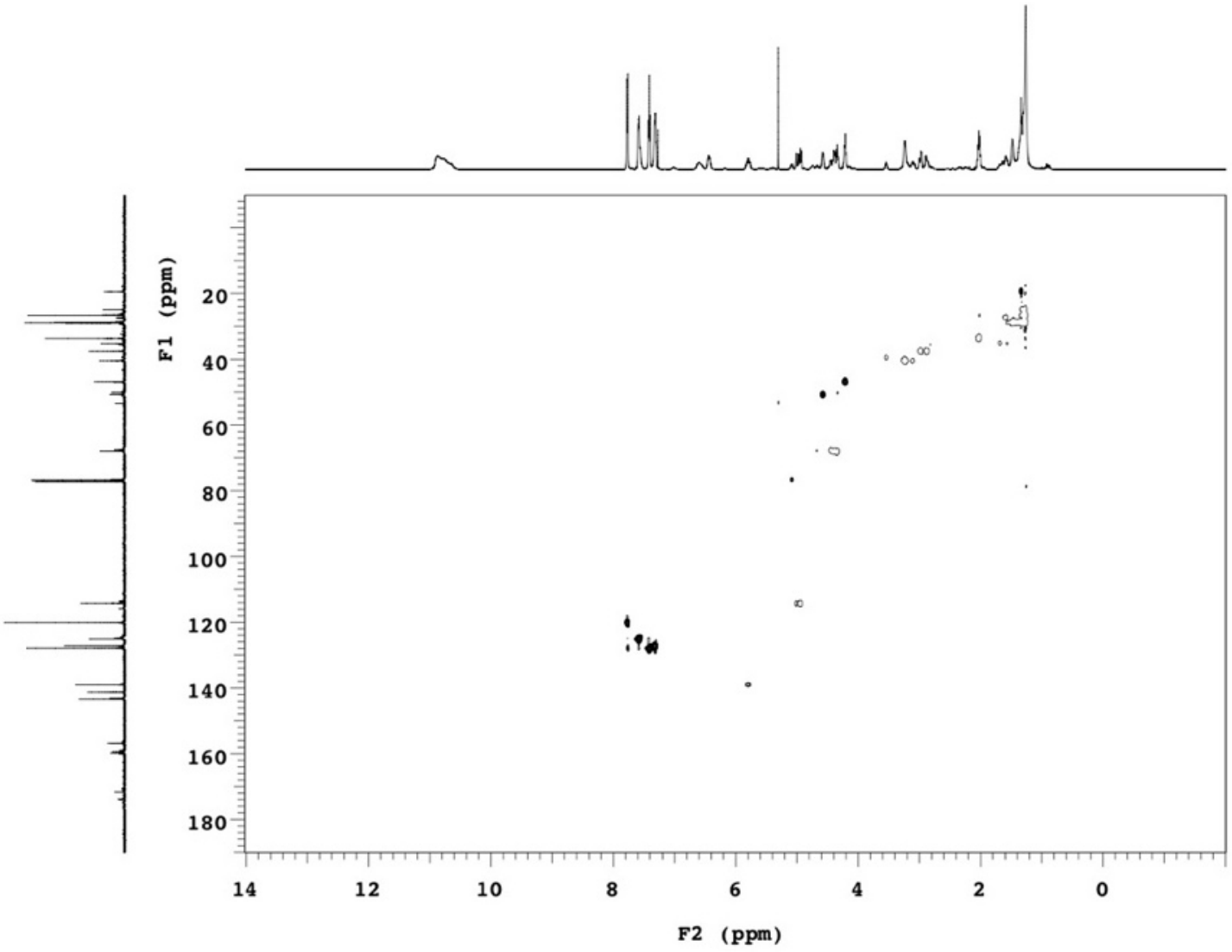


**Figure S142**. HSQC data for compound **QX2003**.

**12-bromododec-1-ene (QX2009)**

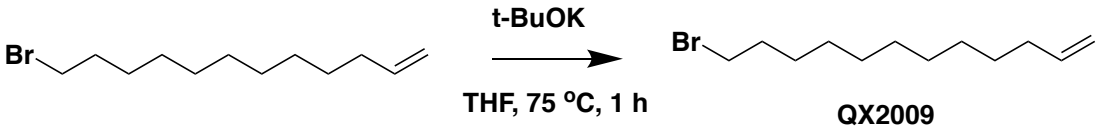


Yield: 54.4% To a stirred solution of 1,12-dibromododecane (1.64 g, 5 mmol) in 10 mL THF was added dropwise a solution of t-BuOK (561 mg, 5 mmol) in THF (5 mL) at 75 ºC over 30 min. The reaction mixture was kept stirring for 30 min at this temperature and then cooled back to room temperature. After standard workup with Et2O, the crude product was purified by flash column chromatography with hexanes as mobile phase to afford the title compound as colorless clear oil (672 mg, 54%). MS(ESI-TOF) m/z calc. for $C_{12}H_{23}BrH^+$ 247.10, found 247.10 [M+H$^+$]; $^1$H NMR (500 MHz, Chloroform-d) δ 5.82 (ddt, J = 16.9, 10.1, 6.7 Hz, 1H), 5.00 (dq, J = 17.2, 1.8 Hz, 1H), 4.94 (ddd, J = 10.2, 2.1, 1.1 Hz, 1H), 3.42 (t, J = 6.9 Hz, 2H), 2.05 (q, J = 6.7 Hz, 2H), 1.86 (dt, J = 14.5, 7.0 Hz, 2H), 1.45 – 1.35 (m, 4H), 1.29 (s, 10H). 13C NMR (126 MHz, Chloroform-*d*) δ 139.19, 114.11, 34.02, 33.81, 32.84, 29.48, 29.44, 29.42, 29.12, 28.93, 28.77, 28.18.

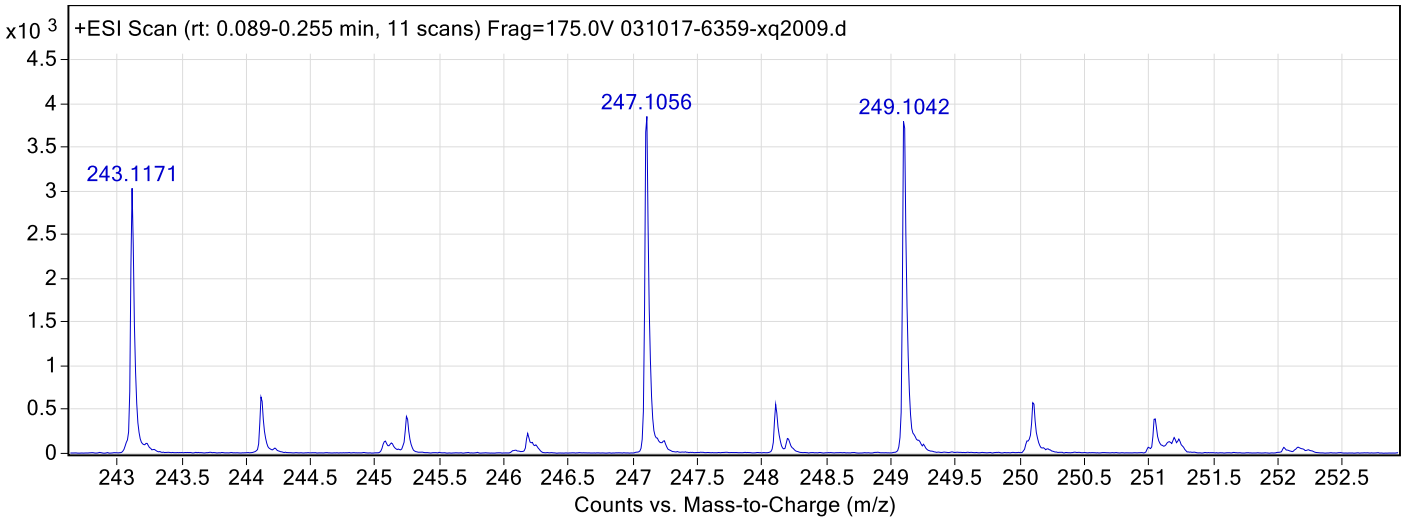


**Figure S143**. ESI-TOF MS data for compound **QX2009**.

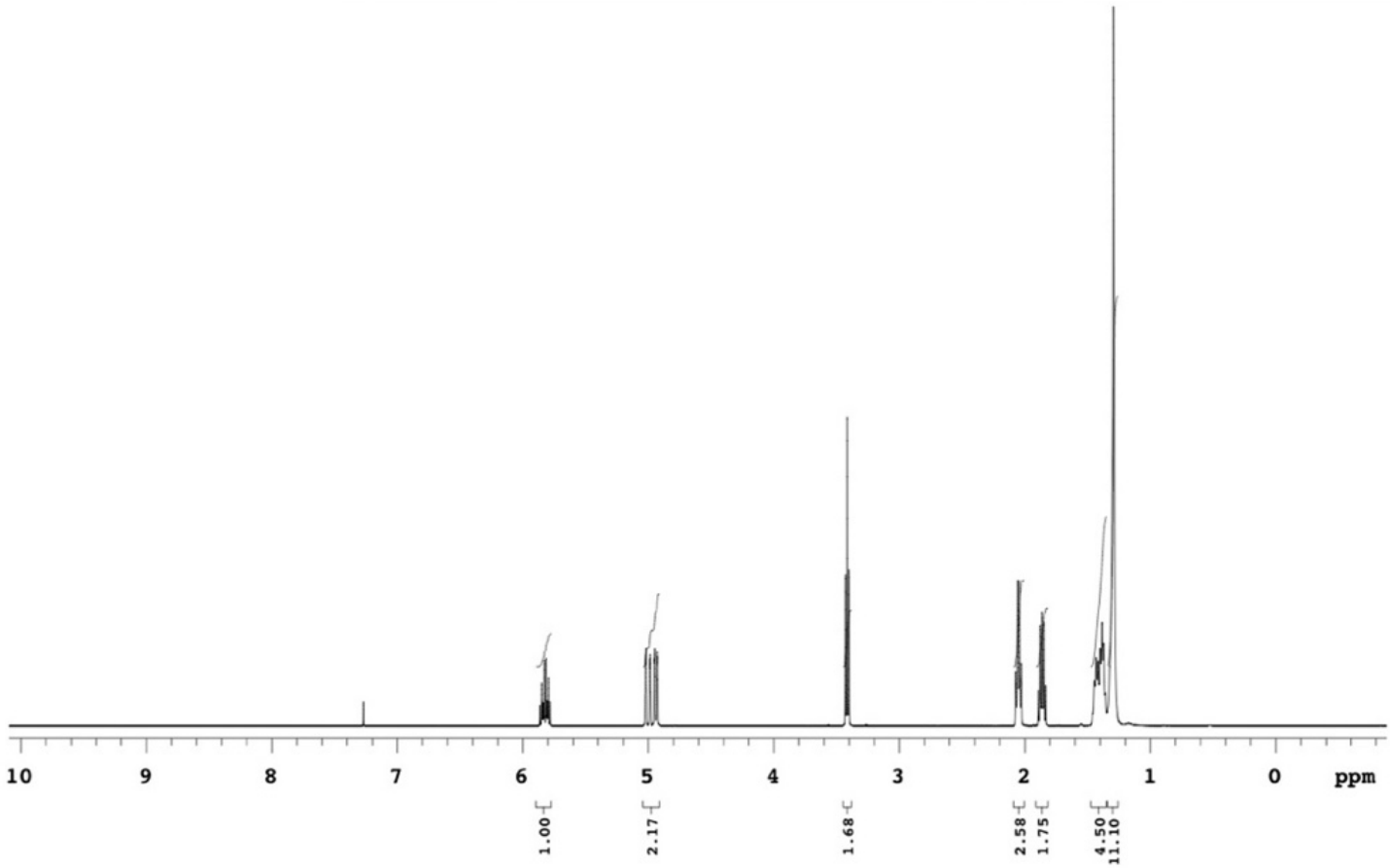


**Figure S144**. $^{1}$H NMR data for compound **QX2009**.

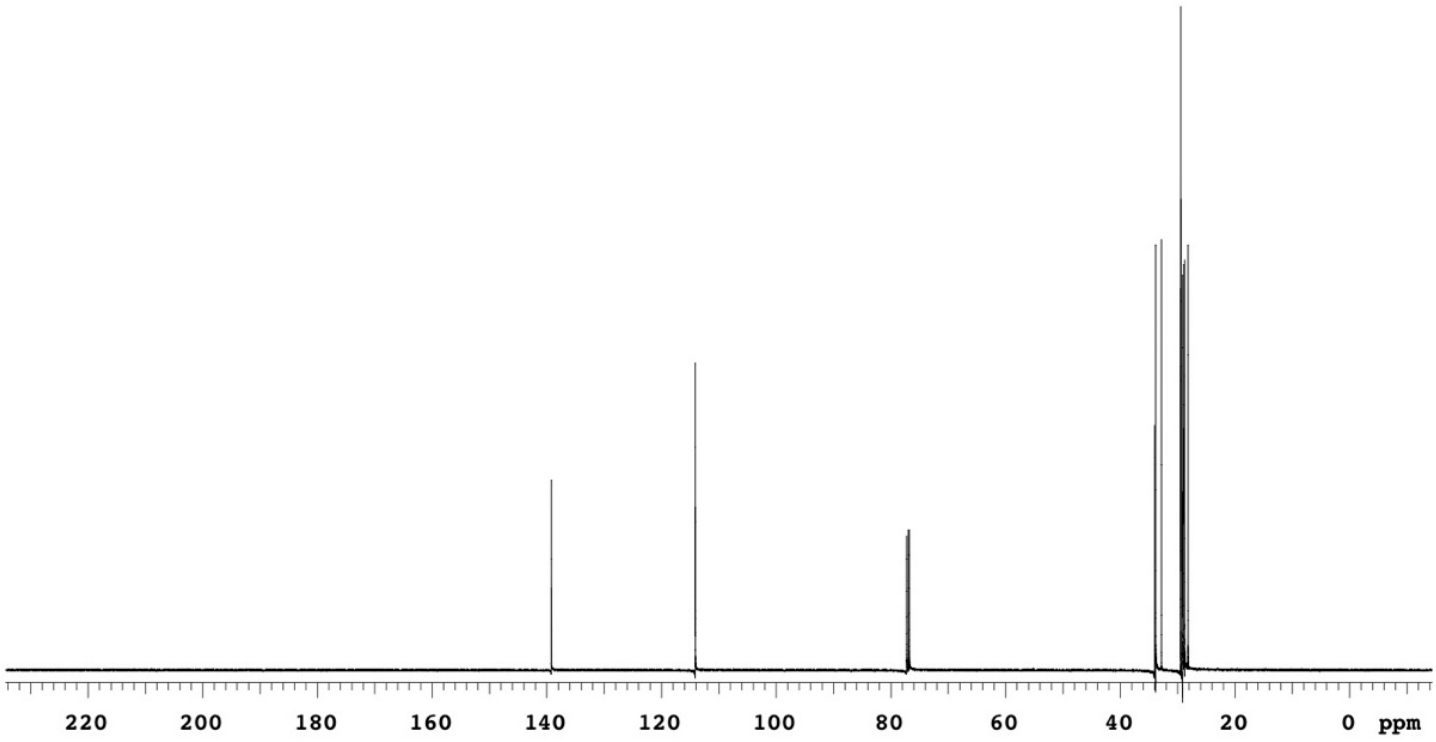


**Figure S145**. $^{13}$C NMR data for compound **QX2009**.

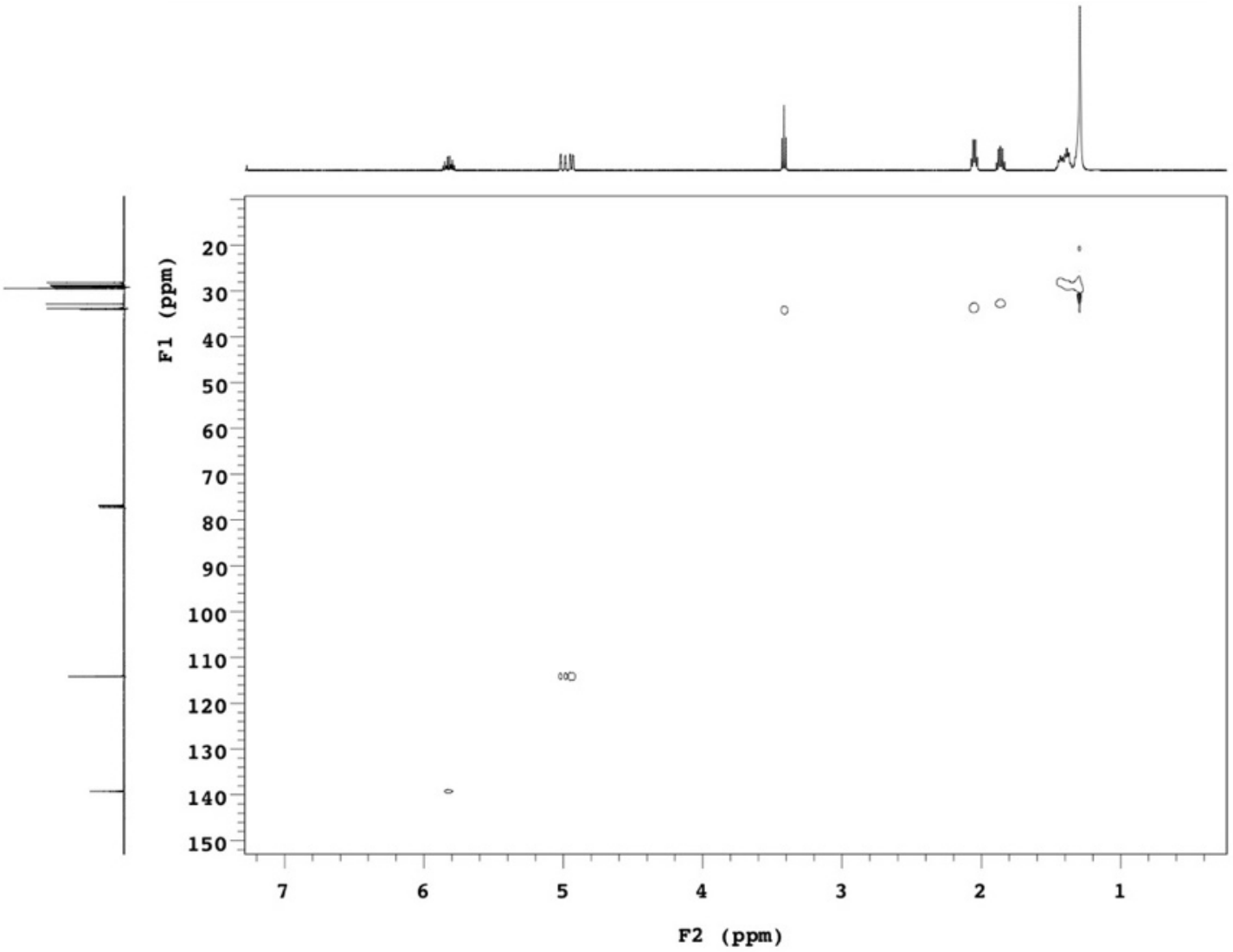


**Figure S146**. HSQC data for compound **QX2009**.

**dodec-11-en-1-amine (QX2013)**

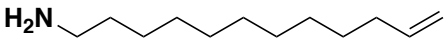

**QX2013**

Procedure was performed as described above for compound QX1015 but using QX2009 as starting material. Yield: 73.6% MS(ESI-TOF) m/z calc. for $C_{12}H_{25}NH^+$ 184.20, found 184.20 [M+H$^+$]; $^1$H NMR (300 MHz, Chloroform-*d*) δ 8.15 (b.r.s, 2H), 5.82 (ddt, *J* = 16.9, 10.2, 6.7 Hz, 1H), 5.00 (dd, *J* = 17.4, 1.8 Hz, 1H), 4.94 (d, *J* = 10.3 Hz, 1H), 3.01 (s, 2H), 2.05 (q, *J* = 7.0 Hz, 2H), 1.79 (t, *J* = 7.6 Hz, 2H), 1.47 – 1.18 (m, 14H).

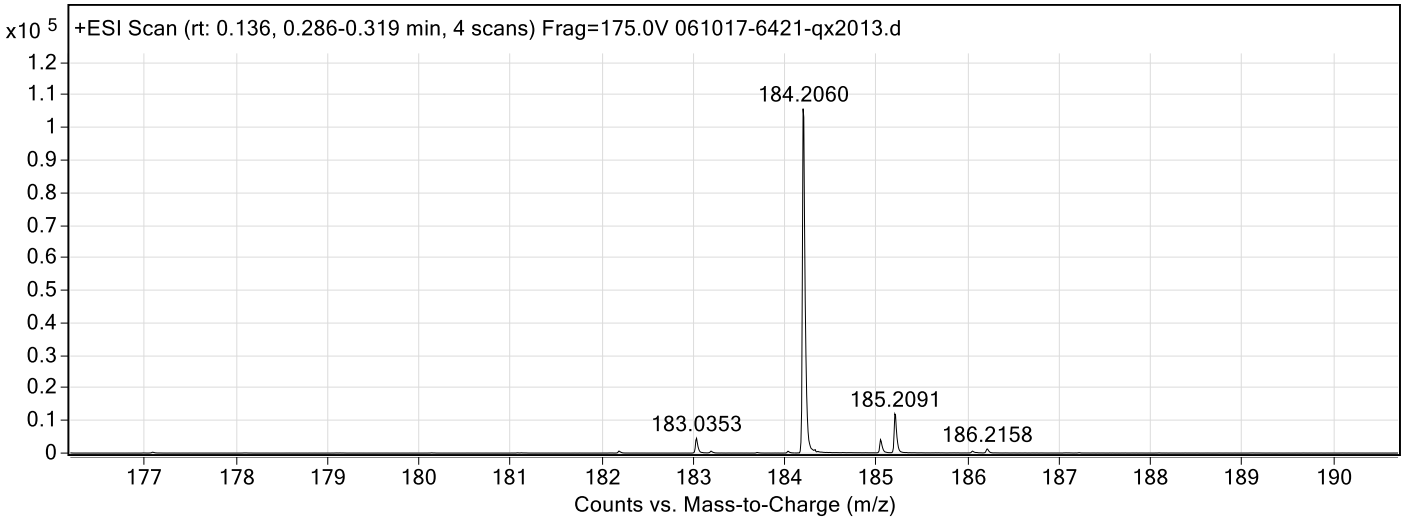


**Figure S147**. ESI-TOF MS data for compound **QX2013**.

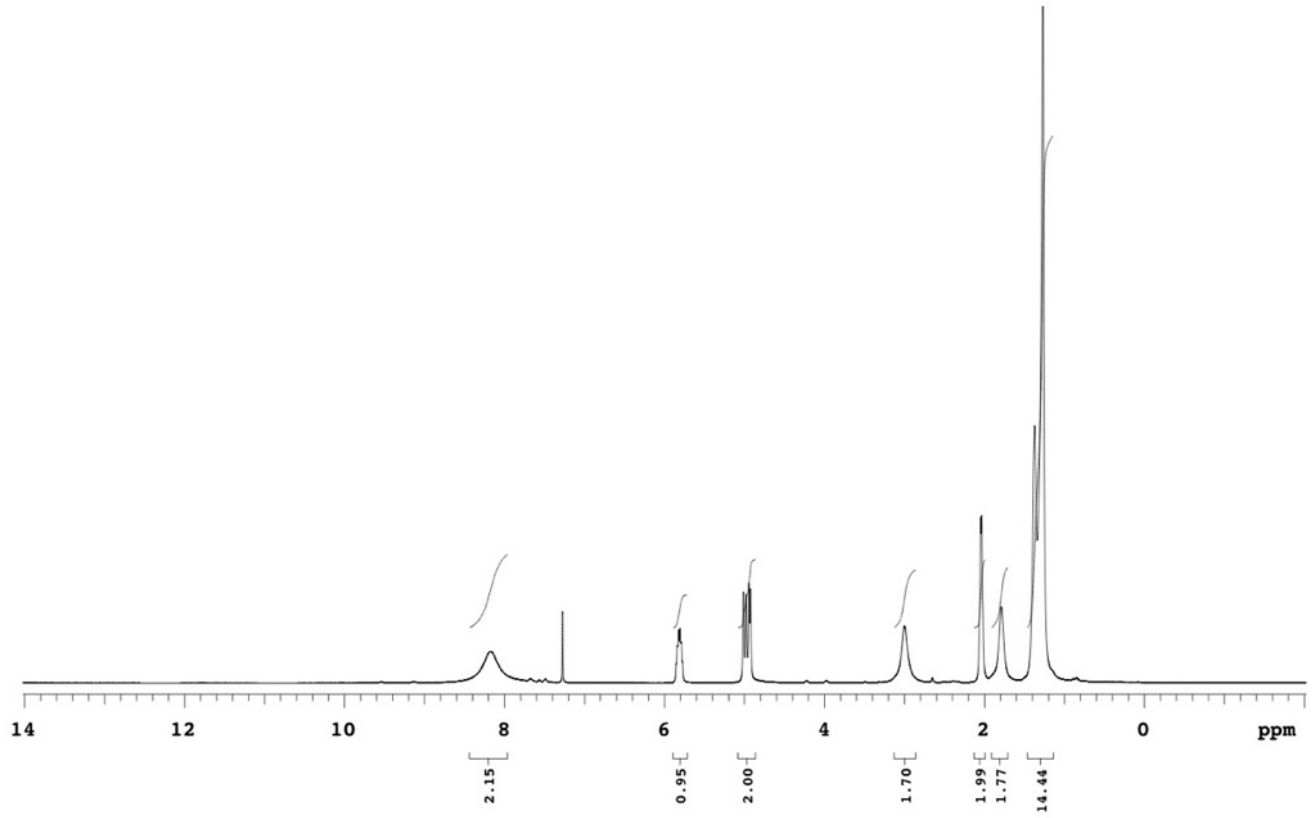

**Figure S148**. $^{1}$H NMR data for compound **QX2013**.

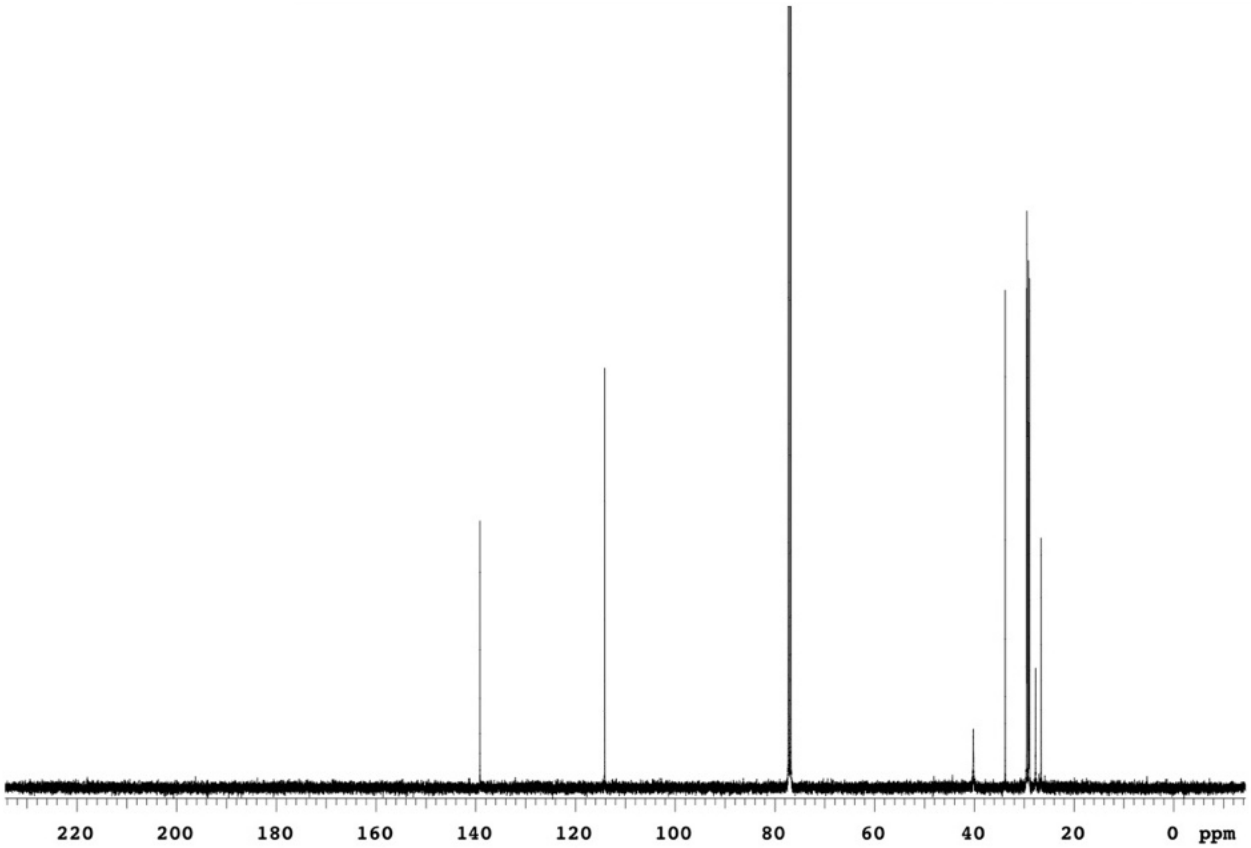


**Figure S149**. $^{13}$C NMR data for compound QX2013.

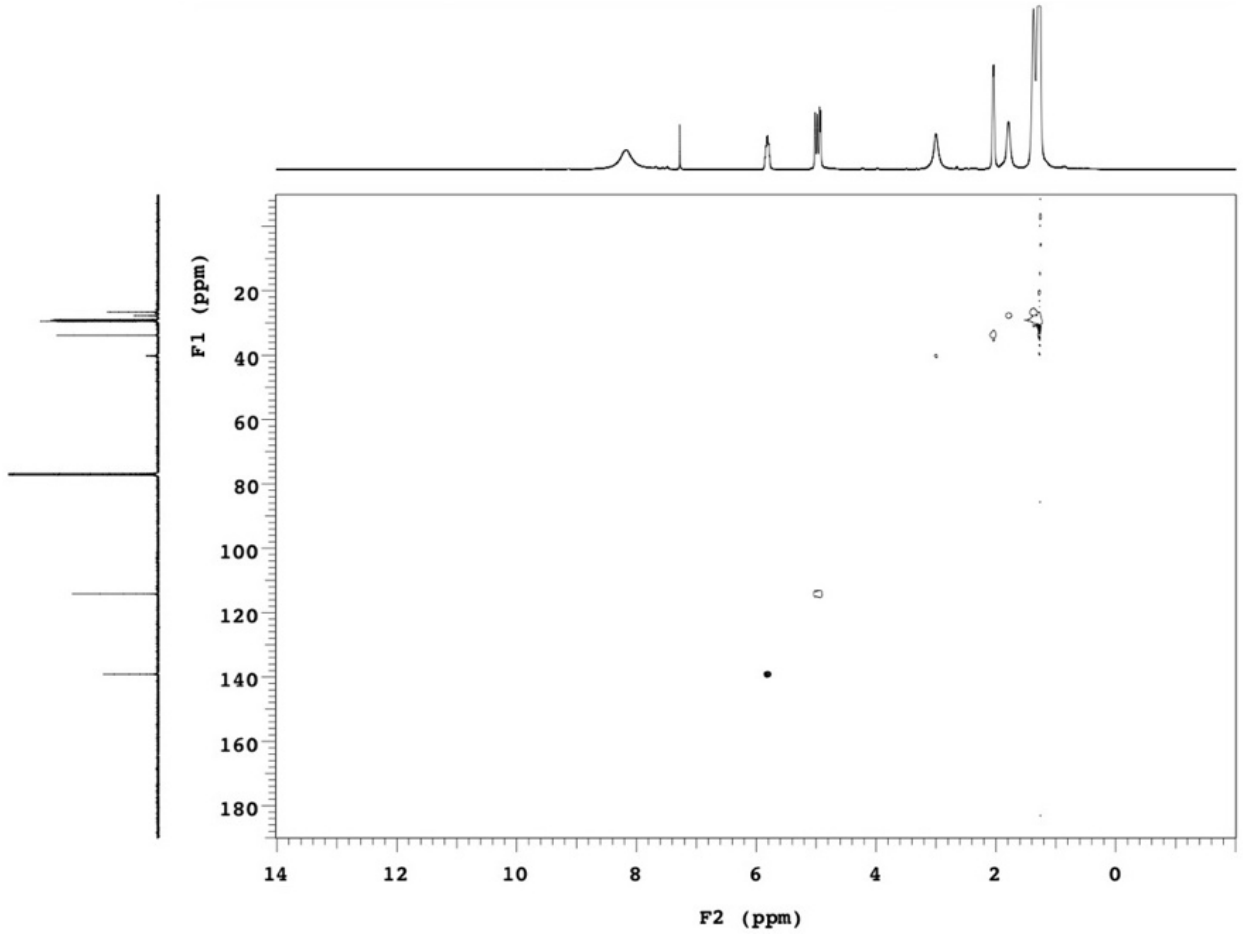


**Figure S150**. HSQC data for compound **QX2013**.

---

**<u>*tert*-butyl $N^2$-(((9*H*-fluoren-9-yl)methoxy)carbonyl)-$N^4$-(dodec-11-en-1-yl)-*L*-asparaginate (QX2015)</u>**

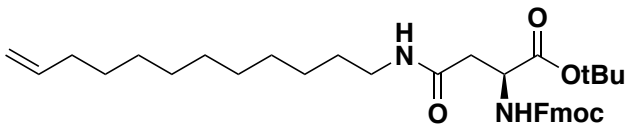


**QX2015**

Procedure was performed as described above for compound QX1017 but using QX2013 as starting material. Yield: 57.4% MS(ESI-TOF) m/z calc. for $C_{35}H_{48}N_2O_5H^+$ 577.36, found 577.3648 [M+H$^+$]; $^1$H NMR (300 MHz, Chloroform-*d*) δ 7.79 (d, *J* = 7.5 Hz, 2H), 7.64 (dd, *J* = 7.5, 2.2 Hz, 2H), 7.43 (t, *J* = 7.4 Hz, 2H), 7.34 (t, *J* = 7.4 Hz, 2H), 6.12 (d, *J* = 8.2 Hz, 1H), 5.84 (ddt, *J* = 16.9, 10.1, 6.7 Hz, 1H), 5.66 (s, 1H), 5.02 (dd, *J* = 17.1, 1.9 Hz, 1H), 4.96 (dd, *J* = 10.4, 2.1 Hz, 1H), 4.50 (dt, *J* = 8.3, 4.5 Hz, 1H), 4.41 (d, *J* = 7.4 Hz, 1H), 4.34 (t, *J* = 8.8 Hz, 1H), 4.25 (t, *J* = 7.1 Hz, 1H), 3.26 (q, *J* = 7.0 Hz, 2H), 2.90 (dd, *J* = 15.6, 4.7 Hz, 1H), 2.73 (dd, *J* = 15.7, 4.5 Hz, 1H), 2.06 (q, *J* = 7.9 Hz, 2H), 1.51 (s, 9H), 1.45 – 1.22 (m, 16H). $^{13}$C NMR (75 MHz, Chloroform-*d*) δ 170.01, 169.67, 156.25, 143.93, 143.79, 141.27, 139.23, 127.70, 127.70, 127.07, 127.07,125.25, 125.20, 125.18, 119.97, 119.97, 114.13, 82.39, 67.19, 51.46, 47.14, 39.67, 38.10, 33.83, 29.62, 29.54, 29.54, 29.48, 29.29, 29.15, 28.95, 27.94, 27.94, 27.94, 26.92.

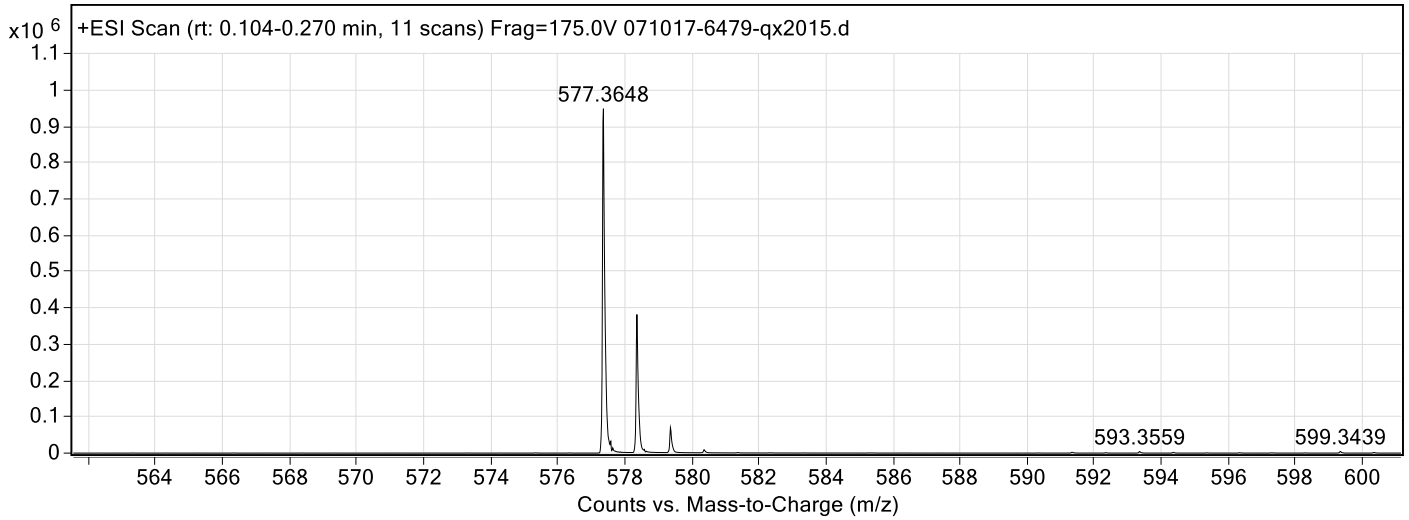


**Figure S151**. ESI-TOF MS data for compound **QX2015**.

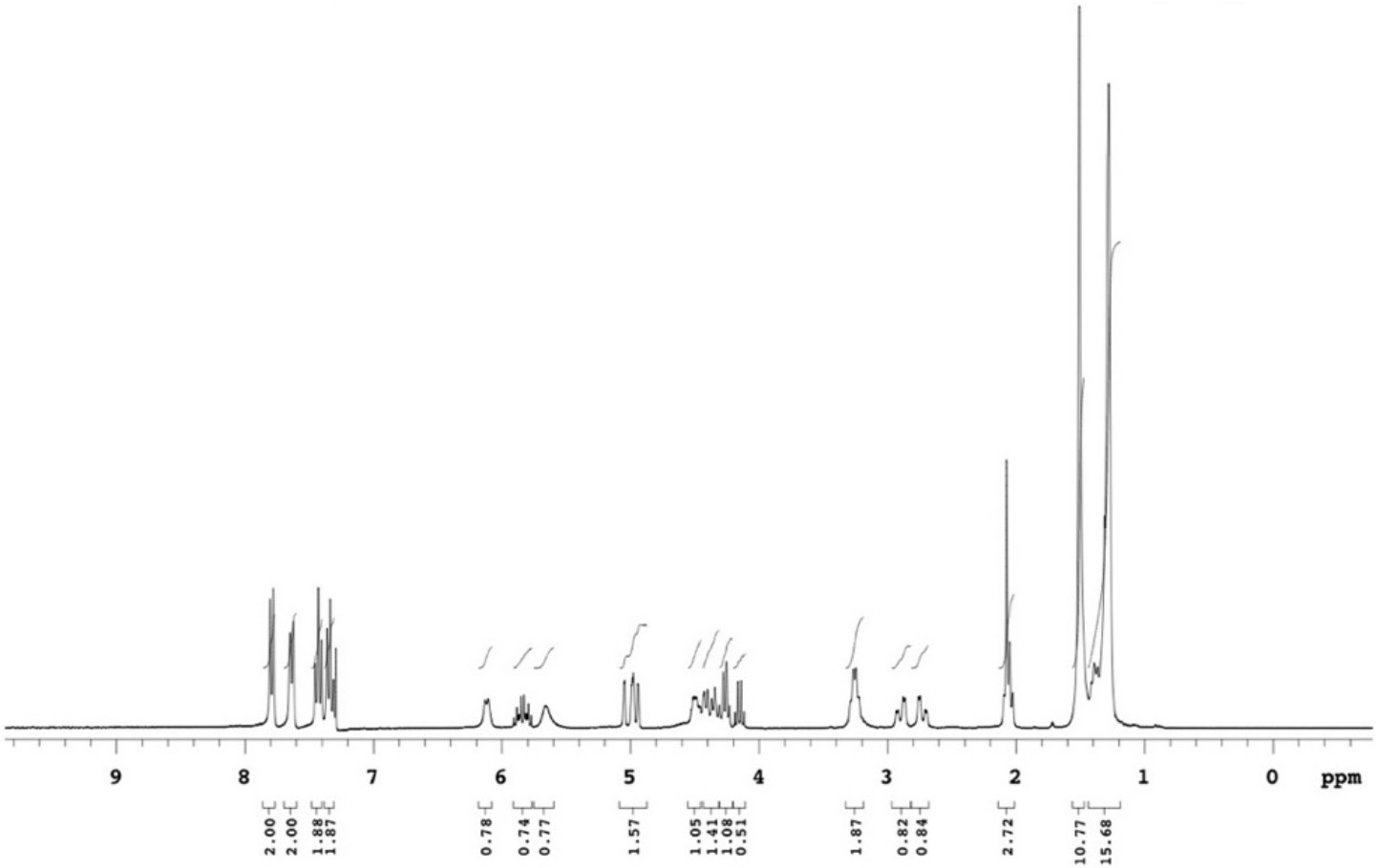


**Figure S152**. $^{1}$H NMR data for compound **QX2015**.

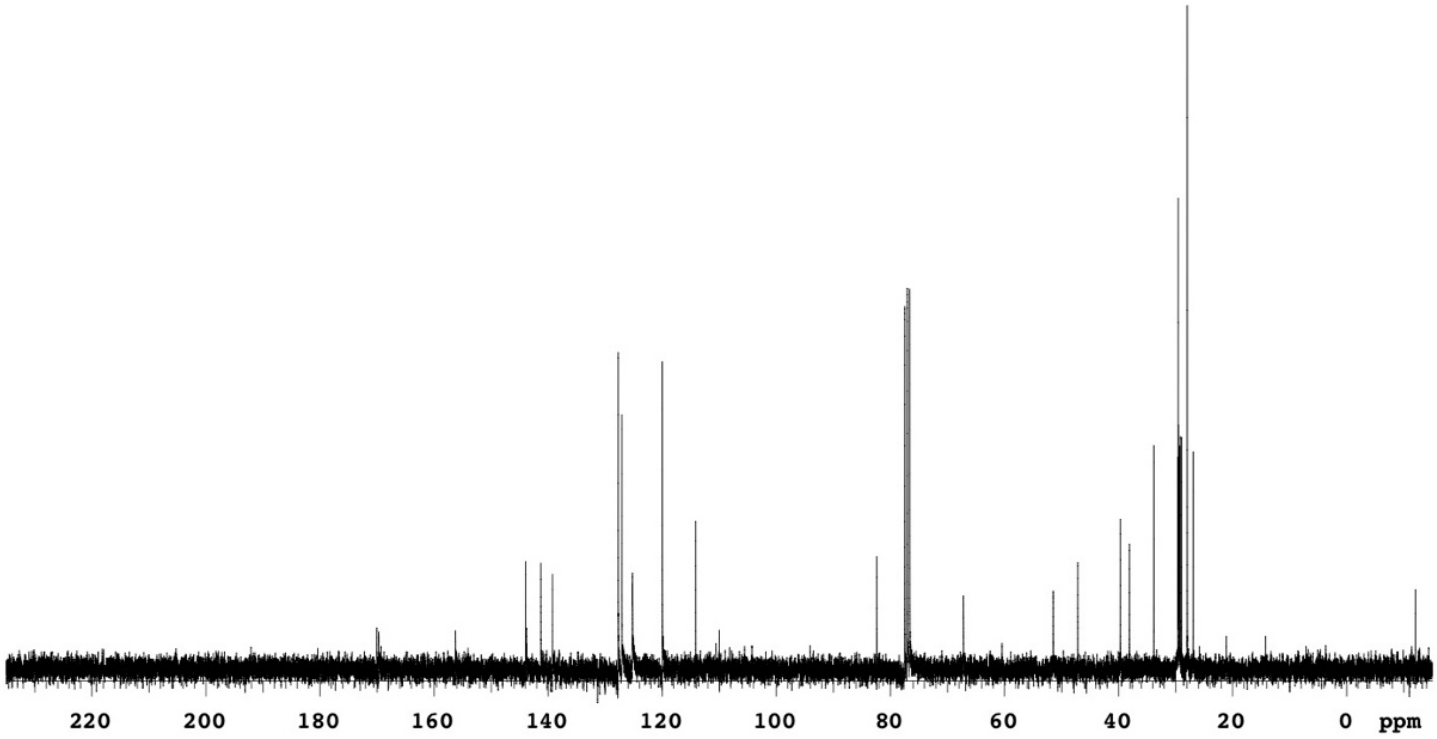


**Figure S153**. $^{13}C$ NMR data for compound **QX2015**.

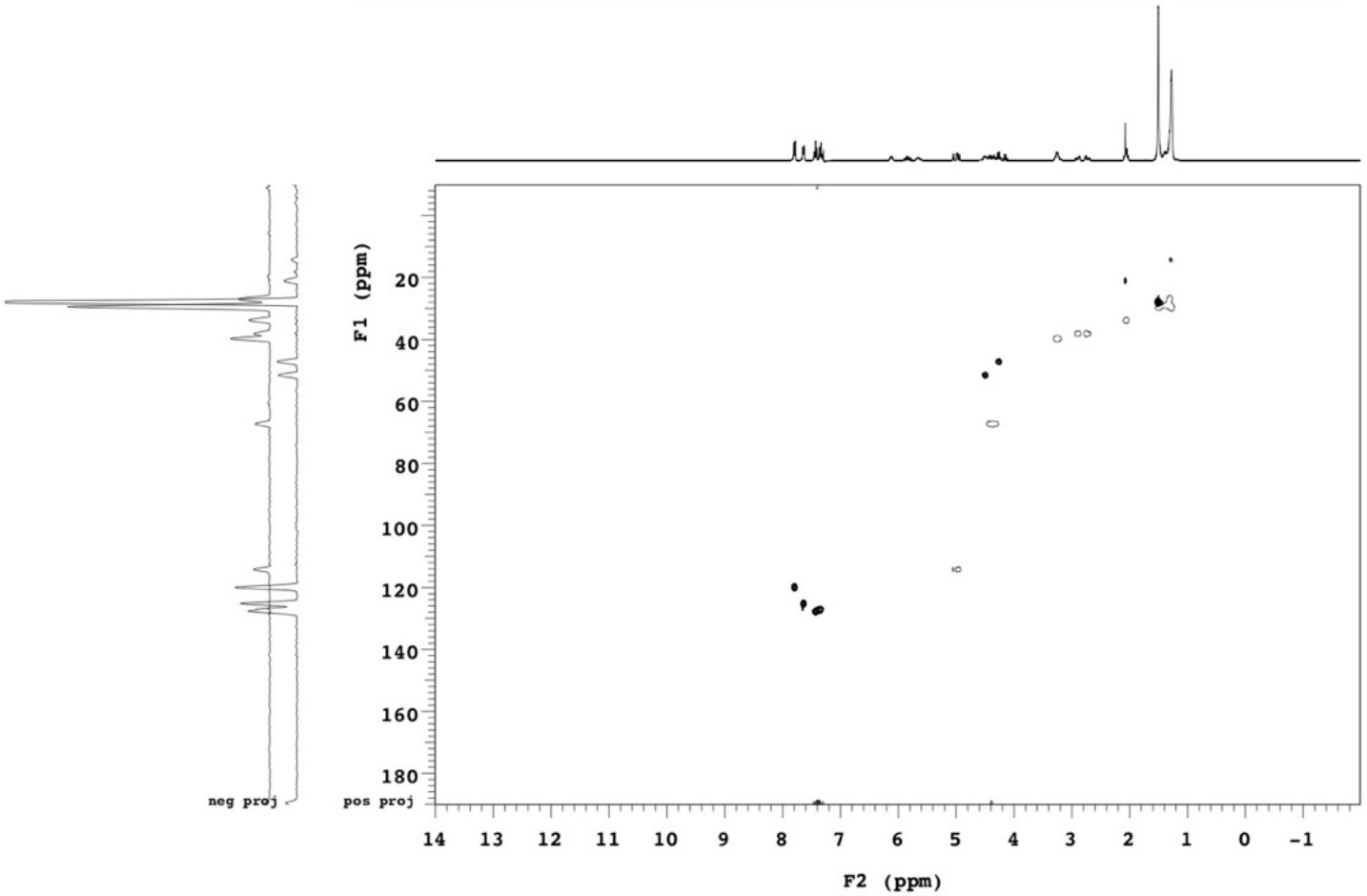


**Figure S154**. HSQC data for compound **QX2015**.

**$N^2$-(((9*H*-fluoren-9-yl)methoxy)carbonyl)-$N^4$-(dodec-11-en-1-yl)-*L*-asparagine (QX2017)**

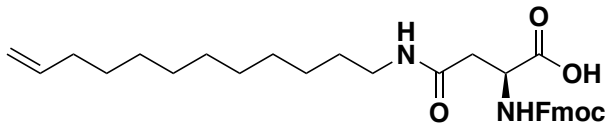


**QX2017**

Procedure was performed as described above for compound QX1019 but using QX2015 as starting material. Yield: quantitative; MS(ESI-TOF) m/z calc. for $C_{31}H_{40}N_2O_5H^+$ 521.30, found 521.30 [M+H$^+$]; $^1$H NMR (300 MHz, Chloroform-*d*) δ 10.99 (b.r.s., 1H), 7.80 (d, *J* = 7.5 Hz, 2H), 7.61 (d, *J* = 7.4 Hz, 2H), 7.44 (t, *J* = 7.4 Hz, 2H), 7.34 (t, *J* = 7.4 Hz, 2H), 6.46 (s, 1H), 6.39 (d, *J* = 6.5 Hz, 1H), 5.84 (ddt, *J* = 16.9, 10.2, 6.6 Hz, 1H), 5.02 (d, *J* = 17.5 Hz, 1H), 4.96 (d, *J* = 11.0 Hz, 2H), 4.57 (s, 1H), 4.41 (qd, *J* = 10.4, 7.3 Hz, 2H), 4.24 (t, *J* = 7.0 Hz, 1H), 3.29 (q, *J* = 6.9 Hz, 2H), 3.02 (dd, *J* = 15.8, 3.9 Hz, 1H), 2.87 (dd, *J* = 15.9, 7.5 Hz, 1H), 2.06 (q, *J* = 7.0 Hz, 2H), 1.45 – 1.20 (m, 16H). $^{13}$C NMR (75 MHz, Chloroform-*d*) δ 173.51, 171.76, 156.68, 143.42, 143.26, 141.31, 139.23, 127.92, 127.18, 125.06, 120.10, 114.13, 109.99, 77.46, 67.94, 50.62, 46.89, 40.54, 37.62, 35.38, 33.82, 29.51, 29.46, 29.17, 29.13, 28.93, 26.77, 25.03.

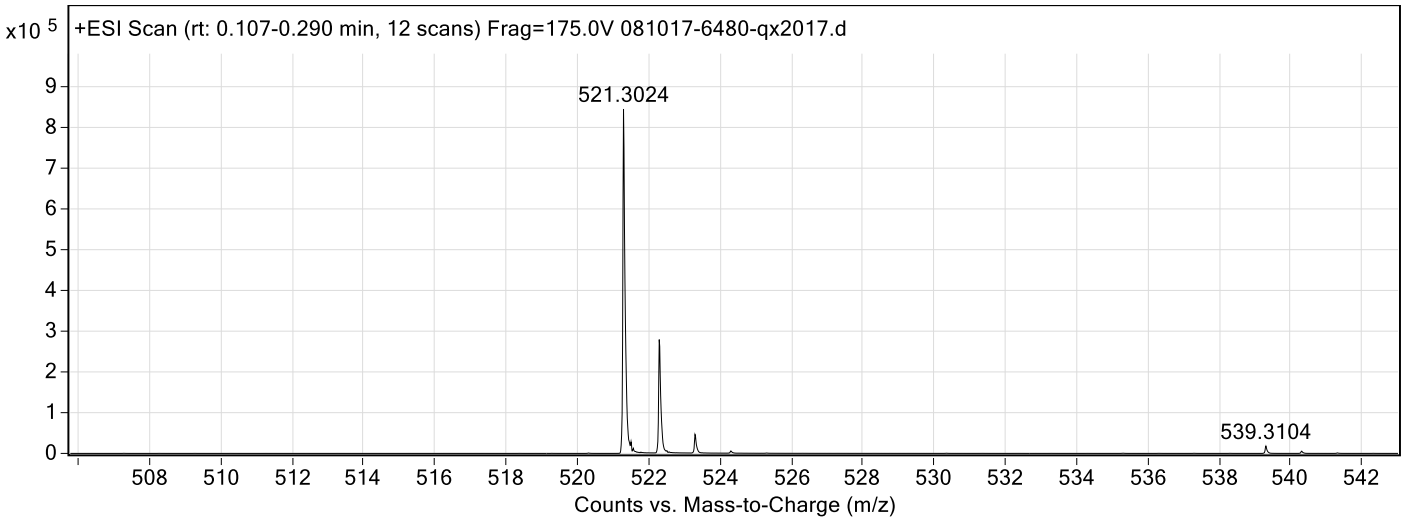


**Figure S155**. ESI-TOF MS data for compound **QX2017**.

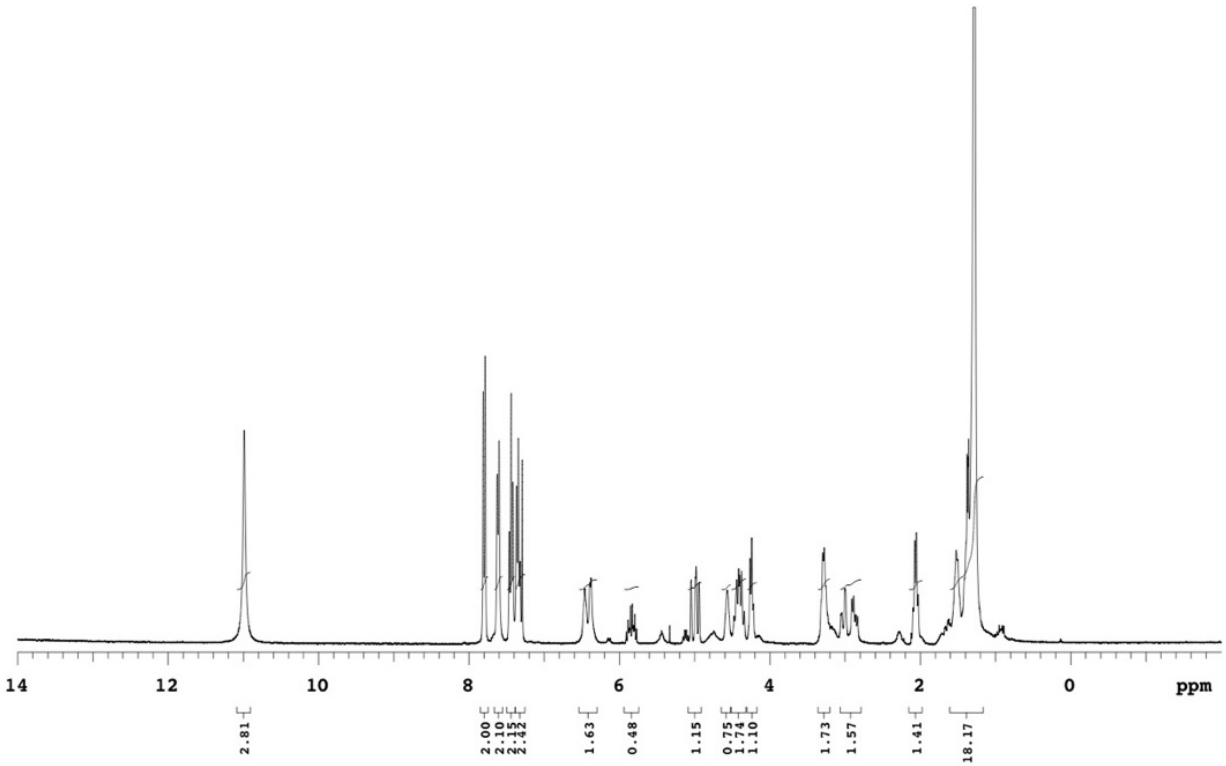


**Figure S156**. [1]H NMR data for compound **QX2017**.

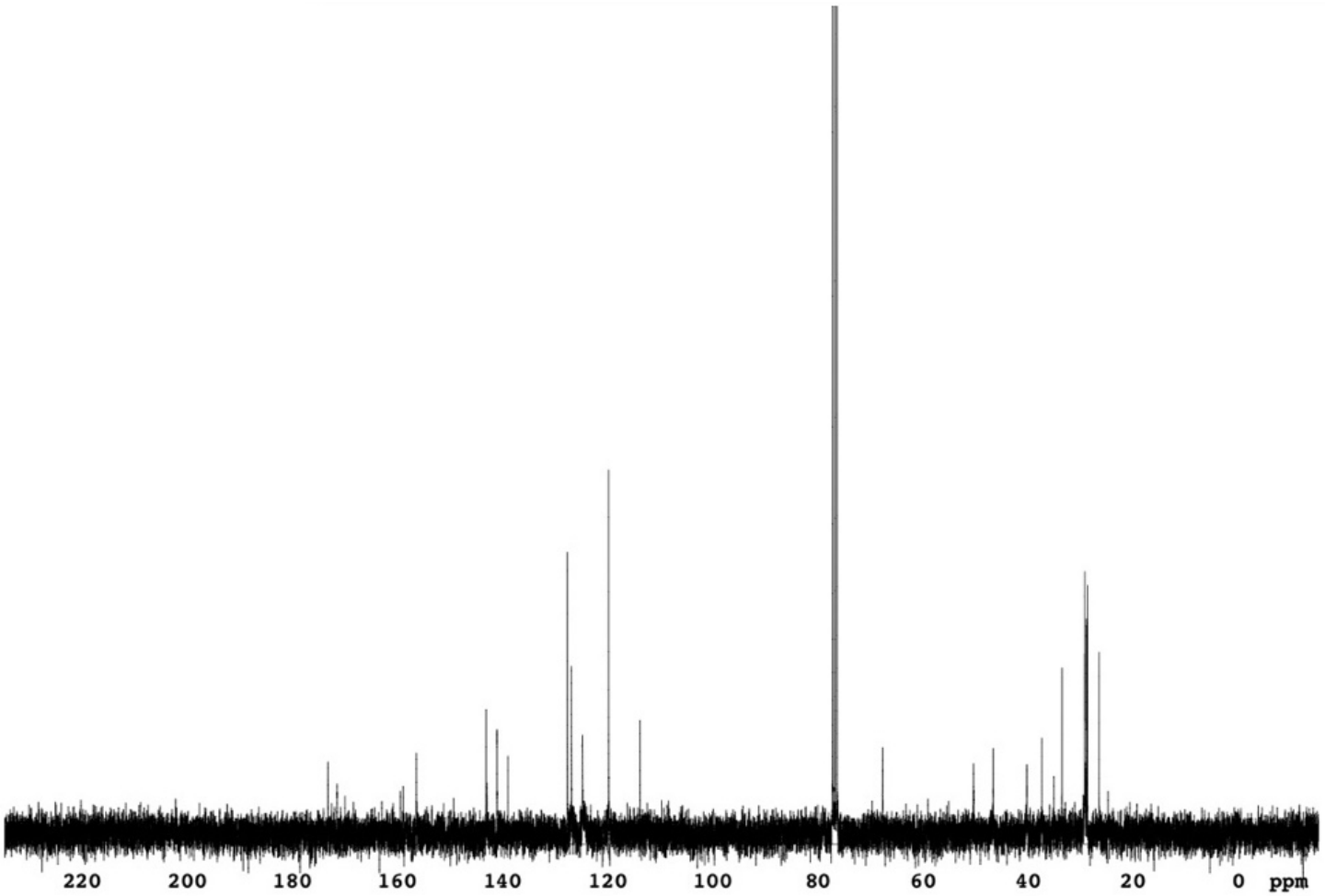


**Figure S157**. [13]C NMR data for compound **QX2017**.

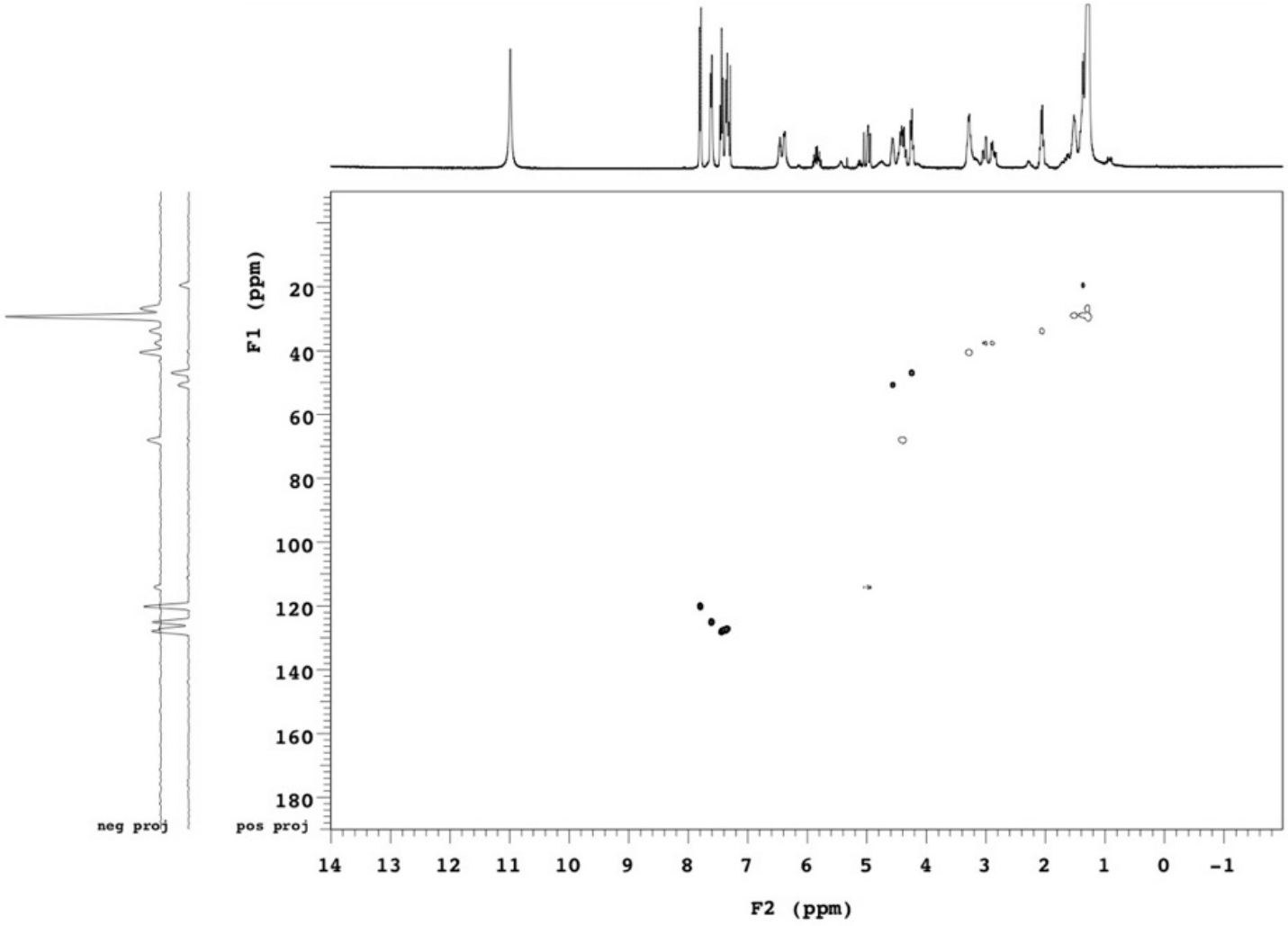


**Figure S158**. HSQC data for compound **QX2017**.